WHEAT BIOFORTIFICATION TO ALLEVIATE GLOBAL MALNUTRITION

EDITED BY: Om Prakash Gupta, Velu Govindan, Alexander Arthur Theodore, Henrik Brinch-Pedersen, Miroslav Nikolic and Victor Taleon

PUBLISHED IN: Frontiers in Nutrition

frontiers Research Topics

ISSN 1664-8714
ISBN 978-2-83250-377-5
DOI 10.3389/978-2-83250-377-5

About Frontiers

Frontiers is more than just an open-access publisher of scholarly articles: it is a pioneering approach to the world of academia, radically improving the way scholarly research is managed. The grand vision of Frontiers is a world where all people have an equal opportunity to seek, share and generate knowledge. Frontiers provides immediate and permanent online open access to all its publications, but this alone is not enough to realize our grand goals.

Frontiers Journal Series

The Frontiers Journal Series is a multi-tier and interdisciplinary set of open-access, online journals, promising a paradigm shift from the current review, selection and dissemination processes in academic publishing. All Frontiers journals are driven by researchers for researchers; therefore, they constitute a service to the scholarly community. At the same time, the Frontiers Journal Series operates on a revolutionary invention, the tiered publishing system, initially addressing specific communities of scholars, and gradually climbing up to broader public understanding, thus serving the interests of the lay society, too.

Dedication to Quality

Each Frontiers article is a landmark of the highest quality, thanks to genuinely collaborative interactions between authors and review editors, who include some of the world's best academicians. Research must be certified by peers before entering a stream of knowledge that may eventually reach the public - and shape society; therefore, Frontiers only applies the most rigorous and unbiased reviews.
Frontiers revolutionizes research publishing by freely delivering the most outstanding research, evaluated with no bias from both the academic and social point of view. By applying the most advanced information technologies, Frontiers is catapulting scholarly publishing into a new generation.

What are Frontiers Research Topics?

Frontiers Research Topics are very popular trademarks of the Frontiers Journals Series: they are collections of at least ten articles, all centered on a particular subject. With their unique mix of varied contributions from Original Research to Review Articles, Frontiers Research Topics unify the most influential researchers, the latest key findings and historical advances in a hot research area! Find out more on how to host your own Frontiers Research Topic or contribute to one as an author by contacting the Frontiers Editorial Office: frontiersin.org/about/contact

WHEAT BIOFORTIFICATION TO ALLEVIATE GLOBAL MALNUTRITION

Topic Editors:
Om Prakash Gupta, Indian Institute of Wheat and Barley Research (ICAR), India
Velu Govindan, International Maize and Wheat Improvement Center (Mexico), Mexico
Alexander Arthur Theodore Johnson, The University of Melbourne, Australia
Henrik Brinch-Pedersen, Aarhus University, Denmark
Miroslav Nikolic, University of Belgrade, Serbia
Victor Taleon, International Food Policy Research Institute, United States

Citation: Gupta, O. P., Govindan, V., Johnson, A. A. T., Brinch-Pedersen, H., Nikolic, M., Taleon, V., eds. (2022). Wheat Biofortification to Alleviate Global Malnutrition. Lausanne: Frontiers Media SA. doi: 10.3389/978-2-83250-377-5

Table of Contents

frontiers | Frontiers in Nutrition

TYPE Editorial
PUBLISHED 16 September 2022
DOI 10.3389/fnut.2022.1001443

OPEN ACCESS

EDITED BY
Akbar Hossain,
Bangladesh Wheat and Maize Research Institute, Bangladesh

REVIEWED BY
Debojyoti Moulick,
Independent Researcher, Kolkata, India
Biswajit Pramanick,
Dr. Rajendra Prasad Central Agricultural University, India

*CORRESPONDENCE
Om Prakash Gupta
op.gupta@icar.gov.in

SPECIALTY SECTION
This article was submitted to Nutrition and Food Science Technology, a section of the journal Frontiers in Nutrition

RECEIVED 23 July 2022
ACCEPTED 26 August 2022
PUBLISHED 16 September 2022

CITATION
Ibba MI, Gupta OP, Govindan V, Johnson AAT, Brinch-Pedersen H, Nikolic M and Taleon V (2022) Editorial: Wheat biofortification to alleviate global malnutrition.
Front. Nutr. 9:1001443.
doi: 10.3389/fnut.2022.1001443

Editorial: Wheat biofortification to alleviate global malnutrition

Maria Itria Ibba[1], Om Prakash Gupta[2]*, Velu Govindan[3], Alexander Arthur Theodore Johnson[4], Henrik Brinch-Pedersen[5], Miroslav Nikolic[6] and Victor Taleon[7]

[1]Wheat Chemistry and Quality Laboratory, International Center for the Improvement of Wheat and Maize (CIMMYT), Texcoco, Mexico, [2]Division of Quality and Basic Sciences, ICAR-Indian Institute of Wheat and Barley Research, Karnal, India, [3]Global Wheat Breeding, International Center for the Improvement of Wheat and Maize (CIMMYT), Texcoco, Mexico, [4]School of Bioscience, University of Melbourne, Parkville, VIC, Australia, [5]Department of Agroecology, Aarhus University, Aarhus, Denmark, [6]Institute for Multidisciplinary Research, University of Belgrade, Belgrade, Serbia, [7]International Food Policy Research Institute, Washington, DC, United States

KEYWORDS

wheat biofortification, malnutrition, micronutrient, bioavailability, GWAS—genome-wide association study

Editorial on the Research Topic
Wheat biofortification to alleviate global malnutrition

According to the latest FAO report on the state of food security and nutrition in the world (1), more than 720 million people faced hunger, and around 3 billion people did not have access to a healthy diet. All these problematics, exacerbated by the current COVID-19 crisis, led to an increase in the number of people affected by the so-called hidden hunger, caused by an inadequate intake of essential micronutrients (MNs) such as iron (Fe), zinc (Zn), selenium (Se) and provitamin A. Biofortification, intended as the improvement of the nutritional quality of food crops through either conventional breeding, agronomic practices or modern biotechnologies, represents a sustainable, cost-effective and long-term approach to alleviate micronutrient-deficiency. Staple crops are typically the major target of most biofortification studies, given their central role in human diet. Wheat, specifically, contributes to around 20% of the total energy and protein intake and to around 30% of the Fe and Zn intake worldwide. However, the current level of MNs present in most wheat-derived food products is not enough to meet the minimum daily intake, especially in the poorest regions of the world. For these reasons, continuing to work on wheat biofortification is fundamental to ensure the production of nutritious and sustainable food and to contribute to the reduction of MNs deficiency.

This special issue of Frontiers in Nutrition presents some of the most recent discoveries on wheat biofortification with studies spanning from the development of genetic tools to speed up conventional breeding, genetic engineering and novel agronomic methods to increase the MNs content in wheat grain. In this issue, Wang Y. et al. report on the identification of different quantitative trait loci (QTL) associated with variation in the grain Fe and Zn content using a bread wheat recombinant inbred line (RIL) population grown across nine different environments. Results of this study revealed the presence of seven different genomic regions associated with grain

Zn content (explaining 2.2 to 25.1% variation), and four genomic regions associated with grain Fe accumulation (explaining 2.3 to 30.4% variation). Interestingly, three of the QTL identified in this study appeared to be associated with the accumulation of both Fe and Zn content. These QTL were therefore transformed into high-throughput Kompetitive Allele Specific PCR (KASP) markers that could be readily used to speed-up biofortification within a conventional breeding program. Similarly, Krishnappa et al. also investigated the genetic control of Fe and Zn accumulation in wheat grains using a RIL population grown in several environments. In this case, however, additional traits associated with grain quality (grain protein content and thousand kernel weight) were also included. Thanks to the high marker density and to the high D-genome coverage, several QTL associated with either Fe, Zn and protein content and thousand kernel weight could be identified. Among them, several were located on the D genome, with the chromosome 7D harboring several QTL associated with all the analyzed traits. Putative candidate genes responsible for the observed phenotypic variation were also identified, paving the road for more detailed future studies which would likely allow the characterization of the specific gene(s) responsible for the variation of these essential traits.

Identification of the genes (and relative enzymes) directly responsible for the accumulation, bioavailability or degradation of anti-nutrients, is undoubtly the final goal of most genetic studies as it could greatly facilitate genetic biofortification though either conventional breeding or transgenic approaches. For this reason, Yu and Tian reported the role of the Carotenoid Cleavage Dioxygenase 4 (CCD4) gene on the wheat grain carotenoid accumulation using a set of Targeting Induced Local Lesions in Genomes (TILLING) durum wheat lines. Results revealed that the CCD4 homeolog genes do not appear to have a significant impact on grain carotenoid content even if changes in the carotenoid composition could be identified in both wheat grains and leaves.

The idneitification of genomic regions associated with higher MN contents and development of genetic tools for the fast transfer of the high MN traits, are not the only approaches used to facilitate the development of MN rich wheat. Several studies have indeed shown that agronomic biofortification is an efficient and effective method to increase wheat grain micronutrient content in the short-term, especially if combined with genetic biofortification (Gupta et al.). Here, Gupta et al. have comprehensively reviwed the recent progress made in utilizing natural genetic diversity, genome-wide association mapping, genomic selection, and genome editing technologies to improve the MN content and their bioavailability in wheat. Yu et al. studied the potential of Zn foliar application on the wheat grown in the Quzhou County of China, a region where more than 90% of the population is engaged in agriculture and where ∼39% of the children suffer from Zn deficiency. The result indicated that compared to control, wheat with Zn foliar application had 97.7 and 68.2% higher Zn content in wheat grain and flour, respectively withoput a significant change in wheat yield. However, according to the author's prediction, implementing this practice could significantly increase the daily Zn intake, reduce the disability-adjusted life years (DALYs) for both infants and children, and increase the overall economic income of this Chinese region. Similar results were reported by Hafeez et al. who investifgated the effect of soil Fe, Zn or Fe and Zn application, on the overall grain MN accumulation, grain quality and plant performance on Zn-efficient wheat variety (Zincol-16) and Zn-inefficient variety (Anaj-17). As expected, the plants grown on the soil treated with either of the three applications, exhibited significantly higher MN content and yield compared with the controls. Also, the Zn-efficient variety was able to accumulate higher Zn and Fe content, confirming that the combination of genetic and agronomic biofortification is an effective strategy to improve MN intake.

Even if agronomic biofortification has been widely proven to be an efficient biofortification approach, the dynamics of absorption and translocation of the applied MNs are complex and influenced by several factors including the chemical form of the MNs, application rate and its method of application. Ramkissoon et al. reported on the time-dependent changes in the absorption, transformation and distribution of Se applied to wheat leaves at two growth stages with or without the inclusion of urea. Results revealed that, independent of the treatment, grain Se content increased to a level adequate for biofortification even if the time of application and the presence of nitrogen (N) in the formulation significantly influenced the assimilation of Se. More studies focused on the optimization of the formulation of Se and other MN fertilizers, and on the best methods and timing of application will be fundamental to refine current agronomic biofortification practices and to optimize the micronutrient accumulation in grain.

When considering agronomic biofortification, the possible detrimental effect that this practice could have on the environment should also be considered. Microbial-assisted biofortification could be a solution to combine the short-term effects of the classic agronomic biofortification while reducing the negative impact that the increased fertilizer application could have on both soils and waters. Using an endophytic strain of *Bacillus altitudinis*, Sun et al. confirm the potential of this technique for wheat Fe biofortification. In this innovative study, the authors test two different inoculation methods and proved that, especially after spraying the microbe inoculum in the soil, the grain Fe accumulation significantly increased and that this *B. altitudinis* strain could efficiently colonize and translocate within wheat. Even if more studies will enable to understand the benefits and effectiveness of this method, microbial-assisted biofortification is an exciting emerging area of investigation that could significantly help create more nutrient-rich and sustainable grains.

Wheat biofortification however could not be enough if most of the micronutrients accumulated in the grains are lost during food processing. Before being consumed in fact, wheat grains are typically milled into refined flour and the bran, which is the part of the grain with the highest mineral content, is typically discarded as a by-product of the milling process. For this reason, Wang H. et al. investigated the effect of bran size and quantity on the quality of Chinese steamed bread, a staple food typically produced with refined flour. Results of this study revealed that addition of 5% wheat bran with medium particle size (D50 = 122.3 ± 7.1 μm) was able to significantly increase the Zn content present in the final product while maintaing an acceptable end-use quality. Nevertheless, independently from the utilization of refined or whole meal flour, regular adoption of biofortified wheat varieties is associated with an increased intake of zinc. As reported by Lowe et al. in fact, regular consumption of food products obtained from biofortified wheat, is associated with a 30% to 60% increased daily zinc intake. These results were obtained using an individually-randomized, double-blind, placebo-controlled cross over design and recruiting 50 households representative of a population with widespread zinc deficiency.

To conclude, development of nutrient-dense wheat has the potential to mitigate the micronutrient deficiency problems that affect a significant part of the world population, typically from developing or under-developed countries. Up to now, tremendous progresses have been made on wheat biofortification, but new knowledge and innovations must be generated to ensure a significant reduction in the incidence of hidden hunger. The studies presented in this issue well represent the latest discoveries and approaches proposed to increase the wheat micronutrient content, underlying the importance of addressing biofortification from different angles by combining both genetic and agronomic approaches.

Author contributions

All authors listed have made a substantial, direct, and intellectual contribution to the work and approved it for publication.

Conflict of interest

The authors declare that the research was conducted in the absence of any commercial or financial relationships that could be construed as a potential conflict of interest.

Publisher's note

All claims expressed in this article are solely those of the authors and do not necessarily represent those of their affiliated organizations, or those of the publisher, the editors and the reviewers. Any product that may be evaluated in this article, or claim that may be made by its manufacturer, is not guaranteed or endorsed by the publisher.

References

1. FAO, IFAD, UNICEF, WFP, WHO. In Brief to The State of Food Security and Nutrition in the World 2021. In: *Transforming food systems for food security, improved nutrition and affordable healthy diets for all*. Rome: FAO (2020).

frontiers in Nutrition

ORIGINAL RESEARCH
published: 09 June 2021
doi: 10.3389/fnut.2021.680391

QTL Mapping for Grain Zinc and Iron Concentrations in Bread Wheat

Yue Wang[1†], Xiaoting Xu[1†], Yuanfeng Hao[1], Yelun Zhang[2], Yuping Liu[2], Zongjun Pu[3], Yubing Tian[1], Dengan Xu[1], Xianchun Xia[1], Zhonghu He[1,4] and Yong Zhang[1*]*

[1] National Wheat Improvement Centre, Institute of Crop Sciences, Chinese Academy of Agricultural Sciences, Beijing, China, [2] Hebei Laboratory of Crop Genetics and Breeding, Institute of Cereal and Oil Crops, Hebei Academy of Agricultural and Forestry Sciences, Shijiazhuang, China, [3] Institute of Crop Sciences, Sichuan Academy of Agricultural Sciences, Chengdu, China, [4] International Maize and Wheat Improvement Center (CIMMYT) China Office, Chinese Academy of Agricultural Sciences, Beijing, China

Deficiency of micronutrient elements, such as zinc (Zn) and iron (Fe), is called "hidden hunger," and bio-fortification is the most effective way to overcome the problem. In this study, a high-density Affymetrix 50K single-nucleotide polymorphism (SNP) array was used to map quantitative trait loci (QTL) for grain Zn (GZn) and grain Fe (GFe) concentrations in 254 recombinant inbred lines (RILs) from a cross Jingdong 8/Bainong AK58 in nine environments. There was a wide range of variation in GZn and GFe concentrations among the RILs, with the largest effect contributed by the line × environment interaction, followed by line and environmental effects. The broad sense heritabilities of GZn and GFe were 0.36 ± 0.03 and 0.39 ± 0.03, respectively. Seven QTL for GZn on chromosomes 1DS, 2AS, 3BS, 4DS, 6AS, 6DL, and 7BL accounted for 2.2–25.1% of the phenotypic variances, and four QTL for GFe on chromosomes 3BL, 4DS, 6AS, and 7BL explained 2.3–30.4% of the phenotypic variances. QTL on chromosomes 4DS, 6AS, and 7BL might have pleiotropic effects on both GZn and GFe that were validated on a germplasm panel. Closely linked SNP markers were converted to high-throughput KASP markers, providing valuable tools for selection of improved Zn and Fe bio-fortification in breeding.

Keywords: ***Triticum aestivum***, **mineral biofortification, quantitative trait locus, 50K SNP array, KASP marker**

OPEN ACCESS

Edited by:
Velu Govindan, International Maize and Wheat Improvement Center, Mexico

Reviewed by:
Peipei Zhang, Agricultural University of Hebei, China
Raja Khanal, Agriculture and Agri-Food Canada, Canada

***Correspondence:**
Zhonghu He
hezhonghu02@caas.cn
Yong Zhang
zhangyong05@caas.cn

[†] These authors have contributed equally to this work

Specialty section:
This article was submitted to Nutrition and Food Science Technology, a section of the journal Frontiers in Nutrition

Received: *14 March 2021*
Accepted: *20 April 2021*
Published: *09 June 2021*

Citation:
Wang Y, Xu X, Hao Y, Zhang Y, Liu Y, Pu Z, Tian Y, Xu D, Xia X, He Z and Zhang Y (2021) QTL Mapping for Grain Zinc and Iron Concentrations in Bread Wheat. Front. Nutr. 8:680391. doi: 10.3389/fnut.2021.680391

INTRODUCTION

Wheat provides the starch, protein, and mineral nutrition needs for 35–40% of the world population (1). Mineral nutrition is crucial for a healthy diet. Over 17% of people suffer from malnutrition worldwide due to lack of mineral nutrition and more than 100,000 children under the age of five die from zinc (Zn) deficiency annually (2–4). The CIMMYT Harvest-Plus program initiated in the early 21st century aimed to address the "hidden hunger" issue by increasing micronutrient concentrations in staple food grains by plant breeding (5). Zn and Fe deficiency were identified as major causes of malnutrition, especially in underdeveloped regions where cereal grains make up most of the food (6).

Zn is a crucial cofactor in many enzymes and regulatory proteins, such as carbonic anhydrase, alkaline phosphatase, and DNA polymerase enzyme synthesis (7). Zn deficiency, first reported in 1961, affects the immune system, taste perception, site, and sexual function (4). Fe deficiency in humans most commonly leads to nutritional anemia in women and children (8). Therefore, it is very important to improve the nutritional quality of wheat by enhancing the Zn (GZn) and Fe (GFe) concentrations in grain (9, 10).

Bio-fortification in wheat breeding demands identification of genetic resources with high GZn and GFe (9). Wide ranges in variation in GZn and GFe have been reported in bread wheat (11–13) and its cultivated and wild relatives (12, 14, 15). Quantitative trait locus (QTL) mapping was used to identify genetic loci affecting GZn and GFe in biparental mapping populations, including recombinant inbred lines (RILs) (16–18). Genome-wide association studies (GWAS) with high-density single-nucleotide polymorphism (SNP) arrays were also used; for example, Alomari et al. (19) performed a GWAS for GZn concentration in 369 European wheats using the 90K and 35K SNP arrays and detected 40 marker–trait associations on chromosomes 2A, 3A, 3B, 4A, 4D, 5A, 5B, 5D, 6D, 7A, 7B, and 7D and 10 candidate genes on chromosomes 3B and 5A. With wide application of molecular markers, such as SSR, DArT, and SNPs, increasing numbers of QTLs for GZn and GFe were detected, including 35 and 32 QTL for GZn and GFe in the A genome, 37 and 30 in the B genome, and 15 and 12 in the D genome, respectively (**Supplementary Table 1**). The GZn QTL in homoeologous groups 1 to 7 were 9, 10, 13, 11, 13, 12, and 19, respectively, whereas the corresponding numbers of GFe QTL were 6, 17, 10, 8, 15, 7, and 11. QTL pleiotropic for GZn and GFe were identified in homoeologous group 3, 4, 5, and 7 chromosomes.

Cultivar Jingdong 8, with high yield and resistance to stripe rust, leaf rust, and powdery mildew, was released in the early 1990s in the China Northern Winter Wheat Region. It was used widely as a parent in breeding and was verified to have high GZn and GFe levels across environments (13). Bainong AK58, a high yielding cultivar in the Southern Yellow-Huai Valley Winter Wheat Region, has wide adaptability and good resistance to stripe rust, powdery mildew, and lodging, but has lower GZn and GFe. The main goals of the present study were to (1) identify QTL for GZn and GFe in the Jingdong 8/Bainong AK58 RIL population using inclusive composite interval mapping, and (2) develop and validate breeder-friendly markers for marker-assisted selection (MAS) for Zn and Fe biofortification in wheat breeding programs.

MATERIALS AND METHODS

Plant Materials

Two hundred fifty-four F_6 RILs developed from Jingdong 8/Bainong AK58 cross were used for QTL mapping of GZn and GFe concentrations. A germplasm panel, including 145 cultivars/lines with a wide range of variation in GZn and GFe from the Chinese wheat germplasm bank (13), were used for validation of QTL for GZn and GFe identified in the RIL population.

Field Trials and Phenotyping

The field trials were conducted at the wheat breeding station of the Institute of Crop Sciences (ICS, CAAS) located at Gaoyi (37°33′N, 114°26′E) and Shijiazhuang (37°27′N, 113°30′E) in Hebei province and Beijing (39°56′N, 116°20′E) during 2016 to 2019 cropping seasons. The parents and RILs were planted in randomized complete blocks with two replications in each environment. Each plot comprised a 1-m row with an inter-row spacing of 20 cm, and a parental check was sown every 30 plots. Standard agronomic practices were applied at each location, along with a soil application of 25 kg/ha $ZnSO_4{\cdot}7H_2O$ in all fields except Beijing.

Grain samples were hand-harvested and cleaned to avoid potential contamination of mineral elements. Micronutrient analysis of grain samples collected from the 2016–2017 cropping season was performed at the Institute of Quality Standards and Testing Technology for Agro-products of CAAS using inductively coupled plasma atomic emission spectrometry (ICP-AES, OPTIMA 3300 DV) after samples were digested in a microwave system with HNO_3-H_2O_2 solution (20). For grain samples from the 2017–2018 and 2018–2019 cropping seasons and the germplasm panel, a "bench-top," nondestructive, energy-dispersive X-ray fluorescence spectrometry (EDXRF) instrument (model X-Supreme 8000, Oxford Instruments plc, Chengdu) was used to measure GZn and GFe, following the standard method for high-throughput screening of micronutrients in whole wheat grain (21).

Statistical Analysis

Analysis of variance (ANOVA) was performed by PROC MIXED with method type3 and all effects were treated as fixed in SAS 9.4 software (SAS Institute, Cary, NC). Variance and covariance components for genotype and genotype by environment interaction effects were estimated using PROC MIXED, assuming all effects as random. A similar model was also performed by PROC MIXED with genotype effect as fixed, while environment, replication nested in environment, and interactions involving environment as random, to estimate best linear unbiased estimate (BLUE). Broad-sense heritabilities ($H_b{}^2$) on the basis of BLUE value were estimated using the following equation and standard errors were calculated following Holland et al. (22):

$$H_b^2 = \frac{\sigma_{\mathbf{g}}^{\mathbf{2}}}{\left(\sigma_{\mathbf{g}}^{\mathbf{2}} + \frac{\sigma_{\mathbf{ge}}^{\mathbf{2}}}{\mathbf{e}} + \frac{\sigma_{\varepsilon}^{\mathbf{2}}}{\mathbf{re}}\right)}$$

where σ_g^2 represents the variance of genotypes, σ_{ge}^2 and σ_ε^2represent the variances of genotype × environment interaction and error, and e and r represent environments and number of replicates per environment, respectively. Phenotypic and genotypic correlations and their standard errors were estimated after Becker (23). Student's t test was performed by PROC TTEST.

SNP Genotyping and QTL Analysis

Genomic DNA extracted from fresh seedling leaves of RILs and parents by CTAB method (24) were used for genotyping by the wheat 50K SNP Array. The wheat 50K SNP Array was developed in collaboration by CAAS and Capital-Bio, Beijing, China (https://www.capitalbiotech.com/). Linkage analysis was performed with JoinMap v4.0 using the regression mapping algorithm (25). QTL analysis was performed by inclusive composite interval mapping with the ICIM-ADD function using

QTL IciMapping v4.1 (http://www.isbreeding.net). Phenotypic values of RILs averaged from two replicates in each environment and BLUE value across nine environments were used for analyses. QTL detection was done using a logarithm of odds (LOD) threshold of 2.5. Pleiotropic QTL were analyzed using the module JZmapqtl of multi-trait composite interval mapping (MCIM) in Windows QTL Cartographer v2.5 (26). QTL pyramids were plotted using ggplot2 in R (27). Physical maps for the positional comparisons of GZn and GFe QTL with previous reports were exhibited using MapChart v2.3 (28).

Conversion of SNPs to KASP Markers

Kompetitive Allele Specific PCR (KASP) markers were developed from SNPs tightly linked with the targeted QTL, each including two competitive allele-specific forward primers and one common reverse primer. Each forward primer incorporated an additional tail sequence that corresponds to only one of the two universal fluorescence resonance energy transfers. Primers were designed from information in the PolyMarker website (http://polymaker.tgac.ac.uk/). PCR procedures and conditions followed Chandra et al. (29). Gel-free fluorescence signal scanning and allele separation were conducted by microplate reader (Multiscan Spectrum BioTek, Synegy/H1) with Klustercaller 2.24.0.11 software (LGC, Hoddesdon, UK) (30).

RESULTS

Phenotypic Evaluation

ANOVA showed that GZn and GFe were significantly influenced by lines, environments, and line by environment interaction effects, with line by environment interaction effects contributing the highest variation, followed by line and environment effects (**Table 1**). The broad-sense heritabilities of GZn and GFe were 0.36 ± 0.03 and 0.39 ± 0.03, respectively. Jingdong 8 accumulated significantly higher GZn and GFe than Bainong AK58. Wide-ranging continuous variation among the RILs suggests polygenic inheritance (**Table 2**, **Figure 1**). Significant and positive correlations of GZn ($r = 0.25$–0.67, $P < 0.01$) and GFe ($r = 0.26$–0.70, $P < 0.01$) were observed across the nine environments (**Table 3**). Additionally, positive phenotypic and genotypic correlations between GZn and GFe ($r = 0.78 \pm 0.01$ and 0.81 ± 0.03, $P < 0.001$) (**Figure 2**), indicated that GZn and GFe were, to some degree, simultaneously accumulated.

Linkage Map Construction

Among 54,680 SNP markers in the 50K SNP array, 20,060 were polymorphic after removal of markers that were monomorphic, absent in more than 20% of assays, and minor allele frequency was <30%. A high-density linkage map spanning 3423 cM and including all 21 chromosomes was constructed using 3328 representative SNP markers of each bin. The average chromosome length was 163 cM, ranging from 116.72 cM (1B) to 237.40 cM (5A) (**Supplementary Table 2**).

TABLE 1 | Analysis of variance of GZn and GFe in 254 RILs derived from the cross Jingdong 8/Bainong AK58 grown in nine environments.

Source of variation	DF	Sum square	
		Zn	Fe
Line	253	39,148**	50,429**
Environment (Env)	8	67,264**	24,847**
Line×Env	2,024	74,960**	91,715**
Rep (Env)	9	3,385**	1,658**
Error	2021	46,076	49,910
Heritability		0.36 ± 0.03	0.39 ± 0.03

***Significant at $P < 0.01$.*

QTL Mapping of GZn and GFe using ICIM and MCIM

Seven QTL for GZn were mapped on chromosomes 1DS, 2AS, 3BS, 4DS, 6AS, 6DL, and 7BL, explaining 2.2–25.1% of the phenotypic variances (**Table 4**, **Supplementary Table 3**, and **Figure 3**), with five favorable alleles coming from Jingdong 8, and with the other two, i.e., *QZn.caas-1DS* and *QZn.caas-3BS*, coming from Bainong AK58. Four QTL for GFe were detected on chromosomes 3BL, 4DS, 6AS, and 7BL, explaining 2.3–30.4% of the phenotypic variances (**Table 4**, **Supplemenatry Table 3**, and **Figure 3**), with all superior alleles coming from Jingdong 8. Among these QTL, three were identified for both GZn and GFe at the same or overlapping location on chromosomes 4DS, 6AS, and 7BL.

Three chromosomal intervals were detected using MCIM including 4DS, 6AS, and 7BL, corresponding to co-localized QTL for GZn and GFe by ICIM-ADD (**Table 5**). Two intervals on chromosomes 4DS and 6AS were detected in most environments for GZn and GFe, while the one on chromosome 7BL was found in most environments for GZn but only one environment for GFe.

QTL Pyramids and Validation

It indicated that superior alleles of pleiotropic QTL on 4DS, 6AS, and 7BL were all from Jingdong 8. Accumulation effect of the three co-localization QTL for GZn and GFe was calculated based on the closely linked markers. The average concentration of GZn increased from 37.79 to 44.43 mg/kg and that of GFe increased from 41.02 to 50.37 mg/kg, with lines containing zero to three favorable alleles (**Supplementary Figure 1**).

Flanking SNPs closely linked to the QTL on chromosomes 4DS and 7BL and a SNP near QTL region of 6AS were converted to KASP markers and validated in the germplasm panel (**Tables 6**, **7**). Cultivars with the same superior allele as Jingdong 8 had significantly higher GZn and GFe than those with the inferior allele from Bainong AK58 for all QTL, except for *QFe.caas-6AS*. The difference between the superior and inferior allele of the QTL on chromosomes 4DS, 6AS, and 7BL was 1.7, 2.8, and 3.5 mg/kg for GZn and 1.4, 1.0, and 4.7 mg/kg for GFe, respectively (**Table 7**).

TABLE 2 | Mean and range of GZn and GFe (mg/kg) in the Jingdong 8/Bainong AK58 RIL population among nine environments.

Trait	Environment	Parents		RILs	
		Jingdong 8	Bainong AK58	Range	Mean ± SD
Zn (mg/kg)	E1	42.1	35.1	25.4–52.6	38.9 ± 4.6
	E2	41.5	34.1	25.2–56.6	39.1 ± 5.6
	E3	53.4	46.4	29.5–60.7	43.5 ± 5.7
	E4	41.3	34.5	28.7–52.6	38.0 ± 4.1
	E5	52.1	44.1	33.5–62.2	46.4 ± 4.7
	E6	46.2	36.9	28.9–54.3	41.3 ± 5.3
	E7	40.7	33.7	25.7–49.0	34.6 ± 3.9
	E8	55.0	42.3	34.6–62.5	47.6 ± 6.0
	E9	48.6	34.7	27.0–57.9	40.0 ± 5.8
Fe (mg/kg)	E1	51.0	43.0	32.8–62.6	47.3 ± 5.2
	E2	53.5	40.9	34.5–68.9	48.0 ± 6.5
	E3	53.2	42.8	34.2–64.0	48.5 ± 6.3
	E4	46.6	40.2	35.3–52.3	42.2 ± 3.2
	E5	49.8	42.3	37.0–59.5	44.9 ± 3.8
	E6	49.2	34.5	31.1–65.1	42.7 ± 5.5
	E7	54.2	37.8	32.0–67.2	45.0 ± 6.7
	E8	56.6	39.7	33.9–69.2	49.2 ± 6.2
	E9	55.0	38.0	28.0–63.9	47.1 ± 6.4

E1–E9, Shijiazhuang 2016–2017, Gaoyi 2016–2017, Beijing 2016–2017, Shijiazhuang 2017–2018, Gaoyi 2017–2018, Beijing 2017–2018, Shijiazhuang 2018–2019, Gaoyi 2018–2019, and Beijing 2018–2019.

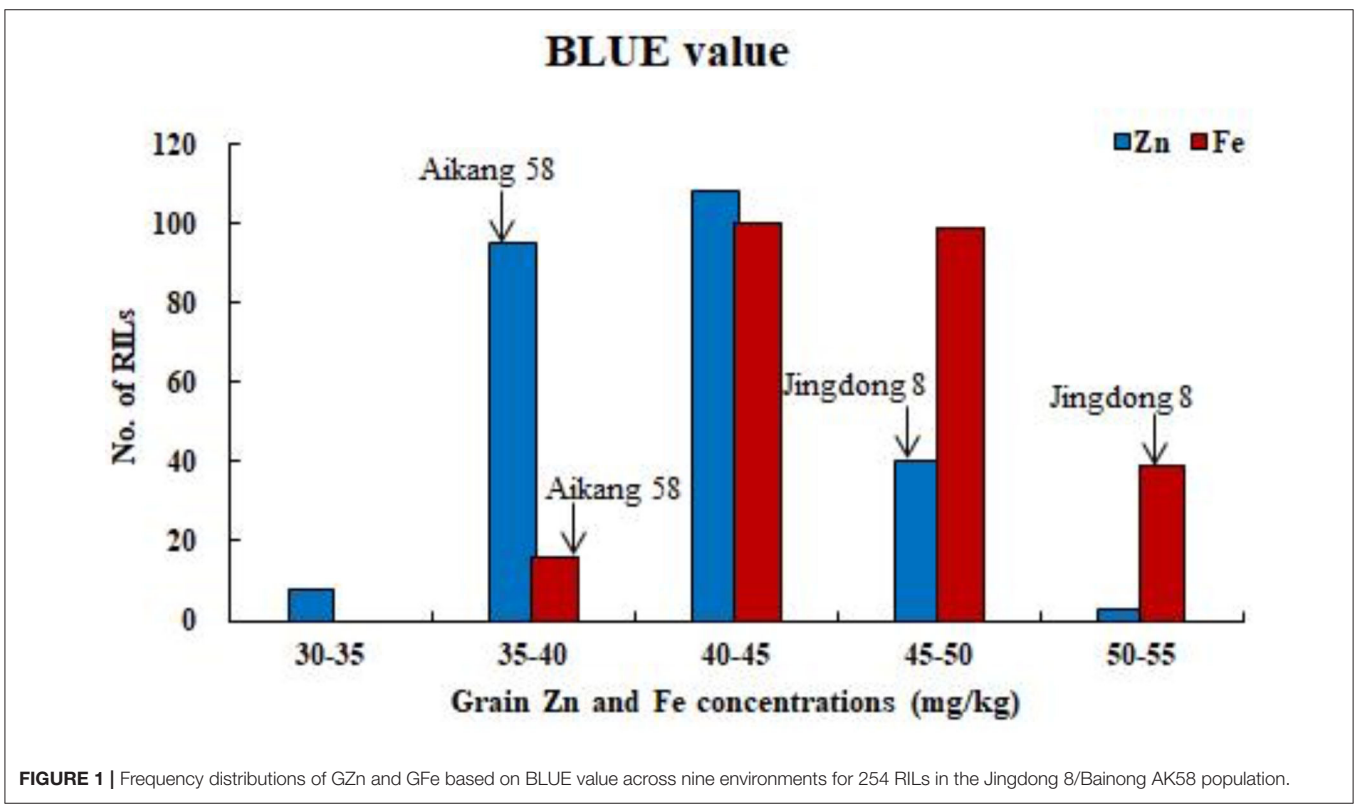

FIGURE 1 | Frequency distributions of GZn and GFe based on BLUE value across nine environments for 254 RILs in the Jingdong 8/Bainong AK58 population.

TABLE 3 | Pearson correlation coefficients of GZn and GFe in the Jingdong 8/Bainong AK58 RIL population among nine environments.

Environment	E1	E2	E3	E4	E5	E6	E7	E8	E9
E1		0.45***	0.32***	0.40***	0.37***	0.48***	0.36***	0.47***	0.48***
E2	0.70***		0.25***	0.41***	0.46***	0.52***	0.27***	0.43***	0.39***
E3	0.52***	0.52***		0.40***	0.33***	0.40***	0.34***	0.34***	0.36***
E4	0.44***	0.47***	0.47***		0.49***	0.57***	0.40***	0.52***	0.51***
E5	0.40***	0.46***	0.42***	0.40***		0.50***	0.31***	0.58***	0.46***
E6	0.51***	0.51***	0.44***	0.53***	0.51***		0.50***	0.67***	0.60***
E7	0.53***	0.54***	0.46***	0.55***	0.51***	0.63***		0.47***	0.43***
E8	0.41***	0.47***	0.45***	0.51***	0.48***	0.53***	0.62***		0.55***
E9	0.26***	0.28***	0.31***	0.38***	0.32***	0.38***	0.41***	0.39***	

****Significant at $P < 0.001$.*

Upper right triangle: Correlation coefficients between environments for GZn.

Lower left triangle: Correlation coefficients between environments for GFe.

E1–E9, Shijiazhuang 2016–2017, Gaoyi 2016–2017, Beijing 2016–2017, Shijiazhuang 2017–2018, Gaoyi 2017–2018, Beijing 2017–2018, Shijiazhuang 2018–2019, Gaoyi 2018–2019, and Beijing 2018–2019.

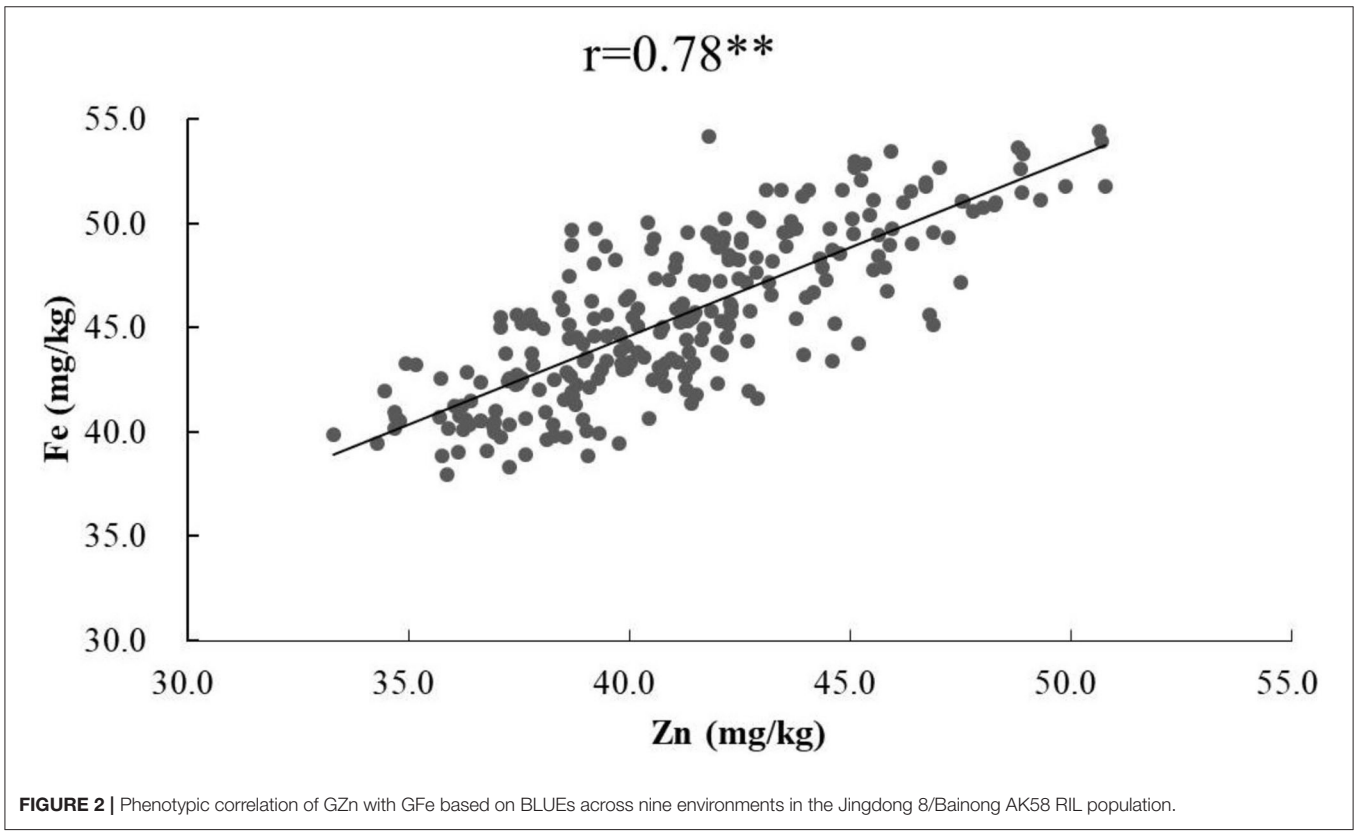

FIGURE 2 | Phenotypic correlation of GZn with GFe based on BLUEs across nine environments in the Jingdong 8/Bainong AK58 RIL population.

DISCUSSION

Comparisons With Previous Reports

In this study, QTL for GZn and GFe were mapped on chromosomes 1D, 2A, 3B, 4D, 6A, 6D, and 7B, and on chromosomes 3B, 4D, 6A, and 7B, respectively. Previously identified QTL are summarized in **Supplementary Table 1** and partly shown in **Figure 3**. In addition to consensus maps, the IWGSC RefSeq v1.0 Chinese Spring reference sequence (31) was used for comparisons of QTL identified in different studies.

QZn.caas-1DS

QZn.caas-1DS, flanked by SNP markers *AX-95235028* and *AX-94939596* at 32.5–38.8 Mb, was detected in three environments. Velu et al. (18) identified *QGZn.ada-1D* linked with a DArT marker *wPt-6979* at 303.4 Mb. Gorafi

TABLE 4 | QTL for GZn and GFe identified by inclusive composite interval mapping in the Jingdong 8/Bainong AK58 RIL population.

Trait	QTL	Environment	Physical interval[a]	Marker interval	LOD[b]	PVE(%)[c]	Add[d]
Zn	*QZn.caas-1DS*	E3	32.5–38.8	*AX-95235028–AX-94939596*	3.0	3.5	1.1
		E6			2.7	3.4	0.9
		E8			6.0	6.0	1.5
	QZn.caas-2AS	E5	46.1–48.4	*AX-94592263–AX-108732889*	4.1	2.2	−1.1
		E8			9.2	9.3	−1.8
	QZn.caas-3BS	E2	42.5–59.1	*AX-110975262–AX-109911679*	3.7	5.7	1.3
		E4			4.8	5.5	1.0
	QZn.caas-4DS	E1	16.0–19.5	*AX-89593703–AX-89445201*	10.8	12.1	−1.8
		E2			4.6	7.2	−1.5
		E4			9.0	10.7	−1.4
		E5			4.4	2.4	−1.1
		E6			17.1	25.1	−2.5
		E7			3.5	4.9	−0.9
		E8			13.1	14.3	−2.3
		E9			8.5	11.2	−1.9
	QZn.caas-6AS	E4	77.1–100.3	*AX-108951317–AX-110968221*	4.4	5.2	−1.0
		E6			3.7	4.8	−1.1
	QZn.caas-6DL	E3	454.1–459.4	*AX-109058428–AX-111841126*	7.3	8.5	−1.7
		E4			3.0	3.5	−0.8
	QZn.caas-7BL	E1	721.8–725.4	*AX-95658138–AX-89745787*	4.2	4.3	−1.0
		E3			5.4	6.4	−1.5
		E6			5.4	6.9	−1.3
		E8			6.3	6.3	−1.5
		E9			5.0	6.2	−1.4
Fe	*QFe.caas-3BL*	E5	764.7–822.9	*AX-111016352–AX-94835626*	3.1	5.8	−0.9
		E6			2.8	2.9	−0.9
	QFe.caas-4DS	E1	16.0–17.1	*AX-89593703–AX-89398511*	16.8	20.4	−2.5
		E2			18.7	27.0	−3.4
		E3			12.3	19.4	−2.7
		E4			24.1	24.3	−1.9
		E5			6.2	9.0	−1.1
		E6			20.6	25.6	−2.7
		E7			20.8	30.4	−3.4
		E8			11.2	5.5	−2.3
		E9			4.6	2.3	−1.7
	QFe.caas-6AS	E1	77.1–106.9	*AX-108951317–AX-109304443*	4.7	5.1	−1.2
		E6			7.0	7.5	−1.5
	QFe.caas-7BL	E1	718.5–725.4	*AX-95631535–AX-89745787*	2.8	2.9	−0.9
		E6			6.2	6.9	−1.4

[a] *Physical interval; Mb, according to IWGSC RefSeq v1.0 (31), http://www.wheatgenome.org/.*

[b] *LOD; likelihood of odds ratio for genetic effects.*

[c] *PVE; percentage of phenotypic variance explained by individual QTL.*

[d] *Add; Additive effect of QTL; negative values indicate that the superior allele came from Jingdong 8, whereas positive values indicate that the superior allele was from Bainong AK58. E1–E9, Shijiazhuang 2016–2017, Gaoyi 2016–2017, Beijing 2016–2017, Shijiazhuang 2017–2018, Gaoyi 2017–2018, Beijing 2017–2018, Shijiazhuang 2018–2019, Gaoyi 2018–2019, and Beijing 2018–2019.*

et al. (32) detected a QTL linked with SSR marker *Xcfd63* at physical position 440 Mb. The present QTL appears to be new.

QZn.caas-2AS

QZn.caas-2AS, flanked by *AX-94592263* and *AX-108732889* at physical positions of 46.1 and 48.4 Mb, was identified in two

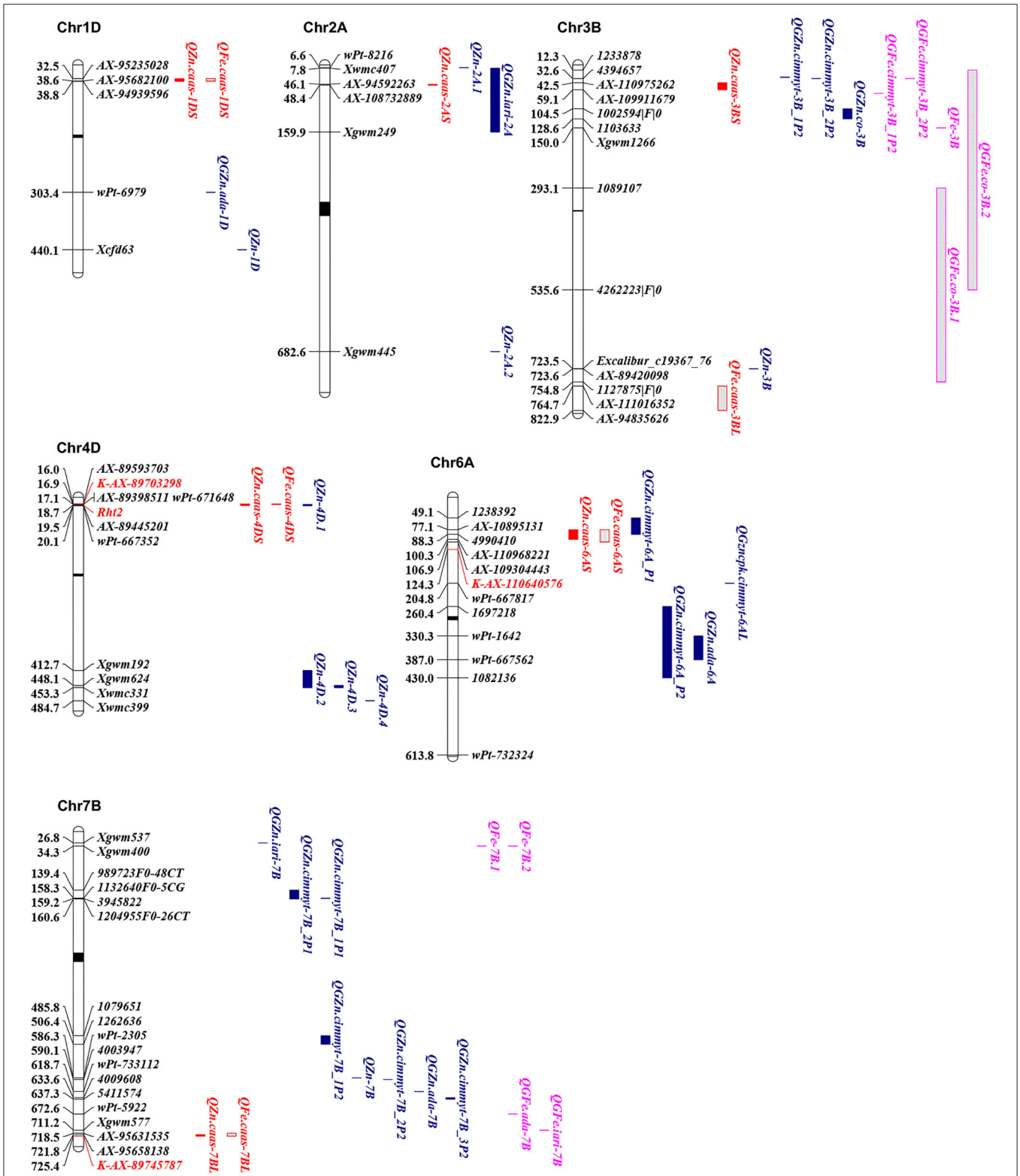

FIGURE 3 | Physical maps for the positional comparisons of GZn and GFe QTL reported on chromosomes 1DS, 2AS, 3BL, 4DS, 6AS, and 7BL with those identified in the present study. QTL linked markers are shown on the right, physical positions are shown on the left, and centromere is shown in the middle (black bar). KASP markers developed in the present study were shown in red. QTL for GZn and GFe in the present study were in red; QTL for GZn in previous studies were in blue; QTL for GFe in previous studies were in purple.

TABLE 5 | Chromosomal intervals for GZn and GFe identified by multi-trait composite interval mapping (MCIM).

Chromosomes	Flanking markers	Physical position (Mb)	Traits (Environment)
4DS	*AX-89593703–AX-89398511*	16.0–17.1	GZn (E1, E2, E4, E6, E7, E8, E9, BLUE value)
			GFe (E1, E2, E4, E5, E6, E7, E8, E9, BLUE value)
6AS	*AX-108951317–AX-110968221*	77.1–100.3	GZn (E1, E2, E4, E6, E7, BLUE value)
			GFe (E1, E2, E4, E6, BLUE value)
7BL	*AX-95658138–AX-89745787*	721.8–725.4	GZn (E1, E3, E6, E7, E8, E9, BLUE value)
			GFe (E6)

TABLE 6 | Kompetitive allele specific PCR (KASP) markers converted from single-nucleotide polymorphisms (SNPs) tightly linked to identified QTL on three chromosomes.

Chromosome	SNP name	Physical position (Mb)	KASP primer	Primer sequence
4DS	*AX-89703298*	16.9	*K-AX-89703298*	5′-GAAGGTGACCAAGTTCATGCTCTAACCATTGGATAGGGCGAC-3′
				5′-GAAGGTCGGAGTCAACGGATTCTAACCATTGGATAGGGCGAA-3′
				5′-CCCAGCTTCAGCCCATGA-3′
6AS	*AX-110640576*	124.3	*K-AX-110640576*	5′-GAAGGTGACCAAGTTCATGCTCACAGATGTTCTCCACTCTCTG-3′
				5′-GAAGGTCGGAGTCAACGGATTCACAGATGTTCTCCACTCTCTC-3′
				5′-CCCTCCAAGGTCCATGGGT−3′
7BL	*AX-89745787*	725.4	*K-AX-89745787*	5′-GAAGGTGACCAAGTTCATGCTGGAGGACATTGTGCAACCG-3′
				5′-GAAGGTCGGAGTCAACGGATTGGAGGACATTGTGCAACCT-3′
				5′-AGGATTGGTTCTGCAATCCA-3′

TABLE 7 | Mean values of GZn and GFe for genotype classes in the germplasm panel.

Trait	QTL	Marker	Genotype	Number	Mean (mg/kg)	*T* value
GZn	*QZn.caas-4DS*	*K-AX-89703298*	CC	79	32.4	−2.28*
			AA	66	30.7	
	QZn.caas-6AS	*K-AX-110640576*	GG	19	34.0	−2.54*
			CC	126	31.2	
	QZn.caas-7BL	*K-AX-89745787*	GG	11	34.7	−2.41*
			TT	134	31.4	
GFe	*QFe.caas-4DS*	*K-AX-89703298*	CC	79	39.4	−2.58*
			AA	66	38.0	
	QFe.caas-6AS	*K-AX-110640576*	GG	19	39.6	−1.18
			CC	126	38.6	
	QFe.caas-7BL	*K-AX-89745787*	GG	11	43.1	−2.55*
			TT	134	38.4	

**Significant at $P < 0.05$.*

environments. Peleg et al. (33) identified *QZn-2A.1* and *QZn-2A.2* linked with *wPt-8216* and *Xgwm445* at 6.6 and 682.6 Mb, respectively. Krishnappa et al. (34) mapped *QGZn.iari-2A* flanking by *Xwmc407* and *Xgwm249* at physical position 28.2 and 159.9 Mb, respectively. *QZn.caas-2AS* detected in the present study was located within the region of *QGZn.iari-2A*; therefore, these two QTL may be the same.

QZn.caas-3BS

QZn.caas-3BS, flanked by *AX-110975262* and *AX-109911679* at physical positions of 42.5 and 59.1 Mb, was detected in two environments. Crespo-Herrera et al. (17) identified two QTL for GZn on this chromosome. *QGZn.cimmyt-3B_2P2* was at the physical position 32.6 Mb linked with DArT markers *4394657*, and *QGZn.cimmyt-3B_1P2* flanked by 3533713 and 1007339 is much more near the distal end of 3BS than *QGZn.cimmyt-3B_2P2* on the basis of the genetic map, although both markers were not on chromosome 3B with the result of blast. Furthermore, Liu et al. (35) mapped *QGZn.co-3B* flanked by DArT markers *1002594|F|0* and *1103633* at physical positions of 104.5 and 128.6 Mb, respectively. Alomari et al. (19) identified a locus for GZn on chromosome 3BL, linked with *AX-89420098* at 723.5 Mb. Thus, the previous QTL were around 10 Mb from *QZn.caas-3BS*, indicating that *QZn.caas-3BS* is likely a new QTL.

QFe.caas-3BL

QFe.caas-3BL, flanked by *AX-111016352* and *AX-94835626* at physical positions of 764.7 and 822.9 Mb, was detected in

two environments. Crespo-Herrera et al. (17) identified two QTL for GFe that were at the similar position as QTL for GZn as mentioned previously, both of which were on the short arm of chromosome 3B. Peleg et al. (33) mapped a QTL on chromosome 3B, closely linked with *Xgwm1266* at physical position 150 Mb. Liu et al. (35) identified *QGFe.co-3B.1* and *QGFe.co-3B.2* flanked by DArT markers *1089107* and *1127875|F|0*, *1233878-4262223|F|0* at physical positions 37.2–754.8 and 12.3–536.6 Mb, respectively. These five QTL were at least 10 Mb distant from *QFe.caas-3BL*. Therefore, *QFe.caas-3BL* is likely a new QTL for GFe.

QZn.caas-4DS and *QFe.caas-4DS*

QZn.caas-4DS and *QFe.caas-4DS*, flanked by *AX-89593703* and *AX-89445201* at physical positions of 16.0 and 19.5 Mb were detected in eight and nine environments, respectively. Pu et al. (36) identified a QTL for GZn at the same position, flanked by *wPt-671648* and *wPt-667352* located between 17.1 and 20.1 Mb on chromosome 4D, with reduced height gene *Rht2* (*Rht-D1b*) located in this region. Using a limited number of isogenic lines, Graham et al. (37) found that lower GZn and GFe in wheat was associated with reduced height genes. Velu et al. (38) verified this association using nine bread wheat (*Triticum aestivum*) and six durum (*T. turgidum*) isogenic line pairs differing at the *Rht1* (*Rht-B1*) locus and one bread wheat pair differing at the *Rht2* locus, indicating that the presence of reduced height genes decreased GZn by 1.9 to 10.0 ppm and GFe by 1.0 to 14.4 ppm. In this study, Bainong AK58 carried *Rht2* (*Rht-D1b*), while Jingdong 8 had *rht2* (*Rht-D1a*) (39). A gene-specific KASP marker *K-AX-86170701* was identified for *Rht2* (40), and lines with allele from Bainong AK58 had significantly lower GZn and GFe than that with allele from Jingdong 8 (**Supplementary Figure 2**). Therefore, it was possible that the lower concentrations of Zn and Fe in Bainong AK58 was associated with the *Rht2* allele.

QZn.caas-6AS and *QFe.caas-6AS*

QZn.caas-6AS and *QFe.caas-6AS*, flanked by *AX-108951317* and *AX-110968221* at physical positions of 77.1 and 106.9 Mb, were detected in four environments. No QTL for GFe was detected on chromosome 6AS previously, while two QTL for GZn were reported. Crespo-Herrera et al. (17) identified *QGZn.cimmyt-6A_P1*, linked with *1238392* and *4990410* at physical positions of 49.1 and 88.2 Mb. Hao et al. (16) mapped *QGZn.cimmyt-6AL* at 204.8 Mb with nearest marker *wPt-667817*. The present QTL was somewhat near the *QGZn.cimmyt-6A_P1*, indicating that they might be the same.

QZn.caas-6DL

QZn.caas-6DL, flanked by *AX-109058428* and *AX-11184112* at physical positions of 454.1 and 459.4 Mb, was detected in two environments. It is likely a new one since no previous QTL for GZn was mapped on this chromosome.

QZn.caas-7BL and *QFe.caas-7BL*

Markers *AX-95631535* and *AX-89745787* at positions 718.5 and 725.4 Mb flanking *QZn.caas-7BL* and *QFe.caas-7BL* are distally located on chromosome 7BL. Several QTL were previously identified on this chromosome. Krishnappa et al. (34) mapped *QGZn.iari-7B* with closest marker *Xgwm537* at 26.8 Mb. Peleg et al. (33) detected *QZn-7B* linked with *wPt-2305* at 586.3 Mb. Crespo-Herrera et al. (17) identified five QTL, including *QGZn.cimmyt-7B_2P1*, *QGZn.cimmyt-7B_1P1*, *QGZn.cimmyt-7B_1P2*, *QGZn.cimmyt-7B_2P2*, and *QGZn.cimmyt-7B_3P2* at physical positions of 139.4–160.6, 158.3–159.2, 485.8–506.4, 590.1, and 633.6–637.3 Mb, respectively. Velu et al. (18) reported *QGZn.ada-7B*, which was located at around 618.7 Mb with closely linked marker *wPt-733112*. All these eight QTL were well proximal (>80 Mb) from the QTL in this study, indicating that *QZn.caas-7BL* was reported for the first time. In addition, four QTL for GFe were mapped on chromosome 7B, among which two of them were at the same physical position of 34.3 Mb (*QFe-7B.1* and *QFe-7B.2*), and the other two were at 672.6 Mb (*QGFe.ada-7B*) and 711.2 Mb (*QGFe.iari-7B*), respectively (18, 28, 29, 41). *QGFe.iari-7B* and *QFe.caas-7BL* might be the same, since their distance is <10 Mb.

Pleiotropic Effects of QTL

The co-localization QTL for GZn and GFe on chromosomes 4DS, 6AS, and 7BL might be pleiotropic QTL based on the same or overlapping region detected using MCIM, in agreement with the significant positive phenotypic and genotypic correlations ($r = 0.78 \pm 0.01$ and 0.81 ± 0.03, $P < 0.01$) between GZn and GFe. Gorafi et al. (32) identified a significant and positive phenotypic correlation between GZn and GFe ($r = 0.78$) and a pleiotropic QTL on chromosome 5D; significant and positive correlations between GZn and GFe were also found in other studies (11, 42). It has been reported that some transporters, chelators, and genes regulated GZn and GFe simultaneously in a high frequency (10, 43). These findings indicated that Zn and Fe could be improved simultaneously in breeding programs targeting mineral biofortification.

Potential Implication in Wheat Breeding

MAS has been applied in crop breeding for more than two decades. Therefore, it would be effective for traits that were controlled by low numbers of major QTL (37). The phenotypic analysis on GZn and GFe was time-consuming and laborious, indicating that identification of molecular markers linked to GZn and GFe would be of interest for improvement of nutritional quality in wheat. In the present study, pleiotropic QTL on chromosomes 4D, 6A, and 7B were detected in multiple environments. SNP markers linked to some of these QTL were converted to KASP markers, and the QTL were verified in a germplasm panel, indicating potential application in wheat breeding programs.

DATA AVAILABILITY STATEMENT

The original contributions presented in the study are included in the article and/or **Supplementary Material**, further inquiries can be directed to the corresponding authors.

AUTHOR CONTRIBUTIONS

YoZ and ZH conceived the idea. YW and XXu conducted the experiments, analyzed the data, and prepared the manuscript. YeZ, YL, ZP, YT, and DX contributed to mapping population development, phenotyping and statistical analysis. XXi and YH assisted in writing and revising the manuscript. All authors contributed to the article and approved the submitted version.

FUNDING

This study was supported by the Agricultural Science and Technology Innovation Program of CAAS (CAAS-XTCX20190025-2, CAAS-ZDRW202002, and CAAS-S2021ZD04).

ACKNOWLEDGMENTS

The authors are very grateful to Prof. R.A. McIntosh, Plant Breeding Institute, University of Sydney, Australia, for reviewing this manuscript.

SUPPLEMENTARY MATERIAL

The Supplementary Material for this article can be found online at: https://www.frontiersin.org/articles/10.3389/fnut.2021.680391/full#supplementary-material

REFERENCES

1. Sharma S, Chunduri V, Kumar A, Kumar R, Khare P, Kondepudi KK, et al. Anthocyanin bio-fortified colored wheat: nutritional and functional characterization. *PLoS ONE.* (2018) 13:e0194367. doi: 10.1371/journal.pone.0194367
2. Shah D, Sachdev HPS. Zinc deficiency in pregnancy and fetal outcome. *Nutr Rev.* (2006) 64:15–30. doi: 10.1111/j.1753-4887.2006.tb00169.x
3. Wessells KR, Brown KH. Estimating the global prevalence of zinc deficiency: results based on zinc availability in national food supplies and the prevalence of stunting. *PLoS ONE.* (2012) 7:e50568. doi: 10.1371/journal.pone.0050568
4. Black RE, Victora CG, Walker SP, Bhutta ZA, Christian P, de Onis M, et al. Maternal and child undernutrition and overweight in low-income and middle-income countries. *Lancet.* (2013) 382:427–51. doi: 10.1016/S0140-6736(13)60937-X
5. Bouis HE, Welch RM. Biofortification—A sustainable agricultural strategy for reducing micronutrient malnutrition in the global south. *Crop Sci.* (2010) 50:S20–32. doi: 10.2135/cropsci2009.09.0531
6. Sands DC, Morris CE, Dratz EA, Pilgeram AL. Elevating optimal human nutrition to a central goal of plant breeding and production of plant-based foods. *Plant Sci.* (2009) 177:377–89. doi: 10.1016/j.plantsci.2009.07.011
7. Deshpande J, Joshi M, Giri P. Zinc: the trace element of major importance in human nutrition and health. *Int J Med Sci.* (2013) 2:1–6. doi: 10.5455/ijmsph.2013.2.1-6
8. Stoltzfus RJ. Defining iron-deficiency anemia in public health terms: a time for reflection. *J Nutr.* (2001) 131:565S—7. doi: 10.1093/jn/131.2.565S
9. Crespo-Herrera LA, Velu G, Singh RP. Quantitative trait loci mapping reveals pleiotropic effect for grain iron and zinc concentrations in wheat. *Ann Appl Biol.* (2016) 169:27–35. doi: 10.1111/aab.12276
10. Tong J, Sun M, Wang Y, Zhang Y, Rasheed A, Li M, et al. Dissection of molecular processes and genetic architecture underlying iron and zinc homeostasis for biofortification: from model plants to common wheat. *Int J Mol. Sci.* (2020) 21:9280. doi: 10.3390/ijms21239280
11. Morgounov A, Gómez-Becerra HF, Abugalieva A, Dzhunusova M, Yessimbekova M, Muminjanov H, et al. Iron and zinc grain density in common wheat grown in Central Asia. *Euphytica.* (2007) 155:193–203. doi: 10.1007/s10681-006-9321-2
12. Tiwari VK, Rawat N, Chhuneja P, Neelam K, Aggarwal R, Randhawa GS, et al. Mapping of quantitative trait loci for grain iron and zinc concentration in diploid A genome wheat. *J Hered.* (2009) 100:771–6. doi: 10.1093/jhered/esp030
13. Zhang Y, Song Q, Yan J, Tang J, Zhao R, Zhang Y, et al. Mineral element concentrations in grains of Chinese wheat cultivars. *Euphytica.* (2010) 174:303–13. doi: 10.1007/s10681-009-0082-6
14. Srinivasa J, Arun B, Mishra VK, Singh GP, Velu G, Babu R, et al. Zinc and iron concentration QTL mapped in a *Triticum spelta*×*T. aestivum* cross. *Theor Appl Genet.* (2014) 127:1643–51. doi: 10.1007/s00122-014-2327-6
15. Velu G, Ortiz-Monasterio I, Cakmak I, Hao Y, Singh RP. Biofortification strategies to increase grain zinc and iron concentrations in wheat. *J Cereal Sci.* (2014) 59:365–72. doi: 10.1016/j.jcs.2013.09.001
16. Hao Y, Velu G, Peña RJ, Singh S, Singh RP. Genetic loci associated with high grain zinc concentration and pleiotropic effect on kernel weight in wheat (*Triticum aestivum* L.). *Mol Breeding.* (2014) 34:1893–902. doi: 10.1007/s11032-014-0147-7
17. Crespo-Herrera LA, Govindan V, Stangoulis J, Hao Y, Singh RP. QTL Mapping of grain Zn and Fe concentrations in two hexaploid wheat RIL populations with ample transgressive segregation. *Front Plant Sci.* (2017) 8:1800. doi: 10.3389/fpls.2017.01800
18. Velu G, Tutus Y, Gomez-Becerra HF, Hao Y, Demir L, Kara R, et al. QTL mapping for grain zinc and iron concentrations and zinc efficiency in a tetraploid and hexaploid wheat mapping populations. *Plant Soil.* (2017) 411:81–99. doi: 10.1007/s11104-016-3025-8
19. Alomari DZ, Eggert K, von Wirén N, Alqudah AM, Polley A, Plieske J, et al. Identifying candidate genes for enhancing grain Zn concentration in wheat. *Front Plant Sci.* (2018) 9:1313. doi: 10.3389/fpls.2018.01313
20. Zarcinas BA, Cartwright B, Spouncer LR. Nitric acid digestion and multi-element analysis of plant material by inductively coupled plasma spectrometry. *Soil Sci Plant Anal.* (1987) 18:131–46. doi: 10.1080/00103628709367806
21. Paltridge NG, Milham PJ, Ortiz-Monasterio JI, Velu G, Yasmin Z, Palmer LJ, et al. Energy-dispersive X-ray fluorescence spectrometry as a tool for zinc, iron and selenium analysis in whole grain wheat. *Plant Soil.* (2012) 361:261–9. doi: 10.1007/s11104-012-1423-0
22. Holland JB, Nyquist WE, Cervantes-Matinez CT. Estimating and interpreting heritability for plant breeding: an update. *Plant Breed Rev.* (2003) 22:9–111. doi: 10.1002/9780470650202.ch2
23. Becker WA. *Manual of Quantitative Genetics,* 4th ed. Pullman, WA: Academic Enterprises (1984).
24. Doyle J, Doyle JL. A rapid DNA isolation procedure from small quantities of fresh leaf tissues. *Phytochem Bull.* (1987) 19:11–5.
25. Stam P (1993) Construction of integrated genetic linkage maps by means of a new computer package: join Map. *Plant J.* (1993) 3:739–744. doi: 10.1111/j.1365-313X.1993.00739.x
26. Jiang CJ, Zeng ZB. Multiple trait analysis of genetic mapping for quantitative trait loci. *Genetics.* (1995) 140:1111–27. doi: 10.1093/genetics/140.3.1111
27. Wickham H. *ggplot2: Elegant Graphics for Data Analysis.* New York, NY: Springer-Verlag.
28. Voorrips RE. MapChart: software for the graphical presentation of linkage maps and QTLs. *J Hered.* (2002) 93:77–78. doi: 10.1093/jhered/93.1.77
29. Chandra S, Singh D, Pathak J, Kumari S, Kumar M, Poddar R, et al. SNP discovery from next-generation transcriptome sequencing data and their validation using KASP assay in wheat (*Triticum aestivum* L.). *Mol Breeding.* (2017) 37:92. doi: 10.1007/s11032-017-0696-7
30. Jia A, Ren Y, Gao F, Yin G, Liu J, Guo L, et al. Mapping and validation of a new QTL for adult-plant resistance to powdery mildew in Chinese

elite bread wheat line Zhou8425B. *Theor Appl Genet.* (2018) 131:1063–71. doi: 10.1007/s00122-018-3058-x
31. Appels R, Eversole K, Stein N, Feuillet C, Keller B, Rogers J, et al. Shifting the limits in wheat research and breeding using a fully annotated reference genome. *Science.* (2018) 361:eaar7191. doi: 10.1126/science.aar7191
32. Gorafi YSA, Ishii T, Kim J-S, Elbashir AAE, Tsujimoto H. Genetic variation and association mapping of grain iron and zinc contents in synthetic hexaploid wheat germplasm. *Plant Genet Resour.* (2018) 16:9–17. doi: 10.1017/S1479262116000265
33. Peleg Z, Cakmak I, Ozturk L, Yazici A, Jun Y, Budak H, et al. Quantitative trait loci conferring grain mineral nutrient concentrations in durum wheat × wild emmer wheat RIL population. *Theor Appl Genet.* (2009) 119:353–69. doi: 10.1007/s00122-009-1044-z
34. Krishnappa G, Singh AM, Chaudhary S, Ahlawat AK, Singh SK, Shukla RB, et al. Molecular mapping of the grain iron and zinc concentration, protein content and thousand kernel weight in wheat (*Triticum aestivum* L.). *PLoS ONE.* (2017) 12:e0174972. doi: 10.1371/journal.pone.0174972
35. Liu J, Wu B, Singh RP, Velu G. QTL mapping for micronutrients concentration and yield component traits in a hexaploid wheat mapping population. *J Cereal Sci.* (2019) 88:57–64. doi: 10.1016/j.jcs.2019.05.008
36. Pu ZE, Yu M, He QY, Chen GY, Wang JR, Liu YX, et al. Quantitative trait loci associated with micronutrient concentrations in two recombinant inbred wheat lines. *J Integr Agric.* (2014) 13:2322–9. doi: 10.1016/S2095-3119(13)60640-1
37. Graham R, Senadhira D, Beebe S, Iglesias C, Monasterio I. Breeding for micronutrient density in edible portions of staple food crops: conventional approaches. *Field Crops Res.* (1999) 60:57–80. doi: 10.1016/S0378-4290(98)00133-6
38. Velu G, Singh RP, Huerta J, Guzmán C. Genetic impact of *Rht* dwarfing genes on grain micronutrients concentration in wheat. *Field Crops Res.* (2017) 214:373–7. doi: 10.1016/j.fcr.2017.09.030
39. Li X, Xia X, Xiao Y, He Z, Wang D, Trethowan R et al. QTL mapping for plant height and yield components in common wheat under water-limited and full irrigation environments. *Crop Pasture Sci.* (2015) 66:660–70. doi: 10.1071/CP14236
40. Rasheed A, Wen W, Gao F, Zhai S, Jin H, Liu J, et al. Development and validation of KASP assays for genes underpinning key economic traits in bread wheat. *Theor Appl Genet.* (2016) 129:1843–60. doi: 10.1007/s00122-016-2743-x
41. Shi RL, Tong YP, Jing RL, Zhang FS, Zou CQ. Characterization of quantitative trait loci for grain minerals in hexaploid wheat (*Triticum aestivum* L.). *J Integr Agric.* (2013) 12:1512–21. doi: 10.1016/S2095-3119(13)60559-6
42. Zhao FJ, Su YH, Dunham SJ, Rakszegi M, Bedo Z, McGrath SP, et al. Variation in mineral micronutrient concentrations in grain of wheat lines of diverse origin. *J Cereal Sci.* (2009) 49:290–5. doi: 10.1016/j.jcs.2008.11.007
43. Shanmugam V, Lo JC and Yeh KC. Control of Zn uptake in *Arabidopsis halleri*: a balance between Zn and Fe. *Front Plant Sci.* (2013) 4:281. doi: 10.3389/fpls.2013.00281

Conflict of Interest: The authors declare that the research was conducted in the absence of any commercial or financial relationships that could be construed as a potential conflict of interest.

frontiers in Nutrition

ORIGINAL RESEARCH
published: 15 June 2021
doi: 10.3389/fnut.2021.669444

Identification of Novel Genomic Regions for Biofortification Traits Using an SNP Marker-Enriched Linkage Map in Wheat (*Triticum aestivum* L.)

Gopalareddy Krishnappa[1,2], Nagenahalli Dharmegowda Rathan[1], Deepmala Sehgal[3], Arvind Kumar Ahlawat[1], Santosh Kumar Singh[1†], Sumit Kumar Singh[1], Ram Bihari Shukla[1], Jai Prakash Jaiswal[4], Ishwar Singh Solanki[5], Gyanendra Pratap Singh[1†] and Anju Mahendru Singh[1]*

[1] Division of Genetics, Indian Council of Agricultural Research-Indian Agricultural Research Institute, New Delhi, India, [2] Division of Crop Improvement, Indian Council of Agricultural Research-Indian Institute of Wheat and Barley Research, Karnal, India, [3] International Maize and Wheat Improvement Center, Texcoco, Mexico, [4] Department of Genetics and Plant Breeding, Govind Ballabh Pant University of Agriculture and Technology, Pantnagar, India, [5] Indian Council of Agricultural Research-Indian Agricultural Research Institute, Regional Station, Samastipur, India

Micronutrient and protein malnutrition is recognized among the major global health issues. Genetic biofortification is a cost-effective and sustainable strategy to tackle malnutrition. Genomic regions governing grain iron concentration (GFeC), grain zinc concentration (GZnC), grain protein content (GPC), and thousand kernel weight (TKW) were investigated in a set of 163 recombinant inbred lines (RILs) derived from a cross between cultivated wheat variety WH542 and a synthetic derivative (*Triticum dicoccon* PI94624/*Aegilops tauschii* [409]//BCN). The RIL population was genotyped using 100 simple-sequence repeat (SSR) and 736 single nucleotide polymorphism (SNP) markers and phenotyped in six environments. The constructed genetic map had a total genetic length of 7,057 cM. A total of 21 novel quantitative trait loci (QTL) were identified in 13 chromosomes representing all three genomes of wheat. The trait-wise highest number of QTL was identified for GPC (10 QTL), followed by GZnC (six QTL), GFeC (three QTL), and TKW (two QTL). Four novel stable QTL (*QGFe.iari-7D.1, QGFe.iari-7D.2, QGPC.iari-7D.2*, and *QTkw.iari-7D*) were identified in two or more environments. Two novel pleiotropic genomic regions falling between *Xgwm350–AX-94958668* and *Xwmc550–Xgwm350* in chromosome 7D harboring co-localized QTL governing two or more traits were also identified. The identified novel QTL, particularly stable and co-localized QTL, will be validated to estimate their effects on different genetic backgrounds for subsequent use in marker-assisted selection (MAS). Best QTL combinations were identified by the estimation of additive effects of the stable QTL for GFeC, GZnC, and GPC. A total of 11 RILs (eight for GZnC and three for GPC) having favorable QTL combinations identified in this study can be used as potential donors to develop bread wheat varieties with enhanced micronutrients and protein.

Keywords: biofortification, QTLs, malnutrition, SNPs, SSRs, mapping

OPEN ACCESS

Edited by:
Victor Taleon, International Food Policy Research Institute, United States

Reviewed by:
Shailender Kumar Verma, Central University of Himachal Pradesh, India
Parveen Chhuneja, Punjab Agricultural University, India

***Correspondence:**
Anju Mahendru Singh
anju.singh@icar.gov.in

†Present address:
Santosh Kumar Singh, Department of Microbiology, Biochemistry & Immunology, Morehouse School of Medicine, Atlanta, GA, United States
Gyanendra Pratap Singh, ICAR-Indian Institute of Wheat and Barley Research, Karnal, India

Specialty section:
This article was submitted to Nutrition and Food Science Technology, a section of the journal Frontiers in Nutrition

Received: *18 February 2021*
Accepted: *19 May 2021*
Published: *15 June 2021*

Citation:
Krishnappa G, Rathan ND, Sehgal D, Ahlawat AK, Singh SK, Singh SK, Shukla RB, Jaiswal JP, Solanki IS, Singh GP and Singh AM (2021) Identification of Novel Genomic Regions for Biofortification Traits Using an SNP Marker-Enriched Linkage Map in Wheat (Triticum aestivum L.). Front. Nutr. 8:669444. doi: 10.3389/fnut.2021.669444

INTRODUCTION

Wheat (*Triticum* spp.) is a major staple cereal crop contributing about 20% calories to the diet and at least 30% of Fe and Zn intake worldwide. Even though it has the highest levels of micronutrients among the three major cereals viz., wheat, rice, and maize, most wheat-based diets fail to deliver the required quantity of essential nutrients, such as iron and zinc. Malnutrition due to insufficient intake of micronutrients, such as iron and zinc, has been recognized as one of the major global health issues affecting nearly three billion people across the globe. The intensity of the risk is high in nations dominated by cereal-based diets (1). Around 25% of the global population is affected by anemia because of Fe deficiency (2), and the leading risk groups for this global public health concern are children 0–5 years of age, and pregnant and lactating women. Anemic complex due to severe iron deficiency leads to several life-threatening diseases, namely, chronic kidney and heart failure, and inflammatory bowel disease (3).

Zinc is an essential element for a wide range of biochemical and immunological functions, and acute zinc deficiency leads to major health difficulties, such as altered growth and development, immunity, pregnancy, and neurobehavioral adversities (4). Estimates indicate that around 17% of the global population suffers from zinc deficiency-related diseases (5). Grain protein quantity and quality determine both the nutritional and end-product quality of wheat. Lack of secondary immunity due to protein energy malnutrition (PEM) is one of the common causes of several infections in humans. Acute PEM in children is clinically defined as marasmus (chronic wasting) or kwashiorkor (edema and anemia) (6). Chronic PEM in children results in impaired cognitive development (7). Micronutrient malnutrition and PEM are leading risk factors for health loss in developing countries, with pregnant women and young children forming the most vulnerable groups (8).

Micronutrient and protein malnutrition can be overcome by consuming nutrient-rich diverse diet and/or by supplementation and fortification. However, the majority of populations in which the malnutrition problem is alarming may not be able to afford either of the two options, particularly the remote rural poor (9). Moreover, these interventions are not sustainable. Enhancing the nutritive levels of crop plants by conventional and molecular breeding approaches, termed as "biofortification," has been recognized as a cost-effective and sustainable approach to reduce global protein and micronutrient malnutrition. Currently, the development of biofortified crop varieties in many countries has gained momentum, particularly after reaching self-sufficiency in food grains.

Grain mineral density depends on a plethora of physiological and biochemical processes, such as mineral absorption, translocation, redistribution, and remobilization to the sink, which makes micronutrient accumulation in grain a complex trait (10). Therefore, breeding programs need to be re-oriented to broaden the genetic base using wild relatives and landraces, and dissecting the genetic basis of these nutritional quality traits (11). Landraces are one of the most important sources of wheat biofortification with high levels of micronutrients (12). Conventional breeding approaches have been successfully used to incorporate higher grain zinc content into elite breeding materials by crossing high-yielding elite wheat lines with *A tauschii*-based synthetic hexaploid wheats or *Triticum spelta* accessions (13). Substitution lines of the 6B chromosome obtained from *Triticum dicoccoides* are one of the most common genetic resources to improve zinc concentration in wheat (14). The *Gpc-B1* locus mapped on the short arm of the 6B chromosome, derived from *T dicoccoides*, has a pleiotropic effect on zinc and iron in addition to grain protein (15). An NAC transcription factor (NAM-B1) encoded by *Gpc-B1* is responsible for the increase in zinc as well as iron levels, possibly by stimulating leaf senescence, and thus remobilization of zinc and iron from flag leaves into seeds (16). Synthetic wheat derived from *Ae. tauschii* contains higher grain zinc and can act as a valuable genetic resource to increase the grain zinc levels of cultivated wheat (17).

Genetic dissection of complex nutritional traits is important for their improvement through marker-assisted selection (MAS). Identification of tightly linked molecular markers to the genomic regions governing the traits would help in the improvement of otherwise difficult to breed complex traits like protein and micronutrients. Reports have indicated significant effects of the environment and genotype-by-environment interaction (GEI) in the expression of PC and TKW (18–23), iron, and zinc (19, 24, 25). Molecular mapping of polygenic traits by identifying quantitative trait loci (QTL) harboring genes for protein, micronutrient, and TKW would allow plant breeders to more efficiently develop biofortified cultivars.

QTL have been identified for grain iron (19, 26–38), grain zinc (13, 19, 27–33, 35–41), grain protein content (19, 27, 31, 35, 36, 42–50), and thousand kernel weight (19, 27, 29, 45, 51–54). However, most investigations on mapping nutritional quality have exploited low-density maps, which have resulted in large interval QTL that have rarely been exploited in breeding.

Previous mapping of the same RIL population was carried out with 136 polymorphic SSR markers, which led to the identification of 16 QTL for four traits (55). The linkage map was coarse because of low marker frequency per chromosome ranging from 6 (1A and 2A) to 11 markers per chromosome (7B). Also, no QTL were mapped on the D genome because of low marker coverage. In this study, a 35K SNP chip was used for genotyping the RIL population, and a combined dataset of SSR and SNP markers was used to identify QTL for nutritional traits.

MATERIALS AND METHODS

Plant Material

A set of 286 RILs from a cross between Indian bread wheat variety WH 542 and a synthetic derivative (*T. dicoccon* PI94624/*Ae. tauschii* [409]//BCN) received from CIMMYT (International Maize and Wheat Improvement Center), Mexico, was used in the earlier mapping study with SSR markers (55). A subset of 163 randomly selected RILs from this population was used for this investigation.

Field Trials and Phenotyping

The details of field experimentation, sample collection, and phenotyping have been described in detail in the earlier study (55). The phenotypic data for GFeC, GZnC, GPC, and TKW recorded for the earlier study were converted into the best linear unbiased predictors (BLUPs) and used in this study. Phenotypic correlations among traits, heritability, and ANOVA were conducted using the MetaRv6.0 (Multi Environment Trial Analysis with R) software. BLUPs of each RIL obtained for an individual year and combined across years were used further in QTL analysis. Phenotypic data of all the six environments are presented as **Supplementary Table 1**.

Genotyping

RILs and parental genomic DNA were extracted from the leaves of 21-day-old seedlings by following the CTAB method of Murray and Thompson (56).

Genotyping With Single Nucleotide Polymorphism Markers

The 163 RILs and parental lines were genotyped using Axiom Wheat Breeder's Genotyping Array (Affymetrix, Santa Clara, CA, United States) with 35,143 SNPs (https://www.cerealsdb.uk.net).

Genotyping With Simple-Sequence Repeat Markers

A total of 714 SSR markers (57, 58) were used for the parental polymorphism survey. These selected 714 SSRs cover all the chromosome arms of the bread wheat genome. Polymorphic markers and genotypic data are presented as **Supplementary Table 2**.

Linkage Analysis and Quantitative Trait Locus Mapping

Monomorphic markers between the two parents and markers with more than 30% missing data and minor allele frequency $\leq$5 and $\geq$95% were eliminated. Furthermore, markers that showed significant segregation distortion ($p < 0.0001$) from the expected

TABLE 1 | Heritability and variance components of grain iron, zinc, protein, and thousand kernel weight in RIL population grown across three locations for 2 years.

Trait	Environment	Parental mean		RIL population h^2 (bs) and variance			
		WH542 (P1)	Synthetic derivative (P2)	h^2 (bs)	Genotype Variance	LSD	CV%
Grain iron (ppm)	ICAR-IARI_Y1	33.8	49.6	0.76	6.44***	3.49	4.90
	ICAR-IARI_Y2	33.8	45.0	0.78	10.30***	4.20	5.90
	GBPUA&T_Y1	30.3	45.8	0.54	3.46***	3.54	6.67
	GBPUA&T_Y2	32.1	42.0	0.82	11.98***	4.10	5.92
	Pusa Bihar_Y1	30.0	45.2	0.66	3.76***	3.16	5.66
	Pusa Bihar_Y2	30.0	44.7	0.72	5.93***	3.62	6.08
	Pooled mean	31.7	45.4	0.81	3.93***	2.41	5.86
Grain zinc (ppm)	ICAR-IARI_Y1	37.7	48.8	0.81	17.98***	5.10	6.84
	ICAR-IARI_Y2	37.2	52.3	0.87	23.91***	4.85	6.44
	GBPUA&T_Y1	27.7	39.3	0.73	9.81***	4.51	9.05
	GBPUA&T_Y2	26.9	38.5	0.86	17.75***	4.42	8.19
	Pusa Bihar_Y1	39.8	45.9	0.90	26.57***	4.55	5.65
	Pusa Bihar_Y2	41.1	51.0	0.86	20.56***	4.69	6.05
	Pooled mean	35.1	46.0	0.77	8.28***	3.81	6.87
Grain protein	ICAR-IARI_Y1	14.6	18.6	0.78	1.21***	1.43	5.04
content (%)	ICAR-IARI_Y2	12.4	18.5	0.65	1.17***	1.78	7.74
	GBPUA&T_Y1	12.8	16.3	0.78	1.40***	1.54	6.24
	GBPUA&T_Y2	11.3	14.6	0.67	1.11***	1.69	8.16
	Pusa Bihar_Y1	15.9	19.1	0.78	1.08***	1.35	4.64
	Pusa Bihar_Y2	15.7	17.8	0.78	1.88***	1.80	6.45
	Pooled mean	13.8	17.5	0.84	0.81***	1.01	6.34
Thousand kernel	ICAR-IARI_Y1	28.1	35.0	0.92	12.93***	2.83	4.49
weight (gm)	ICAR-IARI_Y2	29.1	36.9	0.96	27.32***	3.00	4.10
	GBPUA&T_Y1	29.6	35.1	0.91	9.96***	2.66	4.36
	GBPUA&T_Y2	31.2	33.8	0.96	25.01***	2.94	3.99
	Pusa Bihar_Y1	26.8	32.7	0.89	10.57***	2.94	5.09
	Pusa Bihar_Y2	25.1	35.9	0.93	21.35***	3.49	5.44
	Pooled mean	28.3	34.9	0.91	11.99***	2.91	4.57

****Significant at $p < 0.001$; Y1: 2012–13; Y2: 2013–14; P1: WH542; P2: synthetic derivative; h^2 (bs), heritability (broad sense); LSD, least significant difference; CV, coefficient of variation.*

1:1 ratio and redundant markers were discarded using bin function in QTL ICIM Mapping v4.2. Finally, a high-quality filtered set of 836 informative markers (736 SNPs + 100 SSRs) was utilized for the QTL analysis.

Both linkage and QTL analysis were conducted with the IciMapping v4.2 software (http://www.isbreeding.net). The chromosome location of SNP inferred by BLAST of the sequences and previously mapped SSR markers (55) was used as the anchoring information. A LOD threshold of 3 was specified for grouping the markers. After all the markers were correctly grouped, they were ordered using the k-Optimality algorithm. Then, Rippling was done to fine-tune the ordered chromosomes in the linkage groups using a 5 cM window size. ICIM-ADD method was employed, which conducts inclusive composite interval mapping for identifying QTL. Missing phenotypic data were considered as deletion during QTL mapping and a relaxed threshold LOD score of 2.5 was specified for declaring significant QTL.

In silico Analysis of Quantitative Trait Loci

An *in silico* search of candidate genes was performed in the Ensemble Plants database (http://plants.ensembl.org/index.html) of the bread wheat genome with the Basic Local Alignment Search Tool (BLAST) using default parameters. The sequences of the markers present within the peak of the QTL and the flanking markers were used to conduct the search.

RESULTS

Variability, Heritability, and Trait Correlations

The heritability and variance components of GFeC, GZnC, GPC, and TKW in a RIL population are presented in **Table 1**. Parents were contrasting for all the studied traits and P2 was superior over P1 with 43, 31, 26, and 23%, respectively, for GFeC, GZnC, GPC, and TKW. Environment-wise heritability ranged from 0.54 (GFeC at GBPUA&T_Y1) to 0.96 (TKW at

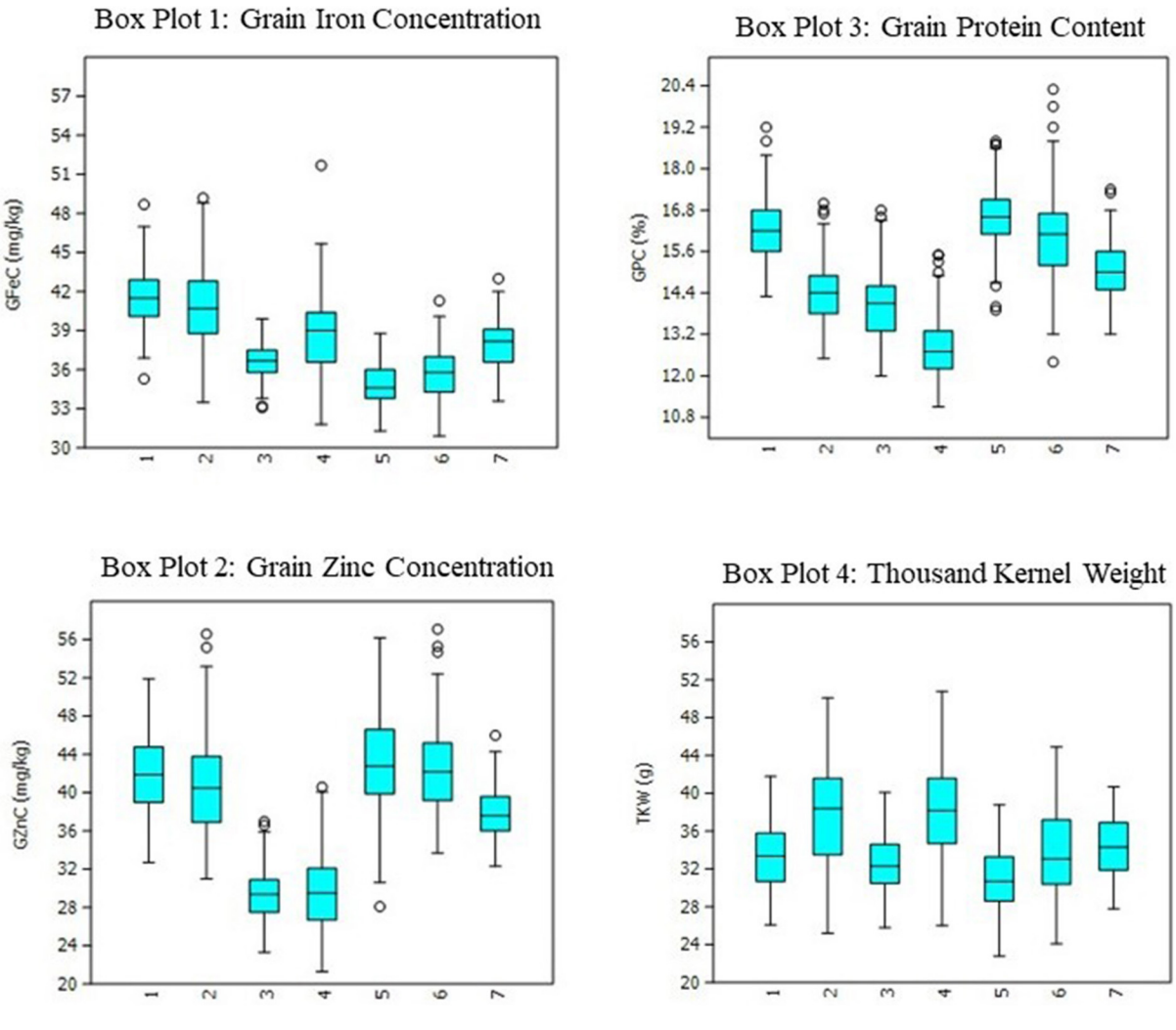

FIGURE 1 | Boxplots for grain iron, zinc, protein, and thousand kernel weight in RIL population grown across three locations for 2 years. 1: ICAR-IARI_Y1; 2: ICAR-IARI_Y2; 3: GBPUA&T_Y1; 4: GBPUA&T_Y2: 5: Pusa Bihar_Y1; 6: Pusa Bihar_Y2; 7: Pooled mean.

ICAR-IARI_Y2 and GBPUA&T_Y2) across the traits. The lowest pooled heritability was observed for GZnC (0.77), whereas, highest pooled heritability was recorded for TKW (0.91). Trait heritability corroborates the variance components; GZnC (6.87%) and TKW (4.57%) recorded the highest and lowest CV, respectively. The genotypic variance was highly significant for all the studied traits across the environments. The environment-wise pooled mean is also represented graphically in **Figure 1**. All the studied traits exhibited a near-normal distribution (**Figure 2**). Genetic correlation coefficients among GFeC, GZnC, GPC, and TKW are presented in **Table 2**. All the associations among the studied traits are positive and significant, except, between TKW and GPC in the Pusa Bihar_Y1 ($r_g = -0.03$) and Pusa Bihar_Y2 environments (0.1) (**Table 2**).

Quantitative Trait Locus Mapping

The total genetic length of the linkage map was 7,057 cM, and it contained 736 SNPs and 100 SSRs. The chromosome and genome-wise distribution of markers is presented in **Table 3**. The B genome had the highest number of mapped markers (361) followed by the A (265) and D genomes (210). Chromosome-wise distribution of the markers ranged between 17 (6A chromosome) to 81 (7A chromosome).

The mapped QTL across the locations and years are presented in **Table 4**, and the linkage map with the identified QTL position is depicted in **Figure 3**. A total of 21 QTL were identified in 13 chromosomes representing all three genomes of wheat. Two, five, and 14 QTL were mapped on the A, B, and D genomes, respectively. Chromosome 7D represented the maximum number of seven QTL. A total of 21 QTL were mapped between 16 flanked regions (**Table 4**); the maximum number of four QTL was identified between flanking markers *Xgwm350–AX-94958668*, followed by three QTL between *Xwmc550–Xgwm350* in the7D chromosome. Trait-wise highest QTL were identified for GPC (10 QTL), followed by GZnC (six QTL), GFeC (three QTL), and TKW (two QTL). QTL for GFeC were mapped in chromosomes 6D and 7D; for GZnC in chromosomes 3B, 1D, 2D, and 7D; for GPC in chromosomes 1A,7A, 5B, 6B, 3D, 4D, 5D, and 7D and for TKW in chromosomes 1B and 7D.

Quantitative Trait Loci for Micronutrients

Three QTL governing GFeC were identified and are presented in **Table 4**. QTL governing GFeC explained 16–42.13% of the phenotypic variance. *QGFe.iari-7D.2*, flanked between *Xgwm350–AX-94958668*, was mapped in three environments (GBPUAT_Y1, PusaBihar_Y1, and PusaBihar_Y2) as well as in pooled mean, and contributed 20.19% to the phenotypic variance, followed by *QGFe.iari-7D.1* in three environments (ICAR-IARI_Y1, ICAR-IARI_Y2, and GBPUAT_Y2) and flanked between *Xwmc550–Xgwm350. QGFe.iari-7D.1* explained 42.13% of the phenotypic variance. Another QTL, *QGFe.iari-6D,* flanked between *Xgwm325–Xbarc202*, was mapped for pooled mean although it explained only 5.61% of the phenotypic variance. A total of six QTL were identified for GZnC and are presented in **Table 4**. QTL governing GZnC explained 5.01–13.07% of phenotypic variance. *QGZn.iari-7D.2*, flanked between

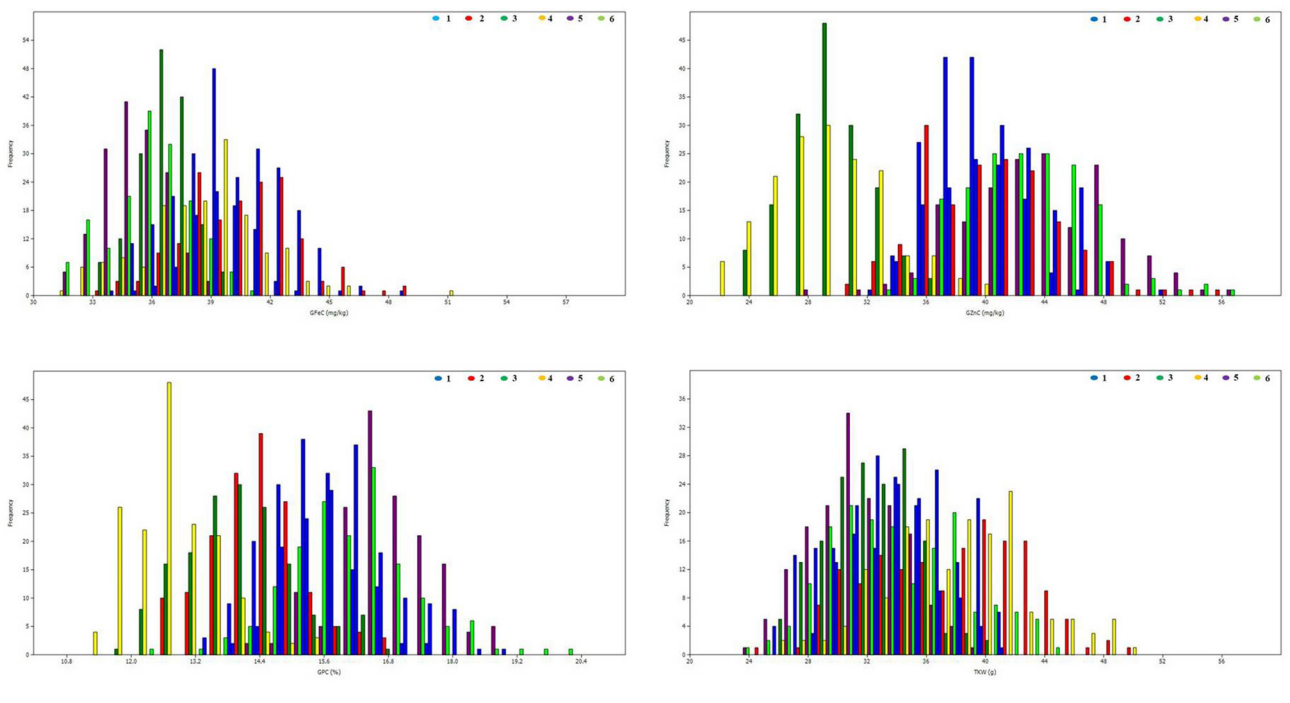

FIGURE 2 | Frequency distributions for grain iron, zinc, protein, and thousand kernel weight in RIL population grown across three locations for 2 years. 1: ICAR-IARI_2012–13; 2: ICAR-IARI_2013–14; 3: GBPUA&T_2012–13; 4: GBPUA&T_2013–14: 5: Pusa Bihar_2012–13; 6: Pusa Bihar_2013–14.

TABLE 2 | Genetic correlation coefficients among grain iron, zinc, protein, and thousand kernel weight in RIL population grown across three locations for 2 years.

	Traits	GFeC	GZnC	GPC
ICAR-IARI_Y1	GZnC	0.65***		
	GPC	0.68***	0.61***	
	TKW	0.55***	0.43***	0.24**
ICAR-IARI_Y2	GZnC	0.64***		
	GPC	0.76***	0.56***	
	TKW	0.58***	0.36***	0.46***
GBPUAT_Y1	GZnC	0.73***		
	GPC	0.54***	0.34***	
	TKW	0.62***	0.52***	0.21**
GBPUAT_Y2	GZnC	0.45***		
	GPC	0.27***	0.10	
	TKW	0.50***	0.37***	0.27***
Pusa Bihar_Y1	GZnC	0.48***		
	GPC	0.53***	0.37***	
	TKW	0.50***	0.21**	−0.03
Pusa Bihar_Y2	GZnC	0.38***		
	GPC	0.55***	0.32***	
	TKW	0.51***	0.34***	0.10
Pooled mean	GZnC	0.97***		
	GPC	0.95***	0.57***	
	TKW	0.81***	0.94***	0.52***

***Significant at $p < 0.01$; ***significant at $p < 0.001$; Y1: 2012–13; Y2: 2013–14; GZnC, grain zinc concentration; GFeC, grain iron concentration; GPC, grain protein content; TKW, thousand kernel weight.*

TABLE 3 | Number of markers grouped by each wheat chromosome and genome in the RIL mapping population.

Chromosome	*Triticum aestivum* genome		
	A	B	D
Chromosome 1	48	26	31
Chromosome 2	20	63	22
Chromosome 3	21	64	25
Chromosome 4	54	50	33
Chromosome 5	24	61	50
Chromosome 6	17	34	27
Chromosome 7	81	63	22
Total	265	361	210

Xgwm350–AX-94958668, was identified in GBPUAT_Y1 along with pooled mean and explained 13.07% of the phenotypic variance. *QGZn.iari-3B*, flanked between *AX-94405870–AX-94940814*, was identified at ICAR-IARI_Y2 and explained 5.01% of the phenotypic variance. *QGZn.iari-1D*, flanked between *AX-95628763–AX-94385394*, was mapped at Pusa Bihar_Y1 and explained 5.28% of the phenotypic variance. *QGZn.iari-2D.1* was identified in ICAR-IARI_Y1 with an explained phenotypic variance of 8.11% and flanked between *Xgwm349–Xwmc309*. *QGZn.iari-2D.2*, flanked between *Xbarc11–Xgwm349*, was mapped for pooled mean and explained only 5.05% of the phenotypic variance. *QGZn.iari-7D.1*, flanked between *Xwmc550–Xgwm350*, was mapped in ICAR-IARI_Y2 with 6.05% of the phenotypic variance.

Quantitative Trait Loci for Grain Protein Content and Thousand Kernel Weight

Ten QTL governing GPC were identified and are presented in **Table 4**. QTL governing GPC explained 4.67% (*QGPC.iari-7D.2* at GBPUAT_Y2) to 11.39% (*QGPC.iari-5B.1* at ICAR-IARI_Y1). *QGPC.iari-7D.2*, flanked between *Xgwm350–AX-94958668*, was mapped in two environments (GBPUAT_Y2, Pusa Bihar_Y2) as well as pooled mean with 9.57% of the phenotypic variance, followed by *QGPC.iari-5B.1* at ICAR-IARI_Y1 and pooled mean with 11.39% of the phenotypic variance and flanked between *Xcfd7–Xbarc109*. The remaining eight QTL, i.e., *QGPC.iari-1A*, *QGPC.iari-7A*, *QGPC.iari-5B.2*, *QGPC.iari-6B*, *QGPC.iari-3D*, *QGPC.iari-4D*, *QGPC.iari-5D*, and *QGPC.iari-7D.1* were mapped in one environment each with an explained phenotypic variance of 4.73, 10.53, 9.19, 9.05, 6.33, 6.71, 8.06, and 6.15%, respectively. Two QTL governing the expression of TKW were identified in chromosomes 1B and 7D (**Table 4**). *QTkw.iari-7D* was identified at all the six tested environments and pooled means. It was flanked between *Xgwm350–AX-94958668* and explained 26.53% of the phenotypic variance. Another QTL, *QTkw.iari-1B,* was mapped at Pusa Bihar_Y2 and flanked between *Xbarc137–Xwmc626*. This QTL explained 4.22% of the phenotypic variance.

Quantitative Trait Locus Additive Effects

The additive effects of the stable QTL were investigated for GFeC, GZnC, and GPC (**Table 5**). For the estimation of additive effects, we used all the novel and stable QTL identified in this study along with a stable genomic region identified in chromosome 2A in the previous study. For GFeC, *QGFe.iari-7D.2* had the largest effect individually, and there is no significant increase by combining the additional QTL and this QTL was identified in 31RILs. For GZnC, the two QTL combinations, *viz.*, *QGZn.iari-2D.1* and *QGZn.iari-7D.1*, showed the highest average GZnC across the environments, and this combination was identified in eight RILs. For GPC, the four QTL combinations viz., *QGPC.iari-2A*, *QGPC.iari-5B*, *QGPC.iari-7D.1*, and *QGPC.iari-7D.2* showed the highest average GPC across the environments, and this combination was identified in three RILs.

In silico Analysis

The *in silico* analysis identified many important candidate genes underlying 10 QTL, with the highest PVE and pleiotropic for GFeC, GZnC, GPC, and TKW (**Table 6**). A pleotropic genomic region on chromosome 2A in our previous study (55) was also considered. Most significantly, QTL *QGZn.iari-2A*, *QGFe.iari-2A*, *QGpc.iari-2A*, *QGFe.iari-7D.2*, *QGZn.iari-7D.2*, *QGGpc.iari-7D.2*, *QTkw.iari-7D*, *QGFe.iari-7D.1*, *QGZn.iari-7D.1*, and *QGpc.iari-7D.1* were located in regions where genes coding for various transcription factors (TraesCS2A02G063800, TraesCS7D02G521500), transporters (TraesCS7D02G338100, TraesCS7D02G521400, and

TABLE 4 | QTL identified for grain iron, zinc, protein, and thousand kernel weight in RIL population grown across three locations for 2 years.

Trait	QTL name	Environment	Position	Flanking markers	LOD	PVE (%)	Add	Confidence interval
GFeC	*QGFe.iari-7D.1*	ICAR-IARI_Y1	11	*Xwmc550–Xgwm350*	14.07	32.10	−1.22	7.5–18.5
		ICAR-IARI_Y2	12		17.92	42.13	−1.68	9.5–12.5
		GBPUAT_Y2	12		6.26	16.21	−1.28	6.5–24.5
	QGFe.iari-7D.2	GBPUAT_Y1	13	*Xgwm350–AX-94958668*	5.90	15.42	−0.55	7.5–27.5
		PusaBihar_Y1	21		6.73	16.00	−0.92	12.5–30.5
		PusaBihar_Y2	19		7.76	20.19	−1.16	8.5–30.5
		Pooled mean	13		18.48	37.44	−1.05	10.5–19.5
	QGFe.iari-6D	Pooled mean	11	*Xgwm32–Xbarc202*	2.57	5.61	−0.41	0–25.5
GZnC	*QGZn.iari-7D.2*	GBPUAT_Y1	21	*Xgwm350–AX-94958668*	3.58	13.07	−1.03	4.5–41.5
		Pooled mean	18		4.39	10.65	−0.80	6.5–35.5
	QGZn.iari-2D.2	Pooled mean	73	*Xbarc11–Xgwm349*	3.26	5.05	−0.56	52.5–87.5
	QGZn.iari-2D.1	ICAR-IARI_Y1	89	*Xgwm349– Xwmc309*	2.98	8.11	−1.23	73.5–104.5
	QGZn.iari-3B	ICAR-IARI_Y2	170	*AX-94405870– AX-94940814*	2.67	5.01	0.95	169.5–170.5
	QGZn.iari-7D.1	ICAR-IARI_Y2	11	*Xwmc550– Xgwm350*	2.97	6.05	−1.04	2.5–30.5
	QGZn.iari-1D	PusaBihar_Y1	343	*AX-95628763– AX-94385394*	2.55	5.28	−1.25	338.5–354.5
GPC	*QGPC.iari-5B.1*	ICAR-IARI_Y1	0	*Xcfd7– Xbarc109*	5.72	11.39	−0.35	0–7.5
		Pooled mean	0		2.60	4.76	−0.19	0–11.5
	QGPC.iari-7D.2	GBPUAT_Y2	13	*Xgwm350– AX-94958668*	2.57	4.67	−0.24	4.5–34.5
		PusaBihar_Y2	20		4.05	9.57	−0.57	9.5–31.5
		Pooled mean	21		3.38	12.91	−0.31	7.5–35.5
	QGPC.iari-7A	ICAR-IARI_Y2	185	*Xbarc222–Xwmc525*	3.37	10.53	−0.31	178.5–193.5
	QGPC.iari-1A	GBPUAT_Y1	72	*AX-94600120–AX-95231896*	2.87	4.73	−0.25	70.5–72.5
	QGPC.iari-4D	GBPUAT_Y1	199	*AX-94383222–AX-94462801*	4.09	6.71	0.31	194.5–199.5
	QGPC.iari-5D	GBPUAT_Y1	522	*AX-94940145–AX-95248961*	4.79	8.06	−0.33	508.5–522
	QGPC.iari-5B.2	GBPUAT_Y2	450	*Xgwm499–AX-95113708*	2.52	9.19	−0.33	430.5–465.5
	QGPC.iari-6B	PusaBihar_Y1	87	*AX-94974451–AX-95195535*	2.69	9.05	0.32	69.5–100.5
	QGPC.iari-3D	PusaBihar_Y1	0	*Xgwm314–Xbarc132*	3.24	6.33	0.26	0–8.5
	QGPC.iari-7D.1	PusaBihar_Y1	10	*Xwmc550–Xgwm350*	2.62	6.15	−0.26	2.5–31.5
TKW	*QTkw.iari-7D*	ICAR-IARI_Y1	30	*Xgwm350–AX-94958668*	6.70	21.05	−2.18	20.5–39.5
		ICAR-IARI_Y2	28		10.78	26.53	−3.75	19.5–37.5
		GBPUAT_Y1	20		5.73	11.02	−1.32	12.5–32.5
		GBPUAT_Y2	27		6.22	21.19	−2.61	10.5–41.5
		PusaBihar_Y1	27		7.01	23.12	−1.93	13.5–37.5
		Pooled mean	26		11.85	27.30	−2.17	18.5–35.5
		PusaBihar_Y2	27		8.84	21.89	−3.27	13.5–36.5
	QTkw.iari-1B	PusaBihar_Y2	323	*Xbarc137–Xwmc626*	2.68	4.22	1.45	311.5–336.5

GFeC, grain iron concentration; GZnC, grain zinc concentration; GPC, grain protein content; TKW, thousand kernel weight; Y1: 2012–13; Y2: 2013–14. Positive value indicates that the allele was inherited from WH542, and negative value indicates that the allele was inherited from synthetic derivative.

TraesCS7D02G338100), and signaling and catalytic molecules were present (TraesCS2A02G192400, TraesCS2A02G063900, TraesCS7D02G521700, TraesCS7D02G338400, and TraesCS7D02G521200) (**Table 6**).

DISCUSSION

Genetic biofortification is the most cost-effective and sustainable strategy to control malnutrition. Understanding the genetic basis of complex traits like micronutrients, protein, and thousand kernel weight by QTL mapping will help in devising appropriate breeding strategies through MAS. The expression of all the studied traits in this study is greatly affected by the environment and GEI. Similar results of greater magnitude of the environment and GEI have been reported in previous studies for PC and TKW (18–20) and also for iron and zinc (13, 19, 59). Among the studied traits, GZnC was the most variable, whereas, TKW was the most stable. The lowest and highest pooled heritability was observed for GZnC and TKW, respectively, and a reverse trend was observed for CV (GZnC: 6.87; TKW: 4.57). Although both location and year effects were visible for all the traits, the magnitude of the location effect was found to be more pronounced than the year effect (**Figure 1**). The positive and

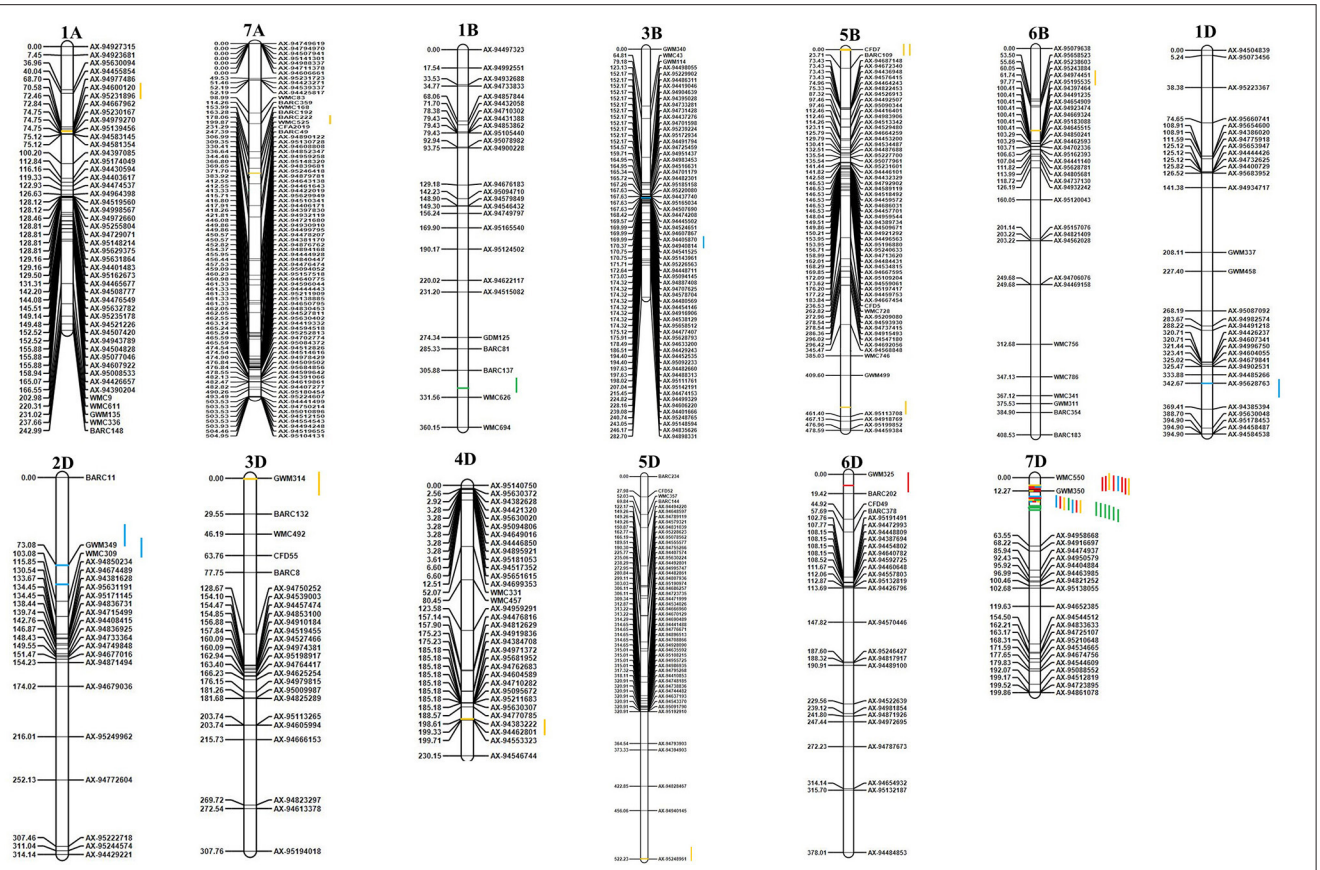

FIGURE 3 | Genetic linkage map and QTL positions identified in A, B, and D genomes of RILs derived from WH 542 × synthetic derivative cross. Red color indicates QTLs for GFeC; Blue color indicates QTLs for GZnC; Yellow color indicates QTLs for grain GPC; Green color indicates QTLs for TKW.

significant associations among GFeC, GZnC, GPC, and TKW found in this study have also been reported in earlier studies (27, 29). In most of the earlier studies, the associations between GPC and TKW were negative. In this study, the associations between GPC and TKW were significantly positive in four out of six studied environments and non-significant negative in the Pusa Bihar_Y1 environment ($r_g = -0.03$), and non-significant positive in the Pusa Bihar_Y2 environment ($r_g = 0.1$). Similar results of both positive and negative associations between GPC and TKW have also been reported in some earlier studies (19, 27, 45, 60). The lowest and highest pooled heritability of GZnC and TKW, respectively, is also congruent with earlier studies (28, 44).

The linkage map was constructed with 836 high-quality informative markers (736 SNPs + 100 SSRs) and utilized for the QTL analysis. In the previous study conducted on the same population, the SSR-based genetic map had a very low frequency of markers in the D genome (55). As a result, none of the QTL is localized in the D genome. The addition of SNPs improved D genome marker density and distribution, particularly in the 7D chromosome. Enrichment of genetic linkage map with SNPs greatly helped in the mining of novel genomic regions in the D genome. As a result, a maximum number of novel QTL were also identified in the D genome (14 QTL).

The D genome generally shows a low level of polymorphism in naturally occurring hexaploid bread wheat due to its well-known evolutionary history and low recombination during its post-evolution era (61, 62). For this reason, synthetic hexaploid wheats (SHWs) were created by crossing tetraploid durum wheats with multiple accessions of *Ae. tauschii* (the D genome donor), which increased the diversity of the D genome (63–65). Studies have shown that the D genome diversity of SHW is considerably greater than that of bread wheat (66, 67). In this study, since a synthetic parent was involved in the cross, D genome polymorphism improved significantly and 25.1% (210) of the markers mapped on the D genome (**Table 3**). A similar trend in marker distribution has been observed in earlier studies involving SHWs as one of the parents in creating mapping populations (30).

A total of 21 QTL were identified in 13 chromosomes representing all three genomes of wheat. Intriguingly, the alleles at most of the QTL responsible for increased GFeC, GZnC, GPC, and TKW were inherited from the synthetic derivative parent. Three QTL (*QGFe.iari-6D*, *QGFe.iari-7D.1*, and *QGFe.iari-7D.2*)

TABLE 5 | RILs with best combination of QTL for biofortification traits in wheat.

QTL	Markers	Marker type	No. of RILs	1	2	3	4	5	6	Mean
Grain iron concentration										
2A	*Xgwm249 + Xgwm359*	B+B	45	42.1	41.1	36.7	38.6	35.3	35.7	38.3
7D.1	*Xwmc550 + Xgwm350*	B+B	41	42.8	41.9	37.3	38.6	35.7	36.2	38.8
7D.2*	*Xgwm350 + AX-94958668*	B+A	31	42.6	41.5	37.6	40.3	35.7	35.8	38.9
2A+7D.1	*Xgwm249 + Xgwm359 + Xwmc550 + Xgwm350*	B+B+B+B	25	42.7	41.9	37.2	39.1	35.6	36.6	38.9
Grain zinc concentration										
2A	*Xgwm249 + Xgwm359*	B+B	45	43	41.4	30.1	30	44.9	43.5	38.8
2D.1	*Xgwm349 + Xwmc309*	A+A	20	43.4	40.8	29.9	30.4	45.1	42.9	38.8
7D.1	*Xwmc550 + Xgwm350*	B+B	41	43.4	42.1	30.5	30.5	44.5	43.3	39.1
7D.2	*Xgwm350 + AX-94958668*	B+A	31	43	42.4	30.8	30.8	43.4	43.1	38.9
2D.1+7D.1*	*Xgwm349 + Xwmc309 + Xwmc550 + Xgwm350*	A+A+B+B	8	44.2	43.5	31.9	31.9	45.3	43.7	40.1
Grain protein content										
2A	*Xgwm249 + Xgwm359*	B+B	45	16.4	14.6	14.4	13	16.7	16.4	15.3
5B.1	*Xcfd7 + Xbarc109*	B+A	22	16.6	14.4	14.1	13	16.9	16.5	15.3
7D.1	*Xwmc550 + Xgwm350*	B+B	41	16.6	14.8	14.7	13.3	16.9	16.5	15.5
7D.2	*Xgwm350 + AX-94958668*	B+A	31	16.5	14.7	14.5	12.9	16.9	16.2	15.3
5B.1+7D.2	*Xcfd7 + Xbarc109 + Xgwm350 + AX-94958668*	B+A+B+A	4	17.4	15.5	14.3	14.1	17.8	17.1	16.0
2A+5B.1+7D.1+7D.2*	*Xgwm249 + Xgwm359 + Xcfd7 + Xbarc109 + Xwmc550 + Xgwm350 + Xgwm350 + AX-94958668*	B+B+B+A+B+B+B+A	3	17.8	15.8	14.6	14.3	18.2	17.2	16.3

**Best combination of QTL, A—Parent 1 type, B—Parent 2 type.*

governing GFeC were identified in chromosomes 6D and 7D. Also, in the earlier study, grain iron QTL have been identified in chromosome 7D (34) with different marker intervals, whereas QTL (*QGFe.iari-6D*) mapped on 6D in this study is novel and not reported by earlier studies. For grain zinc, a total of six QTL (*QGZn.iari-2D.1*, *QGZn.iari-3B*, *QGZn.iari-7D.1*, *QGZn.iari-7D.2*, *QGZn.iari-1D*, and *QGZn.iari-2D.2*) were identified. The localization of QTL for GZnC reported in earlier studies on 3B (30, 39), 1D (39), 2D (39), and 7D (30) in different mapping populations corroborate the involvement of these chromosomes.

For GPC, 10 QTL were identified and designated as *QGPC.iari-5B.1*, *QGPC.iari-7A*, *QGPC.iari-1A*, *QGPC.iari-4D*, *QGPC.iari-5D*, *QGPC.iari-5B.2*, *QGPC.iari-7D.1*, *QGPC.iari-6B*, *QGPC.iari-3D*, and *QGPC.iari-7D.2*. The association of genomic regions for GPC in chromosomes 1A (42, 68), 5B (36, 47), 6B (36, 42), 3D (45), and 5D (45, 47) was also reported in previous studies. Additionally, five novel QTL were identified in 7A (*QGPC.iari-7A*), 4D (*QGPC.iari-4D*), 5D (*QGPC.iari-5D*), and 7D (*QGPC.iari-7D.1* and *QGPC.iari-7D.2*), which were missing in the earlier studies. Interestingly, one novel QTL (*QGPC.iari-7D.2*) was also found to be stable. There were two QTL (*QTkw.iari-1B* and *QTkw.iari-7D*) identified in chromosomes 1B and 7D governing TKW. The genomic regions associated with TKW in these two chromosomes have also been reported in the previous studies (40, 42).

In the earlier study, a total of 16 QTL were identified including four QTL for GFeC, five QTL for GZnC, two QTL for GPC, and five QTL for TKW. The QTL together explained 20, 32, 24.1, and 32.3% of the phenotypic variance, respectively, for GFeC, GZnC, GPC, and TKW. In contrast to the earlier study, where the D genome was completely missing, this study identified the majority of QTL from the D genome. This is due to fairly good marker coverage in all the three genomes in this study, unlike the earlier study, wherein, marker coverage in the D genome was very sparse. The total phenotypic variance explained for all the QTL for any given trait except TKW was higher in this study compared with the earlier studies. Similarly, for two traits, i.e., GFeC and TKW, the highest explained phenotypic variance for an individual QTL was higher compared with the earlier identified QTL. The highest explained phenotypic variance for an individual QTL was 42.13% for GFeC and 26.53% for TKW compared with the earlier identified QTL with 6.8 and 10.4%, respectively.

The environment and GEI play a key role in the expression of quantitative traits. Identification of stable genotypes with the high buffering ability and of QTL is of paramount importance to use in breeding programs. Genetic dissection of complex traits by the identification of stable QTL will complement varietal development by molecular breeding approaches. In this study, four stable QTL (*QTkw.iari-7D*, *QGFe.iari-7D.2*, *QGFe.iari-7D.1*, and *QGPC.iari-7D.2*) were identified in two or more environments. *QTkw.iari-7D* was identified in all the six tested environments and pooled mean, followed by *QGFe.iari-7D.2* and *QGFe.iari-7D.1*, which were identified in three environments

TABLE 6 | Putative candidate genes for grain iron (GFeC), zinc (GZnC), protein (GPC), and thousand kernel weight in the RIL population.

QTL	Chr.	TraesID	Putative candidate genes (overlapping/nearby)	Molecular function
QGZn.iari-2A	2A	TraesCS2A02G192500	Alpha/beta hydrolase fold	–
QGFe.iari-2A		TraesCS2A02G192400	GIY-YIG endonuclease	DNA binding
QGpc.iari-2A		TraesCS2A02G063800	Homeobox-like domain superfamily/SANT/Myb domain	DNA binding
		TraesCS2A02G063900	Protein kinase-like domain superfamily	Protein kinase activity, ATP binding
QGFe.iari-7D.2	7D	TraesCS7D02G337800	Reticulon-like protein	–
QGZn.iari-7D.2		TraesCS7D02G337900	Ribulose-phosphate binding barrel, N-(5′ phosphoribosyl) anthranilate isomerase (PRAI)	Catalytic activity, phosphoribosylanthranilate isomerase activity
QGPC.iari-7D.2		TraesCS7D02G338100	Aluminum-activated malate transporter	Malate transport
QTkw.iari-7D		TraesCS7D02G521800	WD40/YVTN repeat-like-containing domain superfamily, U3 small nucleolar RNA-associated protein	Protein binding
		TraesCS7D02G521700	RNA-binding S4 domain superfamily, Pseudouridine synthase, catalytic domain superfamily	RNA binding, pseudouridine synthase activity
		TraesCS7D02G521500	Zinc finger, MYND-type	–
		TraesCS7D02G521400	SWEET sugar transporter	Carbohydrate transport
		TraesCS7D02G521200	Serine/threonine protein kinase domain containing protein	–
QGFe.iari-7D.1	7D	TraesCS7D02G337800	Reticulon-like protein	–
QGZn.iari-7D.1		TraesCS7D02G337900	Ribulose-phosphate binding barrel, N-(5′ phosphoribosyl) anthranilate isomerase (PRAI)	Catalytic activity, phosphoribosylanthranilate isomerase activity
QGPC.iari-7D.1		TraesCS7D02G338100	Aluminum-activated malate transporter	Malate transport
		TraesCS7D02G338200	GAT domain superfamily, ENTH/VHS	Intracellular protein transport
		TraesCS7D02G338300	Domain unknown function DUF295	–
		TraesCS7D02G338400	Peptidase C78, ubiquitin fold modifier-specific peptidase 1/2	–

along with pooled mean. Stable QTL identified in more than two environments were also reported for GPC and TKW (42, 45), GPC (39, 47, 68), GFeC and GZnC (30), and GFeC (33, 37).

Identification of the best combination of QTL effects by estimation of additive effects of the stable QTL will provide an opportunity to utilize RILs with the best combination as donors. The best combination of QTL for all the three biofortification traits in RILs was identified. There is no additional advantage of additive QTL over the individual QTL effects in the expression of GFeC. However, the QTL combination of the two QTL combinations, *viz.*, *QGZn.iari-2D.1* and *QGZn.iari-7D.1,* showed the highest average GZnC across the environments, and this combination was identified in eight RILs. For GPC, the four QTL combinations, viz., *QGPC.iari-2A*, *QGPC.iari-5B.1*, *QGPC.iari-7D.1*, and *QGPC.iari-7D.2* showed the highest average GPC across the environments, and this combination was identified in three RILs. Although numerically additive QTL effects for GZnC and GPC are higher than the individual QTL effect, statistically they are at par.

Genomic regions harboring co-located QTL for two or more traits were also identified. This information is helpful in the simultaneous improvement of multiple traits without many additional interventions. Two common genomic regions associated with different co-localized QTL governing two or more traits were identified in chromosome 7D where the genomic region flanked between *Xgwm350–AX-94958668* was associated with the maximum number of four co-localized QTL (*QGFe.iari-7D.2*, *QGZn.iari-7D.2*, *QGPC.iari-7D.2*, and *QTkw.iari-7D*). Another region flanked between *Xwmc550–Xgwm350* was also associated with three co-localized QTL (*QGFe.iari-7D.1*, *QGZn.iari-7D.1*, and *QGPC.iari-7D.1*). Some of the other studies (13, 15, 16, 37–40) have also identified such pleiotropic region(s) associated with two or more traits, namely, GFeC, GZnC, GPC, and TKW. High positive correlations observed in this study also strongly support the co-localization of genomic regions governing GFeC, GZnC, GPC, and TKW. Only few studies have reported the association of TKW in the same region as GPC or even with GZnC and GFeC (42, 44, 45, 68). All these studies reported a positive correlation for GPC and TKW. Considering the positive correlations obtained between TKW and GPC in all the environments, except Pusa Bihar_Y1, in this study, it was not surprising to find such pleiotropic QTL (in 2A and 7D chromosomes). The co-location of GFeC, GZnC, and GPC is well documented. For example, the *Gpc-B1* locus derived from *T dicoccoides* is effective in improving GFeC, GZnC, and GPC by 18, 12, and 38%, respectively (15, 16).

The *in silico* BLAST search identified various potential candidate genes underlying QTL with high PV or pleiotropic QTL for GZnC, GFeC, GPC, and TKW (**Table 6**). Various QTL identified in chromosomes 2A and 7D were located in regions where gene coding for transcription factors, transporters, and kinase-like superfamilies was present. For example, the SANT domain (coded by *TraesCS2A02G063800*) is generally found in combination with domains of Zn finger type transcription factors, such as the C2H2-type and GATA-type transcription factors, the role of which has been suggested to be in Zn uptake and homeostasis in plants (69, 70). Members of serine-threonine/protein kinase-like superfamilies are known to catalyze phosphorylation processes, thus controlling growth and development, and some are known to activate Zn channels and transporters (71). The well-characterized serine/threonine-protein kinase encoding gene in maize (*KNR6*; kernel number per row: six) has been shown to determine the kernel number and ear length in maize (72). Since both maize and wheat are members of the *Poaceae*/*Gramineae* family, it would be interesting to further investigate the functional role of the serine/threonine-protein kinase genes identified here (coded by *TraesCS7D02G521200* and *TraesCS2A02G063900*).

In the past decade, the role of various transporters has been shown in regulating mineral homeostasis in plants. These transporters play critical roles in the transport of small peptides, secondary amino acids, glutathione conjugates, and mineral uptake. Many of these transporters have proven to be involved in long-distance iron transport or signaling in Arabidopsis (73). In this regard, an important role of the aluminum-activated malate transporter (ALM1), in combination with a Zn finger-type transcription factor (STOP1), has been shown in regulating iron homeostasis in Arabidopsis (74). In both the *stop1* and *almt1* mutants, the accumulation of Fe in the root apex was found to be greatly reduced (75).

CONCLUSION

We earlier reported QTL for different biofortification traits, *viz.*, grain zinc, iron, protein, and thousand kernel weight utilizing an SSR-based genetic map of 286 RIL population developed between a cultivated bread wheat variety and a synthetic derivative. In this study, we added 736 informative SNPs and analyzed a smaller subset of the same population for these traits. New QTL were identified in this study, and many of these were found located in the D genome. The co-localization of QTL for different traits was also observed. Chromosome 7D, in particular, harbored seven and three co-localized QTL at different positions. This indicates that at least some common pathways may be involved in the uptake or accumulation of the micronutrients. Several consistent QTL over two or more environments for different traits are identified in this study as well. Best QTL combinations in RILs have been identified through additive effects, and these combinations would be potential donors to be utilized in future breeding programs. Furthermore, the identification of pleiotropic regions for GZnC, GFeC, GPC, and TKW suggests the possibilities for genetic improvement of GZnC and GFeC without compromising grain yield and GPC. Further fine mapping to identify linked or functional markers is envisaged.

DATA AVAILABILITY STATEMENT

The datasets presented in this study can be found in online repositories. The names of the repository/repositories and accession number(s) can be found in the article/**Supplementary Materials**.

AUTHOR CONTRIBUTIONS

AS conceptualized the investigation. Field experimentation at Delhi location was conducted by AS, AA, GS, and SaS at Bihar location by IS and RS, at Pantnagar by JJ and GK. Genotyping was done by SuS and GK. Statistical analysis including QTL mapping was done by NDR and DS. Original draft was prepared by GK, AS, and NDR. Review and editing was done by AS, DS, and GK. All authors contributed to the article and approved the submitted version.

FUNDING

This work was a part outcome of a DBT funded project (BT/AGR/Wheat Bioforti/PH-II/2010) granted to AS. High zinc parent received and calibration of the XRF machine with glass based standards by HarvestPlus is duly acknowledged. Training received under ICAR-World bank funded NAHEP-CAAST project by NDR to analyze the molecular data is also acknowledged. Author's also acknowledge IFPRI/HarvestPlus funding support through grant no. 2020H6458.IIW.

SUPPLEMENTARY MATERIAL

The Supplementary Material for this article can be found online at: https://www.frontiersin.org/articles/10.3389/fnut.2021.669444/full#supplementary-material

REFERENCES

1. Black RE, Victora CG, Walker SP, Bhutta ZA, Christian P, de Onis M, et al. Maternal and child undernutrition and overweight in low-income and middle-income countries. *Lancet.* (2013) 382:427–51. doi: 10.1016/S0140-6736(13)60937-X
2. de Benoist B, McLean E, Egli I, Cogswell M. *Worldwide Prevalence of Anaemia 1993–2005: WHO Global Database on Anaemia.* (2008). Available online at: http://www.who.int/nutrition/publications/micronutrients/anaemia_iron_deficiency/9789241596657/en/
3. Lopez A, Cacoub P, Macdougall IC, Peyrin-Biroulet L. Iron deficiency anaemia. *Lancet.* (2016) 387:907–16. doi: 10.1016/S0140-6736(15)60865-0
4. Holtz C, Brown KH. Assessment of the risk of zinc deficiency in populations and options for its control. *Food Nutr Bull.* (2004) 25:94–204. doi: 10.4067/S0717-75182010000200014

5. Wessells KR, Brown KH. Estimating the global prevalence of zinc deficiency: results based on zinc availability in national food supplies and the prevalence of stunting. *PLoS ONE.* (2012) 7:e50568. doi: 10.1371/journal.pone.0050568
6. Schaible UE, Kaufmann SHE. Malnutrition and infection: complex mechanisms and global impacts. *PLoS Med.* (2007) 4:e115. doi: 10.1371/journal.pmed.0040115
7. Kar BR, Rao SL, Chandramouli BA. Cognitive development in children with chronic protein energy malnutrition. *Behav Brain Funct.* (2008) 4:31. doi: 10.1186/1744-9081-4-31
8. Muller O, Krawinkel M. Malnutrition and health in developing countries. *CMAJ.* (2005) 173:279–86. doi: 10.1503/cmaj.050342
9. Pfeiffer WH, McClafferty B. HarvestPlus: breeding crops for better nutrition. *Crop Sci.* (2007) 47:88–105. doi: 10.2135/cropsci2007.09.0020IPBS
10. Grusak MA, Cakmak I. Methods to improve the crop-delivery of minerals to humans and livestock. In: Broadley MR, White PJ, editors. *Plant Nutritional Genomics*. Oxford: Blackwell Publishing Ltd. (2005). p. 265–6.
11. Cakmak I, Pfeiffer WH, Mcclafferty B. Biofortification of durum wheat with zinc and iron. *Cereal Chem J.* (2010) 87:10–20. doi: 10.1094/CCHEM-87-1-0010
12. Rasheed A, Jin H, Xiao Y, Zhang Y, Hao Y, Zhang Y, et al. Allelic effects and variations for key bread-making quality genes in bread wheat using high-throughput molecular markers. *J Cereal Sci.* (2019) 85:305–9. doi: 10.1016/j.jcs.2018.12.004
13. Velu G, Singh RP, Crespo-Herrera L, Juliana P, Dreisigacker S, Valluru R, et al. Genetic dissection of grain zinc concentration in spring wheat for mainstreaming biofortification in CIMMYT wheat breeding. *Sci Rep.* (2018) 8:13526. doi: 10.1038/s41598-018-31951-z
14. Cakmak I, Torun A, Millet E, Feldman M, Fahima T, Korol A, et al. *Triticum dicoccoides*: an important genetic resource for increasing zinc and iron concentration in modern cultivated wheat. *Soil Sci Plant Nutr.* (2004) 50:1047–54. doi: 10.1080/00380768.2004.10408573
15. Distelfeld A, Cakmak I, Peleg Z, Ozturk I, Yazici AM, Budak H, et al. Multiple QTL-effects of wheat *Gpc-B1* locus on grain protein and micronutrient concentrations. *Plant Physiol.* (2007) 129:635–43. doi: 10.1111/j.1399-3054.2006.00841.x
16. Uauy C, Distelfeld A, Fahima T, Blechl A, Dubcovsky JA. NAC gene regulating senescence improves grain protein, zinc, and iron content in wheat. *Science.* (2006) 314:1298–301. doi: 10.1126/science.1133649
17. Calderini DF, Ortiz-Monasterio I. Are synthetic hexaploids a means of increasing grain element concentrations in wheat. *Euphytica*. (2003) 134:169–78. doi: 10.1023/B:EUPH.0000003849.10595.ac
18. Hernandez-Espinos N, Mondal S, Autrique E, Gonzalez-Santoyo H, Crossa J, Huerta-Espino J, et al. Milling, processing and end-use quality traits of CIMMYT spring bread wheat germplasm under drought and heat stress. *Field Crops Res.* (2018) 215:104–12. doi: 10.1016/j.fcr.2017.10.003
19. Kumar J, Saripalli G, Gahlaut V, Goel N, Meher PK, Mishra KK, et al. Genetics of Fe, Zn, b-carotene, GPC and yield traits in bread wheat (*Triticum aestivum* L.) using multi-locus and multi-traits GWAS. *Euphytica.* (2018) 214:219. doi: 10.1007/s10681-018-2284-2
20. Studnicki M, Wijata M, Sobczynski G, Samborski S, Gozdowski D, Rozbicki J. Effect of genotype, environment and crop management on yield and quality traits in spring wheat. *J Cereal Sci.* (2016) 72:30–7. doi: 10.1016/j.jcs.2016.09.012
21. Khazratkulova S, Sharma RC, Amanov A, Ziyadullaev Z, Amanovi O, Alikulov S, et al. Genotype × environment interaction and stability of grain yield and selected quality traits in winter wheat in Central Asia. *Turk J Agric For.* (2015) 39:920–9. doi: 10.3906/tar-1501-24
22. Rozbicki J, Ceglinska A, Gozdowski D, Jakubczak M, Cacak-Pietrzak G, Madry W, et al. Influence of the cultivar, environment and management on the grain yield and bread-making quality in winter wheat. *J Cereal Sci.* (2015) 61:126–32. doi: 10.1016/j.jcs.2014.11.001
23. Saleem N, Ahmad M, Wani SA, Vashnavi R, Dar ZA. Genotype-environment interaction and stability analysis in wheat (*Triticum aestivum* L.) for protein and gluten contents. *Sci Res Essays.* (2015) 10:260–5. doi: 10.5897/SRE2015.6180
24. Velu G, Singh RP, Huerta-Espino J, Pena RJ, Arun B, Mahendru-Singh A, et al. Performance of biofortified spring wheat genotypes in target environments for grain zinc and iron concentrations. *Field Crops Res.* (2012) 137:261–7. doi: 10.1016/j.fcr.2012.07.018
25. Erba D, Alyssa H, Jessica B, Andrea B. Environmental and genotypic influences on trace element and mineral concentrations in whole meal flour of einkorn (*Triticum monococcum* L. subsp. *monococcum*). *J Cereal Sci.* (2011) 54:250–4. doi: 10.1016/j.jcs.2011.06.011
26. Liu Y, Chen Y, Yang Y, Zhang Q, Fu B, Cai J, et al. A thorough screening based on QTL controlling zinc and copper accumulation in the grain of different wheat genotypes. *Environ Sci Pollut Res.* 28:15043–54. (2020). doi: 10.1007/s11356-020-11690-3
27. Liu J, Wu B, Singh RP, Velu G. QTL mapping for micronutrients concentration and yield component traits in a hexaploid wheat mapping population. *J Cereal Sci.* (2019) 88:57–64. doi: 10.1016/j.jcs.2019.05.008
28. Arora S, Cheema J, Poland J, Uauy C, Chhuneja P. Genome-wide association mapping of grain micronutrients concentration in *Aegilops tauschii*. *Front Plant Sci.* (2019) 10:54. doi: 10.3389/fpls.2019.00054
29. Velu G, Tutus Y, Gomez-Becerra HF, Hao Y, Demir L, Kara R, et al. QTL mapping for grain zinc and iron concentrations and zinc efficiency in a tetraploid and hexaploid wheat mapping populations. *Plant Soil.* (2017) 411:81–99. doi: 10.1007/s11104-016-3025-8
30. Crespo-Herrera LA, Govindan V, Stangoulis J, Hao Y, Singh RP. QTL mapping of grain Zn and Fe concentrations in two hexaploid wheat RIL populations with ample transgressive segregation. *Front Plant Sci.* (2017) 8:1800. doi: 10.3389/fpls.2017.01800
31. Tiwari C, Wallwork H, Arun B, Mishra VK, Velu G, Stangoulis J, et al. Molecular mapping of quantitative trait loci for zinc, iron and protein content in the grains of hexaploid wheat. *Euphytica.* (2016) 207:563–70. doi: 10.1007/s10681-015-1544-7
32. Pu Z-e, Ma YU, He Q-y, Chen G-y, Wang J-r, Liu Y-x, et al. Quantitative trait loci associated with micronutrient concentrations in two recombinant inbred wheat lines. *J Integr Agric.* (2014) 13:2322–9. doi: 10.1016/S2095-3119(13)60640-1
33. Srinivasa J, Arun B, Mishra VK, Singh GP, Velu G, Babu R, et al. Zinc and iron concentration QTL mapped in a *Triticum spelta* × *T. aestivum* cross. *Theor Appl Genet.* (2014) 127:1643–51. doi: 10.1007/s00122-014-2327-6
34. Roshanzamir H, Kordenaeej A, Bostani A. Mapping QTLs related to Zn and Fe concentrations in bread wheat (*Triticum aestivum*) grain using microsatellite markers. *Iran J Genet Plant Breed.* (2013) 2:551–6.
35. Xu Y, Diaoguo A, Dongcheng L, Aimin Z, Hongxing X, Bin L. Molecular mapping of QTLs for grain zinc, iron and protein concentration of wheat across two environments. *Field Crops Res.* (2012) 38:57–62. doi: 10.1016/j.fcr.2012.09.017
36. Peleg Z, Cakmack I, Ozturk L, Yazici A, Budak H, Korol AB, et al. Quantitative trait loci conferring grain mineral nutrient concentrations in durum wheat × wild emmer wheat RIL population. *Theor Appl Genet.* (2009) 119:353–69. doi: 10.1007/s00122-009-1044-z
37. Tiwari VK, Rawat N, Chhuneja P, Neelam K, Aggarwal R, Randhawa GS, et al. Mapping of quantitative trait loci for grain iron and zinc concentration in diploid A genome wheat. *J Hered.* (2009) 100:771–6. doi: 10.1093/jhered/esp030
38. Genc Y, Verbyla A, Torun A, Cakmak I, Willsmore K, Wallwork H, et al. Quantitative trait loci analysis of zinc efficiency and grain zinc concentration in wheat using whole genome average interval mapping. *Plant Soil.* (2009) 314:49–66. doi: 10.1007/s11104-008-9704-3
39. Zhou Z, Shi X, Zhao G, Qin M, Ibba MI, Wang Y, et al. Identification of novel genomic regions and superior alleles associated with Zn accumulation in wheat using a genome-wide association analysis method. *Int J Mol Sci.* (2020) 21:1928. doi: 10.3390/ijms21061928
40. Hao Y, Govindan V, Roberto J, Pen Sukhwinder S, Ravi PS. Genetic loci associated with high grain zinc concentration and pleiotropic effect on kernel weight in wheat (*Triticum aestivum* L.). *Mol Breed.* (2014) 34:1893–902. doi: 10.1007/s11032-014-0147-7
41. Shi R, Li H, Tong Y, Jing R, Zhang F, Zou C. Identification of quantitative trait locus of zinc and phosphorus density in wheat (*Triticum aestivum* L.) grain. *Plant Soil.* (2008) 306:95–104. doi: 10.1007/s11104-007-9483-2
42. Fatiukha A, Filler N, Lupo I, Lidzbarsky G, lymiuk V, Korol AB, et al. Grain protein content and thousand kernel weight QTLs identified in a durum ×

wild emmer wheat mapping population tested in five environments *Theor Appl Genet.* (2020) 133:119–31. doi: 10.1007/s00122-019-03444-8
43. Guo Y, Zhang G, Guo B, Qu C, Zhang M, Kong F, et al. QTL mapping for quality traits using a high-density genetic map of wheat. *PLoS ONE.* (2020) 15:e0230601. doi: 10.1371/journal.pone.0230601
44. Giancaspro A, Giove SL, Zacheo SA, Blanco A, Gadaleta A. Genetic variation for protein content and yield-related traits in a durum population derived from an inter-specific cross between hexaploid and tetraploid wheat cultivars. *Front Plant Sci.* (2019) 10:1509. doi: 10.3389/fpls.2019.01509
45. Goel S, Singh K, Singh B, Grewal S, Dwivedi N, Alqarawi AA, et al. Analysis of genetic control and QTL mapping of essential wheat grain quality traits in a recombinant inbred population. *PLoS ONE.* (2019) 14:e0200669. doi: 10.1371/journal.pone.0200669
46. Marcotuli I, Gadaleta A, Mangini G, Signorile AM, Zacheo SA, Blanco A, et al. Development of a high-density SNP-based linkage map and detection of QTL for β-glucans, protein content, grain yield per spike and heading time in durum wheat. *Int J Mol Sci.* (2017) 18:1329. doi: 10.3390/ijms18061329
47. Mahjourimajd S, Taylor J, Rengel Z, Khabaz-Saberi H, Kuchel H, Okamoto M, et al. The genetic control of grain protein content under variable nitrogen supply in an Australian wheat mapping population. *PLoS ONE.* (2016) 11:e0159371. doi: 10.1371/journal.pone.0159371
48. Sun X, Wu K, Zhao Y, Qian Z, Kong F, Guo Y, et al. Molecular genetic analysis of grain protein content and tour whiteness degree using RILs in common wheat. *J Genet.* (2016) 95:317–24. doi: 10.1007/s12041-016-0639-9
49. Elangovan M, Dholakia BB, Rai R, Lagu MD, Tiwari R, Gupta RK, et al. Mapping QTL associated with agronomic traits in bread wheat (*Triticum aestivum* L.). *J Wheat Res.* (2011) 3:14–23.
50. Sun XC, Marza F, Ma HX, Carver BF, Bai GH. Mapping quantitative trait loci for quality factors in an inter-class cross of US and Chinese wheat. *Theor Appl Genet.* (2010) 120:1041–51. doi: 10.1007/s00122-009-1232-x
51. Zhang H, Chen J, Li R, Deng Z, Zhang K, Liu B, et al. Conditional QTL mapping of three yield components in common wheat (*Triticum aestivum* L.). *Crop J.* (2016) 4:220–8. doi: 10.1016/j.cj.2016.01.007
52. Wei L, Bai S, Li J, Hou X, Wang X, Li H, et al. QTL positioning of thousand wheat grain weight in qaidam basin. *Open J Genet.* (2014) 4:239–44. doi: 10.4236/ojgen.2014.43024
53. Mergoum M, Harilal VE, Simsek S, Alamri MS, Schatz BG, Kianian SF, et al. Agronomic and quality QTL mapping in spring wheat. *J Plant Breed Genet.* (2013) 1:19—33.
54. Nezhad KZ, Weber WE, Roder MS, Sharma S, Lohwasser U, Meyer RC, et al. QTL analysis for thousand-grain weight under terminal drought stress in bread wheat (*Triticum aestivum* L.). *Euphytica.* (2012) 186:127–38. doi: 10.1007/s10681-011-0559-y
55. Krishnappa G, Singh AM, Chaudhary S, Ahlawat AK, Singh SK, Shukla RB, et al. Molecular mapping of the grain iron and zinc concentration, protein content and thousand kernel weight in wheat (*Triticum aestivum* L.). *PLoS ONE.* (2017) 12:e0174972. doi: 10.1371/journal.pone.0174972
56. Murray MG, Thompson WF. Rapid isolation of high molecular weight plant DNA. *Nucleic Acids Res.* (1980) 8:4321–5. doi: 10.1093/nar/8.19.4321
57. Roder MS, Korzun V, Wendehake K, Plaschke J, Tixer M-H, Leroy P, et al. A microsatellite map of wheat. *Genetics.* (1998) 149:2007–23. doi: 10.1093/genetics/149.4.2007
58. Somers DJ, Isaac P, Edwards K. A high-density microsatellite consensus map for bread wheat (*Triticum aestivum* L.). *Theor Appl Genet.* (2004) 109:1105–14. doi: 10.1007/s00122-004-1740-7
59. Khokhar JS, Sareen S, Tyagi BS, Singh G, Wilson L, King IP, et al. Variation in grain Zn concentration, and the grain ionome, in field-grown Indian wheat. *PLoS ONE.* (2018) 13:e0192026. doi: 10.1371/journal.pone.0192026
60. Terasawa Y, Ito M, Tabiki T, Nagasawa K, Hatta K, Nishio Z. Mapping of a major QTL associated with protein content on chromosome 2B in hard red winter wheat (*Triticum aestivum* L.). *Breed Sci.* (2016) 66:471–80. doi: 10.1270/jsbbs.16026
61. Chao S, Zhang W, Akhunov E, Sherman J, Ma Y, Luo M-C, et al. Analysis of gene-derived SNP marker polymorphismin US wheat (*Triticum aestivum* L.) cultivars. *Mol Breed.* (2009) 23:23–33. doi: 10.1007/s11032-008-9210-6
62. Caldwell KS, Dvorak J, Lagudah ES, Akhunov E, Luo MC, Wolters P, et al. Sequence polymorphism in poly-ploid wheat and their D-genome diploid ancestor. *Genetics.* (2004) 167:941–7. doi: 10.1534/genetics.103.016303
63. Masood R, Ali N, Jamil M, Bibi K, Rudd JC, Mujeeb-Kazi A. Novel genetic diversity of the Alien D-genome synthetic hexaploid wheat (2n=6x=42, AABBDD) germplasm for various phenology traits. *Pak J Bot.* (2016) 48:2017–24.
64. Deynze AEV, Dubcovsky J, Gill KS, Nelson JC, Sorrells ME, Dvorak J, et al. Molecular-genetic maps for group 1 chromosomes of Triticeae species and their relation to chromosomes in rice and oat. *Genome.* (1995) 38:45–59. doi: 10.1139/g95-006
65. Rosyara U, Kishii M, Payne T, Sansaloni C-P, Singh RP, Braun H-J, et al. Genetic contribution of synthetic hexaploid wheat to CIMMYT's spring bread wheat breeding germplasm. *Sci Rep.* (2019) 9:12355. doi: 10.1038/s41598-019-47936-5
66. Bhatta M, Morgounov A, Belamkar V, Poland J, Baenziger PS. Unlocking the novel genetic diversity and population structure of Synthetic Hexaploid wheat. *BMC Genomics.* (2018) 19:591. doi: 10.1186/s12864-018-4969-2
67. Zhang P, Dreisigacker S, Melchinger AE, Reif JC, MujeebKazi A, Ginkel M-V, et al. Quantifying novel sequence variation and selective advantage in synthetic hexaploid wheats and their backcross-derived lines using SSR markers. *Mol. Breed.* (2005) 15:1–10. doi: 10.1007/s11032-004-1167-5
68. Cui F, Fan X, Chen M Zhang N, Zhao C, Zhang W, et al. QTL detection for wheat kernel size and quality and the responses of these traits to low nitrogen stress. *Theor Appl Genet.* (2016) 129:469–84. doi: 10.1007/s00122-015-2641-7
69. Milner MJ, Pence NS, Liu J, Kochian LV. Identification of a novel pathway involving a GATA transcription factor in yeast and possibly in plant Zn uptake and homeostasis. *J Integr Plant Biol.* (2014) 56:271–80. doi: 10.1111/jipb.12169
70. Lyons TJ, Gasch AP, Gaither LA, Botstein D, Brown PO, Eide DJ. Genome-wide characterization of the Zap1p zinc-responsive regulon in yeast. *Proc Natl Acad Sci USA.* (2000) 97:7957–62. doi: 10.1073/pnas.97.14.7957
71. Thingholm TE, Ronnstrand L, Rosenberg PA. Why and how to investigate the role of protein phosphorylation in ZIP and ZnT zinc transporter activity and regulation. *Cell Mol Life Sci.* (2020) 77:3085–102. doi: 10.1007/s00018-020-03473-3
72. Jia H, Li M, Li W, Liu L, Jian Y, Yang Z, et al. A serine/threonine protein kinase encoding gene KERNEL NUMBER PER ROW6 regulates maize grain yield. *Nat. Commun.* (2020) 11:988. doi: 10.1038/s41467-020-14746-7
73. Stacey MG, Patel A, McClain WE, Mathieu M, Remley M, Rogers EE, et al. The Arabidopsis AtOPT3 protein functions in metal homeostasis and movement of iron to developing seeds. *Plant Physiol.* (2008) 146:589–601. doi: 10.1104/pp.107.108183
74. Wang X, Wang Z, Zheng Z, Dong J, Song L, Sui L, et al. Genetic dissection of Fe-dependent signaling in root developmental responses to phosphate deficiency. *Plant Physiol.* (2019) 179:300–16. doi: 10.1104/pp.18.00907
75. Balzergue C, Dartevelle T, Godon C, Laugier E, Meisrimler C, Teulon J-M, et al. Low phosphate activates STOP1-ALMT1 to rapidly inhibit root cell elongation. *Nat Commun.* (2017) 8:15300. doi: 10.1038/ncomms15300

Conflict of Interest: The authors declare that the research was conducted in the absence of any commercial or financial relationships that could be construed as a potential conflict of interest.

frontiers in Nutrition

ORIGINAL RESEARCH
published: 28 June 2021
doi: 10.3389/fnut.2021.697817

Foliar Zinc Application to Wheat May Lessen the Zinc Deficiency Burden in Rural Quzhou, China

*Bao-Gang Yu, Yu-Min Liu, Xiu-Xiu Chen, Wen-Qing Cao, Tong-Bin Ding and Chun-Qin Zou**

Key Laboratory of Plant-Soil Interactions, Ministry of Education, College of Resources and Environmental Sciences, National Academy of Agriculture Green Development, China Agricultural University, Beijing, China

Zinc (Zn) malnutrition is a common health problem, especially in developing countries. The human health and economic benefits of the replacement of conventional flour with Zn-biofortified wheat flour in rural household diets were assessed. One hundred forty-five wheat flour samples were collected from rural households in Quzhou County. Then, field experiments were conducted on wheat at two Zn levels (0 and 0.4% $ZnSO_4 \cdot 7H_2O$ foliar application) under 16 diverse agricultural practices in Quzhou County. Foliar Zn application significantly increased the Zn concentration and bioavailability in wheat grain and flour. If rural households consumed Zn-biofortified flour instead of self-cultivated flour or flour purchased from supermarkets, 257–769 or 280–838, 0.46–1.36 million or 0.50–1.49 million disability-adjusted life years (DALYs) lost, respectively, could be saved in Quzhou County and China. Amounts of 2.3–12.0 million and 5.5–22.6 billion RMB could be obtained via Zn-biofortified flour in Quzhou County and China, respectively. The current study indicates that Zn-biofortified flour via foliar Zn application is a win-win strategy to maintain the yield and combat human Zn deficiency in rural households in China. More health and economic benefits could be obtained in rural household dependent on wheat flour purchased from supermarkets than in those dependent on self-cultivated wheat flour.

Keywords: agronomic biofortification, zinc, wheat, health benefits, DALYs, Quzhou county

OPEN ACCESS

Edited by:
Velu Govindan, International Maize and Wheat Improvement Center, Mexico

Reviewed by:
Shahid Hussain, Bahauddin Zakariya University, Pakistan
Raheela Rehman, International Maize and Wheat Improvement Center (CIMMYT), Pakistan

****Correspondence:***
Chun-Qin Zou
zcq0206@cau.edu.cn

Specialty section:
This article was submitted to Nutrition and Food Science Technology, a section of the journal Frontiers in Nutrition

Received: *20 April 2021*
Accepted: *02 June 2021*
Published: *28 June 2021*

Citation:
Yu B-G, Liu Y-M, Chen X-X, Cao W-Q, Ding T-B and Zou C-Q (2021) Foliar Zinc Application to Wheat May Lessen the Zinc Deficiency Burden in Rural Quzhou, China. Front. Nutr. 8:697817. doi: 10.3389/fnut.2021.697817

INTRODUCTION

As an essential micronutrient, zinc (Zn) plays a vital role in crop production and human nutrition. At present, Zn deficiency, also called hidden hunger, is a common public issue worldwide, contributing to many health problems (1). Zn deficiency is one of the five leading risk factors resulting in disease and death, and one-third of the global population suffers from Zn malnutrition (2). In China, more than 86 million people suffered from an insufficient Zn intake, and the development of 10 million children (<5 years) was stunted (3).

The widespread occurrence of Zn malnutrition in humans mainly arises from a low dietary intake of Zn (4). Currently, cereal crops are a major dietary source of calories, protein, and Zn worldwide, especially in developing countries (5). However, approximately half of the soils in cereal cultivation is Zn deficient, resulting in an inadequate Zn content in cereal foods to satisfy the human demand (1).

As one of the three major cereal crops, China ranks at the top in terms of the cultivation area and annual production of wheat globally, and wheat is widely used in staple foods and livestock

feed, especially in rural areas (6). However, the average Zn concentration in wheat grain is only 23.3 mg kg^{-1} in China, indicating a wide gap to the target value of 40 mg kg^{-1} (7). In addition, the Zn concentration in wheat flour is positively correlated with the Zn concentration in wheat grain. However, during grain milling, most Zn is typically lost and bound to phytic acid (PA), which further leads to a marked reduction in the Zn intake (8). Therefore, there is an urgent need to improve the Zn concentration and bioavailability in wheat grain and flour to minimize Zn malnutrition.

In recent years, nutritionists have proposed many strategies to overcome Zn deficiency, such as dietary diversification, food fortification, and supplementation. However, these strategies are difficult to implement in developing countries due to the high cost and other social reasons (9). Biofortification-a new strategy to improve the micronutrient contents in edible parts-is potentially more applicable than are other strategies (1). Previous studies have suggested that agronomic biofortification (i.e., fertilization) is a highly cost-effective strategy to improve human health in the short term over genetic biofortification (10). Among agronomic biofortification techniques, it has been well-established, based on a variety of studies, that foliar Zn application is a much more effective method than soil Zn application in Zn concentration enhancement, and the increase in the Zn concentration in wheat grain and flour via foliar Zn application is nearly 2-fold (11, 12). However, many studies have primarily focused on a given field condition, and there may be a higher practical significance to analyze the effects of foliar Zn application on the Zn concentration and bioavailability in wheat grain and flour under diverse agricultural practices (soil properties, wheat cultivar, fertilization, and management).

Quzhou County is located in Handan city, Hebei Province, China, and 97% of the total population in Quzhou County is engaged in agriculture (13). The cultivated land area of winter wheat is 216.8 km^2 in Quzhou County (41% of the total cultivated land area), consisting of 10 townships and 342 administrative villages. However, a previous survey has revealed that 39% of the children in Handan city suffers from Zn malnutrition (14). As an important county of wheat production in Handan city, the Zn deficiency value could increase in Quzhou County, especially in rural households mainly consuming self-cultivated wheat, due to the low soil DTPA-Zn concentration (15) and relatively high phosphorus (P) fertilization level (16). Therefore, it is feasible and meaningful to study the health impact of the agronomic Zn biofortification of wheat in Quzhou County.

The objectives of this study were (1) to analyze the current Zn intake based on samples of the wheat flour consumed daily in rural households in Quzhou County, (2) to study the effects of foliar Zn application on the Zn concentration and bioavailability in wheat grain and flour under diverse agricultural practices in Quzhou County, and (3) to comprehensively assess the health and economic impacts of the replacement of conventional wheat flour with Zn-biofortified flour in rural household diets in Quzhou County and China via scenario simulation.

MATERIALS AND METHODS

Field Locations and Experimental Design

Field experiments were conducted at 16 locations in Quzhou County (114°50′30″E−115°13′30″E, 36°34′45″N−36°57′57″N) in the North China Plain (**Figure 1**). Quzhou County contains a typical calcareous alluvial soil and has a subtropical humid monsoon climate, with an average annual temperature and precipitation of 13.4°C and 534.9 mm, respectively (13). Information on the NPK fertilizers, soil properties, and wheat cultivars used at each location is listed in **Supplementary Table 1**. The winter wheat-summer maize rotation system was applied at all 16 locations.

Each location included two treatments: the control treatment (conventional farmer practices with no Zn application) and foliar Zn application (0.4% $ZnSO_4 \cdot 7H_2O$, w/v). Foliar Zn was applied twice as follows: the first spraying was conducted at the early milk stage, and the second spraying occurred a week later. A Tween (0.01%, v/v) solution was applied at 800 L ha^{-1} in the foliar Zn application treatment. Spraying was conducted on cloudy days or after sunset under windless conditions across all 16 locations. The area of each plot was 100 m^2 at all 16 locations. In addition to foliar Zn application, routine cropping practices were implemented in the present study, including various seeding rates, fertilizer application, herbicide sprays, and irrigation.

Sample Collection and Analysis

At maturity in June 2019, 3 of 3-m^2 area in each plot of grains were collected to determine the yield and nutrient concentrations. The harvested wheat grain samples were washed three times with tap and distilled water. A subsample was retrieved from each treatment, oven dried at 60–65°C to a constant weight and ground into powder with a stainless-steel grinder. Another wheat grain subsample was milled into flour with a Buhler experimental mill (MLU 220, Uzvil, Switzerland), and the rate of flour extraction was ∼75%, which is similar to the general flour extraction rate in China market (17).

A total of 145 wheat flour samples was also randomly collected from 21 villages (including the 16 test locations) to estimate the current Zn intake via wheat flour consumption in the rural households in Quzhou County. We divided the sources of wheat flour into two groups: (1) flour milled from wheat grain that was self-cultivated by the rural households ($n = 124$). (2) Flour purchased from the supermarket by the rural households ($n = 21$). These two wheat flour types were separately consumed by the rural households in Quzhou County as part of their daily diets.

The wheat grain and flour samples were digested with 6 mL of HNO_3 and 2 mL of H_2O_2 in a microwave-accelerated reaction system (CEM, Matthews, NC, USA). The micronutrient concentrations in the digested solutions were determined via inductively coupled plasma optical emission spectroscopy (ICP-OES, OPTIMA 3300 DV, Perkin-Elmer, USA). Standard wheat grain material (IPE182) was acquired from the Wageningen Evaluation Programs for Analytical Laboratories (WEPAL, Wageningen University, the Netherlands) and used to ensure consistency and quality. The PA concentrations in the wheat grain and flour samples were analyzed according to a previous

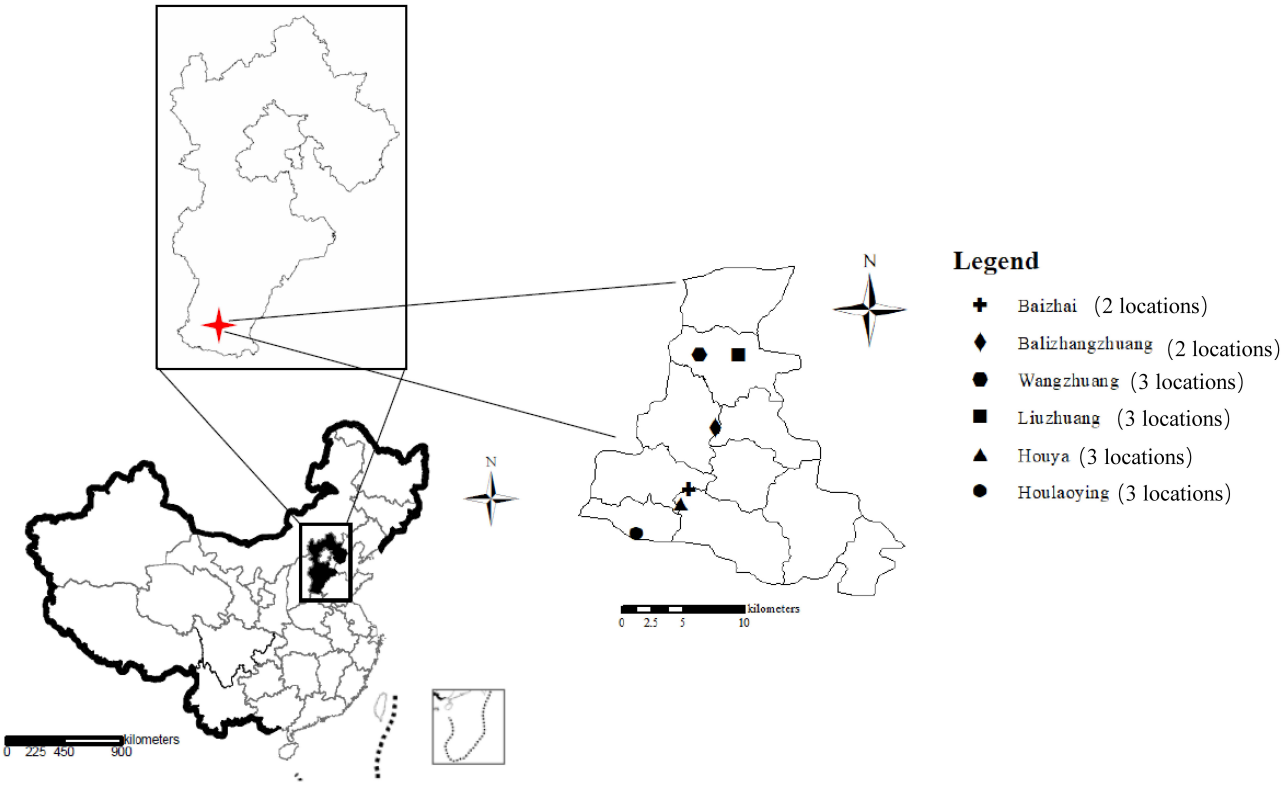

FIGURE 1 | The locations where the field experiments were conducted in Quzhou County, Hebei Province of China. Sixteen experimental locations are located in the 6 villages in Quzhou County.

study (18). Soil samples (0–20 cm) were also collected at each location to analyze the pH and available Zn and P concentrations after air drying and passing through a 1-mm plastic sieve. The soil pH (water/soil, 2.5:1) was determined with a pH meter (PB-10, Sartorius, GER) (19). The soil available Zn concentration (DTPA-Zn) was analyzed via ICP-OES (OPTIMA 3300 DV, Perkin-Elmer, USA) after extraction with 5 mmol L^{-1} diethylene triamine pentaacetic acid (DTPA) (20). The soil available P (Olsen-P) concentration was measured according Olsen (21).

Estimated Zn Bioavailability

A trivariate mathematical model of Zn absorption was adopted to predict the Zn bioavailability (22):

$$TAZ = 0.5 \times 65 \times 100 \times \left\{ A_{MAX} + TDZ + K_R \times \left(1 + \frac{TDP}{K_P}\right) - \sqrt{\left(A_{MAX} + TDZ + K_R \times \left(1 + \frac{TDP}{K_P}\right)\right)^2 - 4 \times A_{MAX} \times TDZ} \right\}$$

where TAZ is the total daily absorbed Zn (mg Zn d^{-1}), TDZ and TDP are the total daily dietary Zn (mmol Zn day^{-1}) and PA (mmol PA day^{-1}), respectively, AMAX is the maximum Zn absorption (0.091), KR is the equilibrium dissociation constant of the Zn-receptor binding reaction (0.680), and KP is the equilibrium dissociation constant of the Zn-PA binding reaction (0.033) (23), while the TAZ model is based on daily wheat grain and flour consumption (300 g day^{-1}) as the sole source of Zn and phytate for adults (24), which is referred to as the estimated Zn bioavailability.

Potential Health and Economic Benefits of Zn-Biofortified Wheat Flour

The framework of the disability-adjusted life years (DALYs) is an *ex ante* assessment tool to estimate the burden of micronutrient malnutrition and the health impact of micronutrient-biofortified wheat flour (25). The current health burden (the DALYs lost) was calculated based on a previous study (26). Infants numbered ∼0.58 thousand and 13.8 million, and children (1–5 years old) numbered 3.8 thousand and 76.5 million in Quzhou County and China, respectively (27). The total DALYs lost (infants and children) due to human Zn deficiency in Quzhou County and China were 0.2 thousand and 3.7 million years, respectively. The potential health benefits (the DALYs saved) of Zn-biofortified wheat flour were calculated with a modified method based on the increased Zn bioavailability rather than the increased Zn concentration (28). The status quo of the daily Zn intake was 4.90 and 6.00 mg day^{-1} for infants and children, respectively (29). Based on the daily consumption level of wheat flour of 300 g d^{-1} for Chinese adults, infants consume 75 g each day, and children consume 150 g each day (28). The daily Zn intake through Zn-biofortified wheat flour was calculated as the sum of the current

daily Zn intake and the increased TAZ level. We assumed that Zn-biofortified wheat flour replaced the self-cultivated flour or the flour purchased by rural households, and no other dietary aspects were changed. Two coverage rates (20% under a pessimistic scenario and 60% under an optimistic scenario) were defined in this study. To simulate the potential impact of the agronomic Zn biofortification of wheat flour in Quzhou County and China, the health benefits (the DALYs saved) of biofortified wheat flour were calculated via the method of Steur et al. (26).

The following equation was adopted to calculate the economic benefit of Zn-biofortified wheat flour:

Economic benefit = total DALYs saved × PCNI – Zn fertilizer cost.

where PCNI is the per capita net income of China based on a previous study (30). Pesticide foliar spraying is a common practice in wheat cropping systems in China, and the effect of foliar Zn application combined with pesticide spraying on the grain Zn concentration is similar to the effect of foliar Zn application alone, which could greatly reduce the labor requirements (31). Hence, in the current study, we only considered the Zn fertilizer cost (90 RMB ha^{-1}) according to Wang et al. (31).

Statistical Analysis

Excel 2010 (Microsoft, USA) and SPSS software (version 26.0) were used for the calculations and statistical analysis. The effects of foliar Zn application on the Zn and PA concentrations and the estimated Zn bioavailability in wheat grain and flour were assessed via one-way analysis of variance (ANOVA) followed by independent *t*-tests ($P < 0.05$). Similarly, the average of the above three parameters (the Zn and PA concentrations and the estimated Zn bioavailability) for the two sources of wheat flour collected from rural households were also compared via independent *t*-tests ($P < 0.05$).

RESULTS

Grain Yield

Foliar Zn application imposed no significant effects on the wheat grain yield at any location (**Figure 2**). The average grain yields were 6.3 and 6.5 t ha^{-1} under the control and foliar Zn treatments, respectively.

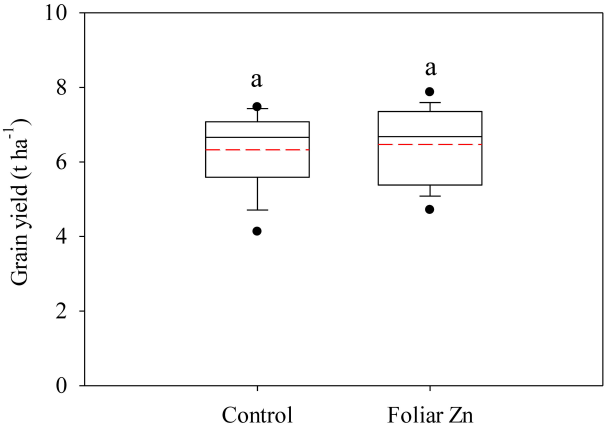

FIGURE 2 | Grain yield (14% water) as affected by foliar Zn application in Quzhou County. The solid and red dashed lines indicate the median and mean values, respectively. The same lowercase letter indicates no significant difference between the foliar Zn application levels via independent *t*-tests at the $P < 0.05$ level.

Zinc and PA Concentrations and Estimated Zn Bioavailability in the Wheat Flour Collected From Rural Households

There was a large variation in the Zn and PA concentrations and estimated Zn bioavailability in the wheat flour samples irrespective of the source. The Zn concentration in the self-cultivated wheat flour was significantly higher than that in the wheat flour purchased from supermarkets. However, no significant differences occurred in the PA concentration and estimated Zn bioavailability between the two sources of wheat flour (**Table 1**).

Zinc and PA Concentrations and Estimated Zn Bioavailability in the Wheat Grain and Flour Obtained From the Field Experiment

Without Zn application, the average Zn concentration in wheat grain and flour was 21.8 and 8.5 mg kg^{-1}, respectively (**Figure 3A**). Foliar Zn application significantly increased the Zn concentration in wheat grain and flour. On average, the increases in the Zn concentration in wheat grain and flour caused by foliar Zn application were 97.7 and 68.2%, respectively (**Figure 3A**). Among the 16 experimental locations, the target grain Zn concentration (40 mg kg^{-1}) was obtained at 12 field locations due to foliar Zn application. Foliar Zn application imposed no significant effects on the PA concentration in wheat grain and flour, and the PA concentration in wheat grain was much higher than that in flour across the 16 locations (**Figure 3B**). Foliar Zn application also significantly increased the Zn bioavailability in wheat grain and flour (**Figure 3C**). On average, the estimated Zn bioavailability in wheat grain and flour increased from 0.73 to 1.38 mg Zn d^{-1} and from 0.90 to 1.71 mg Zn d^{-1}, respectively, via foliar Zn application, resulting in 1.89-fold and 1.90-fold increases, respectively (**Figure 3C**).

Health and Economic Impacts of Zn-Biofortified Wheat Flour in Quzhou County and China

Compared to the self-cultivated wheat flour or the wheat flour purchased by rural households, Zn-biofortified flour increased the daily Zn intake, the percentage of the recommended intake, the DALYs saved for both infants and children, and the potential economic income (**Table 2**). Under the pessimistic scenario (20% coverage rate of Zn-biofortified wheat flour), compared to the self-cultivated flour or the flour purchased by rural households, Zn-biofortified wheat flour reduced 12.93 or 14.09% and 12.33 or 13.43% of the current health burden in Quzhou County and China, respectively (**Table 2**). Under the optimistic scenario (60%

TABLE 1 | Zinc (Zn) and phytic acid (PA) concentrations and estimated Zn bioavailability in the wheat flour collected from the rural households in Quzhou County.

Parameters	Source of flour	Sample number	Minimum	Maximum	Median	Mean[a]	Coefficient of variation (%)
Zn concentration (mg kg^{-1})	Self-cultivated	124	4.03	10.94	8.34	8.28a	15.4
	Supermarkets	21	4.56	8.23	7.02	7.05b	13.3
PA concentration (g kg^{-1})	Self-cultivated	124	1.30	3.93	2.83	2.79a	24.3
	Supermarkets	21	1.37	3.74	2.57	2.51a	26.8
Estimated Zn bioavailability (mg Zn d^{-1})	Self-cultivated	124	0.59	1.57	0.85	0.86a	21.2
	Supermarkets	21	0.52	1.30	0.75	0.79a	27.9

[a]*Means with the same letters indicate no significant difference between two sources of flour at the P < 0.05 level via independent t-tests.*

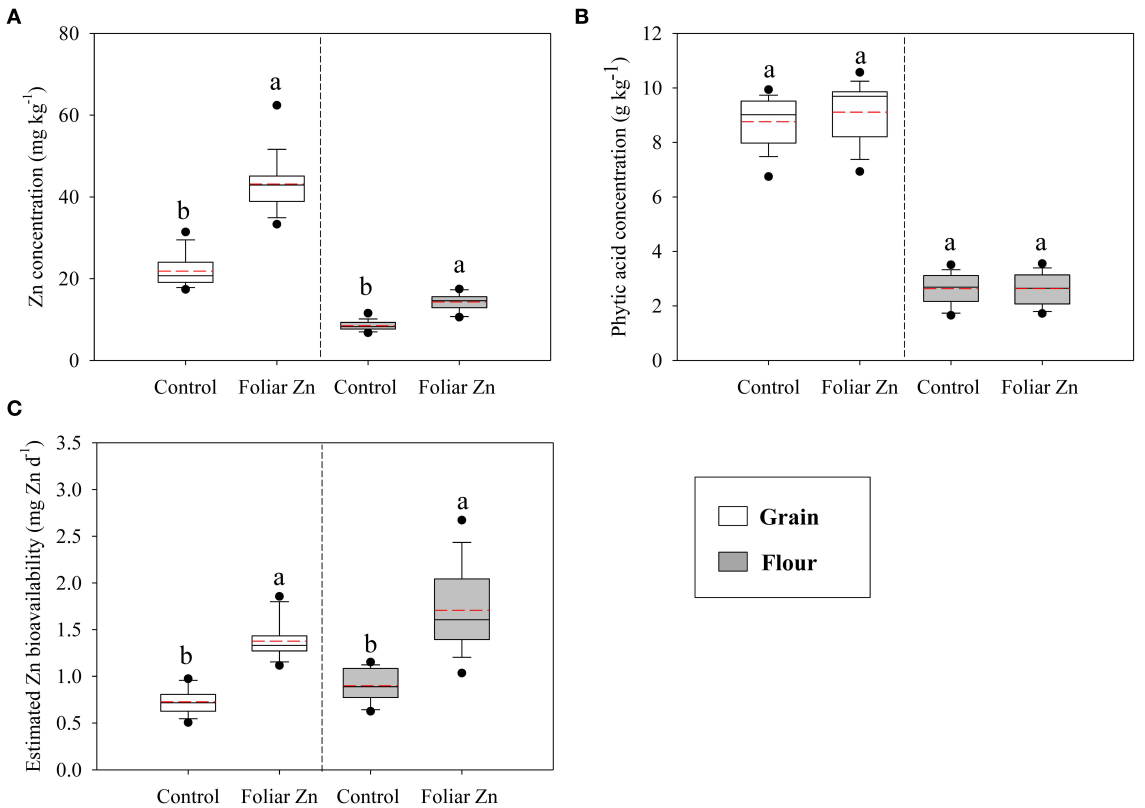

FIGURE 3 | Zinc (Zn) **(A)** and phytic acid **(B)** concentrations and estimated Zn bioavailability **(C)** in wheat grain and flour as affected by foliar Zn application in Quzhou County. The solid and red dashed lines indicate the median and mean values, respectively. The same lowercase letter indicates no significant difference between the foliar Zn application levels via independent *t*-tests at the $P < 0.05$ level. The rate of flour extraction was around 75%.

coverage rate of Zn-biofortified wheat flour), in contrast to the self-cultivated flour or the flour purchased by rural households, Zn-biofortified wheat flour also saved the current health burden in Quzhou County and China, ranging from 38.67 to 42.15% and 38.71 to 40.18%, respectively (**Table 2**).

DISCUSSION

Zinc Concentration and Bioavailability in Wheat Flour Consumed by the Rural Households in Quzhou County

In the current study, the Zn concentration in the wheat flour cultivated by farmers exhibited a large variation, which was consistent with Ashin et al. (32). The variations are attributed to the different agricultural management practices, yields, soil fertilities, wheat cultivars, etc. The average Zn concentration in the wheat flour self-cultivated by the rural households in Quzhou County was 8.3 mg kg^{-1} (**Table 1**). This value was obviously lower than the results of Wang et al. (33). A possible reason for the relatively low Zn concentration in the wheat flour self-cultivated by the rural households in Quzhou County may be the low soil DTPA-Zn concentration (average: 0.82 mg kg^{-1}) (15) and high P application level (average: 62.4 kg P ha^{-1}) (16), which limits the uptake, translocation, and remobilization of Zn to wheat grain (28, 34). Wei and Cen (35) reported that the average Zn concentration in wheat flour purchased from supermarkets

TABLE 2 | Health and economic impacts of Zn-biofortified wheat flour on the rural households in Quzhou County and China.

Parameters		Flour from Self-cultivated		Flour from supermarket	
		Pessimistic scenario	Optimistic scenario	Pessimistic scenario	Optimistic scenario
Daily Zn intake (mg day^{-1}, status quo)					
Infants		4.90	4.90	4.90	4.90
Children		6.00	6.00	6.00	6.00
Daily Zn intake with foliar Zn application (mg day^{-1})					
Infants		5.66	5.66	5.76	5.76
Children		6.76	6.76	6.86	6.86
% of recommended nutrition intake with foliar Zn application (RNI)					
Infants		82.03	82.03	83.48	83.48
Children		84.50	84.50	85.75	85.75
Health impact ("disability-adjusted life years" saved)					
Quzhou	Infants	40	120	44	131
	Children	217	649	237	707
	Total	257	769	280	838
	% reduction in the current health burden	12.93	38.67	14.09	42.15
China	Infants	117,924	353,772	128,389	385,168
	Children	338,208	1,010,403	368,445	1,101,391
	Total	456,132	1,364,175	496,835	1,486,560
	% reduction in the current health burden	12.33	36.87	13.43	40.18
Economic impact (RMB)					
Quzhou		2.3E+06	1.1E+07	2.7E+06	1.2E+07
China		5.5E+09	2.1E+10	6.1E+09	2.3E+10

was 5.4 mg kg^{-1} (n = 188), which was lower than our result of 7.1 mg kg^{-1}. Different manufacturers and production and processing methods may explain this difference. In addition, the current study demonstrated that the Zn concentration in the flour purchased from supermarkets was lower than that in the flour self-cultivated by the rural households. The reason for this may be that the extraction rate of the flour purchased from supermarkets is lower than that of the flour self-cultivated by rural households, and more Zn is lost during milling (36).

Considering Zn homeostasis in human intestines, the Zn bioavailability in wheat flour is more important than the Zn concentration in wheat flour. The observed difference in wheat flour Zn bioavailability between the self-cultivated flour and the flour purchased by rural households suggests a relatively high vulnerability to Zn malnutrition of rural households dependent on wheat flour purchased from supermarkets (**Table 1**). Rosado et al. (24) reported that 3 mg Zn from the consumption of 300 g wheat flour is the target level for human health. In the present survey, 300 g of the self-cultivated wheat flour and the wheat flour purchased by rural households provided only ∼28.7 and 26.3%, respectively, of the daily Zn requirement in Quzhou County.

Zn-Biofortified Wheat in the Field Experiment

In the present study, foliar Zn application imposed no significant effect on the wheat grain yield, which is consistent with previous studies (37, 38). In good agreement with previous results (11, 37), foliar Zn fertilizer application successfully increased the Zn concentration in wheat grain and flour at all farmer field locations. The increase in the grain Zn concentration due to foliar Zn application is above 3-fold in Iran (39) and Turkey (40). The relatively small increase in the grain Zn concentration (1.98-fold) due to foliar Zn application in the current study may be attributed to the lower soil DTPA-Zn concentration in the above studies than that in the current study at the 16 locations. In addition, the climate conditions, wheat cultivars, and spraying period may also directly affect the extent of the Zn concentration increase in wheat grain and flour (37). Irrespective of foliar Zn application, the highest Zn concentrations in wheat grain and flour were observed in Balizhangzhuang-II, which could be explained by the higher soil DTPA-Zn concentration and higher nitrogen (N) application level (synergistic effect between N and Zn) in Balizhangzhuang-II than those at the other locations (**Supplementary Table 1**). In addition, in agreement with the results reported by Hussain et al. (41) and Zou et al. (38), the average grain Zn concentration at the 16 locations increased to 43.1 mg kg^{-1} due to foliar Zn application, which matches the biofortification target of Zn in wheat grain.

As a store of P and energy, PA plays an important role in plant growth and development and functions as an antioxidant and anticarcinogen in the human body (42). Unfortunately, to a certain extent, PA is thought to be an antinutrient that reduces the bioavailability of micronutrients, especially iron and Zn (43). In the current study, the PA concentrations in wheat grain and flour remained unchanged in response to foliar Zn application at all locations, which is consistent with Wang et al. (44). The main

reason may be that foliar Zn application did not significantly affect the wheat grain yield at any of the 16 locations in the current study (**Figure 2**).

The current study suggested that the estimated Zn bioavailability in wheat grain and flour was significantly enhanced by foliar Zn application, which is consistent with the findings of Li et al. (45). Based on the target level of 3 mg Zn obtained from the consumption of 300 g wheat flour (24), the estimated Zn bioavailability in wheat grain and flour in the current study is below this level, and 300 g Zn-biofortified wheat flour could provide ∼57% of the daily Zn requirements. These results indicate that agronomic biofortification (foliar Zn application) in combination with genetic biofortification (breeding of Zn-efficient genotypes) could be a better choice to minimize Zn deficiency in rural households in future research (7). Our results also showed that the estimated Zn bioavailability in wheat flour was higher than that in wheat grain, which is consistent with published results (46, 47). A possible explanation for these results may be the very low PA concentration in wheat endosperm (48). In addition, as cited in the previous paragraphs, a high application level of P fertilizers is a typical phenomenon under the current wheat cropping management practices in Quzhou County, and combined with the results of the field experiment conducted in Quzhou County, there could be another option to increase the Zn bioavailability in wheat grain and flour via P application optimization (49).

Health Impact of Zn-Biofortified Wheat Flour in Quzhou County and China

Considering the role of wheat flour as a staple food in Quzhou County and the estimated Zn bioavailability in Zn-biofortified flour being significantly higher than that in the self-cultivated flour or the flour purchased by rural households, substitution of conventional wheat flour with Zn-biofortified flour in rural household diets could highly alleviate Zn malnutrition.

In the current study, the estimated health impact of Zn-biofortified wheat flour was calculated within the DALY framework. Our results indicated that the human health impact (the DALYs saved) in Quzhou County was greater if Zn-biofortified flour replaced the flour purchased from supermarkets than that if the flour produced on rural household farmlands was replaced. This occurs because the Zn concentration and bioavailability in the flour produced on rural household farmlands were higher than those in the flour purchased from supermarkets. Our results also revealed that the reduction in the burden of Zn deficiency in China (12.33–13.43% under the pessimistic scenario and 36.87–40.18% under the optimistic scenario) due to foliar Zn application was larger than that due to biofortification in India (2–12%) and Pakistan (5–33%) (25, 50). In addition, based on the large area of wheat cultivation in Quzhou County (21.7 thousand ha^{-1}) (51) and China (23.7 million ha^{-1}) (52), a relatively high economic income could be obtained via Zn-biofortified flour in Quzhou County and China, which is consistent with the results of Wang et al. (31). In summary, our results indicate that compared to the flour consumed in rural households on a daily basis, Zn-biofortified wheat flour via foliar Zn application is a feasible strategy to combat human Zn deficiency and potentially increase the economic income in rural households in China.

CONCLUSION

Our farm field experiment demonstrated that foliar Zn application effectively increased the Zn concentration and bioavailability in wheat grain and flour irrespective of the agricultural management practices in Quzhou County. Zn-biofortified wheat flour provided ∼57% of the daily Zn requirement. Based on the defined scenarios, more health and economic benefits could be obtained by the replacement of self-cultivated flour or flour purchased from supermarkets with Zn-biofortified wheat flour in Quzhou County and China. Therefore, foliar Zn application is a win-win agronomic strategy to maintain the yield and combat human Zn deficiency in rural households in China.

DATA AVAILABILITY STATEMENT

The raw data supporting the conclusions of this article will be made available by the authors, without undue reservation.

AUTHOR CONTRIBUTIONS

B-GY: resources, data curation, and writing—original draft. Y-ML, X-XC, W-QC, and T-BD: investigation. C-QZ: conceptualization, writing—review, and editing. All authors contributed to the article and approved the submitted version.

FUNDING

This research was supported by the National Natural Science Foundation of China (NSFC 31672240), the Deutsche Forschungsgemeinschaft (DFG, German Research Foundation)-328017493/GRK 2366 (Sino-German International Research Training Group AMAIZE-P), and Innovative Group Grant of the NSFC (No. 31421092).

SUPPLEMENTARY MATERIAL

The Supplementary Material for this article can be found online at: https://www.frontiersin.org/articles/10.3389/fnut.2021.697817/full#supplementary-material

REFERENCES

1. Cakmak I. Enrichment of cereal grains with zinc: agronomic or genetic biofortification? *Plant Soil.* (2008) 302:1–17. doi: 10.1007/s11104-007-9466-3

2. Kumssa DB, Joy EJM, Ander EL, Watts MJ, Young SD, Walker S, et al. Dietary calcium and zinc deficiency risks are decreasing but remain prevalent. *Sci Rep.* (2015) 5:10974. doi: 10.1038/srep10974

3. Ma G, Jin Y, Li Y, Zhai F, Kok FJ, Jacobsen E, et al. Iron and zinc deficiencies in China: what is a feasible and cost-effective strategy? *Public Health Nutr.* (2008) 11:632–8. doi: 10.1017/S1368980007001085
4. Myers SS, Zanobetti A, Kloog I, Huybers P, Leakey ADB, Bloom AJ, et al. Increasing CO_2 threatens human nutrition. *Nature.* (2014) 510:139–42. doi: 10.1038/nature13179
5. Beal T, Massiot E, Arsenault JE, Smith MR, Hijmans RJ. Global trends in dietary micronutrient supplies and estimated prevalence of inadequate intakes. *PLoS ONE.* (2017) 12:e175554. doi: 10.1371/journal.pone.0175554
6. Shewry PR. Wheat. *J Exp Bot.* (2009) 60:1537–53. doi: 10.1093/jxb/erp058
7. Chen XP, Zhang YQ, Tong YP, Xue YF, Liu DY, Zhang W, et al. Harvesting more grain zinc of wheat for human health. *Sci Rep.* (2017) 7:7016. doi: 10.1038/s41598-017-07484-2
8. Kutman UB, Yildiz B, Ozturk L, Cakmak I. Biofortification of durum wheat with zinc through soil and foliar applications of nitrogen. *Cereal Chem.* (2010) 87:1–9. doi: 10.1094/CCHEM-87-1-0001
9. Frossard E, Bucher M, Machler F, Mozafar A, Hurrell R. Potential for increasing the content and bioavailability of Fe, Zn and Ca in plants for human nutrition. *J Sci Food Agric.* (2000) 80:861–79. doi: 10.1002/(SICI)1097-0010(20000515)80:7<861::AID-JSFA601>3.0.CO;2-P
10. Wang Y, Zou CQ, Mirza Z, Li H, Zhang Z, Li D, et al. Cost of agronomic biofortification of wheat with zinc in China. *Agron Sustain Dev.* (2016) 36:1–7. doi: 10.1007/s13593-016-0382-x
11. Li M, Wang S, Tian X, Li S, Chen Y, Jia Z, et al. Zinc and iron concentrations in grain milling fractions through combined foliar applications of Zn and macronutrients. *Field Crop Res.* (2016) 187:135–41. doi: 10.1016/j.fcr.2015.12.018
12. Zhao A, Tian X, Cao Y, Lu X, Liu T. Comparison of soil and foliar zinc application for enhancing grain zinc content of wheat when grown on potentially zinc-deficient calcareous soils. *J Sci Food Agr.* (2014) 94:2016–22. doi: 10.1002/jsfa.6518
13. Zhuang Z, Mu HY, Fu PN, Wan YN, Yu Y, Wang Q, et al. Accumulation of potentially toxic elements in agricultural soil and scenario analysis of cadmium inputs by fertilization: a case study in Quzhou county. *J Environ Manage.* (2020) 269:110797. doi: 10.1016/j.jenvman.2020.110797
14. Zhao LY, Zhao SY, Liu Y. Zinc contents in 464 children hair under 7 years old in Handan city. *Stud Trace Elem Health.* (2000) 4:34.
15. Yu BG, Zhang TM, Li KL, Wang C, Zou CQ. Spatial variability characteristics of soil available micronutrients and their influencing factors in Quzhou. *Chinese J Soil Sci.* (2019) 50:395–400. doi: 10.19336/j.cnki.trtb.2019.02.20
16. Wang C, Li X, Gong T, Zhang H. Life cycle assessment of wheat-maize rotation system emphasizing high crop yield and high resource use efficiency in Quzhou County. *J Clean Prod.* (2014) 68:56–63. doi: 10.1016/j.jclepro.2014.01.018
17. Zhang YQ, Shi RL, Rezaul KM, Zhang FS, Zou CQ. Iron and zinc concentrations in grain and flour of winter wheat as affected by foliar application. *J Agric Food Chem.* (2010) 58:12268–74. doi: 10.1021/jf103039k
18. Haug W, Lantzsch H. Sensitive method for the rapid determination of phytate in cereals and cereal products. *J Sci Food Agr.* (1983) 34:1423–6. doi: 10.1002/jsfa.2740341217
19. Bao S. *Soil and Agricultural Chemistry Analysis*. Beijing: Agricultural Press (2000).
20. Lindsay WL, Norvell WA. Development of a DTPA soil test for zinc, iron, manganese, and copper. *Soil Sci Soc Am J.* (1978) 42:421–8. doi: 10.2136/sssaj1978.03615995004200030009x
21. Olsen SR. *Estimation of Available Phosphorus in Soils by Extraction with Sodium Bicarbonate (No. 939)*. Washington, DC: US Department of Agriculture (1954).
22. Miller LV, Krebs NF, Hambidge KM. A mathematical model of zinc absorption in humans as a function of dietary zinc and phytate. *J Nutr.* (2007) 137:135–41. doi: 10.1093/jn/137.1.135
23. Hambidge KM, Miller LV, Westcott JE, Sheng X, Krebs NF. Zinc bioavailability and homeostasis. *Am J Clin Nutr.* (2010) 91:1478S–83. doi: 10.3945/ajcn.2010.28674I
24. Rosado JL, Hambidge KM, Miller LV, Garcia OP, Westcott J, Gonzalez K, et al. The quantity of zinc absorbed from wheat in adult women is enhanced by biofortification. *J Nutr.* (2009) 139:1920–5. doi: 10.3945/jn.109.107755
25. Meenakshi JV, Johnson NL, Manyong VM, DeGroote H, Javelosa J, Yanggen DR, et al. How cost-effective is biofortification in combating micronutrient malnutrition? An ex ante assessment. *World Dev.* (2010) 38:64–75. doi: 10.1016/j.worlddev.2009.03.014
26. Steur HD, Gellynck X, Blancquaert D, Lambert W, Straeten DVD, Qaim M. Potential impact and cost-effectiveness of multi-biofortified rice in China. *New Biotechnol.* (2012) 29:432–42. doi: 10.1016/j.nbt.2011.11.012
27. National Bureau of Statistics of China. *China Statistical Yearbook 2009*. Beijing: China Statistics Press (2010).
28. Liu DY, Liu YM, Zhang W, Zou CQ. Agronomic approach of zinc biofortification can increase zinc bioavailability in wheat flour and thereby reduce zinc deficiency in humans. *Nutrients.* (2017) 9:465. doi: 10.3390/nu9050465
29. Chai W. Chinese dietary vitamin intake and deficiency in recent ten years based on systematic analysis. In: *Proceedings of the 2nd International Meeting of the Micronutrient Forum Micronutrients*. Beijing (2009).
30. Liang L, Wang Y, Ridoutt BG, Lal R, Wang D, Wu W, et al. Agricultural subsidies assessment of cropping system from environmental and economic perspectives in North China based on LCA. *Ecol Indic.* (2019) 96:351–60. doi: 10.1016/j.ecolind.2018.09.017
31. Wang X, Liu D, Zhang W, Wang C, Cakmak I, Zou C. An effective strategy to improve grain zinc concentration of winter wheat, Aphids prevention and farmers' income. *Field Crop Res.* (2015) 184:74–9. doi: 10.1016/j.fcr.2015.08.015
32. Ahsin M, Hussain S, Rengel Z, Amir M. Zinc status and its requirement by rural adults consuming wheat from control or zinc-treated fields. *Environ Geochem Health.* (2020) 42:1877–92. doi: 10.1007/s10653-019-00463-8
33. Wang M, Kong F, Liu R, Fan Q, Zhang X. Zinc in wheat grain, processing, and food. *Front Nutr.* (2020) 7:124. doi: 10.3389/fnut.2020.00124
34. Zhang W, Liu DY, Li C, Chen XP, Zou CQ. Accumulation, partitioning, and bioavailability of micronutrients in summer maize as affected by phosphorus supply. *Eur J Agron.* (2017) 86:48–59. doi: 10.1016/j.eja.2017.03.005
35. Wei J, Cen K. Contamination and health risk assessment of heavy metals in cereals, legumes, and their products: a case study based on the dietary structure of the residents of Beijing, China. *J Clean Prod.* (2020) 260:121001. doi: 10.1016/j.jclepro.2020.121001
36. Ma G, Jin Y, Piao J, Kok F, Guusje B, Jacobsen E. Phytate, calcium, iron, and zinc contents and their molar ratios in foods commonly consumed in China. *J Agr Food Chem.* (2005) 53:10285–90. doi: 10.1021/jf052051r
37. Zhang YQ, Sun YX, Ye YL, Karim MR, Xue YF, Yan P, et al. Zinc biofortification of wheat through fertilizer applications in different locations of China. *Field Crop Res.* (2011) 125:1–7. doi: 10.1016/j.fcr.2011.08.003
38. Zou CQ, Du YF, Rashid A, Ram H, Savasli E, Pieterse PJ, et al. Simultaneous biofortification of wheat with zinc, iodine, selenium, and iron through foliar treatment of a micronutrient cocktail in six countries. *J Agr Food Chem.* (2019) 67:8096–106. doi: 10.1021/acs.jafc.9b01829
39. Habib M. Effect of foliar application of Zn and Fe on wheat yield and quality. *Afr J Biotechnol.* (2009) 8:6795–8. doi: 10.5897/AJB2009.000-9526
40. Ozturk L, Yazici MA, Yucel C, Torun A, Cekic C, Bagci A, et al. Concentration and localization of zinc during seed development and germination in wheat. *Physiol Plantarum.* (2006) 128:144–52. doi: 10.1111/j.1399-3054.2006.00737.x
41. Hussain S, Maqsood MA, Rengel Z, Aziz T. Biofortification and estimated human bioavailability of zinc in wheat grains as influenced by methods of zinc application. *Plant Soil.* (2012) 361:279–90. doi: 10.1007/s11104-012-1217-4
42. Shamsuddin AM. Anti-cancer function of phytic acid. *Int J Food Sci Tech.* (2002) 37:769–82. doi: 10.1046/j.1365-2621.2002.00620.x
43. Harland BF, Morris ER. Phytate: a good or a bad food component? *Nutr Res.* (1995) 15:733–54. doi: 10.1016/0271-5317(95)00040-P
44. Wang S, Zhang X, Liu K, Fei P, Chen J, Li X, et al. Improving zinc concentration and bioavailability of wheat grain through combined foliar applications of zinc and pesticides. *Agron J.* (2019) 111:1478–87. doi: 10.2134/agronj2018.09.0597
45. Li M, Wang S, Tian X, Zhao J, Li H, Guo C, et al. Zn distribution and bioavailability in whole grain and grain fractions of winter wheat as affected by

applications of soil N and foliar Zn combined with N or P. *J Cereal Sci.* (2015) 61:26–32. doi: 10.1016/j.jcs.2014.09.009
46. Ryan MH, McInerney JK, Record IR, Angus JF. Zinc bioavailability in wheat grain in relation to phosphorus fertiliser, crop sequence and mycorrhizal fungi. *J Sci Food Agr.* (2008) 88:1208–16. doi: 10.1002/jsfa.3200
47. Zhang P, Ma G, Wang C, Zhu Y, Guo T. Mineral elements bioavailability in milling fractions of wheat grain response to zinc and nitrogen application. *Agron J.* (2019) 111:2504–11. doi: 10.2134/agronj2019.02.0104
48. Tang J, Zou CQ, He Z, Shi R, Ortiz-Monasterio I, Qu Y, et al. Mineral element distributions in milling fractions of Chinese wheats. *J Cereal Sci.* (2008) 48:821–8. doi: 10.1016/j.jcs.2008.06.008
49. Zhang W, Liu DY, Liu YM, Chen XP, Zou CQ. Overuse of phosphorus fertilizer reduces the grain and flour protein contents and zinc bioavailability of winter wheat (*Triticum aestivum* L.). *J Agric Food Chem.* (2017) 65:1473–82. doi: 10.1021/acs.jafc.6b04778
50. Stein AJ, Nestel P, Meenakshi JV, Qaim M, Sachdev HP, Bhutta ZA. Plant breeding to control zinc deficiency in India: how cost-effective is biofortification? *Public Health Nutr.* (2007) 10:492–501. doi: 10.1017/S1368980007223857
51. Handan Statistics Bureau. *Handan Statistical Yearbook 2019*. (2020). Available online at: http://hdzfxxgk.hd.gov.cn/gszbm/auto23694/202004/t20200403_1258882.html
52. National Bureau of Statistics of China. *China Statistical Yearbook*. (2020). Available online at: http://www.stats.gov.cn (accessed Februray 28, 2020).

Conflict of Interest: The authors declare that the research was conducted in the absence of any commercial or financial relationships that could be construed as a potential conflict of interest.

frontiers in Nutrition

ORIGINAL RESEARCH
published: 03 August 2021
doi: 10.3389/fnut.2021.704030

Microbial-Assisted Wheat Iron Biofortification Using Endophytic *Bacillus altitudinis* WR10

Zhongke Sun[1,2]*, *Zonghao Yue*[1], *Hongzhan Liu*[1], *Keshi Ma*[1] and *Chengwei Li*[2]*

[1] College of Life Science and Agronomy, Zhoukou Normal University, Zhoukou, China, [2] College of Biological Engineering, Henan University of Technology, Zhengzhou, China

Microbial-assisted biofortification attracted much attention recently due to its sustainable and eco-friendly nature for improving nutrient content in wheat. An endophytic strain *Bacillus altitudinis* WR10, which showed sophistical regulation of iron (Fe) homeostasis in wheat seedlings, inspired us to test its potential for enhancing Fe biofortification in wheat grain. In this study, assays *in vitro* indicated that WR10 has versatile plant growth-promoting (PGP) traits and bioinformatic analysis predicted its non-pathogenicity. Two inoculation methods, namely, seed soaking and soil spraying, with 10^7 cfu/ml WR10 cells were applied once before sowing of wheat (*Triticum aestivum* L. cv. Zhoumai 36) in the field. After wheat maturation, evaluation of yield and nutrients showed a significant increase in the mean number of kernels per spike (KPS) and the content of total nitrogen (N), potassium (K), and Fe in grains. At the grain filling stage, the abundance of *Bacillus* spp. and the content of N, K, and Fe in the root, the stem, and the leaf were also increased in nearly all tissues, except Fe in the stem and the leaf. Further correlation analysis revealed a positive relationship between the total abundance of *Bacillus* spp. and the content of N, K, and Fe in grains. Seed staining confirmed the enhanced accumulation of Fe, especially in the embryo and the endosperm. Finally, using a hydroponic coculture model, qPCR quantification indicated effective colonization, internalization, translocation, and replication of strain WR10 in wheat within 48 h. Collectively, strain WR10 assisted successful Fe biofortification in wheat in the field, laying a foundation for further large-scale investigation of its applicability and effectiveness.

Keywords: iron biofortification, wheat grain, endophyte, *Bacillus* spp., field study

OPEN ACCESS

Edited by:
Om Prakash Gupta,
Indian Institute of Wheat and Barley Research (ICAR), India

Reviewed by:
Radha Prasanna,
Indian Agricultural Research Institute (ICAR), India
Ummed Singh,
Agriculture University, Jodhpur, India

***Correspondence:**
Zhongke Sun
sunzh@daad-alumni.de
orcid.org/0000-0002-9784-9769
Chengwei Li
lcw@haut.edu.cn

Specialty section:
This article was submitted to Nutrition and Food Science Technology, a section of the journal Frontiers in Nutrition

Received: *01 May 2021*
Accepted: *02 July 2021*
Published: *03 August 2021*

Citation:
Sun Z, Yue Z, Liu H, Ma K and Li C (2021) Microbial-Assisted Wheat Iron Biofortification Using Endophytic Bacillus altitudinis WR10. Front. Nutr. 8:704030. doi: 10.3389/fnut.2021.704030

INTRODUCTION

Iron (Fe) is an essential trace element for the health of both plants and humans; however, most Fe in the soil is not readily accessible to plants (ferric form, Fe^{3+}), resulting in low bioavailability (1). Furthermore, Fe deficiency is one of the most prevalent forms of malnutrition in the world, and one-fifth of the population in China suffers from Fe deficiency (http://www.chinacdc.cn). The long-term acquisition of Fe by humans is mainly through food, highlighting the importance of Fe content in staple crops (2). As one of the most important food crops in the world, wheat provides various nutrients, including Fe, to hundreds of millions of people. The HarvestPlus project suggested that wheat grains should contain 59 mg/kg of Fe to meet the dietary Fe needs of adults (3); however, the average Fe content of 198 wheat varieties was only 29.1 mg/kg in France (4), and that of 260

varieties in the Huanghuai wheat region of China was only 22.2 mg/kg (5). Therefore, Fe deficiency remains one of the most serious global nutritional problems.

Several approaches have been developed to overcome Fe deficiency in humans (6); however, only biofortification, a process of breeding nutrients into food crops, is considered to be a sustainable strategy for tackling malnutrition, especially for those who have limited access to diverse diets or fortified foods. Indeed, the biofortification of staple crops is an evidence-based and cost-effective method to address malnutrition in tens of millions of people (https://www.harvestplus.org/biofortification-nutrition-revolution-now). In general, Fe biofortification can be achieved mainly by plant breeding, transgenic techniques, or agronomic practices (7). Therefore, wheat Fe biofortification is an urgent and economically important task (8). Promoting root absorption of Fe from the soil and increasing Fe accumulation in grains have become the most fundamental, efficient, and sustainable methods of wheat biofortification (9, 10); however, so far, progress in wheat Fe biofortification by traditional plant breeding has not been as successful as in other crops (11). Although transgenic techniques have developed high-iron genotypes, their release is still restricted. Agronomic practices, mainly foliar application of Fe-containing chemical fertilizers, are currently the major methods used for wheat; however, these practices are unappealing due to mineral unsustainability and potential adverse effects on the environment.

It has been confirmed that wheat-associated microbes are widely involved in plant Fe homeostasis, e.g., improving Fe uptake and alleviating Fe toxicity in wheat (12). Different microorganisms can not only increase yield production but also promote absorption and accumulation of certain essential elements in crop grains, a process termed microbial-assisted biofortification (13). In recent years, the use of microorganisms for enhancing wheat biofortification has attracted much attention (14). Microorganisms can significantly improve Fe accumulation in wheat in an efficient and eco-friendly way. Strains of *Bacillus* spp. form spores and are widely explored as plant growth-promoting bacteria (PGPB) in contemporary agriculture for different purposes (15, 16). They secrete siderophores, organic acids, and other compounds to promote the uptake of Fe in the rhizosphere of wheat (17, 18). Furthermore, they can improve the translocation or remobilization of Fe from the roots to the aerial parts and the accumulation in the grains (18, 19). *Bacillus* spp. has been widely recognized for its important role in helping plants obtain Fe to cope with Fe deficiency (20, 21). Field studies have demonstrated as high as a 70% increase of Fe content in wheat grains after inoculation with *B. pichinotyi* or *B. subtilis* (22, 23). In another study, the values of tillers per plant (TTP) and thousand-grain weight (TGW) increased more than 20%, and the levels of grain Fe increased more than 44% (24).

Due to a lower environmental impact and higher colonization ability in plants, endophytic bacteria may have better applicability than the widely used soil bacteria at present (25). We have isolated a series of endophytic bacteria from wheat roots (26). One of them, *B. altitudinis* WR10, has a strong ability to absorb Fe and improves the ability of wheat to tolerate Fe by upregulating the expression of wheat genes encoding ferritin (27). The strain has high phytase activity, produces siderophores, and forms biofilm (28). Therefore, this study was planned to inoculate wheat with this strain using different methods (such as soaking or spraying) to increase Fe content in wheat grains and achieve WR10-assisted Fe biofortification in wheat.

MATERIALS AND METHODS

Bacterial Growth and Characterization

The strain *B. altitudinis* WR10 was previously isolated from the root of wheat (*Triticum aestivum* L. cv. Zhoumai 26) and stored in 20% glycerol at −80°C (27). The glycerol stock of *B. altitudinis* WR10 was streaked on Luria-Bertani (LB) agar. After overnight incubation at 30°C, a single colony was picked into 5 ml sterile LB broth in a glass tube. The tube was agitated at 30°C, 150 rpm for 24 h. For quantitative assay of hormone production, supernatants were collected by centrifugation at 8,000 g for 5 min. The concentrations of indoleacetic acid (IAA), cytokinin (CTK), and gibberellin (GA) in supernatants were assayed with commercial Plant IAA, CTK, or GA ELISA Kits using specific antibodies coated microplate (Enzyme-linked Biotechnology Co. Ltd., Shanghai), by reading absorbance at 450 nm (Abs.450 nm) and calibrating with corresponding standards. For qualitative assay of hydrolytic enzymes production, bacterial suspension was spotted on respective agars using starch, pectin, carboxymethylcellulose, or casein as the sole carbon source (29). A clear halo zone around spotted bacteria after staining indicates the production of corresponding enzymes. The production of hydrogen cyanide (HCN), ammonia, and siderophores was detected, as in a previous report (30). The intrinsic antibiotic spectra were tested on LB agar supplemented with different antibiotics, including ampicillin (100 μg/ml), chloramphenicol (5 μg/ml), erythromycin (5 μg/ml), kanamycin (50 μg/ml), and spectromycin (100 μg/ml). No growth after 24 h of incubation at 30°C was considered as sensitive. All these antibiotics are purchased at biotechnological grade (Sigma-Aldrich, USA). For pathogenicity analysis, the Virulence Factors Database (VFDB, www.mgc.ac.cn/cgi-bin/VFs/v5/main.cgi?fun=VFanalyzer) and the PathogenFinder (https://cge.cbs.dtu.dk/services/PathogenFinder) web-based tools were searched using the reference genome of *B. altitudinis* GR8 (31, 32). Strain GR8 has the highest identity in a marker gene *gyrB* of *B. altitudinis* WR10 (28).

Microbial Inoculants Preparation, Field Application, and Wheat Planting

Bacillus altitudinis WR10 was cultivated in LB broth in 500 ml flasks, under 30°C, and agitating at 200 rpm. Cell pellets were collected from overnight culture fluids after centrifugation at 8,000 g for 5 min. Bacterial cells were washed two times with sterile water and then resuspended in water (10^7 cfu/ml) for field application as microbial inoculants. For soil spraying, fresh inoculants were sprayed onto the surface of the soil using a sprinkling can (0.5 L per m^2) 2 h before sowing. For seed soaking, wheat seeds (*Triticum aestivum* L. cv. Zhoumai 36) were immersed in fresh WR10 inoculants for 1 h under room temperature and agitating at 50 rpm. After incubation, seeds

were dried by airing on a bench for 24 h. For both controls, equal volumes of water without bacteria were simultaneously used. The planting of the wheat was conducted in 2019–2020 at the Field Experimental Center of Zhoukou Normal University (N33°38′, E114°40′), China. Manipulation and application of *B. altitudinis* WR10 in the field were approved by the Institutional Biosafety Committee of Zhoukou Normal University. For each group, about 100 seeds (∼5 g) were manually sowed in two lines, each with a length of 10 m. During growth, there was no extra fertilization or irrigation. Some chemical properties of the soil were assayed according to the respective national guidelines provided in the Supplementary Information (**Supplementary Table 1**).

Wheat Sample Collection, Growth, and Yield Evaluation

At the grain filling stage (Feekes 11.1), 30 whole plants were collected randomly from different planting regions. Two growth parameters, including plant height and total chlorophyll content, were evaluated. Plant height above the ground was measured in centimeters. Then, plants were rinsed with tap water for 10 min to clean off any attachments. The clean plants were further cut into different sections, including the root, the stem, and the leaf (∼5 cm in length). The content of chlorophyll in the leaves was quantified as described elsewhere (33). The total chlorophyll content was calculated according to the formula (20.21 × Abs.645+8.02 × Abs.663). The content was expressed as mg/g dry weight. At the maturity stage (Feekes 11.4), wheat spikes were harvested manually and stored in plastic bags. Among them, 30 spikes were hand thrashed and used for analyzing the number of kernels per spike (KPS) and TGW. The samples used for weighting were dried in a thermo-constant incubator at 60°C until completely dry.

Hydroponic Coculture of Wheat Seedlings and *Bacillus altitudinis* WR10

Hydroponic coculture was carried out according to a previous report with minor modification (27). Briefly, 7-day-old well-grown seedlings of 60 of *Triticum aestivum* L. cv. Zhoumai 36 were planted in 6 plastic boxes each containing 1.2 L dH_2O. These six boxes were allocated into two groups. For the coculture group, each box was supplemented with 1.2 ml concentrated suspension of *B. altitudinis* WR10 (10^9 cfu/ml). For the control group, 1.2 ml autoclaved suspension of *B. altitudinis* WR10 was added to each box. After the addition of bacteria, seedlings were grown at a controlled temperature (25°C) in humid conditions (humidity 70%) under dark or light (12/12 h) for 48 h. Six seedlings from each box were collected at different time points, e.g., 0, 1, 2, 4, 6, 8, 10, 12, 24, and 48 h postinoculation (hpi).

Quantification of Bacterial Abundance

The abundance of *Bacillus* spp. in different tissues, including the root, the stem, and the leaf collected at the grain filling stage was quantified by qPCR assays using genus-specific primers (B_groELF/B_groELR). The abundance of strain WR10 in wheat seedlings, either the root or the sprout, collected during hydroponic coculture was quantified by qPCR assays using strain-specific primers (qR10F/qR10R). For both quantifications, sections of different tissues were first ultra-sonicated for 5 min (2/2 s) in sterile distilled water at room temperature. Second, they were dried at 60°C until constant weight. Third, these wheat tissues from six plants were mixed and grounded in liquid nitrogen with a mortar. Fourth, total genomic DNA was extracted from 20 mg tissue powder using a HiPure Food Microbial DNA Kit according to the user guide (Magen, China). Finally, the abundance of *Bacillus* spp. was evaluated by quantifying the relative gene copy of *groEL*. The abundance of strain WR10 was evaluated by quantifying the relative gene copy of *GAPDH*. The qPCR reaction was conducted in a CFX96 Touch™ Real-Time PCR Detection System (BioRad, USA) using SYBR green qPCR Master Mix (Vazyme, China). The parameters for thermocycler and melting curves were the same as done previously (27). The sequences of the primers and the sizes of amplicons are supplied in the Supplementary Information (**Supplementary Table 2**).

Assays of Nutrient Content in Different Wheat Tissues

Three macronutrients, namely total nitrogen (N), phosphorus (P), and potassium (K), and four micronutrients, namely Fe, zinc (Zn), manganese (Mn), and copper (Cu), were detected in different wheat tissues collected from the field. Tissues (0.1 g) used for macronutrients determination were digested by 5 ml H_2SO_4 and 2 ml H_2O_2 and diluted in 20 ml water. The dilute was neutralized with 10 M NaOH before being used for assays. The content of N was measured using the Kjeldahl method as previously described (34). The contents of P and K were measured with biochemical assay kits purchased from a company, Elabscience® (Wuhan, China). Precisely, the content of P was quantified by reading absorbance at 660 nm using the colorimetric assay kit (Cat. No. E-BC-K245-S). The content of K was quantified by turbidimetry assay at 450 nm using another kit (Cat. No. E-BC-K279-M). The concentrations of all micronutrients were assayed using a flame atomic absorption spectrophotometry (FAAS, Persee, China), as previously described (35). For wheat tissues and grains, a modified protocol was developed for sample processing based on a methodological report (36). Briefly, dry wheat tissues were milled into powder by a universal pulverizer or were grounded in liquid nitrogen with a mortar. Tissue powder was extracted by adding 0.5 M HNO_3 (0.1 g tissue per 20 ml acid) in 50 ml plastic tubes shaking under 37°C at 200 rpm for 2 h. Supernatants were collected after centrifugation at 10,000 g for 5 min and were used for these assays in triplicates. Phytate content was assayed using a rapid colorimetric method described previously, which is based on the reaction between ferric ion and sulfosalicylic acid (37). Sodium phytate was used for the preparation of standard solutions (Sigma, Shanghai, China). Absorbance was read in microtiters at 500 nm for phytate assay. All spectrometric readings using microtiters were read by a SpectraMax i3x microplate reader (Molecular Devices, Sunnyvale, USA).

Grain Iron Staining

Mature grains from different groups were carefully dissected longitudinally or transversely using a stainless steel surgical knife

and stained for 1 h with Perls' Prussian blue staining solution (2% [w/v] potassium hexacyanoferrate [II] and 2% [v/v] hydrochloric acid) as described elsewhere (38). After being washed two times in distilled water, all stained grains were dried at room temperature for 1 h. The stained section of grains was observed using a stereo light microscope NSZ-405 (NOVEL, Ningbo, China) and images were acquired by Echoo Imager (OPLENIC, Hangzhou, China).

Data Analysis

Original data were expressed as mean ± SD of at least three repeats. Statistical analysis was conducted in SPSS 19.0 (SPSS Inc., USA). Significant differences between groups were analyzed by one-way ANOVA using the LSD test. Values of $p < 0.05$ were considered statistically significant. Spearman's correlation coefficients were analyzed among bacterial abundance and different nutrient contents. The coefficient of determination (R^2) was also calculated after linear regression using Microsoft Excel. To show data from different groups in different tissues in figures, they were normalized to corresponding values in the control group (NC). All related data can be found in the Supplementary Information.

RESULTS

Characteristics and Potential Pathogenicity of *Bacillus altitudinis* WR10

Some characteristics of *B. altitudinis* WR10, including common PGP traits, were screened *in vitro* (**Table 1**). Briefly, ELISA assays using culture supernatants revealed the production of phytohormones, such as IAA and GA by strain WR10. The bacterium solubilized both inorganic (calcium phosphate) and organic (phytate) phosphorus. Production of ammonia and siderophores were also detected according to obvious phenotypes. Biofilm formation, exopolysaccharide secretion, and early colonization of wheat root were observed as well. For antagonistic traits, strain WR10 was sensitive to antibiotics, including ampicillin, chloramphenicol, erythromycin, kanamycin, and spectromycin under the tested concentrations. Strain WR10 was ACC deaminase positive and produced HCN. Regarding hydrolytic enzymes, strain WR10 produced amylase, cellulose, pectinase, and chitinase. Comprehensive analysis of pathogenicity factors by VFDB indicated the absence of most major virulence factors in *Bacillus* spp., albeit there were a few genes involved in capsule synthesis that may contribute to immune evasion. Detail results are provided in Supplementary Information (**Supplementary Table 3**). Further genome prediction by the PathogenFinder service confirmed strain WR10 as a non-human pathogen, as no matched pathogenic family was found.

TABLE 1 | Production of enzymes and other characters of *B. altitudinis* WR10 related to plant growth-promoting (PGP) and antagonism.

Character	*B. altitudinis* WR10
PGP traits	
IAA	31.5 pmol/ml
Cytokinin	–
Gibberelin	74.6 pmol/ml
Phosphorus solubilization	+
Siderophore production	+
Ammonia production	+
Biofilm formation	+
Exopolysaccharide	+
Early colonization	+
Antagonistic traits	
Antibiotic spectra	Amp^-, Cm^-, Erm^-, Kan^-, Spe^-
HCN production	+
ACC deaminase	+
Hydrolytic enzymes	
Chitinase	+
Protease	–
Cellulase	+
Amylase	+
Pectinase	+

+, positive; –, negative; $^-$, sensitive; Amp, ampicillin (100 μg/ml); Cm, chloramphenicol (5 μg/ml); Erm, erythromycin (5 μg/ml); Kan, kanamycin (50 μg/ml); Spe, spectromycin (100 μg/ml); HCN, hydrogen cyanide.

Effect of Microbial Inoculation on Yield and Nutrients of Wheat Grains

After wheat harvest, the TGW and KPS were calculated for evaluating the impact of microbial inoculation on grain yield production. The data indicated that there was no change in TGW among the different groups (**Supplementary Table 4**). In contrast, the relative numbers of KPS were significantly larger in the two treated groups, e.g., increased by 24.67 and 16.44% in groups sprayed or soaked in WR10, respectively (**Figure 1A**). For macronutrients, quantification using whole wheat flour showed a significant increase of N and K contents, except P. For example, both total N and K contents were increased by more than 50% (**Figures 1B,C**). For micronutrients, there was no difference in the contents of Zn, Mn, and Cu after inoculation of WR10; however, Fe content was significantly increased by about 30 and 19% (exactly, 29.94 and 18.67%) in the spraying and soaking groups, respectively (**Figure 1D**). The absolute concentration of Fe in Zhoumai 36 was increased from 33.55 to 43.60 mg/kg in the spraying group. For all these changed indices except N, stronger effects were observed in the soil-spraying group than in the seed-soaking group. In addition, the phytate assay showed a slight decrease (∼5%) in relative phytate content in the spraying group although there was no significant difference compared with the control (**Supplementary Table 4**).

Effect of Microbial Inoculation on Wheat Vegetative Organs

At the grain filling stage, two parameters were monitored to evaluate the impact of microbial inoculation on wheat growth (**Supplementary Table 5**). Compared with NC, there was no difference in plant height among the three groups; however, there was a significant increase in total chlorophyll content in leaves collected from the two inoculated groups. Precisely,

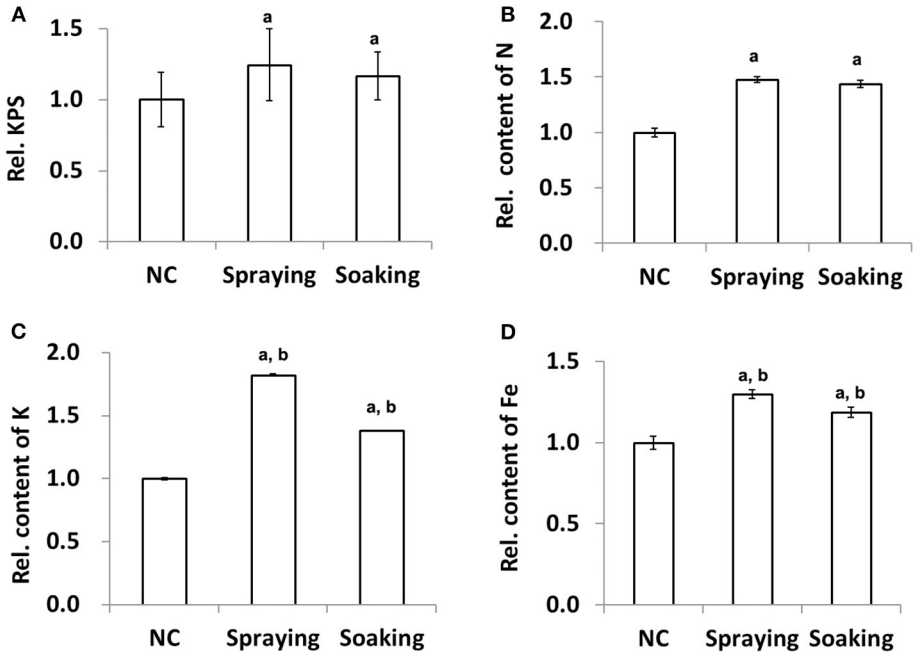

FIGURE 1 | Effect of WR10 inoculation on wheat grain yield production and nutrient content. **(A)** The relative mean number of kernels per spike (KPS) of 30 wheat plants; **(B)** Relative content of total N in grains; **(C)** Relative content of K in grains; **(D)** Relative content of Fe in grains. Content of macronutrients was calculated as mg/g, and that of micronutrients was calculated as mg/kg dry weight (DW). Original data were analyzed by ANOVA pair-wise comparisons using LDS-test and $p < 0.05$ was considered significant. All data in the figure were normalized to their counterparts in the control group (NC) without inoculation of bacteria. In spraying, soils were sprayed with *B. altitudinis* WR10 before sowing of wheat; in soaking, wheat seeds were soaked in *B. altitudinis* WR10 suspension before sowing. a, statistically different from NC; b, significantly different between spraying and soaking groups.

the content of total chlorophyll was increased by 42.07 and 22.85% in groups sprayed or soaked WR10, respectively. The qPCR quantification of *Bacillus* spp. showed a positive influence of microbial inoculation as the relative abundance was always higher after the inoculation of *B. altitudinis* WR10 (**Figure 2A**). In particular, the abundance of *Bacillus* spp. increased more than 7- or 3-fold in the root after being sprayed or soaked with WR10, respectively. In both the root and the leaf, the relative abundance of *Bacillus* spp. was higher in the spraying group than in the soaking group, suggesting a stronger influence of the former application method. Regarding nutrients, on the one hand, the inoculation of WR10 constantly increased the contents of N and K in all tested tissues, including the root, the stem, and the leaf (**Figures 2B,C**). On the other hand, the inoculation with WR10 had different impacts on Fe content in different tissues. In general, inoculation with WR10 significantly increased the relative content of Fe in the root but decreased the relative content in the stem and the leaf (**Figure 2D**, **Supplementary Table 6**).

Iron Staining and the Relationship Between *Bacillus* spp. Abundance and Nutrient Content

Spearman's correlation analysis showed that a positive relationship exists between the changed nutrient contents and the abundance of endophytic *Bacillus* spp. (**Supplementary Table 7**). In particular, Spearman's correlation coefficient was 0.937 or 0.933 for K or Fe and bacterial abundance ($p < 0.01$). As shown in **Figure 3A**, the nutrient content in grains has a high linear correlation to the total abundance of *Bacillus* spp. in all vegetative organs. For example, the R^2 between either K or Fe content and the total abundance of *Bacillus* spp. is higher than 0.9. To further investigate the distribution of Fe in grains, Fe staining was performed. Whether dissected longitudinally (left panel) or transversely (right panel), Perls' Prussian blue staining of grains showed the distribution of iron (**Figure 3B**). In contrast to NC, much intense blue staining could be observed in aleurone, embryo, and endosperm from grains harvested in the spraying and the soaking groups.

The Colonization, Internalization, Translocation, and Replication of *B. altitudinis* WR10 in Wheat

In the control group, *B. altitudinis* WR10 could not be detected by qPCR from all wheat samples, indicating its absence in Zhoumai 36; however, it could be constantly detected from seedlings of Zhoumai 36 as endophyte, after its addition for hydroponic coculture (**Figure 4**). To be precise, within 1 h (1 hpi), WR10 could even be detected in the root, suggesting its fast colonization and internalization. After that, the relative abundance of WR10 was improved sharply by nearly 200-fold within 10 h (10 hpi), indicating quick internalization and/or replication; however, the

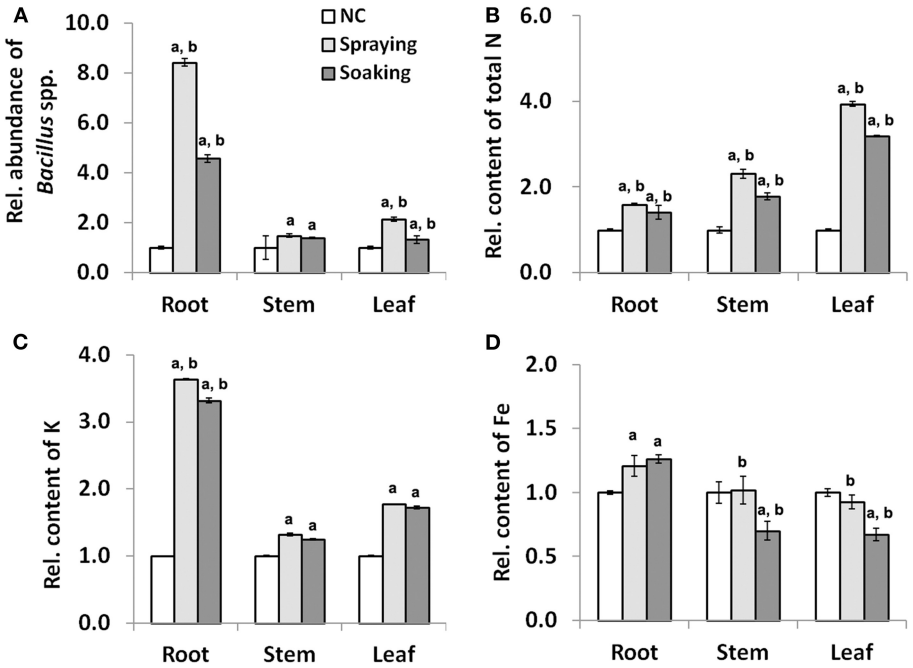

FIGURE 2 | Effect of WR10 inoculation on the abundance of endophytic *Bacillus* spp. and nutrient content in different wheat tissues at the grain filling stage. **(A)** The relative abundance of endophytic *Bacillus* spp. in different wheat tissues; **(B)** Relative content of N in different wheat tissues; **(C)** Relative content of K in different wheat tissues; **(D)** Relative content of Fe in different wheat tissues. Content of macronutrients was calculated as mg/g, and that of micronutrients was calculated as mg/kg dry weight. Original data were analyzed by pair-wise comparisons using LDS test, and $p < 0.05$ was considered significant. All data in the figure were normalized to their respective counterparts in the control group (NC) without inoculation of bacteria. In spraying, soils were sprayed with *B. altitudinis* WR10 before sowing of wheat; in soaking, wheat seeds were soaked in *B. altitudinis* WR10 suspension before sowing; a, statistically different from NC; b, significantly different between spraying and soaking groups.

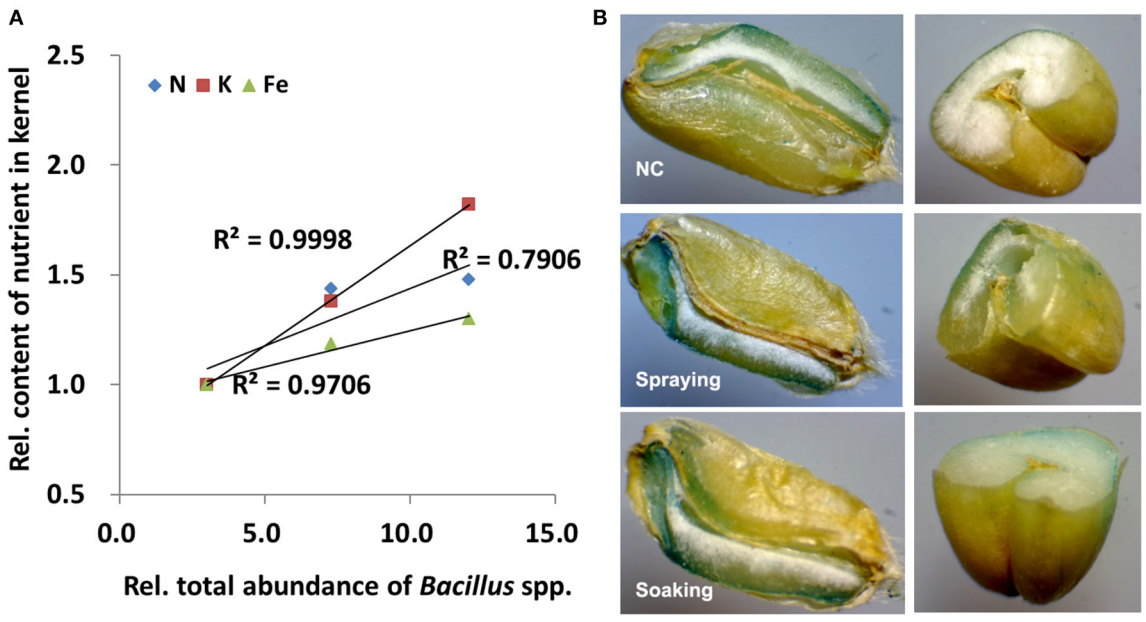

FIGURE 3 | Correlation analysis and iron staining. **(A)** Linear regression and coefficients of determination (R^2) between the total abundances of *Bacillus* spp. and content of three nutrients; **(B)** Perls' Prussian blue staining of grains. All data were normalized to their respective counterparts in the control group (NC) without inoculation of bacteria. In spraying, soils were sprayed with *B. altitudinis* WR10 before sowing of wheat; in soaking, wheat seeds were soaked in *B. altitudinis* WR10 suspension before sowing.

abundance of WR10 reached a plateau after 10 hpi and remained constant within the tested periods (**Figure 4A**). Similarly, WR10 could be detected in the sprout at 1 hpi, suggesting its quick translocation from the root. Further, the relative abundance of WR10 also increased steadily by more than 30-fold within 24 hpi, indicating continuous translocation and/or replication (**Figure 4B**). In addition, the abundance of WR10 was always much lower in the sprout than in the root.

DISCUSSION

Some wheat-associated microbes, mainly the rhizospheric microbes, produce siderophores and other metabolites that increase Fe solubility in the soil and can alleviate Fe-deficiency stress in the plant (12). Therefore, these microbes have been proposed as biofertilizers for enhancing Fe acquisition of crops due to their important role in favoring plant-iron uptake and accumulation under limiting conditions (39). Indeed, through inoculation of versatile microorganisms, enhanced uptake of Fe in wheat had been achieved by many previous studies (14); however, the majority of microbes used have been soil microorganisms and Fe concentration was only tested in the root. Hence, the stability and the effectiveness in practice are highly variable. In this study, we used an endophytic bacterium, *B. altitudinis* WR10, because it has a strong ability to absorb Fe and improves the ability of wheat to tolerate Fe (27). In addition, the strain produces siderophores and secretes phytase (28). These properties made the strain a good candidate for assisting wheat Fe biofortification for three reasons at least. First, WR10 can improve Fe bioaccessibility in soils and improve Fe accumulation in tissues. Second, it can decrease Fe toxicity within wheat tissues. Third, WR10 may degrade phytate, thereby improving Fe bioavailability in grains, which is important from the perspective of human nutrition.

To apply the strain, we first evaluated its pathogenicity and several PGP traits (**Table 1**). Unsurprisingly, strain WR10 was predicted as a non-human pathogen. Considering the strain was isolated from the root of healthy wheat as an endophyte, it should also be non-pathogenic to plants and can be used in agricultural systems. The characteristics listed in **Table 1** suggest that the strain possesses many growth-promoting and antagonistic properties. All these data support its potential application without unseen biosafety concerns (29, 30). As a pilot field experiment, this study tested the potential of *B. altitudinis* WR10 in natural field conditions, without any fertilization or irrigation.

The influence of microbial inoculation on yield and nutrients of grains was first evaluated, as improving yield is always the primary target of wheat planting. A few field studies have demonstrated the positive effect of microbial inoculants on wheat yield (22, 40, 41). It has been reported that stress-tolerant *Viridibacillus arenosi* strain IHB B7171 enhances grain yield by 13.9% in wheat (42). Yadav et al. reported a more than 20% increase in the values of TTP and TGW by inoculation with *Bacillus subtilis* CP4 and Arbuscular mycorrhizal fungi (AMF) (24, 43). This study demonstrated a significant increase in the number of KPS (16.44 or 24.67%) after bacterial inoculation, without influence on TGW (**Figure 1A**, **Supplementary Table 4**). Improvement in the number of KPS has also been reported in wheat after inoculation with AMF (44); however, the real effect of microbial inoculants on total grain yield production still needs comprehensive investigation, as this is often restrained by multiple factors. For example, grain yield is more significantly affected by nitrogen fertilization than AMF inoculation (44). Furthermore, inoculation with an endophytic nitrogen-fixing bacterium, *Paraburkholderia tropica,* had shown little effect on wheat grain yield, either with or without fertilization (45).

Except for increasing yield, the use of microbes for improving nutrient acquisition has also been evaluated across a variety of crops under varying conditions (46). It has been shown that AMF inoculation has a positive effect on Cu, Fe, and Zn content in all tissue types of wheat (40). As high as a 70% increase in Fe content in wheat grains after inoculation with *B. pichinotyi* or *B. subtilis* has been reported (22, 23). In another study, *B. subtilis* CP4 and AMF in combination increased Fe content in wheat grains by more than 44% (24). To fully discover the effect of WR10 application on grain nutrients, we evaluated three macronutrients and four micronutrients in grains. Data demonstrated that the one-time application of *B. altitudinis* WR10 significantly improves the content of N, K, and Fe (**Figure 1**). Especially, among all tested micronutrients, Fe content in grains was increased by about 30 and 19% in the spraying and soaking groups, respectively; however, there was no change in P, Zn, Mn, and Cu (**Supplementary Table 4**). In addition, we assayed phytate content in grains. Phytate is widely recognized as anti-nutritional because of the strong binding potential with minerals, including Fe and Zn (47). Strain WR10 produces phytases that effectively degrade phytate (28). Therefore, the content of phytate can be decreased after inoculation with WR10; however, this data suggest that this is not true in grains (**Supplementary Table 4**), and, as reported in AMF, the positive effect of WR10 on plant Fe accumulation may also be modulated by wheat genotypes, soil pH, texture, and nutrient concentration, as well as agronomic practices, such as N and P fertilization (46, 48).

Due to the importance of plant growth on yield production and nutrient accumulation in grains, we monitored plant height and total chlorophyll content in leaves at the grain filling stage, a vital phase for wheat kernel development. Plant height was measured as the first index due to its crucial role in plant architecture and yield potential (49); however, plant height showed no difference among the different groups (**Figure 1A**). The results agreed with a study that tested 13 single-inoculated bacteria, in which the plant height of wheat seedlings was measured after growing in pots for 80 days (50). Second, it was revealed that plant chlorophyll content is positively correlated with nitrogen content, which is important for crop quality and yield (51, 52). Hence, the total content of chlorophyll is a good indicator of the nutritional status of the plant and has significance for modern precision agriculture in practice. In this study, inoculation with WR10 significantly increased the total content of chlorophyll in leaves, indicating its positive

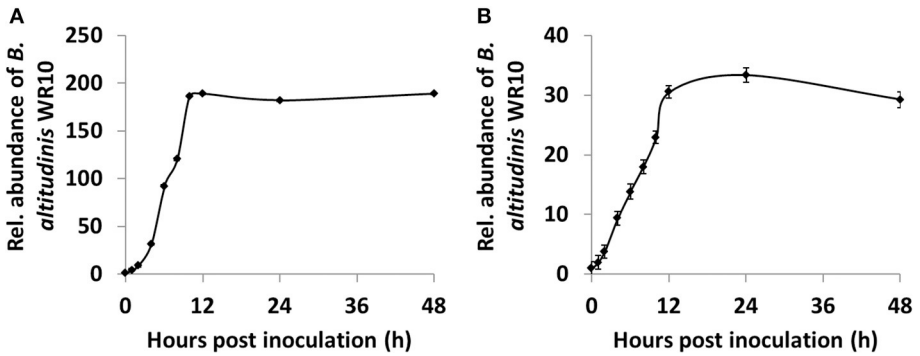

FIGURE 4 | Quantification of *B. altitudinis* WR10 in different wheat tissues during hydroponic coculture by qPCR assay. **(A)** The relative abundance of endophytic *B. altitudinis* WR10 in the root; **(B)** relative abundance of endophytic *B. altitudinis* WR10 in the sprout. At 0 phi, the relative abundances in different tissues were considered as 1. Fold changes were calculated by the $2^{\Delta Cq}$ method, which uses the copy numbers of the *GAPDH* gene representing the abundance of *B. altitudinis* WR10. Data were mean of three repeats from the genomic DNA mixture of six seedlings.

effect on wheat nutrition and potentially on yield production (**Figure 1B**). In line with our observation, a large number of studies have reported an increase in chlorophyll content or a decrease in its loss by different PGPB in wheat grown under various conditions (53–56).

Although there is no doubt that microbes play an important role in plant nutrition, quantitative estimations of microbial-plant interactions are still scarce, especially under field conditions (57). By quantification of the abundance of endophytic *Bacillus* spp., a major group of bacteria explored in contemporary agriculture, this study showed a complex effect of microbial inoculation on a certain genus within different tissues of wheat (**Figure 2A**). At the same time, quantification of Fe content in different tissues provided insights into how Fe hemostasis in the plant is regulated by bacteria. For example, at the grain filling stage, Fe content was improved in the root but decreased in the stem and the leaf (**Figure 2B**). The results indicate microbial inoculants, like *B. altitudinis* WR10, may enhance Fe uptake of roots from soils and strengthen Fe translocation in stems and remobilization in leaves. Therefore, much Fe can be acquired in the root, with less Fe in the stem and the leaf after inoculation of bacteria. Taken together, inoculation with *B. altitudinis* WR10 improved the abundance of *Bacillus* spp., which in turn improved Fe accumulation in grains, mainly by increasing Fe acquisition in roots from soils.

In addition, the formulation and application method showed an obvious impact on the effect of microbial inoculants (58). As a pilot study, we evaluated the two most widely applied methods and did not consider formulation in this study. Nearly, all indicators showed that liquid soil spraying has a stronger influence than seed soaking (**Figures 1**, **2**). For example, the abundance of *Bacillus* spp. was higher in all tissues in the spraying group than in the soaking group. This might be because more *B. altitudinis* WR10 were introduced into soils by soil spraying than by seed soaking or WR10 replicated/colonized much more easily in the former application method. Although it was reported that all inoculation methods, including in-furrow inoculation, soil spraying, foliar spraying, and seed soaking of *Azospirillum brasilense* increased the abundance of diazotrophic bacteria in wheat tissues, soil inoculations favored root and rhizosphere colonization (59). Root and rhizosphere colonization is important for the function of inoculants, as Fe can only be absorbed by the roots from the rhizospheric soil (12). In tobacco plants, soil inoculation led to pronounced bacterial-induced effect than seed inoculation in a mine soil contaminated with heavy metals (60). In Italian ryegrass, it was also showed that soil spraying performed better than seed soaking using different microbial inoculants, which further showed that the beneficial effect was correlated with the colonization efficiency of the inoculated strains (61). Therefore, it seems soil spraying is a more effective method for microbial inoculation than seed soaking, especially considering the feasibility and stability at a commercial scale (62). Furthermore, this study demonstrated a high correlation between the total abundance of *Bacillus* spp. in all vegetative organs and some nutrient content in grains (**Figure 3A**). A positive correlation exists between the total abundance of *Bacillus* spp. and the contents of N, K, and Fe in grains (**Figure 3A**, **Supplementary Table 7**). The result is reasonable as nutrient accumulation in grains is determined by both uptakes in roots, translocation in stems, and remobilization/distribution in leave; however, different regulations by the same bacterium can be seen in different nutrients (**Figure 2**). For example, in all tissues, the contents of N and K were higher along with a higher abundance of *Bacillus* spp. In contrast, Fe content was higher in the root but lower in leaves when having more *Bacillus* spp; however, the complex and different regulation of nutrient content in different wheat tissues by microbial inoculants are frequently reported in previous studies (13, 22–24, 43).

To quantify the relative abundance of the inoculant WR10, a hydroponic coculture model was used. A sharp increase in the relative abundance of WR10 was detected by qPCR assays in both the root and the sprout after bacterial inoculation, contrasting with uninoculated controls (**Figure 4**). The results indicated quick and efficient colonization, internalization, translocation, and/or replication of *B. altitudinis* WR10 in Zhoumai 36.

Indeed, the relative abundance of WR10 is always much higher in the root than in the sprout at the same time point and effective colonization of AMF, as well as other PGPB, has also been reported in the root of wheat (24, 44); however, this experiment provided more information regarding the quantitative or dynamic distribution of microbial inoculants in different tissues of wheat. It was also shown that exogenous WR10 reached a plateau in both the root and the sprout after a certain number of hours (e.g., 10 or 12 hpi).

In summary, strain *B. altitudinis* WR10 is a non-pathogen with versatile PGP and antagonistic traits. The strain can efficiently colonize and translocate within wheat. Its inoculation significantly enhances Fe biofortification in wheat grains (*Triticum aestivum* L. cv. Zhoumai 36) in the field, prospecting a promising potential for further investigation of WR10-assisted Fe biofortification. Also, Fe content in grains was positively correlated with the total abundance of endogenous *Bacillus* spp. in wheat. In addition, soil spraying is much more effective than seed soaking in increasing grain Fe content. To pave the way for microbial-assisted biofortification, the influence of application routines, soil chemicals, fertilization regimes, as well as the genotypes of wheat also need to be evaluated in the future.

DATA AVAILABILITY STATEMENT

The raw data supporting the conclusions of this article will be made available by the authors, without undue reservation.

AUTHOR CONTRIBUTIONS

ZS and CL designed the experiment, wrote the manuscript, discussed the results, and finalized the manuscript. ZS, ZY, and HL carried out the experiments. ZS and KM analyzed the data. All authors contributed to the article and approved the submitted version.

FUNDING

This work was partially supported by a grant from the National Natural Science Foundation of China (No. 32071478).

ACKNOWLEDGMENTS

We thank Mr. Xiaoqi Zhang and Dr. Yongchuang Liu for processing several wheat samples during their academic training in our lab. We also acknowledge Huazhi Yinyang Co. Ltd (www.nutri-all.com) for assisting plant management in the field.

SUPPLEMENTARY MATERIAL

The Supplementary Material for this article can be found online at: https://www.frontiersin.org/articles/10.3389/fnut.2021.704030/full#supplementary-material

REFERENCES

1. Singh D, Prasanna R. Potential of microbes in the biofortification of Zn and Fe in dietary food grains. a review. *Agrono Sustain Dev.* (2020) 40:1–21. doi: 10.1007/s13593-020-00619-2
2. Garg M, Sharma N, Sharma S, Kapoor P, Kumar A, Chunduri V, et al. Biofortified crops generated by breeding, agronomy, and transgenic approaches are improving lives of millions of people around the world. *Front Nutr.* (2018) 5:12. doi: 10.3389/fnut.2018.00012
3. Bouis HE, Hotz C, McClafferty B, Meenakshi JV, Pfeiffer WH. Biofortification: a new tool to reduce micronutrient malnutrition. *Food Nutr Bull.* (2011) 32:S31–40. doi: 10.1177/15648265110321S105
4. Baize D, Bellanger L, Tomassone R. Relationships between concentrations of trace metals in wheat grains and soil. *Agron Sustain Dev.* (2009) 29:297–312. doi: 10.1051/agro:2008057
5. Fu Z, Song A, Guo S, Song C, Zhang Z. Determination on Fe content in main wheat germplasm resources in Huanhuai wheat area. *J Anhui Agri Sci.* (2008) 36:14018–20. doi: 10.1016/S1002-0160(08)60059-4
6. Bathla S, Arora S. Prevalence and approaches to manage iron deficiency anemia (IDA). *Crit Rev Food Sci Nutr.* (2021) 7:1–14. doi: 10.1080/10408398.2021.1935442
7. Liberal Â, Pinela J, Vívar-Quintana AM, Ferreira ICFR, Barros L. Fighting iron-deficiency anemia: innovations in food fortificants and biofortification strategies. *Foods.* (2020) 9:1871. doi: 10.3390/foods9121871
8. Balk J, Connorton JM, Wan Y, Lovegrove A, Moore KL, Uauy C, et al. Improving wheat as a source of iron and zinc for global nutrition. *Nutr Bull.* (2019) 44:53–9. doi: 10.1111/nbu.12361
9. Vinoth A, Ravindhran R. Biofortification in millets: a sustainable approach for nutritional security. *Front Plant Sci.* (2017) 8:29. doi: 10.3389/fpls.2017.00029
10. Moretti D. Plant-based diets and iron status. In: Mariotti F, editor. *Vegetarian and Plant-Based Diets in Health and Disease Prevention*. San Diego, CA: Academic Press. (2017). p. 715–27. doi: 10.1016/B978-0-12-803968-7.00039-3
11. Connorton JM, Balk J. Iron biofortification of staple crops: lessons and challenges in plant genetics. *Plant Cell Physiol.* (2019) 60:1447–56. doi: 10.1093/pcp/pcz079
12. He L, Yue Z, Chen C, Li C, Li J, Sun Z. Enhancing iron uptake and alleviating iron toxicity in wheat by plant growth-promoting bacteria: theories and practices. *Int J Agric Biol.* (2020) 23:190–6. doi: 10.17957/IJAB/15.1276
13. Yasin M, El-Mehdawi AF, Anwar A, Pilon-Smits EA, Faisal M. Microbial-enhanced selenium and iron biofortification of wheat (*Triticum aestivum* L.) - applications in phytoremediation and biofortification. *Int J Phytoremediation.* (2015) 17:341–7. doi: 10.1080/15226514.2014.922920
14. Shi Y, Li J, Sun Z. Success to iron biofortification of wheat grain by combining both plant and microbial genetics. *Rhizosphere.* (2020) 15:100218. doi: 10.1016/j.rhisph.2020.100218
15. Hashem A, Tabassum B, Fathi Abd Allah E. Bacillus subtilis: a plant-growth promoting rhizobacterium that also impacts biotic stress. *Saudi J Biol Sci.* (2019) 26:1291–7. doi: 10.1016/j.sjbs.2019.05.004
16. Miljaković D, Marinković J, Balešević-Tubić S. The significance of Bacillus spp. in disease suppression and growth promotion of field and vegetable crops. *Microorganisms.* (2020) 8:1037. doi: 10.3390/microorganisms8071037
17. Zhou C, Guo J, Zhu L, Xiao X, Xie Y, Zhu J, et al. Paenibacillus polymyxa BFKC01 enhances plant iron absorption via improved root systems and activated iron acquisition mechanisms. *Plant Physiol Biochem.* (2016) 105:162–73. doi: 10.1016/j.plaphy.2016.04.025
18. LeTourneau MK, Marshall MJ, Grant M, Freeze PM, Strawn DG, Lai B, et al. Phenazine-1-carboxylic acid-producing bacteria enhance the reactivity of iron minerals in dryland and irrigated wheat rhizospheres. *Environ Sci technol.* (2019) 53:14273–84. doi: 10.1021/acs.est.9b03962
19. Mitter B, Pfaffenbichler N, Flavell R, Compant S, Antonielli L, Petric A, et al. A new approach to modify plant microbiomes and traits by introducing beneficial bacteria at flowering into progeny seeds. *Front Microbiol.* (2017) 8:11. doi: 10.3389/fmicb.2017.00011

20. Freitas MA, Medeiros FH, Carvalho SP, Guilherme LR, Teixeira WD, Zhang H, et al. Augmenting iron accumulation in cassava by the beneficial soil bacterium Bacillus subtilis (GBO3). *Front Plant Sci.* (2015) 6:596. doi: 10.3389/fpls.2015.00596
21. Verma P, Yadav AN, Khannam KS, Guilherme LR, Teixeira WD, Zhang H, et al. Molecular diversity and multifarious plant growth promoting attributes of Bacilli associated with wheat (*Triticum aestivum* L.) rhizosphere from six diverse agro-ecological zones of India. *J Basic Microb.* (2016) 56:44–58. doi: 10.1002/jobm.201500459
22. Yasin M, El-Mehdawi AF, Pilon-Smits EA, Faisal M. Selenium-fortified wheat: potential of microbes for biofortification of selenium and other essential nutrients. *Int J Phytoremediation.* (2015) 17:777–86. doi: 10.1080/15226514.2014.987372
23. Singh D, Geat N, Rajawat MVS, Prasanna R, Kar A, Singh AM, et al. Prospecting endophytes from different Fe or Zn accumulating wheat genotypes for their influence as inoculants on plant growth, yield, micronutrient content. *Ann Microbiol.* (2018) 68:815–33. doi: 10.1007/s13213-018-1388-1
24. Yadav R, Ror P, Rathore P, Kumar S, Ramakrishna W. *Bacillus subtilis* CP4, isolated from native soil in combination with arbuscular mycorrhizal fungi promotes biofortification, yield and metabolite production in wheat under field conditions. *J Appl Microbiol.* (2020) 131:339–59. doi: 10.1111/jam.14951
25. Adeleke BS, Babalola OO. The endosphere microbial communities, a great promise in agriculture. *Int Microbiol.* (2021) 24:1–17. doi: 10.1007/s10123-020-00140-2
26. Chen C, Yue Z, Chu C, Ma K, Li L, Sun Z. Complete genome sequence of Bacillus sp. strain WR11, an endophyte isolated from wheat root providing genomic insights into its plant growth-promoting effects. *Mol Plant Microbe Interact.* (2020) 33:876–9. doi: 10.1094/MPMI-02-20-0030-A
27. Sun Z, Liu K, Zhang J, Zhang Y, Xu K, Yu D, et al. IAA producing Bacillus altitudinis alleviates iron stress in *Triticum aestivum* L. seedling by both bioleaching of iron and up-regulation of genes encoding ferritins. *Plant Soil.* (2017) 419:1–11. doi: 10.1007/s11104-017-3218-9
28. Yue Z, Shen Y, Chen Y, Liang A, Chu C, Chen C, et al. Microbiological insights into the stress-alleviating property of an endophytic *Bacillus altitudinis* WR10 in wheat under low-phosphorus and high-salinity stresses. *Microorganisms.* (2019) 7:508. doi: 10.3390/microorganisms7110508
29. Borker SS, Thakur A, Kumar S, Kumari S, Kumar R, Kumar S. Comparative genomics and physiological investigation supported safety, cold adaptation, efficient hydrolytic and plant growth-promoting potential of psychrotrophic Glutamicibacter arilaitensis LJH19, isolated from night-soil compost. *BMC Genomics.* (2021) 22:307. doi: 10.1186/s12864-021-07632-z
30. Boubekri K, Soumare A, Mardad I, Lyamlouli K, Hafidi M, Ouhdouch Y, et al. The screening of potassium- and phosphate-solubilizing Actinobacteria and the assessment of their ability to promote wheat growth parameters. *Microorganisms.* (2021) 9:470. doi: 10.3390/microorganisms9030470
31. Cosentino S, Voldby Larsen M, Møller Aarestrup F, Lund O. PathogenFinder - distinguishing friend from foe using bacterial whole genome sequence. *PLoS ONE.* (2013) 8:e77302. doi: 10.1371/journal.pone.0077302
32. Liu B, Zheng DD, Jin Q, Chen LH, Yang J. VFDB 2019: a comparative pathogenomic platform with an interactive web interface. *Nucleic Acids Res.* (2019) 47:D687–92. doi: 10.1093/nar/gky1080
33. Dhanapal AP, Ray JD, Singh SK, Hoyos-Villegas V, Smith JR, Purcell LC, et al. Genome-wide association mapping of soybean chlorophyll traits based on canopy spectral reflectance and leaf extracts. *BMC Plant Biol.* (2016) 16:174. doi: 10.1186/s12870-016-0861-x
34. Cataldo DA, Schrader LE, Youngs VL. Analysis by digestion and colorimetric assay of total nitrogen in plant tissues high in nitrate. *Crop Sci.* (1974) 14:854–6. doi: 10.2135/cropsci1974.0011183X001400060024x
35. Yue Z, Chen Y, Chen C, Ma K, Tian E, Wang Y, et al. Endophytic *Bacillus altitudinis* WR10 alleviates Cu toxicity in wheat by augmenting reactive oxygen species scavenging and phenylpropanoid biosynthesis. *J Hazard Mater.* (2021) 405:124272. doi: 10.1016/j.jhazmat.2020.124272
36. Pohl P, Dzimitrowicz A, Lesniewicz A, Welna M, Szymczycha-Madeja A, Cyganowski P, et al. Room temperature solvent extraction for simple and fast determination of total concentration of Ca, Cu, Fe, Mg, Mn, and Zn in bee pollen by FAAS along with assessment of the bioaccessible fraction of these elements using in vitro gastrointestinal digestion. *J Trace Elem Med Biol.* (2020) 260:126479. doi: 10.1016/j.jtemb.2020.126479
37. Latta M, Eskin M. A simple and rapid colorimetric method for phytate determination. *J Agric Food Chem.* (1980) 28:1313–5. doi: 10.1021/jf60232a049
38. Connorton JM, Jones ER, Rodríguez-Ramiro I, Fairweather-Tait S, Uauy C, Balk J. Wheat vacuolar iron transporter TaVIT2 transports Fe and Mn and is effective for biofortification. *Plant Physiol.* (2017) 174:2434–44. doi: 10.1104/pp.17.00672
39. Zuo Y, Zhang F. Soil and crop management strategies to prevent iron deficiency in crops. *Plant Soil.* (2011) 339:83–95. doi: 10.1007/s11104-010-0566-0
40. Pellegrino E, Öpik M, Bonari Ercoli EL. Responses of wheat to arbuscular mycorrhizal fungi: a meta-analysis of field studies from 1975 to 2013. *Soil Biol Biochem.* (2015) 84:210–7. doi: 10.1016/j.soilbio.2015.02.020
41. Assainar SK, Abbott LK, Mickan BS, Whiteley AS, Siddique KHM, Solaiman ZM. Response of wheat to a multiple species microbial inoculant compared to fertilizer application. *Front Plant Sci.* (2018) 9:1601. doi: 10.3389/fpls.2018.01601
42. Thakur R, Sharma KC, Gulati A, Sud RK, Gulati A. Stress-tolerant Viridibacillus arenosi strain IHB B 7171 from tea rhizosphere as a potential broad-spectrum microbial inoculant. *Indian J Microbiol.* (2017) 57:195–200. doi: 10.1007/s12088-017-0642-8
43. Yadav R, Ror P, Rathore P, Ramakrishna W. Bacteria from native soil in combination with arbuscular mycorrhizal fungi augment wheat yield and biofortification. *Plant Physiol Biochem.* (2020) 150:222–33. doi: 10.1016/j.plaphy.2020.02.039
44. Ercoli L, Schüßler A, Arduini I, Pellegrino E. Strong increase of durum wheat iron and zinc content by field-inoculation with Arbuscular mycorrhizal fungi at different soil nitrogen availabilities. *Plant Soil.* (2017) 419:153–67. doi: 10.1007/s11104-017-3319-5
45. Bernabeu PR, García SS, López AC, Vio SA, Carrasco N, Boiardi JL, et al. Assessment of bacterial inoculant formulated with Paraburkholderia tropica to enhance wheat productivity. *World J MicrobiolBiotechnol.* (2018) 34:81. doi: 10.1007/s11274-018-2461-4
46. Lehmann A, Rillig MC. Arbuscular mycorrhizal contribution to copper, manganese and iron nutrient concentrations in crops - a meta-analysis. *Soil Biol Biochem.* (2015) 81:147–58. doi: 10.1016/j.soilbio.2014.11.013
47. Zhang YY, Stockmann R, Ng K, Ajlouni S. Revisiting phytate-element interactions: implications for iron, zinc and calcium bioavailability, with emphasis on legumes. *Crit Rev Food Sci Nutr.* (2020) 16:1–17. doi: 10.1080/10408398.2020.1846014
48. Hodge A, Storer K. Arbuscular mycorrhiza and nitrogen: implications for individual plants through to ecosystems. *Plant Soil.* (2015) 386:1–19. doi: 10.1007/s11104-014-2162-1
49. Dong H, Yan S, Liu J, Liu P, Sun J. TaCOLD1 defines a new regulator of plant height in bread wheat. *Plant Biotechnol J.* (2019) 17:687–99. doi: 10.1111/pbi.13008
50. Wang J, Li R, Zhang H, Wei G, Li Z. Beneficial bacteria activate nutrients and promote wheat growth under conditions of reduced fertilizer application. *BMC Microbiol.* (2020) 20:38. doi: 10.1186/s12866-020-1708-z
51. Filella I, Serrano L, Serra J, Penuelas J. Evaluating wheat nitrogen status with canopy reflectance indices and discriminant analysis. *Crop Sci.* (1995) 35:1400–5. doi: 10.2135/cropsci1995.0011183X003500050023x
52. Zhang J, Han W, Huang L, Zhang Z, Ma Y, Hu Y. Leaf chlorophyll content estimation of winter wheat based on visible and near-infrared sensors. *Sensors.* (2016) 16:437. doi: 10.3390/s16040437
53. Khan N, Bano A, Babar MDA. The stimulatory effects of plant growth promoting rhizobacteria and plant growth regulators on wheat physiology grown in sandy soil. *Arch Microbiol.* (2019) 201:769–85. doi: 10.1007/s00203-019-01644-w
54. Khan N, Bano A. Exopolysaccharide producing rhizobacteria and their impact on growth and drought tolerance of wheat grown under rain fed conditions. *PLoS ONE.* (2019) 14:e0222302. doi: 10.1371/journal.pone.0222302
55. Seleiman MF, Ali S, Refay Y, Rizwan M, Alhammad BA, El-Hendawy SE. Chromium resistant microbes and melatonin reduced Cr uptake and toxicity,

improved physio-biochemical traits and yield of wheat in contaminated soil. *Chemosphere.* (2020) 250:126239. doi: 10.1016/j.chemosphere.2020.126239
56. Arkhipova T, Martynenko E, Sharipova G, Kuzmina L, Ivanov I, Garipova M, et al. Effects of plant growth promoting rhizobacteria on the content of abscisic acid and salt resistance of wheat plants. *Plants.* (2020) 9:1429. doi: 10.3390/plants9111429
57. Saad MM, Eida AA, Hirt H. Tailoring plant-associated microbial inoculants in agriculture: a roadmap for successful application. *J Exp Bot.* (2020) 71:3878–901. doi: 10.1093/jxb/eraa111
58. Alori ET, Babalola OO. Microbial inoculants for improving crop quality and human health in Africa. *Front Microbiol.* (2018) 9:2213. doi: 10.3389/fmicb.2018.02213
59. Fukami J, Nogueira MA, Araujo RS, Hungria M. Accessing inoculation methods of maize and wheat with Azospirillum brasilense. *AMB Express.* (2016) 6:3. doi: 10.1186/s13568-015-0171-y
60. Álvarez-López V, Prieto-Fernández A, Janssen J, Herzig R, Vangronsveld J, Kidd PS. Inoculation methods using *Rhodococcus erythropolis* strain P30 affects bacterial assisted phytoextraction capacity of *Nicotiana tabacum*. *Int J Phytoremediation.* (2016) 18:406–15. doi: 10.1080/15226514.2015.1109600
61. Afzal M, Yousaf S, Reichenauer TG, Sessitsch A. The inoculation method affects colonization and performance of bacterial inoculant strains in the phytoremediation of soil contaminated with diesel oil. *Int J Phytoremediation.* (2012) 14:35–47. doi: 10.1080/15226514.2011.552928
62. O'Callaghan M. Microbial inoculation of seed for improved crop performance: issues and opportunities. *Appl Microbiol Biotechnol.* (2016) 100:5729–46. doi: 10.1007/s00253-016-7590-9

Conflict of Interest: The authors declare that the research was conducted in the absence of any commercial or financial relationships that could be construed as a potential conflict of interest.

Publisher's Note: All claims expressed in this article are solely those of the authors and do not necessarily represent those of their affiliated organizations, or those of the publisher, the editors and the reviewers. Any product that may be evaluated in this article, or claim that may be made by its manufacturer, is not guaranteed or endorsed by the publisher.

frontiers in Nutrition

ORIGINAL RESEARCH
published: 08 September 2021
doi: 10.3389/fnut.2021.740286

Assessing the Role of *Carotenoid Cleavage Dioxygenase 4* Homoeologs in Carotenoid Accumulation and Plant Growth in Tetraploid Wheat

*Shu Yu and Li Tian**

Department of Plant Sciences, University of California, Davis, Davis, CA, United States

The dietary needs of humans for provitamin A carotenoids arise from their inability to synthesize vitamin A *de novo*. To improve the status of this essential micronutrient, special attention has been given to biofortification of staple foods, such as wheat grains, which are consumed in large quantities but contain low levels of provitamin A carotenoids. However, there remains an unclear contribution of metabolic genes and homoeologs to the turnover of carotenoids in wheat grains. To better understand carotenoid catabolism in tetraploid wheat, Targeting Induced Local Lesions in Genomes (TILLING) mutants of *CCD4*, encoding a Carotenoid Cleavage Dioxygenase (CCD) that cleaves carotenoids into smaller apocarotenoid molecules, were isolated and characterized. Our analysis showed that *ccd4* mutations co-segregated with *Poltergeist-like* (*pll*) mutations in the TILLING mutants of A and B subgenomes, hence the *ccd-A4 pll-A*, *ccd-B4 pll-B*, and *ccd-A4 ccd-B4 pll-A pll-B* mutants were analyzed in this study. Carotenoid profiles are comparable in mature grains of the mutant and control plants, indicating that CCD4 homoeologs do not have a major impact on carotenoid accumulation in grains. However, the neoxanthin content was increased in leaves of *ccd-A4 ccd-B4 pll-A pll-B* relative to the control. In addition, four unidentified carotenoids showed a unique presence in leaves of *ccd-A4 ccd-B4 pll-A pll-B* plants. These results suggested that CCD4 homoeologs may contribute to the turnover of neoxanthin and the unidentified carotenoids in leaves. Interestingly, abnormal spike, grain, and seminal root phenotypes were also observed for *ccd-A4 pll-A*, *ccd-B4 pll-B*, and *ccd-A4 ccd-B4 pll-A pll-B* plants, suggesting that CCD4 and/or PLL homoeologs could function toward these traits. Overall, this study not only reveals the role of CCD4 in cleavage of carotenoids in leaves and grains, but also uncovers several critical growth traits that are controlled by CCD4, PLL, or the CCD4-PLL interaction.

Keywords: wheat, carotenoid cleavage dioxygenase, *ccd4*, poltergeist-like, TILLING

OPEN ACCESS

Edited by:
Alexander Arthur Theodore Johnson, The University of Melbourne, Australia

Reviewed by:
Yueliang Zhao, Shanghai Ocean University, China
Mohamed Fawzy Ramadan Hassanien, Zagazig University, Egypt

***Correspondence:**
Li Tian
ltian@ucdavis.edu
orcid.org/0000-0001-6461-6072

Specialty section:
This article was submitted to Nutrition and Food Science Technology, a section of the journal Frontiers in Nutrition

Received: *12 July 2021*
Accepted: *18 August 2021*
Published: *08 September 2021*

Citation:
Yu S and Tian L (2021) Assessing the Role of Carotenoid Cleavage Dioxygenase 4 Homoeologs in Carotenoid Accumulation and Plant Growth in Tetraploid Wheat. Front. Nutr. 8:740286. doi: 10.3389/fnut.2021.740286

INTRODUCTION

Wheat is among the most widely cultivated and consumed staple food crops around the world. Wheat grains are a rich source of starch and proteins for human nutrition (1). In recent years, efforts have been directed toward enhancing the production of provitamin A carotenoids, particularly β-carotene, in wheat grains through breeding and biotechnology for improved vitamin

A nutrition (2). However, provitamin A carotenoids produced in wheat grains may be subjected to degradation by carotenoid cleavage dioxygenases (CCDs) that cleave carotenoids (C_{40}) into smaller apocarotenoid molecules (3). Therefore, it is imperative to better understand the activity and function of CCDs in wheat grains for achieving a high level of provitamin A carotenoid accumulation. Previous comparative analyses using CCDs from mouse [β-carotene 15,15′-monooxygenase-1 (BCMO1), BCMO2, and retinal pigment epithelium 65 (RPE65)], *Synechocystis* sp. PCC 6803 [lignostilbene dioxygenase (ACO)], and maize [9-*cis*-epoxycarotenoid dioxygenase (VP14)] revealed that CCDs from different kingdoms all contain four conserved histidine residues and additional acidic amino acids for binding of iron through hydrogen bonding, which is essential for the activity of the iron-dependent CCD enzymes (4).

Of the four CCDs (CCD1, CCD4, CCD7, and CCD8) identified in different plant species, CCD7 and CCD8 are dedicated to the biosynthesis of apocarotenoid phytohormones strigolactones, whereas CCD1 and CCD4 contribute to the production of various other apocarotenoid molecules in diverse tissues (5). Our recent study showed that *CCD1* and *CCD4* homoeologs are differentially expressed in tetraploid and hexaploid wheat grains (6). When assayed for enzyme activity using recombinant proteins, wheat CCD1 homoeologs, but not CCD4 homoeologs, converted β-carotene, lutein, and zeaxanthin to apocarotenoids, suggesting a role of CCD1 homoeologs in carotenoid degradation in wheat grains (6). However, genetic studies with *Arabidopsis* seeds demonstrated that *At*CCD4 plays a major role in degradation of β-carotene during desiccation of *Arabidopsis* seeds, though *At*CCD4 exhibited low *in vitro* enzyme activity toward β-carotene (7). Additionally, total carotenoids in chrysanthemum petals and the violaxanthin content in potato tubers were increased when *CCD4* expression was downregulated via RNA interference (RNAi) in these tissues, suggesting its role in carotenoid cleavage *in planta* (8, 9). Taking into consideration these reports from wheat and other plants, it remains to be determined whether CCD4 could catalyze carotenoid cleavage reactions in wheat, which could be interrogated through genetic manipulation of CCD4 enzyme activity or gene expression. Emerging evidence has suggested the role of apocarotenoid signaling molecules, other than strigolactones and abscisic acid [ABA; produced by nine-*cis*-epoxycarotenoid dioxygenases (NCEDs)], in controlling plant growth, development, and interactions with the environment (5). Therefore, it will be important to also understand the function of apocarotenoid molecules generated by CCD4 in wheat.

To investigate the function of CCD4 homoeologs in carotenoid metabolism and plant growth in tetraploid wheat, we isolated Targeting Induced Local Lesions in Genomes (TILLING) mutants of *CCD4* homoeologs from a tetraploid wheat mutant library in this study. *CCD4* is located near a gene annotated as *Poltergeist-like* (*PLL*) on chromosome 6 of tetraploid wheat (**Figure 1A**). PLL and its homolog Poltergeist (POL) belong to the protein phosphatase type 2C (PP2C) family and contain metal ion-interacting domains with highly conserved amino acid residues (10). The *Arabidopsis* POL and PLL1 were shown to function in maintenance and differentiation of stem cells as well as additional developmental pathways such as formation of the central vasculature and embryo development (10–15). Although the *Arabidopsis pol* and *pll1* single mutants only displayed weak developmental phenotypes relative to wild-type plants (10, 15), the *pol pll1* double mutants were seedling lethal, indicating that both POL and PLL1 are crucial for plant development (13). Besides PLL1, there are four additional PLLs in *Arabidopsis*: PLL2-PLL5. While the mutant analysis demonstrated that PLL4 and PLL5 regulate leaf morphology, *pll2* and *pll3* mutants did not exhibit any distinguishable growth phenotypes when compared to wild-type plants, suggesting that PLL2 and PLL3 may not play a developmental role in *Arabidopsis* (12).

Our analysis showed that the *ccd4* TILLING mutant lines isolated in this study also contain mutations in *PLL* and that the *ccd4* mutations are linked to the *pll* mutations in both A and B subgenomes in the backcrossed (BCed) progenies. Because *CCD4* and *PLL* are closely located in the same chromosomal region, there is a low frequency of recombination between the two genes during meiosis and they are inherited together in the next generation. As such, the double (*ccd-A4 pll-A* and *ccd-B4 pll-B*) and quadruple (*ccd-A4 ccd-B4 pll-A pll-B*) mutants were analyzed in this study for biochemical and growth phenotypes and agronomic traits.

MATERIALS AND METHODS

Plant Growth and Tissue Collection

Wheat seeds were surface-sterilized using 1% (w/v) sodium hypochlorite solution containing 0.1% (v/v) Triton X-100, and rinsed with running water for at least 3 times. The sterilized seeds were placed on two layers of damp germination paper (Hoffman Manufacturing, Inc., Corvallis, OR) in a petri dish and stored at 4°C for 3 d to synchronize germination. The cold-treated seeds were subsequently moved to room temperature (∼22°C) and germinated in the dark for 2–4 d to allow root development. The seedlings were then transplanted in soil and grown in a climate-controlled greenhouse (∼22°C) under long-day conditions (16-h light/8-h dark). For leaf carotenoid and gene expression analyses, the fourth leaf counted from the top on the primary tiller of 4-week-old plants was collected, frozen in liquid nitrogen, and stored at −80°C until analysis. For grain carotenoid, spike, and grain yield analyses, spikes were collected from wheat plants at the harvest-ready stage and dried at room temperature (∼22°C) for 1 week before the measurements. Grains were hand-cleaned to remove dry husks, and those harvested from the same plant were pooled and considered as one biological replicate. For grain carotenoid analysis, 25 whole grains were randomly sampled from each biological replicate and used for extraction.

TILLING Mutant Screening and Crossing

Mutants of *CCD-A4* and *CCD-B4* (i.e., *ccd-A4* and *ccd-B4*) were identified from the exome-sequenced TILLING mutant library of tetraploid wheat cv. Kronos (https://dubcovskylab.ucdavis.edu/wheat_blast) using the respective DNA sequences as queries. To reduce the additional mutations caused by ethyl methanesulfonate (EMS), the M_4 *ccd-A4* (line T4-0842) and *ccd-B4* (line T4-3179) mutants were BCed to the wild-type parental

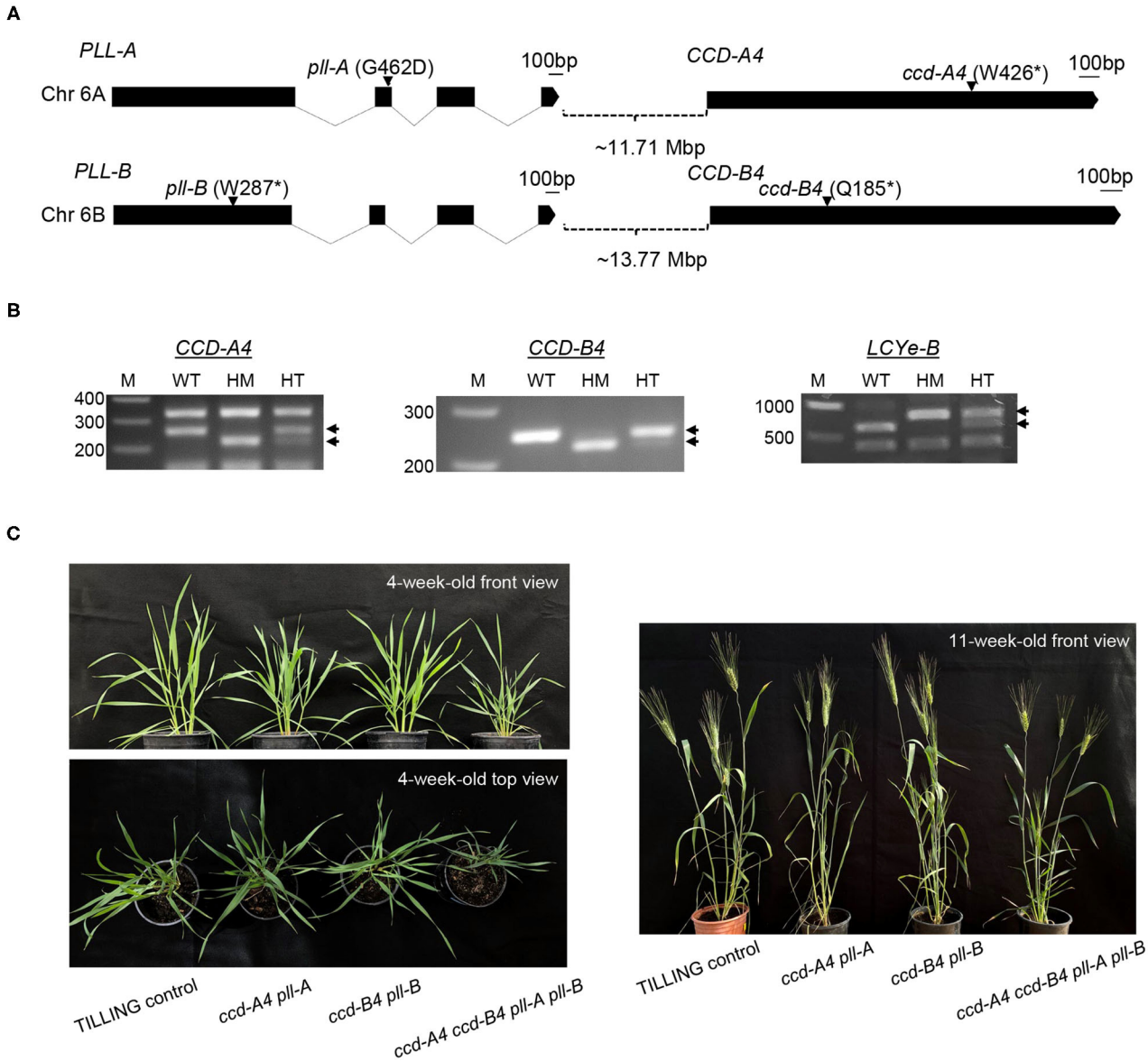

FIGURE 1 | Tetraploid wheat TILLING mutants of *CCD-A4*, *CCD-B4*, *PLL-A*, and *PLL-B*. **(A)** Exon-intron diagrams of *CCD-A4*, *CCD-B4*, *PLL-A*, and *PLL-B*. Exons and introns are shown by black boxes and solid lines, respectively. The black bar denotes 100 bp. Locations of mutations are indicated with arrows. Mutant alleles of *CCD4* and *PLL* homoeologs are linked and co-segregated in progenies of *ccd-A4* and *ccd-B4* mutants. Chr, chromosome; Mbp, megabase pair; *stop codon. **(B)** Cleaved Amplified Polymorphic Sequences (CAPS) and derived CAPS (dCAPS) markers for genotyping of wild-type and mutant *CCD-A4*, *CCD-B4*, and *LCYe-B* alleles. The PCR products were digested with HphI (*CCD-A4* primer pair), RsaI (*CCD-B4* primer pair), and DdeI (*LCYe-B* primer pair). Diagnostic bands for each marker are indicated with arrows. WT, homozygous wild type for the target gene; HM, homozygous mutant; HT, heterozygous mutant; M, DNA size marker. **(C)** Images of 4-week-old and 11-week-old TILLING control as well as *ccd-A4 pll-A*, *ccd-B4 pll-B*, and *ccd-A4 ccd-B4 pll-A pll-B* mutant plants.

plant Kronos for one generation. The BC_1 *ccd-A4* and *ccd-B4* mutant plants were then intercrossed and the heterozygous progenies harboring *ccd-A4* and *ccd-B4* mutant alleles were chosen for self-pollination. From the segregating population of the self-pollinated plants, mutants that are homozygous for *ccd-A4* or *ccd-B4*, or both *ccd-A4* and *ccd-B4* were selected. TILLING controls are plants containing wild-type *CCD-A4* and *CCD-B4* alleles, and have a mutational load similar to that of *ccd-A4*, *ccd-B4*, and *ccd-A4 ccd-B4* mutants; TILLING controls were also selected from the segregating population. Cleaved Amplified Polymorphic Sequences (CAPS) and derived CAPS (dCAPS) markers were designed for *CCD-A4* and *CCD-B4* and used in the genotyping analysis (**Supplementary Table 1**).

A mutated *lycopene ε-cyclase-B* (*LCYe-B*) allele is also present in the M_4 *ccd-B4* plant (line T4-3179), but segregated independently from the *ccd-B4* mutation when BCed to

the wild-type Kronos plants. TILLING control and the homozygous BC_1 *ccd-A4*, *ccd-B4*, and *ccd-A4 ccd-B4* mutants were inspected for *LCYe-B* alleles using a CAPS marker (**Supplementary Table 1**); all of the above-mentioned genotypes contain the wild-type *LCYe-B* allele and were used in this study. The *PLL* homoeologs were amplified from the *ccd-A4*, *ccd-B4*, *ccd-A4 ccd-B4* mutants and TILLING control and subjected to DNA sequencing (primer pairs are listed in **Supplementary Table 2**). This confirmed that the *ccd-A4* mutant harbored *pll-A* and *PLL-B* alleles, the *ccd-B4* mutant contained *PLL-A* and *pll-B* alleles, and the *ccd-A4 ccd-B4* mutant carried *pll-A* and *pll-B* alleles. TILLING control plants were verified to possess only wild-type *CCD-A4*, *CCD-B4*, *PLL-A*, and *PLL-B* alleles. Because the *ccd4* mutants also contain homozygous *pll* mutations, they were therefore designated the *ccd-A4 pll-A*, *ccd-B4 pll-B*, and *ccd-A4 ccd-B4 pll-A pll-B* mutants.

Multiple Sequence Alignment

The GenBank accession numbers of the selected proteins are: *Synechocystis* sp. PCC 6803 lignostilbene dioxygenase, BAA18428; maize VP14, AAB62181; tetraploid wheat CCD-A4, KU975448; tetraploid wheat CCD-B4, KU975449; *At*PLL1, NP_181078; *At*POL, NP_850463; tetraploid wheat PLL-A, XP_037447847 (this sequence from *Triticum dicoccoides* is identical to PLL-A from *T. turgidum*); tetraploid wheat PLL-B, XP_037453069 (this sequence from *T. dicoccoides* is identical to PLL-B from *T. turgidum*). The protein sequences were aligned using Clustal Omega (16) and the alignment diagrams were prepared using BoxShade (https://embnet.vital-it.ch/software/BOX_form.html).

Carotenoid Analysis

Leaves and mature whole grains were ground into fine powder in liquid nitrogen using a mortar and pestle. Total carotenoids were extracted from ∼50 mg leaves and ∼300 mg whole grain flour using the methods described in (6) and (17), respectively. Carotenoids extracted from grain flour were saponified using 2 M KOH [dissolved in methanol containing 0.01% (w/v) butylated hydroxytoluene]. Following saponification in dark for 30 min, equal volumes of diethyl ether and H_2O were added for phase separation. Re-extraction of carotenoids from the water phase, pooling and washing the diethyl ether layers, and drying and re-dissolving of carotenoid residues were carried out as described (17). Ten microliter of leaf or grain carotenoid extract (resuspended in ethyl acetate) was injected on a reverse-phase HPLC column and analyzed using a previously established gradient (18).

Gene Expression Analysis

Total RNA was extracted from ∼50 mg of ground leaves using a cetyltrimethylammonium bromide (CTAB)-based method (19). After treatment with RNase-free DNase I (Fermentas, Glen Burnie, MD), reverse transcription was carried out using the iScript™ Advanced cDNA Synthesis Kit (BioRad, Hercules, CA) following the manufacturer's instructions. For each qPCR reaction, 0.1 μl first-strand cDNA (equivalent to 6.25 ng total RNA) was used as template for amplification with the iTaq™ Universal SYBR® Green Supermix (BioRad). Primers used for the real-time qPCR analysis of *CCD-A4* and *CCD-B4*, as well as the reference genes *Ta2291* and *Ta54227*, were as previously described (6).

Measurement of Plant Growth Traits

For analysis of spike and grain traits, nine plants of TILLING control or each of the mutant genotypes were assessed for the total number of spikes per plant. The number of spikelets on each spike was counted and averaged for all spikes in the same plant to be considered as one biological replicate. To determine the length of primary spike, the spike on the first tiller of the plant was measured for the distance between the base and the top of the spike without the awn. The total number of grains was counted for each plant. Grain weight was then calculated by dividing the weight of all grains harvested from a plant by the number of grains for that plant. Images of grains were captured using an Epson V600 scanner (Epson, Los Alamitos, CA) with the crease side down. The grain length and width were determined using ImageJ (20) and averaged for all grains collected from each plant.

For analysis of seminal root traits, one sterilized and cold-treated wheat seed was placed in between a piece of germination paper and a clear sheet protector with the crease side of the seed oriented toward the germination paper and the embryo end pointing downwards. The seeds were grown vertically at the room temperature (∼22°C) either entirely in the dark or under long-day conditions (16-h light/8-h dark) with a light intensity of 120 $\mu mol\ m^{-2}\ s^{-1}$. After germinating at room temperature for 3 d, the seedlings were scanned using an Epson V600 scanner (Epson) and images saved as TIFF files. Coleoptiles and seminal roots were hand-traced in the images and the trait parameters were determined using ImageJ (20).

Statistical Analysis

One-way Analysis of Variation (ANOVA) followed by Tukey's Honestly Significant Difference test were performed for the carotenoid quantification, gene expression, spike, grain, and seminal root data using JMP (SAS Institute, Cary, NC).

RESULTS

The *ccd4* TILLING Mutants Used in This Study Do Not Contain Mutations in Other Carotenoid Metabolic Gene Homoeologs, but Carry *pll-A* and *pll-B* Mutations

By searching an exome-sequenced tetraploid wheat TILLING mutant library (21), 78 and 109 lines were identified that contain mutations in the open reading frame (ORF) of *CCD-A4* and *CCD-B4*, respectively. Of these mutations, three led to premature stop codons in CCD-A4: W426* in line T4-0842, W441* in line T4-2477, and Q628* in line T4-0594, and one in CCD-B4: Q181* in line T4-3179. Lines T4-0842 (W426*) and T4-3179 (Q181*) were used in this study and designated as *ccd-A4* and *ccd-B4*. The W426* mutation in *ccd-A4* truncated 203 amino acids out of the 628 amino acids of CCD-A4. The Q181* mutation in *ccd-B4* led to a CCD-B4 protein missing 452 amino

acids from the C-terminus (**Figure 1A**). These truncated CCD-A4 and CCD-B4 proteins do not contain the entire four-His and three-Glu iron coordination system essential for CCD enzyme activity, suggesting that they are loss-of-function mutations (**Supplementary Figure 1**) (22).

The exome sequences of *ccd-A4* and *ccd-B4* were also analyzed for possible mutations in other carotenoid metabolic genes, including *lycopene β-cyclase* (*LCYb*), *LCYe*, *β-carotene hydroxylase 1* (*HYD1*), *HYD2*, and *CCD1*. The absence of mutations was verified for all of these gene homoeologs (i.e., both A and B subgenomes) except for *LCYe-B*; *ccd-B4* (line T4-3179 at the M_4 generation) also contained a mutation in *LCYe-B*. The *ccd-A4* and *ccd-B4* mutants were each BCed to the wild-type parental line Kronos for one generation. The *LCYe-B/lcye-B* (chromosome 3) and *CCD-B4/ccd-B4* (chromosome 6) alleles segregated independently during BC as they are located on different chromosomes. We confirmed that all the *ccd4* mutants used in this study (at the BC_1 generation) only contain the wild-type *LCYe-B* alleles according to genotyping analysis using a CAPS marker (**Figure 1B**). The BC_1 *ccd-A4* and *ccd-B4* mutants were crossed and the progenies genotyped to select the *ccd-A4 ccd-B4* double mutants using CAPS and dCAPS markers (**Figure 1B**).

Genes surrounding *CCD4* on chromosome 6 were also inspected for mutations using the exome sequences of *ccd-A4* and *ccd-B4*. Both *ccd-A4* and *ccd-B4* mutants carried mutated *PLL* alleles (**Figure 1A**) and we confirmed that *pll* mutations were linked with *ccd4* mutations in the BC_1 *ccd4* mutants by DNA sequencing (data not shown). The mutation of *PLL-A* led to an amino acid substitution (G462D) and the mutation of *PLL-B* led to a truncated PLL-B (W287*) protein (**Figure 1A**). These mutated proteins miss either a critical amino acid in a highly conserved region (pll-A) or essential functional components of protein phosphatases (pll-B), suggesting that they are likely loss-of-function mutations (**Supplementary Figure 2**). Taken together from the mutant analysis, the *ccd-A4*, *ccd-B4,* and *ccd-A4 ccd-B4* mutants used in this study are indeed *ccd-A4 pll-A*, *ccd-B4 pll-B*, and *ccd-A4 ccd-B4 pll-A pll-B*, respectively. In addition to these mutant genotypes, TILLING control plants that are wild-type for the *CCD-A4*, *CCD-B4*, *PLL-A*, and *PLL-B* alleles, and carry a similar mutational load as the mutants were analyzed in parallel with the mutants.

Mutations of *CCD-A4* and *CCD-B4* Are Associated With Altered Carotenoid Profiles and Varied Expression of *CCD4* Homoeologs in Leaves

To understand the impact of *ccd4* mutations on carotenoid accumulation, total carotenoids were extracted from leaves and mature whole grains of TILLING control and the mutant plants and analyzed on high performance liquid chromatography (HPLC) (**Figure 2**; **Tables 1**, **2**). In leaves, a small but significant increase was observed in neoxanthin levels in *ccd-B4 pll-B* and *ccd-A4 ccd-B4 pll-A pll-B*, in violaxanthin levels in *ccd-A4 pll-A* and *ccd-B4 pll-B*, in lutein levels in *ccd-B4 pll-B*, and in total carotenoids in *ccd-B4 pll-B* and *ccd-A4 ccd-B4 pll-A pll-B*, relative to TILLING control (**Table 1**). There was no significant change in the β-carotene content between TILLING control and the mutants (**Table 1**). Although accumulated at very low levels, two unidentified peaks eluted at 8.89 min (peak 1) and 10.01 min (peak 2) showed differential accumulation only in *ccd-A4 ccd-B4 pll-A pll-B* (**Figure 2B**; **Supplementary Table 1**). Additionally, two unidentified peaks eluted at 13.28 min (peak 3) and 13.39 min (peak 4) were present in the leaf carotenoid extracts of *ccd-A4 ccd-B4 pll-A pll-B* but absent in other genotypes (**Figure 2B**; **Supplementary Table 3**). Peaks 1–4 appear to be carotenoid molecules as they possess the characteristic three-peak absorption profiles for carotenoids (**Figure 2C**). In mature whole grains, lutein, β-carotene, and total carotenoids were not significantly different among TILLING control and the mutant genotypes (**Table 2**).

To examine whether the mutation of one *CCD4* homoeolog may cause changes in the expression of the other *CCD4* homoeolog, transcript levels of *CCD-A4* and *CCD-B4* in leaves of the mutant and TILLING control plants were determined using real-time qPCR (**Figure 3**). Expression levels of the mutated *CCD-A4* and *CCD-B4* alleles were only about 30% of the wild-type alleles in TILLING control, suggesting that the mutations not only led to premature stop codons, but also reduced the stability of the respective mRNAs (**Figure 3**). While the expression of *CCD-B4* in *ccd-A4 pll-A* maintained at a level comparable to that in TILLING control, the expression of *CCD-A4* was slightly higher in *ccd-B4 pll-B* than TILLING control, suggesting that the *ccd-B4* mutation may induce *CCD-A4* expression (**Figure 3**).

The *ccd-A4 ccd-B4 pll-A pll-B* Mutant Differed Greatly in Spike and Grain Phenotypes

When grown in the greenhouse under long-day conditions, *ccd-A4 ccd-B4 pll-A pll-B* plants were apparently smaller than *ccd-A4 pll-A*, *ccd-B4 pll-B*, and TILLING control plants at both early (4-week-old, prior to the emergence of spikes) and late (11-week-old, physiological maturity) developmental stages (**Figure 1C**). To evaluate the effect of *ccd4* and *pll* mutations on plant performance and grain quality, several agronomic traits related to grain yield were determined that include the number of spikes per plant, number of spikelets per spike, grain number per plant, grain weight, and grain size (length and width) (**Figure 4**). When evaluated using tissues collected at the harvest-ready stage of mature plants, *ccd-A4 ccd-B4 pll-A pll-B* has 120% more spikes per plant than TILLING control, and ∼50% more spikes than *ccd-A4 pll-A* and *ccd-B4 pll-B* (**Figure 4A**). However, *ccd-A4 ccd-B4 pll-A pll-B* has 40% less spikelets per spike than TILLING control, and ∼30% less spikelets per spike than *ccd-A4 pll-A* and *ccd-B4 pll-B* (**Figure 4B**). As a result of the reduced number of spikelets on the spike, the primary spike in *ccd-A4 ccd-B4 pll-A pll-B* was ∼12% shorter compared with other genotypes (**Figures 4C,D**).

Besides the visibly different spike phenotypes (**Figure 4D**), grains harvested from *ccd-A4 ccd-B4 pll-A pll-B* appeared to be slightly smaller than those from TILLING control and other

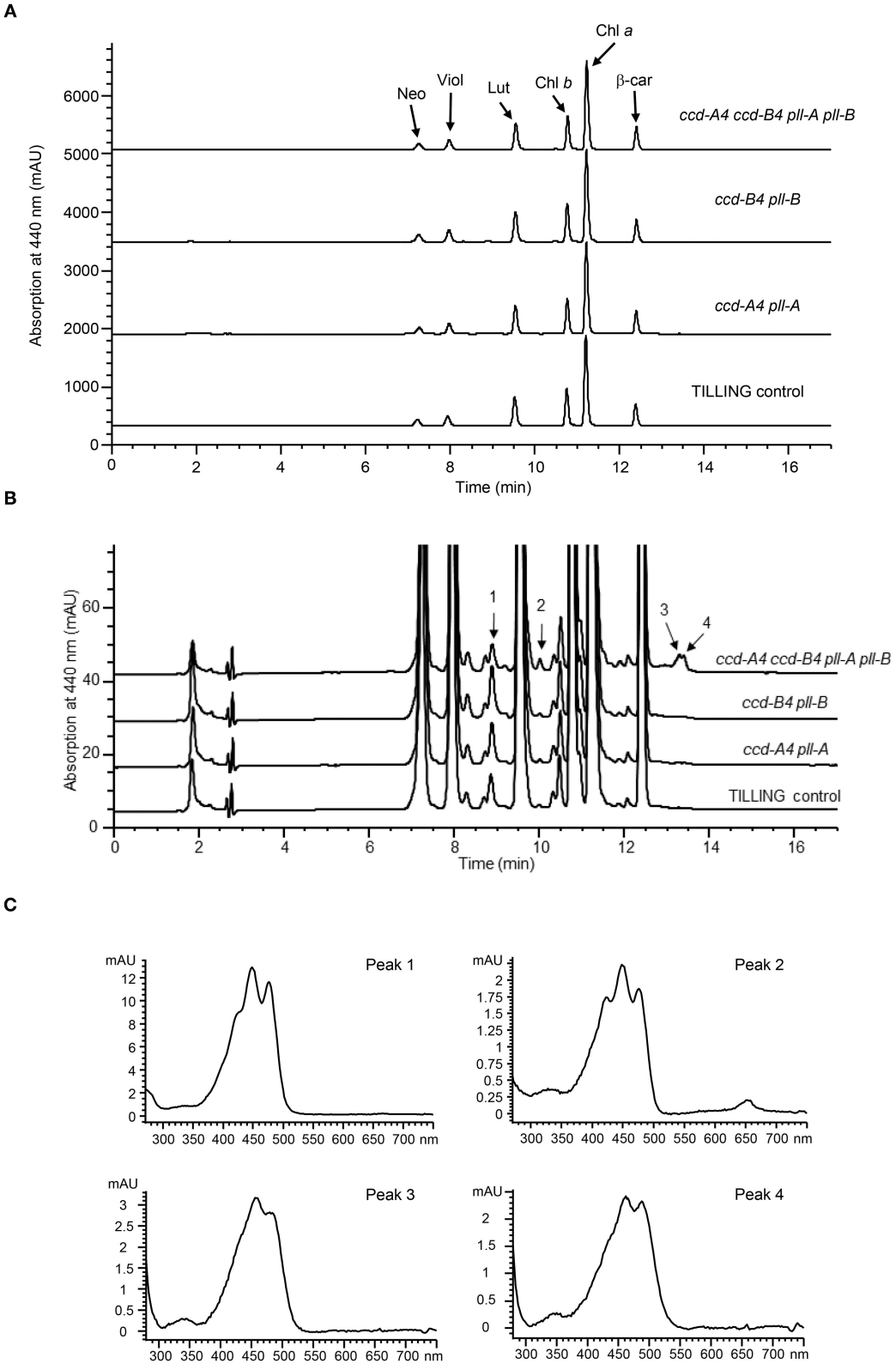

FIGURE 2 | HPLC analysis of carotenoid profiles in leaves of TILLING control and mutant plants. **(A)** HPLC chromatograms of TILLING control, *ccd-A4 pll-A*, *ccd-B4 pll-B*, and *ccd-A4 ccd-B4 pll-A pll-B*. Neo, neoxanthin; Viol, violaxanthin; Lut, lutein; Chl *b*, chlorophyll *b*; Chl *a*, chlorophyll *a*; β-car, β-carotene. **(B)** A zoomed view of HPLC chromatograms showing peaks that are differentially accumulated in *ccd-A4 ccd-B4 pll-A pll-B* and TILLING control. **(C)** Absorption spectra of peaks 1–4.

TABLE 1 | Carotenoids (mmol mol^{-1} chlorophylls *a* + *b*) in leaves of 4-week-old TILLING control and mutant plants.

Genotype	Neoxanthin	Violaxanthin	β-carotene	Lutein	Total
TILLING control	20.36 ± 0.69^{a}	24.19 ± 1.21^{a}	47.31 ± 2.28^{a}	70.25 ± 1.73^{a}	162.11 ± 3.02^{a}
ccd-A4 pll-A	21.48 ± 1.01^{ab}	26.78 ± 1.61^{b}	45.33 ± 2.67^{a}	72.38 ± 0.92^{ab}	165.97 ± 3.84^{ab}
ccd-B4 pll-B	21.78 ± 0.98^{b}	27.13 ± 1.81^{b}	47.90 ± 4.16^{a}	73.15 ± 1.17^{b}	165.95 ± 1.86^{b}
ccd-A4 ccd-B4 pll-A pll-B	22.48 ± 0.52^{b}	26.14 ± 0.91^{ab}	47.77 ± 1.11^{a}	70.87 ± 1.09^{ab}	167.25 ± 3.37^{b}

Data presented are mean ± standard deviation of 4–8 biological replicates. Different letters indicate statistically significant differences (P < 0.05) within a column.

TABLE 2 | Carotenoids (nmol g^{-1} flour) in mature whole grains of TILLING control and mutant plants.

Genotype	Lutein	β-carotene	Total
TILLING control	4.94 ± 1.14^{a}	0.21 ± 0.05^{a}	5.15 ± 1.16^{a}
ccd-A4 pll-A	5.20 ± 1.56^{a}	0.20 ± 0.04^{a}	5.40 ± 1.53^{a}
ccd-B4 pll-B	3.98 ± 1.53^{a}	0.21 ± 0.06^{a}	4.18 ± 1.58^{a}
ccd-A4 ccd-B4 pll-A pll-B	5.30 ± 1.27^{a}	0.20 ± 0.05^{a}	5.50 ± 1.26^{a}

Data presented are mean ± standard deviation of 5-6 biological replicates. Different letters indicate statistically significant differences (P < 0.05) within a column.

mutants (**Figure 4E**). When quantified, *ccd-A4 ccd-B4 pll-A pll-B* grains were 3% shorter than TILLING control and other mutants, whereas grain width was comparable for grains of all genotypes (**Figures 4F,G**). On the other hand, the number of grains per plant and grain yield were more drastically reduced for *ccd-A4 ccd-B4 pll-A pll-B* relative to TILLING control, *ccd-A4 pll-A*, and *ccd-B4 pll-B*, suggesting that the *ccd-A4 ccd-B4 pll-A pll-B* mutant has reduced fertility (**Figures 4H,I**). Indeed, we observed that spikes on the lateral tillers of *ccd-A4 ccd-B4 pll-A pll-B* were sterile despite its large number of lateral tillers (data not shown). Consistent with the relatively smaller grains, the average weight of grains was also decreased by ∼11% in *ccd-A4 ccd-B4 pll-A pll-B* compared to TILLING control and other mutants (**Figure 4J**).

The *ccd-A4 ccd-B4 pll-A pll-B* Mutant Exhibited Distinct Seminal Root Phenotypes in Seedlings Grown in the Dark and Under Long-Day Conditions

In mature plants at harvest, *ccd-A4 ccd-B4 pll-A pll-B* plants possess a largely reduced root volume, which may lead to less biomass production and yield as the root system is responsible for taking up water and mineral nutrients from the soil (**Figure 5A**). Wheat plants contain both seminal roots that develop from the radical and nodal (aka. crown or adventitious) roots that develop from nodes of the stem. To understand whether the *ccd4* and/or *pll* mutations affect root growth, seminal root traits of seedlings were analyzed for 3-day-old seedlings grown in dark or long-day conditions, as both lighting schemes have been used in wheat seed germination (**Figures 5**, **6**). A total of seven seminal root traits were evaluated, including network width, network depth, network width to depth ratio, convex hull area (the area of the smallest convex polygon to enclose the root system), number of seminal roots, seminal root length, and seminal root angle (the angle between the outermost seminal roots). Coleoptile lengths of the seedlings were also measured.

For dark-grown seedlings, the network width, depth, width to depth ratio, convex hull area, and angle of seminal roots were 26–80% reduced in *ccd-A4 ccd-B4 pll-A pll-B* relative to TILLING control (**Figures 5D–G**). While the reduced seminal root angle was due to a lack of seminal roots 4 and 5 in *ccd-A4 ccd-B4 pll-A pll-B* seedlings after 3 d of germination, the reduced network depth and width resulted from a slower growth of seminal roots 1 (depth) and 2 and 3 (width) in this mutant (**Figures 5D,E,L**). In fact, the emergence of the fourth seminal root was only observed in very few 11-day-old *ccd-A4 ccd-B4 pll-A pll-B* seedlings, indicating that the initiation of the fourth seminal root was severely delayed in this mutant (**Supplementary Figure 3**). The combined absence of seminal roots 4 and 5 and a slow growth of seminal roots 1–3 also led to the reduced network width-depth ratio and convex hull area in 3-day-old *ccd-A4 ccd-B4 pll-A pll-B* seedlings. The total length of seminal roots #1-3 of *ccd-A4 ccd-B4 pll-A pll-B* was 75% shorter than that of TILLING control (**Figure 5I**). Although the 3-day-old *ccd-A4 pll-A* and *ccd-B4 pll-B* seedlings possessed 5 seminal roots, their total seminal root lengths were ∼30% shorter than TILLING control (**Figures 5I–K**). The coleoptile lengths correlated with seminal root lengths (seminal roots 1–5) in all mutant genotypes with *ccd-A4 pll-A* and *ccd-B4 pll-B* showing 35–45% reduced length, and *ccd-A4 ccd-B4 pll-A pll-B* 85% reduced length compared to TILLING control (**Figure 5M**).

For three-day-old seedlings grown under long-day conditions, the network width, depth, width to depth ratio, convex hull area, and angle of seminal roots in *ccd-A4 ccd-B4 pll-A pll-B* were largely decreased relative to TILLING control. These observed root phenotypes are similar to those observed for the dark-grown seedlings (**Figures 6A–E**). When compared to TILLING control, the total seminal root length was reduced by 80% in *ccd-A4 ccd-B4 pll-A pll-B* (containing only seminal roots 1–3), 31% in *ccd-A4 pll-A*, and 39% in *ccd-B4 pll-B* (**Figures 6I–K**). The coleoptile lengths of *ccd-A4 pll-A*, *ccd-B4 pll-B,* and *ccd-A4 ccd-B4 pll-A pll-B* were 30, 43, and 92% decreased relative to TILLING control, respectively (**Figure 6K**). Interestingly, the long-day-grown seedlings generally exhibited narrower network width, smaller convex hull area, and more shallow seminal root angles than dark-grown seedlings (**Figures 5**, **6**).

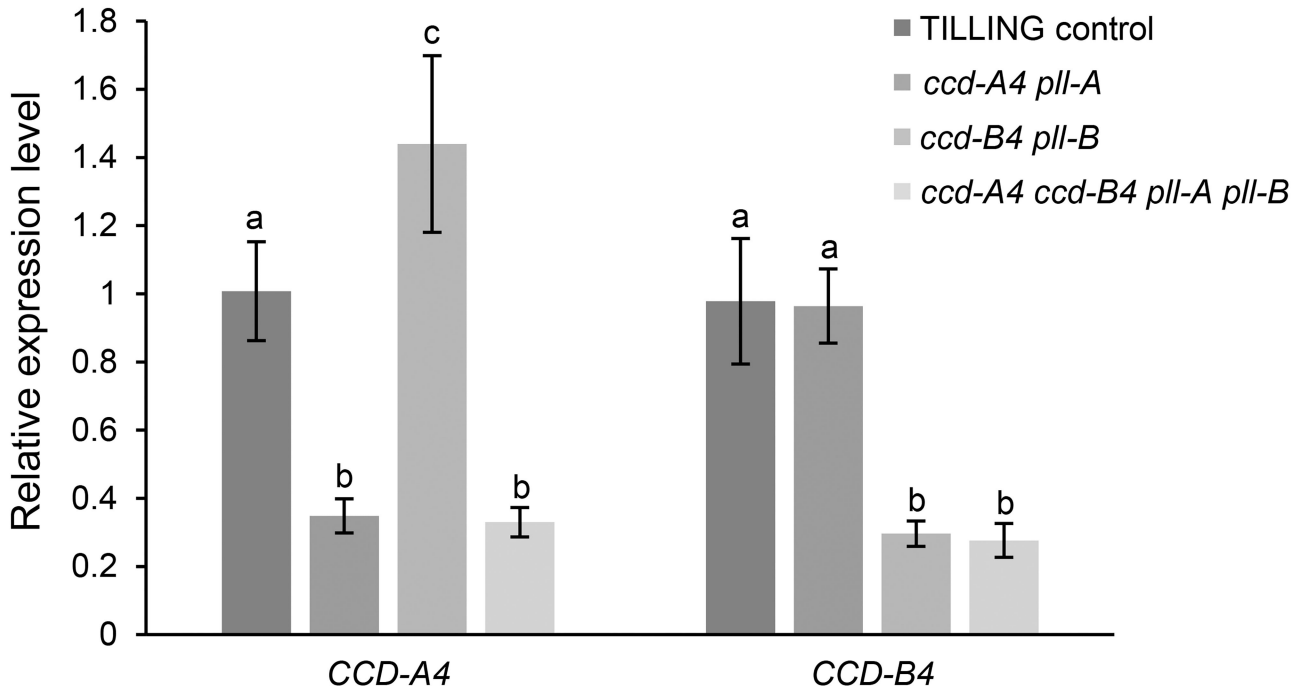

FIGURE 3 | Expression levels of *CCD-A4* and *CCD-B4* in leaves of TILLING control and mutant plants. Data presented are mean ± standard deviation of 4-8 biological replicates. Different letters indicate significantly different expression ($P < 0.05$) for *CCD-A4* or *CCD-B4* in different genotypes.

DISCUSSION

In this study, we isolated, generated, and characterized tetraploid wheat TILLING mutants of *ccd-A4 pll-A*, *ccd-B4 pll-B*, and *ccd-A4 ccd-B4 pll-A pll-B*. The carotenoid content was comparable in grains of TILLING control and the mutants, indicating that CCD4 homoeologs do not play a major role in carotenoid turnover in grains, and therefore their activities do not need to be modified for provitamin A biofortification in tetraploid wheat grains. On the other hand, the moderately increased accumulation of neoxanthin in leaves of *ccd-B4 pll-B* and *ccd-A4 ccd-B4 pll-A pll-B*, violaxanthin in leaves of *ccd-A4 pll-A* and *ccd-B4 pll-B*, and lutein in leaves *ccd-B4 pll-B*, suggests a potential role of CCD-A4 and CCD-B4 in turnover of these xanthophylls in this tissue (**Table 1**). By contrast, β-carotene levels were not significantly changed in *ccd-A4 pll-A*, *ccd-B4 pll-B*, and *ccd-A4 ccd-B4 pll-A pll-B* relative to TILLING control in leaves and whole grains (**Tables 1**, **2**), which is consistent with the results of *in vitro* enzyme assays where incubating recombinant CCD-A4 and CCD-B4 proteins with β-carotene did not yield any products (6). It should be noted that the catalytic activity of CCD-A4/CCD-B4 toward neoxanthin and violaxanthin was not examined in the enzyme assays previously (6).

Interestingly, four unidentified carotenoid peaks showed unique accumulation in leaves of *ccd-A4 ccd-B4 pll-A pll-B*, suggests that these carotenoid molecules could be potential substrates for CCD-A4 and CCD-B4 *in planta*. It also indicates that manipulation of CCD4 activities may lead to accumulation of carotenoids that are not normally present in wild-type plants (**Figure 2**; **Supplementary Table 3**). Furthermore, two carotenoids (peaks 3 and 4) are only present in *ccd-A4 ccd-B4 pll-A pll-B* leaves, suggesting that CCD-A4 and CCD-B4 may have overlapping activities toward these two carotenoids and can compensate for each other's missing activity in *ccd-A4 pll-A* and *ccd-B4 pll-B* leaves. This notion of overlapping activities is also supported by the observation that *CCD-A4* expression was induced when CCD-B4 function was abolished in *ccd-B4 pll-B* (**Figure 3**).

Besides analyzing the function of CCD4 homoeologs, the presence of *pll-A* and *pll-B* mutations in the TILLING mutants analyzed in this study also provides an opportunity for examining the role of PLL in wheat plants. Although six putative *PLL* genes were identified in the wheat genome, none of them have been functionally characterized (23). The *ccd-A4 pll-A*, *ccd-B4 pll-B*, and *ccd-A4 ccd-B4 pll-A pll-B* mutants displayed changes in several traits that contribute to wheat plant biomass and yield, including seminal root initiation and architecture, spike fertility, and grain size (**Figures 4**–**6**). These growth phenotypes have not been reported in the *ccd4* or *pol*/*pll* mutants characterized in *Arabidopsis* or other plant species. Conversely, the tetraploid wheat *ccd-A4 ccd-B4 pll-A pll-B* mutant does not exhibit the defective meristem and vasculature development phenotypes reported for the *Arabidopsis pol*/*pll* mutants (**Figure 1**).

Among the growth and agronomic traits altered by *ccd4* and/or *pll* mutations, mutations in the A or B subgenome homoeologs of *CCD4* and *PLL* alone already had a significant impact on the convex hull area of seminal roots, the seminal root length (1-3, 4-5), and the coleoptile length; these mutant

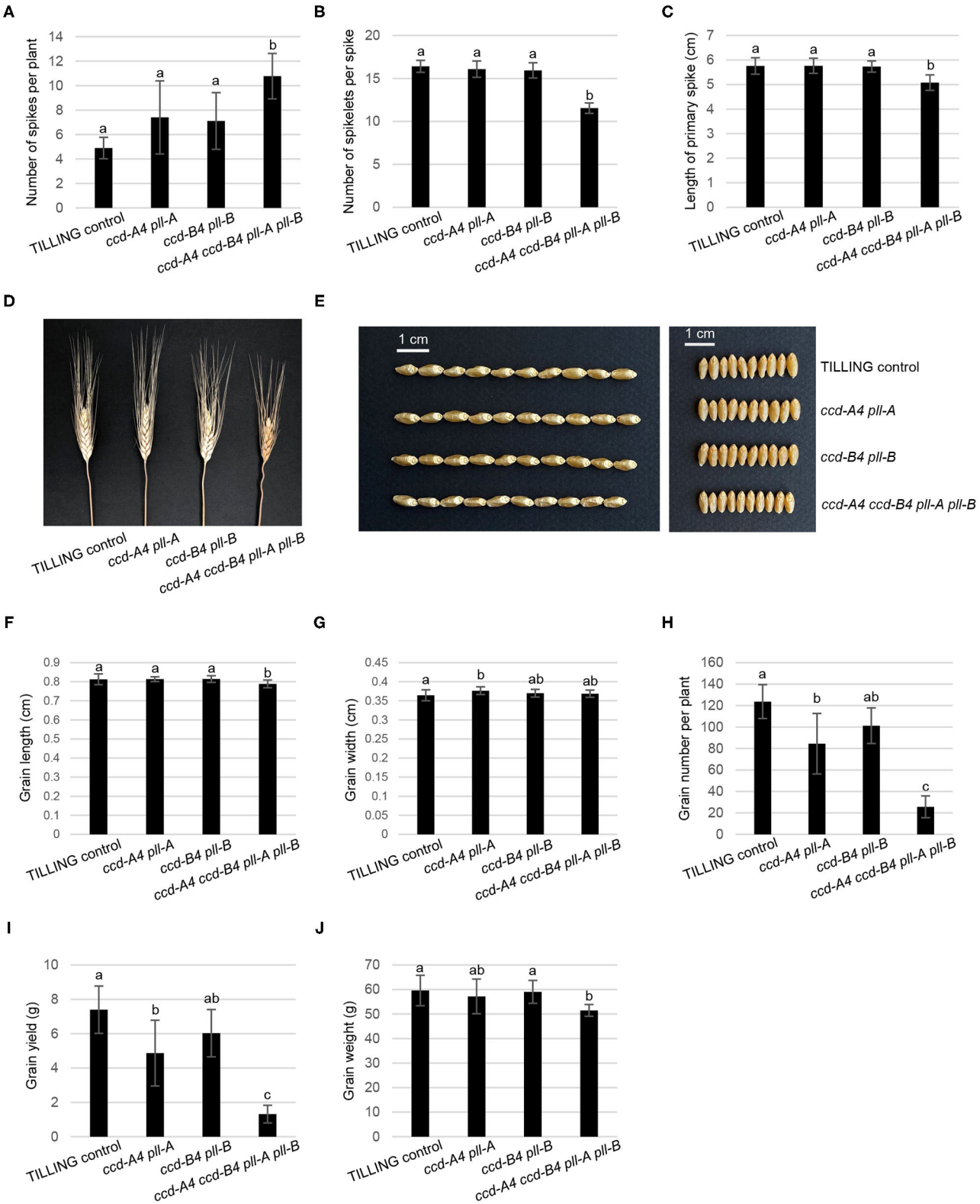

FIGURE 4 | Spike and grain phenotyping of TILLING control and mutant plants. **(A)** Number of spikes per plant. **(B)** Number of spikelets per spike. **(C)** Length of primary spike. **(D)** Image of TILLING control and mutant spikes. **(E)** Images of TILLING control and mutant grains. **(F)** Grain length. **(G)** Grain width. **(H)** Grain number per plant. **(I)** Grain yield. **(J)** Grain weight. The mean ± standard deviation of 9 biological replicates are shown. Different letters denote significantly different ($P < 0.05$) for each spike or grain trait.

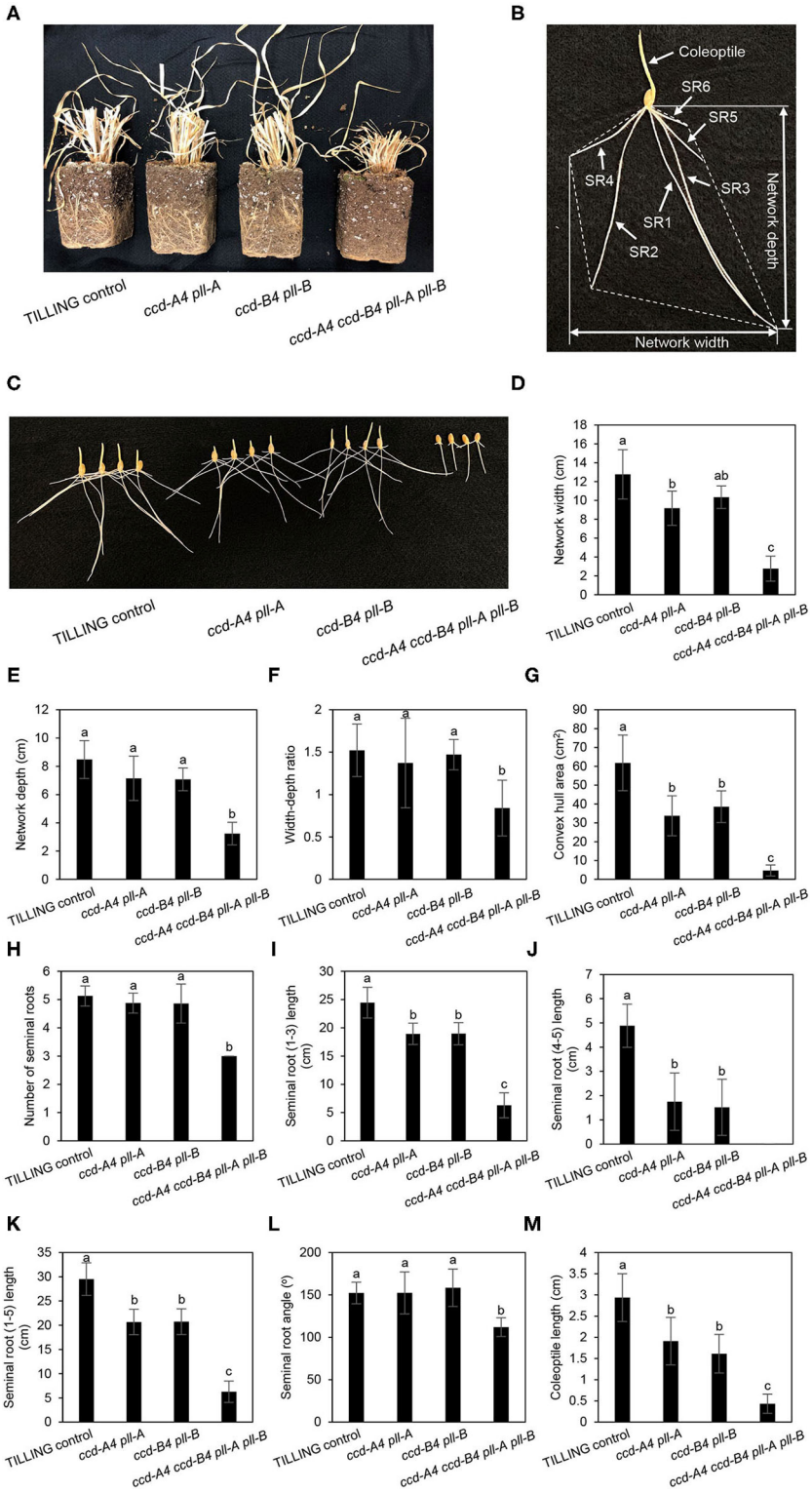

FIGURE 5 | Seminal root phenotyping of TILLING control and mutant seedlings grown in the dark. **(A)** Overview of root growth for TILLING control and mutant plants at harvest. **(B)** Diagram showing analysis of wheat seminal root parameters. The convex hull area refers to the smallest area covered by a convex polygon containing the root system and is delineated with dotted lines. SR, seminal root. **(C)** Image of 3-day-old seedlings grown in the dark. **(D–L)** Represent different seminal root traits. **(M)** Coleoptile length. The mean ± standard deviation of 11 seedlings are shown. Different letters denote significantly different ($P < 0.05$) for each seminal root trait or coleoptile length.

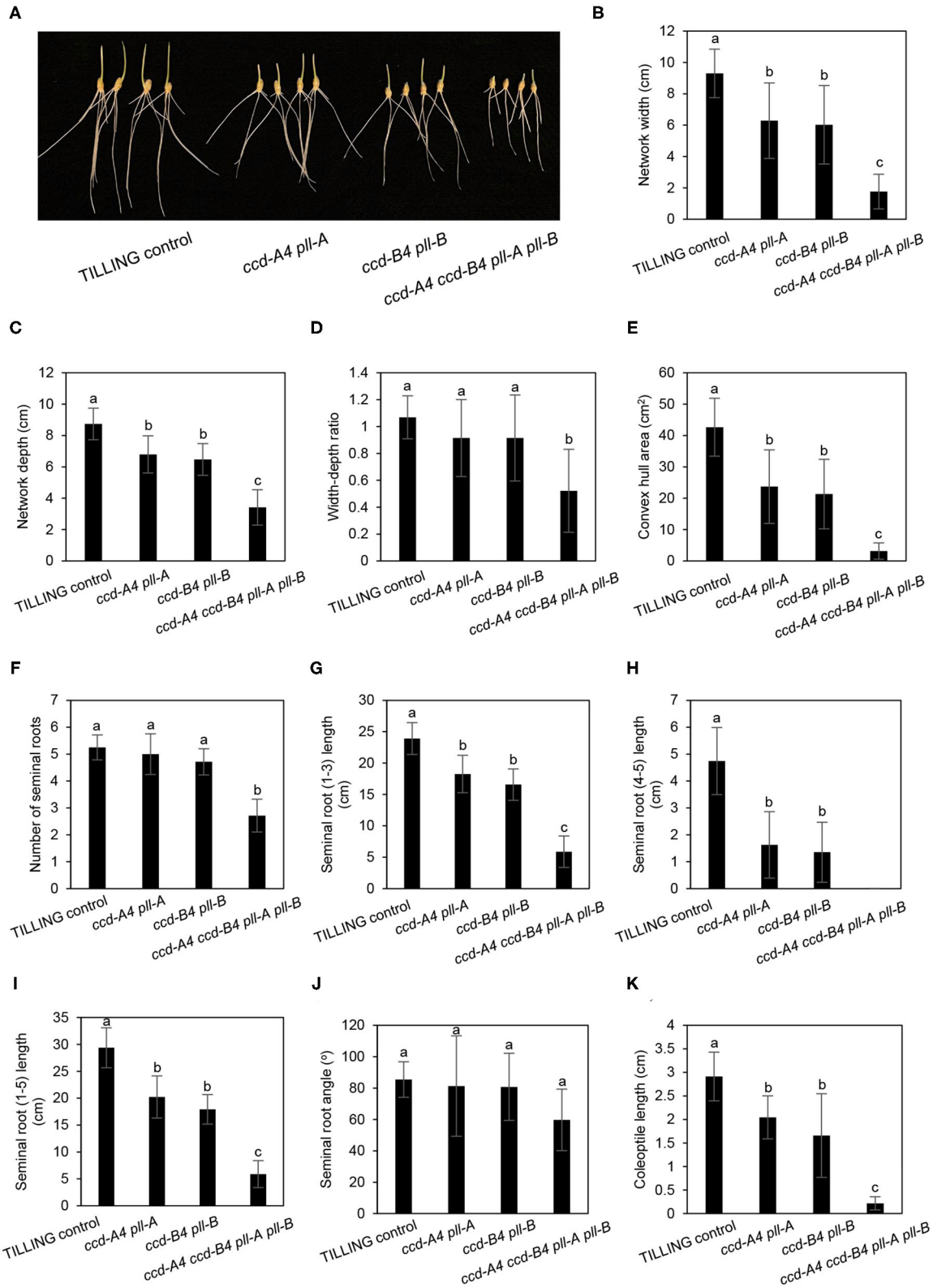

FIGURE 6 | Seminal root phenotyping of TILLING control and mutant seedlings grown under long-day conditions. **(A)** Image of 3-day-old seedlings grown under long-day conditions. **(B–J)** Represent different seminal root traits. **(K)** Coleoptile length. The mean ± standard deviation of 11 seedlings are shown. Different letters denote significantly different ($P < 0.05$) for each seminal root trait or coleoptile length.

phenotypes were exacerbated in *ccd-A4 ccd-B4 pll-A pll-B* where both A and B subgenome homoeologs were knocked out (**Figures 5**, **6**). This suggests that the A and B subgenome homoeologs of CCD4 and/or PLL play distinct roles in controlling the above-mentioned traits. However, for other traits measured, such as number of spikelets per spike, grain yield, and seminal root initiation, significant differences were only observed in *ccd-A4 ccd-B4 pll-A pll-B*, suggesting that CCD4 and/or PLL homoeologs are functionally redundant for these traits.

Taken together, functional characterization of the *ccd-A4 pll-A*, *ccd-B4 pll-B*, and *ccd-A4 ccd-B4 pll-A pll-B* TILLING mutants uncovered the function of CCD4 in carotenoid accumulation in leaves and grains of tetraploid wheat. Additionally, the mutant analysis revealed that CCD4 and/or PLL homoeologs affect key seminal root, grain, and spike traits—traits that are important for not only wheat yield but also human nutrition as wheat grains are a critical dietary source of starch and proteins for human consumption. While the linked *ccd4* and *pll* mutations in the TILLING mutants pose challenges to discerning the role of CCD4, PLL or the interaction of CCD4 and PLL in controlling the plant growth traits, Clustered Regularly Interspaced Short Palindromic Repeats (CRISPR)/CRISPR-associated protein 9 (Cas9) (CRISPR/Cas9) gene editing lines of *CCD4* and *PLL* are currently being generated that mutate each gene individually. These CRISPR/Cas9-induced *ccd4* and *pll* mutant lines will help dissect the function of CCD4 and PLL in plant growth, which will have broad implications in improving wheat yield and nutrient content.

DATA AVAILABILITY STATEMENT

The original contributions presented in the study are included in the article/**Supplementary Material**, further inquiries can be directed to the corresponding author.

AUTHOR CONTRIBUTIONS

SY and LT designed the experiments, analyzed the data, and wrote the manuscript. SY performed the experiments. Both authors contributed to the article and approved the submitted version.

FUNDING

This work was funded by USDA-NIFA (2017-67013-26164 to LT). SY received support from a China Scholarship Council Scholarship, the Henry A. Jastro Research Award, and the UC Davis, Department of Plant Sciences Graduate Research Fellowship.

ACKNOWLEDGMENTS

We thank Dr. Jorge Dubcovsky at University of California, Davis for providing the wheat TILLING mutant materials. We also thank Cody Bekkering for critical reading of the manuscript.

SUPPLEMENTARY MATERIAL

The Supplementary Material for this article can be found online at: https://www.frontiersin.org/articles/10.3389/fnut.2021.740286/full#supplementary-material

Supplementary Figure 1 | Multiple sequence alignment of tetraploid wheat CCD-A4 and CCD-B4 as well as maize VP14 and *Synechocystis* sp. PCC 6803 ACO proteins. The conserved amino acids essential for carotenoid cleavage dioxygenase enzyme activities are indicated with asterisks. The mutated amino acids in CCD-A4 and CCD-B4 are indicated with blue and green arrows, respectively. VP14, 9-*cis*-epoxycarotenoid dioxygenase; ACO, lignostilbene dioxygenase.

Supplementary Figure 2 | Multiple sequence alignment of tetraploid wheat PLL-A and PLL-B as well as *Arabidopsis* POL and PLL1 proteins. The metal interacting domains and conserved amino acids are underlined and indicated with asterisks, respectively. The mutated amino acids in PLL-A and PLL-B are pointed with blue and green arrows, respectively. POL, Poltergeist; PLL, Poltergeist-like.

Supplementary Figure 3 | Images of 11-day-old *ccd-A4 ccd-B4 pll-A pll-B* and TILLING control seedlings grown in the dark. The white arrow points to the emerged seminal root 4 (SR4) in one of the 11-day-old *ccd-A4 ccd-B4 pll-A pll-B* seedlings. The white triangles indicate the places where root growth of TILLING control seedlings was constrained by the size of seed pouches.

Supplementary Table 1 | Primers and restriction enzymes used in the genotyping analysis.

Supplementary Table 2 | Primers used for amplification of the *PLL* homoeologs.

Supplementary Table 3 | Areas (peak area mg^{-1} fresh weight) of peaks 1–4 integrated in the HPLC analysis shown in **Figure 2B**.

REFERENCES

1. Hazard B, Trafford K, Lovegrove A, Griffiths S, Uauy C, Shewry P. Strategies to improve wheat for human health. *Nat Food.* (2020) 1:475–80. doi: 10.1038/s43016-020-0134-6
2. Yu S, Tian L. Breeding major cereal grains through the lens of nutrition sensitivity. *Mol Plant.* (2018) 11:23–30. doi: 10.1016/j.molp.2017.08.006
3. Moreno JC, Mi J, Alagoz Y, Al-Babili S. Plant apocarotenoids: from retrograde signaling to interspecific communication. *Plant J.* (2021) 105:351–75. doi: 10.1111/tpj.15102
4. Poliakov E, Gentleman S, Cunningham FX, Jr., Miller-Ihli NJ, Redmond TM. Key role of conserved histidines in recombinant mouse beta-carotene 15,15'-monooxygenase-1 activity. *J Biol Chem.* (2005) 280:29217–23. doi: 10.1074/jbc.M500409200
5. Felemban A, Braguy J, Zurbriggen MD, Al-Babili S. Apocarotenoids involved in plant development and stress response. *Front Plant Sci.* (2019) 10:1168. doi: 10.3389/fpls.2019.01168
6. Qin X, Fischer K, Yu S, Dubcovsky J, Tian L. Distinct expression and function of carotenoid metabolic genes and homoeologs in developing wheat grains. *BMC Plant Biol.* (2016) 16:155. doi: 10.1186/s12870-016-0848-7
7. Gonzalez-Jorge S, Ha S, Magallanes-Lundback M, Gilliland L, Zhou A, Lipka A, et al. Carotenoid cleavage dioxygenase4 is a negative regulator of β-carotene content in Arabidopsis seeds. *Plant Cell.* (2013) 25:4812–26. doi: 10.1105/tpc.113.119677
8. Campbell R, Ducreux LJM, Morris WL, Morris JA, Suttle JC, Ramsay G, et al. The metabolic and developmental roles of carotenoid cleavage dioxygenase4 from potato. *Plant Physiol.* (2010) 154:656–64. doi: 10.1104/pp.110.158733
9. Ohmiya A, Kishimoto S, Aida R, Yoshioka S, Sumitomo K. Carotenoid cleavage dioxygenase (CmCCD4a) contributes to white color formation

in chrysanthemum petals. *Plant Physiol.* (2006) 142:1193–201. doi: 10.1104/pp.106.087130
10. Yu LP, Miller AK, Clark SE. POLTERGEIST encodes a protein phosphatase 2C that regulates CLAVATA pathways controlling stem cell identity at Arabidopsis shoot and flower meristems. *Curr Biol.* (2003) 13:179–88. doi: 10.1016/S0960-9822(03)00042-3
11. Gagne JM, Clark SE. The protein phosphatases POL and PLL1 are signaling intermediates for multiple pathways in Arabidopsis. *Plant Signal Behav.* (2007) 2:245–6. doi: 10.4161/psb.2.4.3863
12. Song SK, Clark SE. POL and related phosphatases are dosage-sensitive regulators of meristem and organ development in Arabidopsis. *Dev Biol.* (2005) 285:272–84. doi: 10.1016/j.ydbio.2005.06.020
13. Song SK, Hofhuis H, Lee MM, Clark SE. Key divisions in the early arabidopsis embryo require POL and PLL1 phosphatases to establish the root stem cell organizer and vascular axis. *Dev Cell.* (2008) 15:98–109. doi: 10.1016/j.devcel.2008.05.008
14. Song SK, Lee MM, Clark SE. POL and PLL1 phosphatases are CLAVATA1 signaling intermediates required for arabidopsis shoot and floral stem cells. *Development.* (2006) 133:4691–8. doi: 10.1242/dev.02652
15. Yu LP, Simon EJ, Trotochaud AE, Clark SE. POLTERGEIST functions to regulate meristem development downstream of the CLAVATA loci. *Development.* (2000) 127:1661–70. doi: 10.1242/dev.127.8.1661
16. Sievers F, Wilm A, Dineen D, Gibson TJ, Karplus K, Li W, et al. Fast, scalable generation of high-quality protein multiple sequence alignments using Clustal Omega. *Mol Syst Biol.* (2011) 7:539. doi: 10.1038/msb.2011.75
17. Dong OX, Yu S, Jain R, Zhang N, Duong PQ, Butler C, et al. Marker-free carotenoid-enriched rice generated through targeted gene insertion using CRISPR-Cas9. *Nat Commun.* (2020) 11:1178. doi: 10.1038/s41467-020-14981-y
18. Qin X, Zhang W, Dubcovsky J, Tian L. Cloning and comparative analysis of carotenoid (-hydroxylase genes provides new insights into carotenoid metabolism in tetraploid (*Triticum turgidum* ssp. durum) and hexaploid (*Triticum aestivum*) wheat grains. *Plant Mol Biol.* (2012) 80:631–46. doi: 10.1007/s11103-012-9972-4
19. Jaakola L, Pirttilä A, Halonen M, Hohtola A. Isolation of high quality RNA from bilberry (*Vaccinium myrtillus* L.) fruit. *Mol Biotechnol.* (2001) 19:201–3. doi: 10.1385/MB:19:2:201
20. Schneider CA, Rasband WS, Eliceiri KW. NIH Image to ImageJ: 25 years of image analysis. *Nat Methods.* (2012) 9:671–5. doi: 10.1038/nmeth.2089
21. Krasileva KV, Vasquez-Gross HA, Howell T, Bailey P, Paraiso F, Clissold L, et al. Uncovering hidden variation in polyploid wheat. *Proc Natl Acad Sci USA.* (2017) 114:E913–21. doi: 10.1073/pnas.1619268114
22. Sui X, Zhang J, Golczak M, Palczewski K, Kiser PD. Key residues for catalytic function and metal coordination in a carotenoid cleavage dioxygenase. *J Biol Chem.* (2016) 291:19401–12. doi: 10.1074/jbc.M116.744912
23. Yu X, Han J, Wang E, Xiao J, Hu R, Yang G, et al. Genome-wide identification and homoeologous expression analysis of PP2C genes in wheat (*Triticum aestivum* L.). *Front Genet.* (2019) 10:561. doi: 10.3389/fgene.2019.00561

Conflict of Interest: The authors declare that the research was conducted in the absence of any commercial or financial relationships that could be construed as a potential conflict of interest.

Publisher's Note: All claims expressed in this article are solely those of the authors and do not necessarily represent those of their affiliated organizations, or those of the publisher, the editors and the reviewers. Any product that may be evaluated in this article, or claim that may be made by its manufacturer, is not guaranteed or endorsed by the publisher.

frontiers in Nutrition

ORIGINAL RESEARCH
published: 15 October 2021
doi: 10.3389/fnut.2021.732409

Using ^{77}Se-Labelled Foliar Fertilisers to Determine How Se Transfers Within Wheat Over Time

Chandnee Ramkissoon[1,2]*, *Fien Degryse*[1], *Scott Young*[2], *Elizabeth H. Bailey*[2] and *Michael J. McLaughlin*[1]

[1] Fertiliser Technology Research Centre, School of Agriculture, Food and Wine, University of Adelaide, Glen Osmond, SA, Australia, [2] School of Biosciences, University of Nottingham, Loughborough, United Kingdom

OPEN ACCESS

Edited by:
Om Prakash Gupta,
Indian Institute of Wheat and Barley Research (ICAR), India

Reviewed by:
M. J. I. Shohag,
Bangabandhu Sheikh Mujibur Rahman Science and Technology University, Bangladesh
Beata Rutkowska,
Warsaw University of Life Sciences, Poland
Wiesław Szulc,
Warsaw University of Life Sciences, Poland

***Correspondence:**
Chandnee Ramkissoon
chandnee.ramkissoon@adelaide.edu.au

Specialty section:
This article was submitted to Nutrition and Food Science Technology, a section of the journal Frontiers in Nutrition

Received: 29 June 2021
Accepted: 08 September 2021
Published: 15 October 2021

Citation:
Ramkissoon C, Degryse F, Young S, Bailey EH and McLaughlin MJ (2021) Using ^{77}Se-Labelled Foliar Fertilisers to Determine How Se Transfers Within Wheat Over Time. Front. Nutr. 8:732409. doi: 10.3389/fnut.2021.732409

Foliar selenium (Se) fertilisation has been shown to be more efficient than soil-applied fertilisation, but the dynamics of absorption and translocation have not yet been explored. An experiment was undertaken to investigate time-dependent changes in the absorption, transformation, and distribution of Se in wheat when ^{77}Se-enriched sodium selenate (Se_{fert}) was applied to the leaves at a rate of 3.33 μg Se per kg soil (equivalent to 10 g ha^{-1}) and two growth stages, namely stem elongation, Zadoks stage 31/32 (GS1), and heading stage, Zadoks stage 57 (GS2). The effect of urea inclusion in foliar Se fertilisers on the penetration rates of Se was also investigated. Wheat was harvested at 3, 10, and 17 days and 3, 10, and 34 days after Se applications at GS1 and GS2, respectively. Applying foliar Se, irrespective of the formulation, brought grain Se concentration to a level high enough to be considered adequate for biofortification. Inclusion of N in the foliar Se solution applied at an early growth stage increased recoveries in the plants, likely due to improved absorption of applied Se through the young leaves. At a later growth stage, the inclusion of N in foliar Se solutions was also beneficial as it improved the assimilation of applied inorganic Se into bioavailable selenomethionine, which was then rapidly translocated to the grain. The practical knowledge gained about the optimisation of Se fertiliser formulation, method, and timing of application will be of importance in refining biofortification programs across different climatic regimes.

Keywords: selenium, wheat, speciation, biofortification, foliar fertilisation

INTRODUCTION

Micronutrient deficiencies affect one in three people globally (1) as a result of intake patterns or absorption rates that fall below the level required to sustain good health and development (2). Selenium (Se) is one such micronutrient that is currently consumed at lower-than-recommended levels in many parts of the world. Combs (3) estimated that 0.5–1 billion people worldwide were at risk of Se deficiency diseases as a result of inadequate dietary Se intake.

Selenium is an essential nutrient for both humans and animals (4). It has been shown to have antiviral effects, be beneficial for reproduction, and lower autoimmune thyroid disease risks. More recently, its role as an antioxidant and a potential anticarcinogen has been appraised (5, 6).

Although inadequate Se intake can cause general poor health, extremely low levels of Se can cause specific deficiency diseases such as Keshan (cardiomyopathy) and Kashin–Beck (an osteoarthritis disorder); these are seen, for example, in some regions of China and Siberia (7, 8). However, Se can also be toxic if ingested at higher-than-recommended levels. An excess of Se in the body, resulting in "selenosis," is characterised by the loss of hair and nails, and general fatigue (9). The current daily recommended intake of Se is set at 55 and 70 μg person^{-1} for women and men, respectively; more generally, a dietary Se intake range of 40–400 μg day^{-1} is considered safe (10). As a result of increasing concern about the inadequacy of Se intake in many locations around the world, research has, in recent decades, focused on ways to improve dietary Se levels sustainably to preempt or alleviate Se deficiency.

Agronomic biofortification is a term describing the process through which the concentration of micronutrients in edible parts of staple crops is increased through the application of fertilisers enriched with trace elements (2). The efficacy of Se fertilisers to fortify crops depends on several factors, including the chemical form of Se used its application rate, and its method. Selenium is most commonly applied in its oxidised inorganic forms, such as selenate (Se^{VI}) or selenite (Se^{IV}) either to the soil or to the canopy (foliar fertilisation) or as a combination of soil and foliar (11). When soil-applied, selenate is often the preferred source for biofortification because of its higher mobility in the soil and plants. Selenate is highly mobile in the xylem and accumulates in the edible parts of plants before being converted to bioavailable organic forms such as selenomethionine (SeMet). By contrast, Se^{IV}, despite rapid uptake into roots, is generally converted more rapidly to organic forms and accumulates in roots (12). The efficacy of soil-applied Se fertilisers is largely dependent on the chemical speciation of Se and the physicochemical properties of the soil (13). Soil components such as metal oxides, clays, and soil organic matter (SOM) have the potential to adsorb Se strongly, especially Se^{IV}, resulting in reduced mobility and availability of Se in the soil. Selenate, on the other hand, adsorbs *via* a weaker mechanism and hence is more mobile and bioavailable than Se^{IV}. However, selenate is also more prone to leaching than Se^{IV}, especially in acidic environments (14). Moreover, the biogeochemical behaviour of Se in soils is influenced by the presence of environmental microorganisms in the soil, particularly arbuscular mycorrhizal fungus (AMF), such that, it is essential to consider plant–bacteria-fertiliser interactions in soils to optimise Se biofortification (15).

In contrast to soil-applied fertilisers, foliar fertilisers tend to be more efficient due to the reduced losses to the environment by leaching and/or adsorption to soil particles (16, 17). In contrast to soil application, foliar-applied nutrients are absorbed through the leaf epidermis and transferred to the rest of the plant *via* the phloem (18, 19). Effectively, Ros et al. (16) showed that foliar fertilisation could be on average eight times more efficient than Se application to soil. For example, they found that an application rate of 30–60 g ha^{-1} Se^{VI} to the soil would be needed to increase grain Se concentration from 0.07 to 0.1 mg kg^{-1} compared with just 4.5–10 g ha^{-1} Se^{VI} when the foliar application of Se was used (16). However, foliar fertilisers may also be prone to losses, for example, through leaf runoff following rainfall. More information about the penetration rates of foliar-applied Se fertilisers into plants, and subsequently transfer to edible parts of the plant may be useful to mitigate such losses and optimise foliar Se fertilisation.

In previous studies, we demonstrated that the concentration of bioavailable Se (selenomethionine) in wheat grain subject to foliar Se applications could be increased through the addition of small amounts of nitrogen (N), for example, urea (20). Although the exact mechanism for this improved efficiency is not yet fully understood, it was suggested that N aided Se assimilation into organic Se forms in the leaves, which were then transported to the grain. There is also limited literature about the optimum timing of foliar Se application for biofortification. Lyons (17) suggested that the application of nutrients such as Se and I are best made between the booting and early milk stages, preferably around the heading stage, to maximise the area of canopy available for fertiliser interception and uptake. Understanding how Se transfers from the point of application to the rest of the crop at different growth stages may be useful in planning Se fertilisation tactics to optimise crop uptake.

In this study, we aimed to determine the time-dependent changes in Se absorption, assimilation, and transfer to the aboveground biomass, following the application of ^{77}Se-labelled selenate fertilisers to wheat leaves. The use of stable isotope Se tracers, such as enriched ^{77}Se, enables the simultaneous determination of native (soil-derived) and applied Se sources in both plant and soil systems (21, 22). The partitioning of the applied ^{77}Se-fertiliser in wheat was assessed when different (a) foliar treatments (Se $\pm$ N) and (b) application timings (growth stages) were employed. This study provided practical information about the uptake and transformation of foliar-applied Se in wheat, which farmers could use to manage fertiliser application methods and timing to optimise Se biofortification.

MATERIALS AND METHODS

Soil

Sandy loam topsoil was used for the pot trial (**Table 1**). The soil was air-dried and sieved to $<$2 mm prior to characterisation. Soil pH and electrical conductivity (EC) were measured in a 1:2.5 soil-to-solution suspension on an automated Skalar pH/EC system. Soil organic matter content was estimated by the loss-on-ignition method (23). Particle size analysis was determined by laser granulometry following treatment with 40% hydrogen peroxide (H_2O_2), as described in Mathers et al. (22). Extractable P and S (mg kg^{-1}) were determined by the method developed by Olsen et al. (24) and Blair and Lefroy (25). The water holding capacity (WHC) of the soil was determined using ceramic tension plates and hanging water columns (26).

Pot Trial

The pot trial was set up in spring (April–May 2019) in a glasshouse at the University of Nottingham Sutton Bonington Campus (United Kingdom). The crops were grown under natural light conditions, which averaged $\sim$6 h daily. Five seeds of spring wheat (*Triticum aestivum* cv. Willow) were sown directly

TABLE 1 | Physicochemical properties of the soil used in the experiment.

pH (water)	7.9
Electrical conductivity (μS cm^{-1})	1,300
Organic matter (%)	4.1
Clay (%)	13
Sand (%)	72
Extractable P (mg kg^{-1})	3.0
Extractable S (mg kg^{-1})	18

TABLE 2 | The dry matter yield of aboveground plants harvested 3, 10, and 17 days after Se application at stem elongation (GS1) and 3, 10, and 34 days after Se application at the heading stage (GS2) (SE in brackets; $n = 4$).

Growth stage (GS)	Days after sowing (DAS)	Harvest time following Se_{fert} application	Dry matter yield[†]
	D	*d*	g pot^{-1}
1	66	3	3.16 (0.08)^{e}
	73	10	4.65 (0.20)^{d}
	80	17	5.92 (0.29)^{c}
2	122	3	18. 9 (0.56)^{b}
	129	10	21.7 (0.50)^{a}
	153	34	22.2 (0.44)^{a}

$^{a-e}$*Indicate significant differences ($p < 0.05$).*

into free-draining pots containing 1.8 kg soil and thinned to two plants per pot 3 weeks later. Plants were fertilised with 5 ml of an ammonium nitrate solution (16.4 g L^{-1} NH_4NO_3) at stem extension and head emergence. No additional basal fertilisation was applied to the soil as sufficient plant-available nutrients were present (**Table 2**). Pots were arranged in a randomised block design and watered to an estimated weight of 60% WHC of the soil using Milli Q water (18.2 MΩ cm) throughout the experiment. All treatments were replicated four times.

Foliar Selenium Fertiliser Application

Selenium fertilisers (Se_{fert}) were prepared from a ^{77}Se-enriched sodium selenate solution (259 mg L^{-1} $^{77}Se^{VI}$). Selenium was applied at a single, realistic rate of 3.33 μg kg^{-1}; this is equivalent to ∼10 g ha^{-1}, based on a 20-cm depth of topsoil and 1.5 g cm^{-3} bulk density. Three fertilser treatments were used: (i) foliar-applied Se only (F.Se); (ii) foliar-applied Se with a 2% w/v N source in the form of urea (Sigma–Aldrich, 99–100% purity, United Kingdom) (F.Se+N); (iii) control (Ctrl) where neither Se nor N was applied. The foliar Se+N solution was prepared by dissolving 0.21 g of urea in a solution with a ^{77}Se concentration of 180 mg L^{-1}. The foliar solutions contained 0.5% surfactant (Triton-X 100; Sigma–Aldrich), which served to reduce the surface tension between the droplets and the leaf, thereby promoting fertiliser absorption. Foliar solutions were applied as four drops of 5 μl volume droplets to the youngest flag leaves of each plant (two plants per pot). For the control treatment, water with 0.5 % surfactant was applied in a manner similar to foliar Se solutions.

The application was either at growth stage 1 (GS1), which was at stem elongation [growth stage 31/32 on the Zadoks scale and 63 days after sowing (DAS)] or GS2, which was at head emergence [Zadoks stage 57 and 119 DAS; (27)].

The surface of the soil was covered with cling film for a week following foliar fertiliser application and care was taken not to irrigate the plants immediately after foliar fertilisation to prevent any potential runoff into the soil.

Plant Harvest

The aboveground biomass of the wheat plants was harvested at 3, 10, and 17 d (H3, H10, and H17) after fertiliser application at GS1 and 3, 10, and 34 days (H3, H10, and H34) after fertiliser application at GS2. For the plants treated at GS2, wheat heads were harvested separately from the straw and, for the last sampling (H34), wheat heads were further hand-threshed to separate the wheat grains. All the foliar-treated leaves were harvested separately from the straw, washed in 0.1% v/v detergent, and then rinsed with Milli Q water (28). Water rinses were saved to analyse for any unabsorbed applied Se_{fert}. After harvest, all plant parts were dried at 50°C for 72 h or until the constant dry weight was achieved. The dry weights of the different plant parts were recorded. Subsequently, plant material was ground using a centrifugal mill (model ZM 200, Retsch, Germany) fitted with a 0.5 mm titanium screen and stored under ambient conditions prior to digestion and chemical analyses.

Selenium Analyses

Total Se Determination

The total Se concentration in plant samples was measured using inductively coupled plasma mass spectrometry (ICP-MS; model iCapQ, Thermo Fisher Scientific, Bremen, Germany) following microwave-assisted acid digestion. Approximately 0.2 g of plant material was weighed into perfluoroalkoxy vessels and mixed with 6 ml of concentrated nitric acid (HNO_3) before microwave heating (Model Multiwave 3000, fitted with a 48-place rotor; Anton Paar, Graz, Austria). The digested samples were then made to 20 ml final volume using Milli Q water and further diluted 10-fold with 2% HNO_3 prior to analysis.

Speciation Analysis

An enzymatic hydrolysis method was employed to prepare the foliar-treated leaves and wheat grain samples for Se speciation analysis. The method of analysis was adapted from Muleya et al. (29). Four Se species were assayed: selenate, selenite, seleno-L-cysteine (SeCys), and seleno-L-methionine (SeMet). A multistandard solution (10 ml) containing the four Se species nominally at 5 μg L^{-1} concentration was prepared by diluting stock solutions of $^{77}Se^{IV}$ and $^{77}Se^{VI}$ (1,000 mg L^{-1}) and SeCys and SeMet (100 mg L^{-1}); the stock solutions with organic Se were prepared by dissolving the individual salts in Milli Q water. The Se concentrations of the individual Se species standards were verified by analysis (direct aspiration) using ICP-MS, with measured Se concentrations of 6.47, 5.37, 5.28, and 5.30 μg L^{-1}, respectively.

Five millilitres of an enzyme solution containing 0.02 g protease K (Type XIV ≥ 3.5 units mg^{-1} solid from *Streptomyces griseus*) and 0.01 g lipase (Type VII ≥ 700 units mg^{-1} solid from *Candida rugosa*) was added to plant samples (0.2 g) in centrifuge tubes. The samples were incubated in the dark and shaken in a water bath set at 60 rpm at 37°C for 24 h; after incubation, they were centrifuged at 3,000 g for 30 min and filtered through 0.25 μm filters. Enzymatically-hydrolysed samples that were not immediately analysed were stored at 4°C in the dark. Selenium speciation analysis was undertaken using coupled HPLC-ICP-triple quadrupole-MS (ICP-QQQ-MS) instruments (**Supplementary Table 1**). The ICP-QQQ-MS was operated in oxygen cell mode to enable mass shifting of the Se isotopes and thereby minimise interferences; thus, ^{77}Se was mass shifted to m/z 93 and ^{80}Se to m/z 96. Standards were run after every block of 12 samples to monitor drift and enable correction of sample concentrations (22).

Sample processing was undertaken using a version of Chromeleon (Dionex) chromatography software operating within the iCapQ Qtegra software; the peaks generated by the individual Se species were manually integrated for peak area. Raw intensity data (integrated counts-per-second, iCPS) were then imported from the ICP-QQQ-MS at mass:charge (m/z) ratios of 93 and 96.

The enzymatically-hydrolysed plant samples were also analysed for a total ^{80}Se and ^{77}Se by ICP-MS, following a 1:10 dilution of the original enzyme extracts with 2% HNO_3 acid. The final concentrations of the individual Se species were calculated from the proportion of the total extract Se that was measured as the peak area of the individual species, as described in Mathers et al. (22). For example, the concentration (μg L^{-1}) of SeMet (at m/z 93 and 96) was calculated from Equation 1:

$$\mathrm{SeMet_{conc}} = \frac{\mathrm{SeMet_{cps}}}{\sum \mathrm{species_{cps}}} \times \mathrm{Se_{tot,enz}} \quad (1)$$

where $\mathrm{SeMet_{cps}}$ is the peak intensity (iCPS) of SeMet and $\sum \mathrm{species_{cps}}$ the sum for all four species ($\mathrm{SeMet_{cps}}$, $\mathrm{SeCys_{cps}}$, $\mathrm{Se^{IV}_{cps}}$, and $\mathrm{Se^{VI}_{cps}}$), and $\mathrm{Se_{tot,enz}}$ is the total Se concentration (μg L^{-1}) measured in the enzyme-hydrolysed extracts.

The concentration of individual Se species and total Se concentrations was then converted to a gravimetric basis using the dry weights of individual samples and the volume of the different extracts.

Quality Control

Replicate samples of standard reference material (tomato leaves NIST 1573a) were acid digested and analysed for total Se by ICP-MS to provide quality assurance for the analysis of the plant samples. The recovery of Se in the reference material was within 100 ± 10% of the certified value (certified value 0.0543 mg kg^{-1}; analysed value 0.0488 mg kg^{-1} Se)

The extraction efficiency of the enzyme (E_{ext}) was calculated as follows (Equation 2).

$$E_{ext} = \frac{\mathrm{Se_{tot,enz}}}{\mathrm{Se_{tot,acid}}} \times 100 \quad (2)$$

where $\mathrm{Se_{tot,acid}}$ is the total Se concentration measured by acid hydrolysis for individual samples (μg L^{-1}).

Statistical Analyses

The effects of the different fertilisation treatments on grain yield and Se concentrations in plants were determined using the ANOVA procedure in SPSS (IBM SPSS Statistics for Windows, Version 24.0, IBM Corp, Armonk, New York), with a significance threshold of 5%. Duncan's and Tukey's *post-hoc* tests were used to compare treatment means.

RESULTS

Biomass Yield

The yield of plants, calculated as the dry weight of the aboveground biomass, increased significantly with time but no significant differences in yield were observed among the different Se treatments (**Table 2**).

Selenium Distribution in Plants

The recovery of $\mathrm{Se_{fert}}$ in plants harvested at GS1 was > 50%, even after 3 days following application (**Figure 1A**). The partitioning data showed that the majority (>63%) of the applied $\mathrm{Se_{fert}}$ was measured in the treated leaves up to 10 days after application, which decreased to <50% by day 17, suggesting mobilisation from the leaf to the straw. This mobilisation was more efficient for F.Se+N-treated plants, suggesting that the inclusion of N to foliar Se solutions improved the transfer of Se from the point of application to the rest of the aboveground biomass (**Figure 1A**).

For GS2 samples (122–153 DAS), the aboveground biomass was further separated into straw, heads, and leaves (**Figure 1B**). With high $\mathrm{Se_{fert}}$ recoveries in the aboveground biomass, limited losses of the applied foliar Se fertilisers to the environment were observed. This was confirmed by $\mathrm{Se_{fert}}$ levels in the foliar rinses being below analytical detection limits (data not shown for brevity). Within 3 days of application, 43 ± 0.98% $\mathrm{Se_{fert}}$ was translocated from the point of application to the rest of the aerial plant parts, which was equally distributed between the wheat heads and the straw. At the last sampling time (153 DAS), this translocation increased to 56 ± 5.2%, with heads, especially the grains, accumulating significantly more $\mathrm{Se_{fert}}$ than straw ($p < 0.05$). No significant differences in the recovery of $\mathrm{Se_{fert}}$ in the aboveground biomass of plants were observed between foliar Se (±N) treatments at GS2.

In comparison to $\mathrm{Se_{fert}}$ recovery in plants, the recovery of native Se ($\mathrm{Se_N}$) in the aboveground plant biomass was much lower (**Figure 2**), indicating that the applied Se fertiliser was more available for plant uptake than native soil Se. Plants harvested at GS2 had accumulated significantly more $\mathrm{Se_N}$ (4.14 ± 0.33%) than those harvested at GS1 (1.37 ± 0.17%), likely because GS2 plants had a longer contact time with the native Se pool.

Effect of N Addition in Foliar Se Solutions on $\mathrm{Se_{fert}}$ Uptake

The inclusion of N with foliar Se solutions led to greater Se uptake compared with foliar Se application on its own when applied

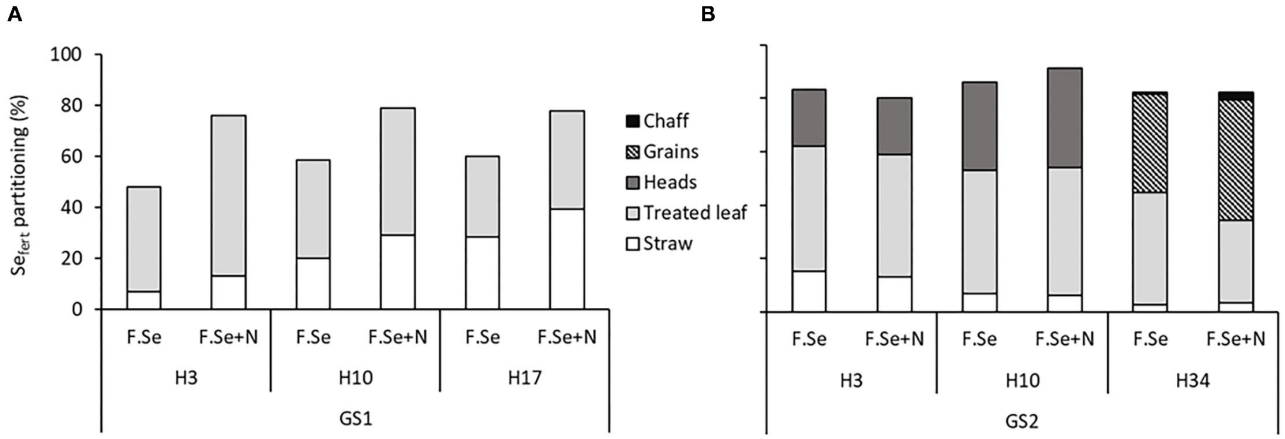

FIGURE 1 | Partitioning of applied foliar Sefert (±N) in the aboveground biomass of plants as a function of harvest time [3, 10, and 17/34 days after application at stem elongation, GS1 **(A)**/heading stage, GS2 **(B)**]. The recovery of applied Sefert was calculated as the percentage of applied fertiliser Se that was recovered in the aboveground plant parts. Note that at H34, wheat heads were hand threshed to separate grains and chaff.

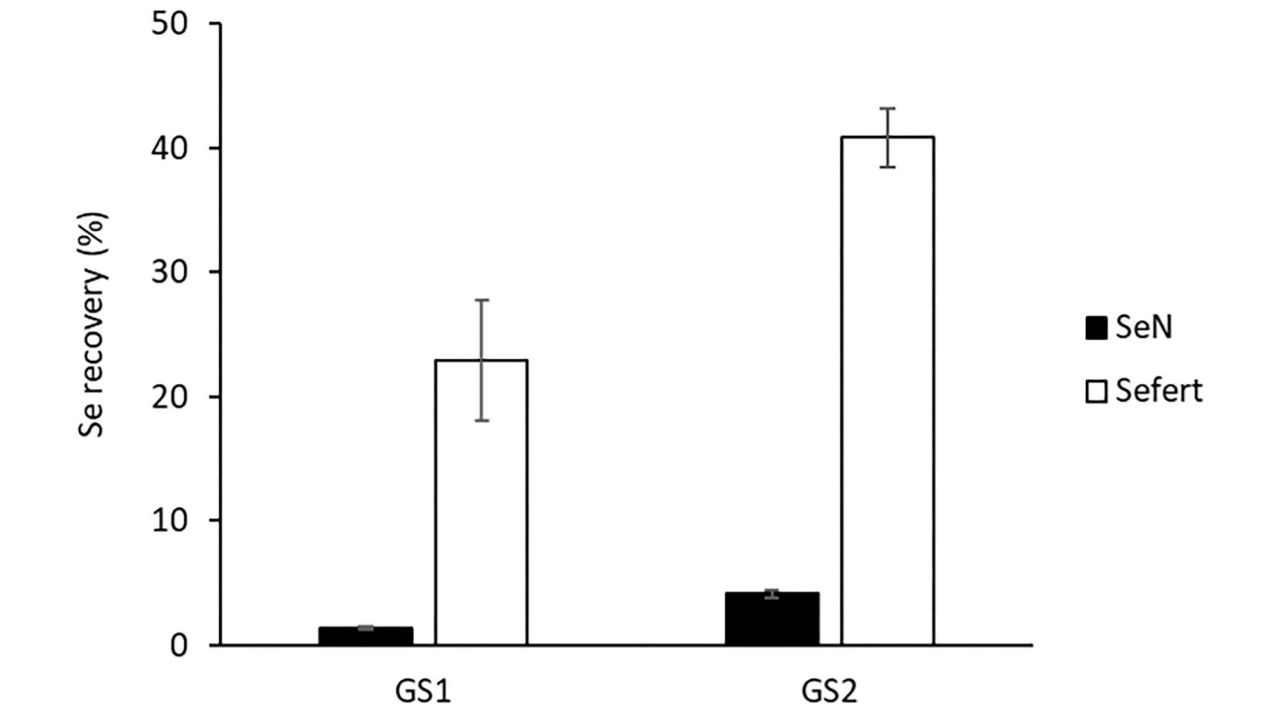

FIGURE 2 | The recovery of native Se (Se_N) and fertiliser-derived Se (Se_{fert}) in the aboveground biomass of plants (excluding the foliar-treated leaves) harvested at stem elongation (GS1) and the heading stage (GS2). The recovery is the percentages of soil Se or fertiliser-applied Se that was recovered in the aboveground plant parts. Error bars represent SEs ($n = 4$).

at GS1, but this was not apparent at GS2 (**Table 3**). At GS2, the translocation of Se_{fert} into the wheat plants increased with growth time but was not affected by the addition of N to the foliar Se formulations.

The effectiveness of N inclusion in foliar Se fertilisers was observed in the grains (**Figure 3**). The average grain Se concentrations for foliar Se+N were 0.26 ± 0.02 and 0.32 ± 0.07 mg kg^{-1}, which accounted for 44 and 54% of the applied Se transferred to the grain, respectively.

Se Speciation in Grain

Protease hydrolysis extracted >60% of the total Se concentration in the wheat grain (Equation 2). Selenomethionine was the most abundant species in the wheat grain, accounting for >90% of

TABLE 3 | The influence of *N* inclusion with foliar Se solutions and harvest time on the accumulation of Se from the fertiliser (Se_{fert}) in the aboveground biomass (foliar-treated leaves excluded) (SE in brackets; $n = 4$).

Time after Se_{fert} application (*d*)	Se_{fert} uptake ($\mu g\ pot^{-1}$)			
	GS1		GS2	
	–N	*+N*	*–N*	*+N*
3	0.495 (0.03)	0.946 (0.36)	2.40 (0.40)	2.31 (0.30)
10	1.44 (0.28)	2.11 (0.49)	2.85 (0.11)	3.12 (0.32)
17/34‡	2.06 (0.25)	2.84 (0.55)	2.90 (0.21)	4.00 (0.51)
Two-way ANOVA				
Day	<0.05		<0.05	
N	<0.10		ns	
Day**N*	ns		ns	

"ns" denotes non-significant interactions at $p < 0.05$.

‡*The last sampling was done 17 and 34 days after Se_{fert} application at GS1 and GS2, respectively.*

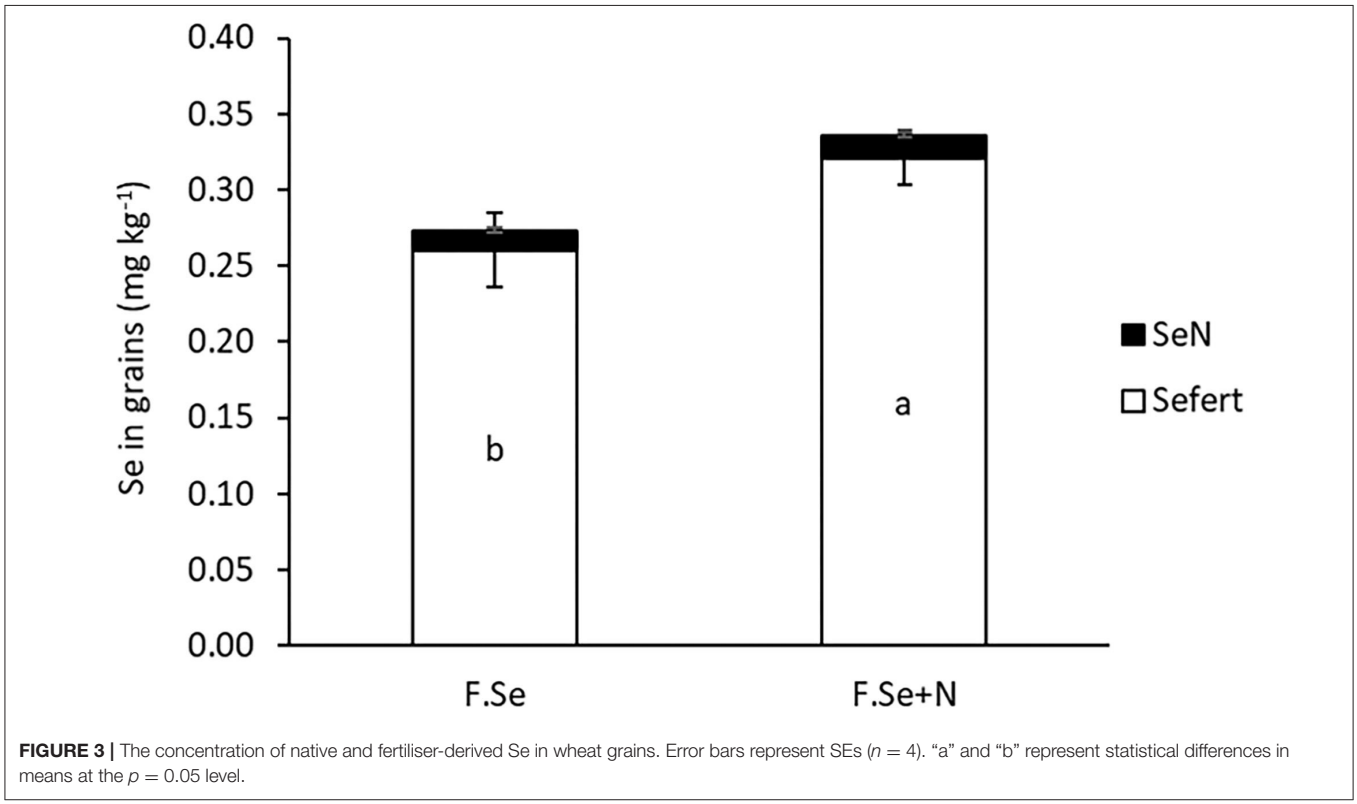

FIGURE 3 | The concentration of native and fertiliser-derived Se in wheat grains. Error bars represent SEs ($n = 4$). "a" and "b" represent statistical differences in means at the $p = 0.05$ level.

the total Se_{fert} in the grain. A small amount of Se^{VI} (<10% of the total Se_{fert}) was also detected in the grain, and no Se^{IV} or SeCys was measured, irrespective of Se treatments (**Table 4**). The inclusion of N in foliar Se solutions led to a significantly higher SeMet concentration in grains (0.21 mg kg^{-1}), compared with F. Se-only fertilisation (0.16 mg kg^{-1}) (**Table 4**).

Se Speciation in Leaves Treated With Foliar Se (±N)

The protease hydrolysis extracted, on average, 72 ± 2.4% of the total Se_{fert} in the foliar-treated leaves. The main species identified in the extracts were Se^{VI} (91 ± 2.0%) and SeMet (8.0 ± 1.9%); negligible concentrations of Se^{IV} and SeCys (<2% of the Se_{fert} in the leaves) were measured (**Figure 4**). For both F.Se and F.Se+N treatments, the distributions of the Se species in wheat were similar.

Selenate was the most abundant species in the foliar-treated leaves, and its proportion did not change significantly over the 153-day experimental period (91 ± 1.6%) (**Figure 4**). By comparison, the proportion of SeMet decreased significantly with harvest time, in a similar way for both GS1 and GS2, which suggests more rapid mobilisation of SeMet to the rest

TABLE 4 | The distribution of the extracted Se species in wheat grain expressed as mean concentration or as % of total extracted grain Se (SE in brackets, $n = 4$).

Treatments	Se species in grain					
	SeMet		Se^{VI}		Se^{IV}	SeCys
	mg kg^{-1}	% of total	mg kg^{-1}	% of total		
F.Se	0.16 (0.02)	92 (0.3)	0.014 (0.00)	8.3 (0.3)	n.d	n.d
F.Se+N	0.21 (0.02)	94 (2.3)	0.010 (0.00)	6.3 (2.3)		

"n.d." denotes non-detectable concentrations of species.

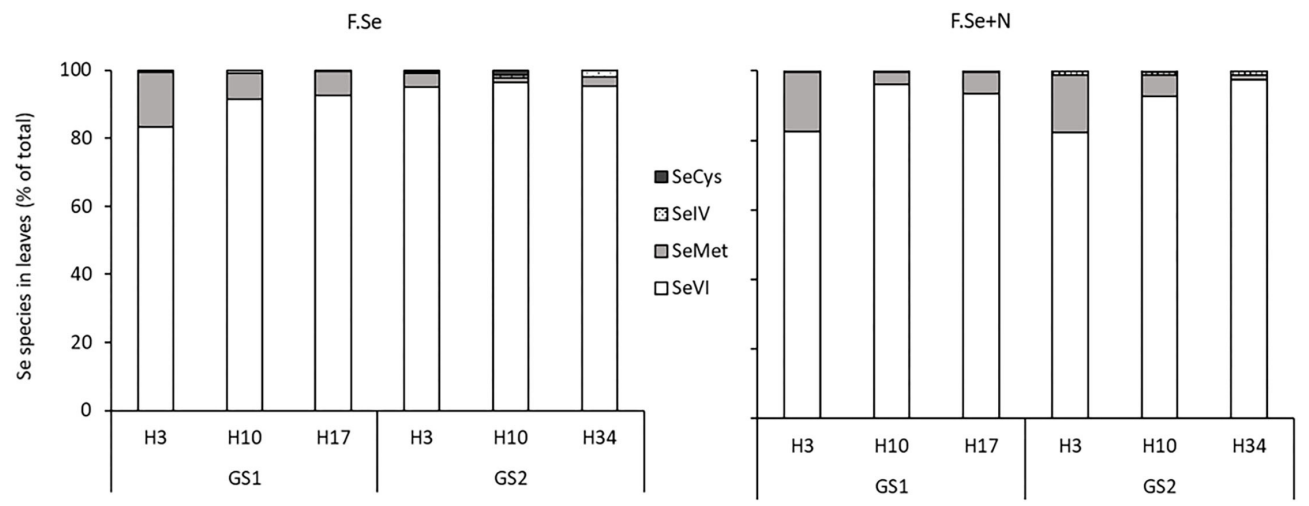

FIGURE 4 | The distribution of Se species as a percentage of the total Se in leaves that were treated with F.Se and F.Se+N and harvested at different times following application at stem elongation (GS1) and heading (GS2).

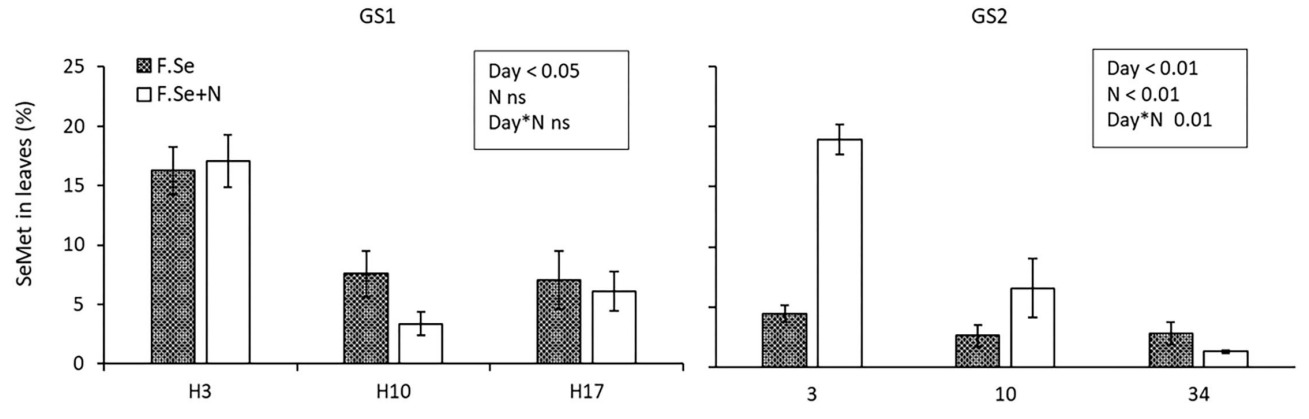

FIGURE 5 | The concentration of SeMet in leaves that were treated with foliar Se and foliar Se+N at stem elongation (GS1) and heading stage (GS2). Results show averages and error bars represent SEs ($n = 4$). The p-values displayed on the graph show statistical significance from a two-way ANOVA.

of the plant compared with other Se species (**Figure 4**). The influence of N on the SeMet concentration in leaves and its translocation was observed only at GS2 (**Figure 5**). The application of F.Se+N led to significantly more transformation of the applied inorganic Se into SeMet, resulting in more rapid translocation of SeMet away from the application leaf (**Figure 5**).

DISCUSSION

Plant biomass was not influenced by the different Se treatments (**Table 2**), which was expected given that Se does not play an essential role in plant nutrition. Although Se can mitigate stress in plants by stimulating the activity of antioxidants (30), its essentiality in higher plants is not proven (31).

The Se concentrations of control plants and grains in the experiment were below the lower threshold of adequacy in the diet of 0.1 mg kg^{-1} dry matter (32), suggesting very low available Se levels in the soil used in this experiment. Accordingly, very low levels of Se_N (0.015 mg kg^{-1}) were observed in the plants and the majority of the Se in the wheat originated from the fertiliser source (Se_{fert}) (**Figure 1**). Similar findings were observed by Muleya et al. (29), who reported a Se_N concentration range of 0.01–0.03 mg kg^{-1} in three crops grown in Se-deficient soils in Malawi.

The application of Se by the foliar method appears to be very successful in promoting Se uptake by wheat, with minimal losses to the environment; recoveries of Se_{fert} in crops ranged from 60 to 100% (**Figure 1**). Such recoveries evidenced the higher effectiveness of foliar fertilisers compared to soil-applied ones for biofortification (16). Broadley et al. (33) and Mathers et al. (22) recovered <20% of applied Se in wheat grain, following 10 g ha^{-1} soil-application of Na_2SO_4 in the UK. Similarly, Lyons et al. (34) and Curtin et al. (35) recovered 13.5 and 17.0% in wheat grain, respectively, from the soil application of Se^{VI}. The efficiency of foliar micronutrient fertilisers can reportedly be further improved by adding small amounts of N in the foliar solutions. Aciksoz et al. (36) observed that the addition of 1% N-urea (w/v) to foliar Fe fertilisers increased grain Fe concentrations, potentially by facilitating the cuticular penetration of foliar-applied Fe. Similarly, in a previous study, we observed that the addition of 2% w/v N in the form of urea or urea ammonium nitrate (UAN) to the foliar Se solution significantly improved grain Se concentrations compared to foliar Se application on its own (20). Effectively, a clear, positive effect of foliar Se coapplication with N on plant and grain Se concentration was observed (**Table 3**); the mechanisms for this positive effect appeared to differ according to the timing of application. At an early growth stage (GS1), the presence of N in foliar Se solutions significantly increased Se accumulation in the aboveground biomass of the plants (**Table 3**), potentially due to improved absorption of the applied Se_{fert} through the cuticle of the wheat leaves and/or improved assimilation of the applied inorganic Se into organic compounds and subsequent translocation. Since the speciation analysis of the foliar-treated leaves at GS1 showed no effect of N on the formation of SeMet (**Table 4**), it is likely that a physiological mechanism was responsible for the greater efficiency of the foliar Se+N fertilisers.

At a later growth stage (GS2), the fertiliser formulations were equally effective in raising plant Se concentrations, but those fertilised with F. Se+N had higher Se concentrations in the grain (**Figure 3**), suggesting improved translocation of Se from the point of application to the grain. Speciation analysis of the foliar-treated leaves suggested that N in the foliar Se solution improved the conversion of Se^{VI} to SeMet in the leaves, which was then more rapidly translocated to the grain (**Table 4**). Given that N and Se share a common metabolic pathway in plants (30), the coapplication of foliar Se with N at a stage where plants have a high metabolic activity (GS2) most likely affected the rate of Se assimilation and translocation within the plant. Hence, the coapplication of foliar Se with N at the heading stage was highly beneficial in improving the nutritional status of the plant, which has important implications for biofortification.

The target grain Se concentration range desired for biofortification, without running the risk of toxic effects, is >0.1 and <1 mg kg^{-1} (32). The application of foliar Se (±N) in this study increased grain Se concentrations to 0.25–0.3 mg kg^{-1} (**Figure 3**), which is optimal for biofortification, based on an RDI of 55–65 μg day^{-1} (17, 37). The application of foliar Se+N resulted in significantly higher Se concentrations in the grain compared with the foliar Se application on its own (**Figure 3**), of which >90% was in the highly bioavailable SeMet form (**Table 4**). These findings confirmed our previous results, whereby the application of F.Se+N doubled the concentration of Se in grain compared with F.Se only (20). It is worth noting that this experiment was carried out under controlled conditions, whereby plants were grown in a glasshouse and foliar fertilisers were applied in a precise manner. This could explain why the recovery of foliar-applied Se fertilisers in plants (>60% at GS1 and >96% at GS2) was considerably higher than those where foliar fertilisers were applied in outdoor conditions. For example, Ducsay et al. (38) recovered 13–15% of Se in grain following foliar application of 10 g ha^{-1} Se^{VI} to wheat in small field experiments. Nevertheless, this is, to the best of our knowledge, the first study to map the transformation and translocation of Se in wheat following its application with and without N at different growth stages and, hence, provide practical information about ways to optimise foliar Se fertilisations.

CONCLUSIONS

Applying foliar Se, irrespective of the formulation, at 10 g ha^{-1} equivalent brought grain Se concentration to a level high enough to be considered adequate for biofortification. Whether applied at an early or a late growth stage, foliar Se fertilisers can be made more efficient by coapplication with 2% w/v N as urea. The application of foliar Se with N to young wheat plants improved its absorption through the leaves, thereby reducing the window of opportunity for fertiliser Se to be lost to the environment either by volatilisation or by leaf runoff. At a later growth stage, the inclusion of N in foliar Se solutions improved the transformation of applied inorganic Se into bioavailable SeMet, which was then more rapidly translocated from the point of application to the grain. From the current study, it appears that the coapplication of foliar Se with 2% N-urea at the heading stage significantly increased the concentration of bioavailable Se in the grain. Farmers could use such information to optimise fertilisation strategies and minimise losses to the environment.

DATA AVAILABILITY STATEMENT

The raw data supporting the conclusions of this article will be made available by the authors, without undue reservation.

AUTHOR CONTRIBUTIONS

CR, SY, and EB: conceptualisation, data analysis and interpretation, and writing the review and editing.

CR: experimental setup, data collection, analysis and interpretation, and writing. MM and FD: data analysis and interpretation and writing the review and editing. All authors contributed to the article and approved the submitted version.

ACKNOWLEDGMENTS

The authors gratefully acknowledge the contribution of the following staff members at the University of Nottingham, Mark Meacham for his help in setting up the crop trial, and Dr. Molly Muleya for her help with the speciation analysis of the plant samples. The authors are also grateful to the University of Adelaide and the University of Nottingham for financially supporting this research project.

SUPPLEMENTARY MATERIAL

The Supplementary Material for this article can be found online at: https://www.frontiersin.org/articles/10.3389/fnut.2021.732409/full#supplementary-material

REFERENCES

1. Fao. *The State of Food and Agriculture 2013: Food Systems for Better Nutrition*. Rome: Food and Agricultural Organization of the United Nations (2013).
2. Bouis HE, Saltzman A. Improving nutrition through biofortification: a review of evidence from HarvestPlus, 2003 through 2016. *Glob Food Sec.* (2017) 12:49–58. doi: 10.1016/j.gfs.2017.01.009
3. Combs GF. Selenium in global food systems. *Br J Nutr.* (2001) 85:517–47. doi: 10.1079/BJN2000280
4. Rayman MP. The importance of selenium to human health. *Lancet.* (2000) 356:233–41. doi: 10.1016/S0140-6736(00)02490-9
5. Reid ME, Duffield-Lillico AJ, Slate E, Natarajan N, Turnbull B, Jacobs E, et al. The nutritional prevention of cancer: 400 mcg per day selenium treatment. *Nutr Cancer.* (2008) 60:155–63. doi: 10.1080/01635580701684856
6. Rayman MP. Selenium and human health. *Lancet.* (2012) 379:1256–68. doi: 10.1016/S0140-6736(11)61452-9
7. Fordyce, F. (2005). Selenium deficiency and toxicity in the environment. In: Selinus O, Alloway BJ, Centeno JA, Finkelman RB, Fuge R, Lindh U, Smedley P, editors. *Essentials of Medical Geology*. Dordrecht: Springer. p. 373–415.
8. Broadley MR, White PJ, Bryson RJ, Meacham MC, Bowen HC, Johnson SE, et al. Biofortification of UK food crops with selenium. *Proc Nutr Soc.* (2006) 65:169–81. doi: 10.1079/PNS2006490
9. Institute of Medicine. *Dietary Reference Intakes for Vitamin C, Vitamin E, Selenium, and Carotenoids.* Meyers LD, Suitor CW, editors. Washington, DC: National Academics Press (2007).
10. Macfarquhar JK, Broussard DL, Melstrom P, Hutchinson R, Wolkin A, Martin C, et al. Acute selenium toxicity associated with a dietary supplement. *Arch Intern Med.* (2010) 170:256–61. doi: 10.1001/archinternmed.2009.495
11. Wang J, Wang Z, Mao H, Zhao H, Huang D. Increasing Se concentration in maize grain with soil- or foliar-applied selenite on the Loess Plateau in China. *Field Crops Res.* (2013) 150:83–90. doi: 10.1016/j.fcr.2013.06.010
12. White PJ, Bowen HC, Parmaguru P, Fritz M, Spracklen WP, Spiby RE, et al. Interactions between selenium and sulphur nutrition in Arabidopsis thaliana. *J Exp Bot.* (2004) 55:1927–37. doi: 10.1093/jxb/erh192
13. Zhang Z, Shen F, Gu M, Liu Y, Pan L, Shohag MJI, et al. Evaluation of selenium bioavailability to Brassica juncea in representative Chinese soils based on diffusive gradients in thin-films (DGT) and chemical extraction methods. *Int J Phytoremediation.* (2020) 22:952–62. doi: 10.1080/15226514.2020.1774502
14. Fernández-Martínez A, Charlet L. Selenium environmental cycling and bioavailability: a structural chemist point of view. *Rev Environ Sci Biotechnol.* (2009) 8:81–110. doi: 10.1007/s11157-009-9145-3
15. Chen X, Zhang Z, Gu M, Li H, Shohag MJI, Shen F, et al. Combined use of arbuscular mycorrhizal fungus and selenium fertilizer shapes microbial community structure and enhances organic selenium accumulation in rice grain. *Sci Total Environ.* (2020) 748:141166. doi: 10.1016/j.scitotenv.2020.141166
16. Ros G, Rotterdam A, Bussink D, Bindraban P. Selenium fertilization strategies for bio-fortification of food: an agro-ecosystem approach. *Plant Soil.* (2016) 404:99–112. doi: 10.1007/s11104-016-2830-4
17. Lyons G. Biofortification of cereals with foliar selenium and iodine could reduce hypothyroidism. *Front Plant Sci.* (2018) 9:730. doi: 10.3389/fpls.2018.00730
18. Xie R, Zhao J, Lu L, Ge J, Brown PH, Wei S, et al. Efficient phloem remobilization of Zn protects apple trees during the early stages of Zn deficiency. *Plant Cell Environ.* (2019) 42:3167–81. doi: 10.1111/pce.13621
19. Tang L, Hamid Y, Liu D, Shohag MJI, Zehra A, He Z, et al. Foliar application of zinc and selenium alleviates cadmium and lead toxicity of water spinach – Bioavailability/cytotoxicity study with human cell lines. *Environ Int.* (2020) 145:106122. doi: 10.1016/j.envint.2020.106122
20. Ramkissoon C, Degryse F, Da Silva RC, Baird R, Young SD, Bailey EH, et al. Improving the efficacy of selenium fertilizers for wheat biofortification. *Sci Rep.* (2019) 9:19520–9. doi: 10.1038/s41598-019-55914-0
21. Di Tullo P, Pannier F, Thiry Y, Le Hécho I, Bueno M. Field study of time-dependent selenium partitioning in soils using isotopically enriched stable selenite tracer. *Sci Total Environ.* (2016) 562:280–8. doi: 10.1016/j.scitotenv.2016.03.207
22. Mathers A, Young SD, Mcgrath S, Zhao F, Crout N, Bailey EH. Determining the fate of selenium in wheat biofortification: an isotopically labelled field trial study. *Plant Soil.* (2017) 420:61–77. doi: 10.1007/s11104-017-3374-y
23. Dean, Jr. Determination of carbonate and organic matter in calcareous sediments and sedimentary rocks by loss on ignition; comparison with other methods. *J Sediment Petrol.* (1974) 44:242–8. doi: 10.1306/74D729D2-2B21-11D7-8648000102C1865D
24. Olsen SR, Cole CV, Watanabe FS, Dean LA. *Estimation of Available Phosphorus in Soils by Extraction With Sodium Bicarbonate*. Washingtonm, DC: US Government Printing Office (1954).
25. Blair G, Lefroy R. Interpretation of soil tests: a review. *Aust J Exp Agric.* (1993) 33:1045. doi: 10.1071/EA9931045
26. Dane JH, Topp GC, Campbell GS. *Methods of Soil Analysis. Part 4, Physical Methods*. Madison, Wis: Soil Science Society of America (2002).
27. Zadoks JC, Chang TT, Konzak CF. A decimal code for the growth stages of cereals. *Weed Res.* (1974) 14:415–21. doi: 10.1111/j.1365-3180.1974.tb01084.x
28. Labanauskas CK. Washing citrus leaves for leaf analysis. *Calif Agric.* (1968) 22:12–13.
29. Muleya M, Young SD, Reina SV, Ligowe IS, Broadley MR, Joy EJM, et al. Selenium speciation and bioaccessibility in Se-fertilized crops of dietary importance in Malawi. *J Food Compos Anal.* (2021) 98:103841. doi: 10.1016/j.jfca.2021.103841
30. Schiavon M, Lima LW, Jiang Y, Hawkesford MJ. Effects of selenium on plant metabolism and implications for crops and consumers. In: Pilon-Smits E, Winkel L, Lin ZQ, editors. Selenium in Plants. *Plant Ecophysiology, Vol. 11*. Cham: Springer (2017). doi: 10.1007/978-3-319-56249-0_150
31. Pilon-Smits EaH, Quinn CF, Tapken W, Malagoli M, Schiavon M. Physiological functions of beneficial elements. *Curr Opin Plant Biol.* (2009) 12:267–74. doi: 10.1016/j.pbi.2009.04.009
32. Hartikainen H. Biogeochemistry of selenium and its impact on food chain quality and human health. *J Trace Elem Med Biol.* (2005) 18:309–18. doi: 10.1016/j.jtemb.2005.02.009
33. Broadley MR, Alcock J, Meacham MC, Norman K, Mowat H, Scott P, et al. Selenium biofortification of high-yielding winter wheat (*Triticum aestivum* L.) by liquid or granular Se fertilization. *Plant Soil.* (2010) 332:5–18. doi: 10.1007/s11104-009-0234-4

34. Lyons G, Stangoulis J, Graham R. High-selenium wheat: biofortification for better health. *Nutr Res Rev.* (2003) 16:45–60. doi: 10.1079/NRR200255
35. Curtin D, Hanson R, Van Der Weerden TJ. Effect of selenium fertilizer formulation and rate of application on selenium concentrations in irrigated and dryland wheat (*Triticum aestivum*). *N Z J Crop Hortic.* (2008) 36:1–7. doi: 10.1080/01140670809510216
36. Aciksoz SB, Yazici A, Ozturk L, Cakmak I. Biofortification of wheat with iron through soil and foliar application of nitrogen and iron fertilizers. *Plant Soil.* (2011) 349:215–25. doi: 10.1007/s11104-011-0863-2
37. Smoleń S, Kowalska I, Czernicka M, Halka M, Keska K, Sady W. Iodine and selenium biofortification with additional application of salicylic acid affects yield, selected molecular parameters and chemical composition of lettuce plants (*Lactuca sativa* L. var capitata). *Front Plant Sci.* (2016) 7:1553. doi: 10.3389/fpls.2016.01553
38. Ducsay L, LoŽek O, Marček M, Varényiová M, Hozlár P, Lošák T. Possibility of selenium biofortification of winter wheat grain. *Plant Soil Environ.* (2016) 62:379–83. doi: 10.17221/324/2016-PSE

Conflict of Interest: The authors declare that the research was conducted in the absence of any commercial or financial relationships that could be construed as a potential conflict of interest.

Publisher's Note: All claims expressed in this article are solely those of the authors and do not necessarily represent those of their affiliated organizations, or those of the publisher, the editors and the reviewers. Any product that may be evaluated in this article, or claim that may be made by its manufacturer, is not guaranteed or endorsed by the publisher.

frontiers in Nutrition

ORIGINAL RESEARCH
published: 10 December 2021
doi: 10.3389/fnut.2021.761708

Effect of Zn-Rich Wheat Bran With Different Particle Sizes on the Quality of Steamed Bread

Huinan Wang[1,2], *Anfei Li*[1], *Lingrang Kong*[1] *and Xiaocun Zhang*[1]*

[1] Agronomy College, State Key Laboratory of Crop Biology, Shandong Agricultural University, Taian, China, [2] Key Laboratory of Food Nutrition and Safety, Ministry of Education, College of Food Science and Engineering, Tianjin University of Science and Technology, Tianjin, China

Bran is the main by-product of wheat milling and the part of the grain with the highest Zn content. We investigated the effects of the particle sizes (coarse, D50 = 375.4 ± 12.3 μm; medium, D50 = 122.3 ± 7.1 μm; and fine, D50 = 60.5 ± 4.2 μm) and addition level (5–20%) of Zn-biofortified bran on the quality of flour and Chinese steamed bread. It was studied to determine if the Zn content of steamed bread could be enhanced without deleterious effects on quality. Dough pasting properties, such as peak viscosity, trough viscosity, final viscosity, breakdown, and setback, decreased significantly as the bran addition level was increased from 5 to 20% but did not significantly differ as a result of different bran particle sizes. Bran incorporation significantly increased hardness, gumminess, chewiness, and adhesiveness, whereas the springiness, cohesiveness, and specific volume of steamed bread decreased with the increase in bran addition. The optimal sensory score of steamed bread samples in the control and Zn fertilizer groups were obtained under 5% bran addition resulting in comparable flavor, and texture relative to control. Meanwhile, the Zn content of the steamed bread in the Zn fertilizer group was 40.2 mg/kg, which was 55.8% higher than that in the control group. Results indicated that adding the appropriate particle size and amount of bran would be an effective and practical way to solve the problem of the insufficient Zn content of steamed bread.

Keywords: Zn biofortification, Zn content, wheat bran, wheat flour, viscoelasticity, steamed bread

OPEN ACCESS

Edited by:
Alexander Arthur Theodore Johnson, The University of Melbourne, Australia

Reviewed by:
Tao Feng, Shanghai Institute of Technology, China
Kingsley George Masamba, Lilongwe University of Agriculture and Natural Resources, Malawi

***Correspondence:**
Xiaocun Zhang
xczhang@sdau.edu.cn

Specialty section:
This article was submitted to Nutrition and Food Science Technology, a section of the journal Frontiers in Nutrition

Received: *20 August 2021*
Accepted: *15 November 2021*
Published: *10 December 2021*

Citation:
Wang H, Li A, Kong L and Zhang X (2021) Effect of Zn-Rich Wheat Bran With Different Particle Sizes on the Quality of Steamed Bread. Front. Nutr. 8:761708. doi: 10.3389/fnut.2021.761708

INTRODUCTION

Zn is one of the most essential trace elements that are closely related to human health. It is a component of more than 100 enzymes in the human body and a participant in the synthesis of nucleic acids and protein. Zn deficiency seriously affects the secretion of enzymes and hormones, thus endangering human health. More than 50% of the world's agricultural soils are deficient in available Zn (1). Approximately 30% of the global population is affected by insufficient Zn intake (2). Every year, ∼20% of deaths in children, especially children in developing countries, under the age of 5 years die from various diseases caused by Zn, Fe, and/or I deficiency (3). The WHO regards Zn deficiency as a major risk factor and an invisible killer threatening human health.

Wheat is one of the major food crops that is considered to be an important candidate for Zn biofortification. In China, the Zn content of wheat grain grown in major wheat-producing areas is <30 mg/kg (4), which is lower than the international recommended standard of 40–60 mg/kg (5). Thus, this level cannot satisfy the Zn demand of the population that consumes wheat as their staple food. Moreover, soils in the main wheat-producing

areas in China are potentially deficient in Zn; this condition seriously affects the accumulation of Zn in wheat. The foliar spraying of Zn fertilizers is an effective measure for increasing the Zn content of wheat grains rapidly (6).

The processing of wheat for consumption always includes two main steps: grinding wheat grain into flour and food preparation. During these processes, bran, which has the highest Zn content, is often discarded, resulting in the large loss of Zn from wheat grains. Therefore, bran can be applied in the processing of steamed bread to improve the content of Zn and increase the utilization rate of Zn in wheat grains. Wheat grain is composed of three components: the bran, embryo, and endosperm. The endosperm is the main ingredient of flour, and the bran is the main by-product of flour processing. Studies have shown that the content of metal elements, such as Zn, in wheat grain embryos, aleurone layers, and seed coats is drastically higher than that in the endosperm (7). The Zn content of the embryo and aleurone layer is approximately 150 mg/kg, whereas that of the endosperm is only 15 mg/kg (8). These values show that wheat bran has a considerably higher Zn content than flour and is rich in dietary fibers, good quality proteins, and antioxidants. Therefore, the reasonable application of bran in steamed bread processing can not only improve the Zn content of steamed bread and the utilization ratio of bran, it is also a safe and effective means of daily Zn supplementation. However, the addition of wheat bran often affects the structure and sensory quality of the resulting food and reduces consumer acceptance. Some researchers have shown that bran particle size has a significant effect on dough properties and product quality, such as the use of MWB (microparticulated wheat bran) could improve the texture as well as the specific volume of whole wheat bread (9). The effects of bran addition levels on noodles (10, 11), baked and steamed bread (12–14), and biscuits have been studied (15, 16). Zhang and Li (11) reported that addition of fine bran (0.21 mm) at 5–10% or medium bran (0.53 mm) at 5% in wheat flour, it is possible to satisfactorily produce fiber-rich dry white Chinese noodle. Sozer et al. (16) observed that particle size reduction of bran increased the biscuit hardness and decreased the starch hydrolysis index of biscuits. Steamed bread is the traditional staple food in China (17). It accounts for approximately 40% of national total wheat consumption (18). Steamed bread plays an important role in the diet structure of China. However, the fortification of steamed bread with Zn-rich wheat bran has not been systematically studied. The current study focused on the effect of adding bran with different particle sizes and proportions on the quality of wheat flour and dough properties, including Zn content and pasting, rheological, and structural properties. We anticipated that the results of this study would provide a new scheme for the rational use of wheat bran and scientific information enabling the quality improvement of Zn-fortified products.

Abbreviations: ICP-MS, Inductively coupled plasma mass spectrometry; 1M, Core powder 1; 2M, Core powder 2; 3M, Core powder 3; 1B, Hide powder 1; 2B, Hide powder 2; 3B, Hide powder 3.

MATERIALS AND METHODS

Plant Materials and Growth Conditions

The winter wheat cultivar used for the study was "Shannong 29," which was bred by Shandong Agricultural University. The field experiment was conducted at the Shandong Agricultural University Research Farm (117°16′69.52″N, 36°16′67.09″E). This area has a warm and semihumid continental monsoon climate, an annual average rainfall of 680 mm, and an annual mean temperature of 12.8°C. During the growing season, Zn fertilizer was sprayed at the jointing, flowering, pre-grouting, and late filling stages for the Zn biofortification of wheat. The foliar treatments were as follows: (1) foliar spraying of water as a control and (2) spraying of $ZnSO_4 \cdot 7H_2O$ (0.4%, w/v) containing 0.01% (v/v) Tween 20 as a surfactant. All the fertilization treatments were performed after sunset. Each plant plot had an area of 50 m^2 (5 m × 10 m) with three replications. The line spacing was 0.25 m, and the plant spacing was 0.02 m.

Preparation of Wheat Flour Samples

After harvesting, part of the samples was milled into flour by using a MM400 Hybrid Ball Mill (Retsch, Beijing, China) for the determination of the Zn concentration of whole grains. The other wheat samples were milled into three core powders (1M, 2M, and 3M), three hide powders (1B, 2B, and 3B), and bran by using a MLU-202 Automatic Laboratory Mill (Buhler, Inc., Wuxi, China) in accordance with the AACC-approved method 26-21A (19).

Preparation of Bran Samples With Different Particle Sizes

The bran collected from the mill was sifted into coarse bran (particle size of 2–2.5 mm) by using a JJSD sieve shaker (Shanghai Jiading Ltd. equipped different sized screens) with differently sized screens. Whole wheat bran was ground by using a fine grinder (KC-701, Kaichuang Instruments Co., Ltd., Beijing, China) into fine-ground bran. The bran samples were then divided into three equal portions. Two were subsequently ground into medium and fine particles by using a Perten 3100 laboratory mill (PerkinElmer Instruments Co., Ltd.) equipped with meshes of different sizes. Coarse bran (D50 = 375.4 ± 12.3 μm) was superfinely ground into medium (D50 = 122.3 ± 7.1 μm) and fine (D50 = 60.5 ± 4.2 μm) bran. The bran samples with different particle sizes were added to the flour at 0, 5, 10, 15, and 20% levels (on a 14% moisture basis). In this work, whole flour was the flour that contained whole grain. Standard flour was a blend of the 1M, 2M, 3M, 1B, 2B, and 3B fractions and was similar to commercially available flour. Coarse flour was a mixture of standard flour and coarse bran. Medium flour was a mixture of standard flour and medium bran. Fine flour was a mixture of standard flour and fine bran.

Nutrient Analysis

The samples were digested with HNO_3-H_2O_2 (4, 2 ml) in a microwave digester reaction system (Multiwave3000, Brabender, Germany). Then, the Zn content of the digested solution was determined through inductively coupled plasma optical emission spectroscopy (X Series 2, Thermo Fisher, USA). After use, all

the instruments used in the experiment were soaked in 20% nitric acid overnight, then rinsed with deionized water and dried. The moisture content, ash content, and falling number of the flour samples were determined in accordance with the Chinese National Standards GB/T 5497-1985, GB/T 5009.4-2003, and GB/T 10361-89, respectively. Protein content on a dry weight basis was determined through the Kjeldahl method in accordance with the International Approved Method 46-12 (19). The sedimentation value of dough was determined in accordance with the AACC International Approved Method 76-31 (19).

Determination of Pasting Properties

The pasting properties of the samples were determined by applying a Rapid Visco Analyzer (RVA-Super 3, Newport Scientific, Australia) in accordance with the AACC International Approved Method 76-21 (19). The test was performed by using 3.5 g (14% moisture basis) blends from each sample mixed with 25 ± 0.1 ml of distilled water (corrected for compensation on a 14% moisture basis).

Whiteness

A Minolta Chroma Meter (Model CR-400, Minolta Co., Osaka, Japan) was used to determine the whiteness of wheat flour and obtain L*, a*, and b* values. L* represents brightness and is a measure of black to white (0–100). Large L* values are indicative of high whiteness and brightness. a* stands for the red–green phase. A positive a* value indicates redness, whereas a negative a* value reflects greenness. b* stands for the yellow–blue phase. If b* is positive, then the sample is yellow. If b* is negative, then the sample is blue.

Gluten Content and Index

The gluten content and index were determined by using a Glutomatic 2200 system (M/S perter, Germany) in accordance with the AACC International Approved Method 38-12.02 (19). A total of 10 g of each dough sample was weighed out, and wet gluten was converted into 14% wet base.

Preparation of Steamed Bread

Steamed bread was prepared with 200 g of flour or flour blended with bran, 2 g of yeast, and water (85% of Mixolab water absorption). Before dough mixing, the yeast was dissolved in water (35°C). Then, the yeast solution and flour were poured into a mixing machine (HL-110, Shaoguan Co. Ltd., Guangzhou, China) and mixed for 5 min. The mixed dough was sheeted 15 times on a tablet pressure machine to remove air bubbles and split into 100 g portions. Each chunk was rolled with heights of approximately 6 cm by hand and then fermented (35°C, 80% relative humidity) for 45 min in a cabinet. After fermentation, the buns were steamed for 20 min in an electric steamer and cooled for 5 min after turning off the fire.

Sensory Evaluation

The steamed bread samples were cooled to room temperature for approximately 1 h before the measurement. The volume of steamed bread was determined by using the rapeseed displacement method. The specific volume was calculated from the volume-to-weight ratio of the steamed bread. GB/T21118-2007 with a few modifications was adopted for the sensory quality analysis of steamed bread. Specific volume, color, surface structure, appearance, internal structure, elasticity, toughness, stickiness, and scent were scored by six trained evaluators. The highest scores for each item were 20, 10, 10, 10, 15, 10, 10, 10, and 5, which provided a total score of 100 (the specific score was accurate to 0.1). The eating quality of the cooked steamed bread was subjectively evaluated by 16 (the male to female ratio was 1:1; the average age range is between 25 and 55.) trained panelists according to Chinese Standard Method GB/T 35991-2018.

Textural Analysis

After sensory evaluation, the steamed bread was subjected to textural profile analysis (TPA) by using a TA XTPlus Texture Analyze apparatus (TA XT Plus; Stable Micro Systems Ltd., Godalming, Surrey, UK) equipped with a P/35 R probe. Before the test, the steamed bread was cooled to room temperature and then cut into 10 mm-thick slices. The two center slices were taken for TPA. The test parameters were as follows: pretest speed of 1.0 mm/s, test speed of 1.0 mm/s, post-test speed of 1.0 mm/s, compression ratio of 50%, trigger force of 5 g, interval time of 5 s, and data collection rate of 200 pps.

Statistical Analysis

All data were collected at least in triplicate. The statistical analysis of the results was carried out with SPSS software (SPSS 19.0, SPSS Inc., Chicago, U.S.A.), and Duncan's test ($p < 0.05$) was used to compare significant differences among the samples.

RESULTS AND DISCUSSION

Effect of Spraying Zn Fertilizer on the Zn Content of Wheat and Flour

The effects of spraying Zn fertilizer on the Zn content of whole grain and different grain components are summarized in **Figure 1A**. The average Zn content of the wheat grain in the control group was 37.1 mg/kg and that of the wheat grain in the Zn fertilizer group was 54.7 mg/kg. Compared with that of the control group, the Zn content of the wheat grain in the Zn fertilizer group had increased by 47.4%. Considering that bran had the highest Zn concentration, it was the part of the wheat grain wherein Zn mainly accumulated. Significant differences were found among the Zn contents of the three core powder flours ($p < 0.05$), which followed the order of 3M > 2M > 1M. By contrast, no significant differences were found among the Zn concentrations of the three hide powder flours. As can be seen from **Figure 1B**, the Zn contents of flour in the control group (7.5 mg/kg) and the fertilizer group (11.9 mg/kg) were significantly higher than those of the flour sold in markets (3.4 mg/kg) ($p < 0.05$). Meanwhile, the Zn content of the Zn fertilizer flour had increased by 58.7% compared with that of the control flour. These results showed that the foliar spraying of Zn fertilizer is an effective way for bioaccumulation (20). **Figure 1C** shows that the Zn concentration of bran with different particle sizes did not significantly differ ($p > 0.05$) between the CK and Zn groups, indicating that the processing of bran into different particle

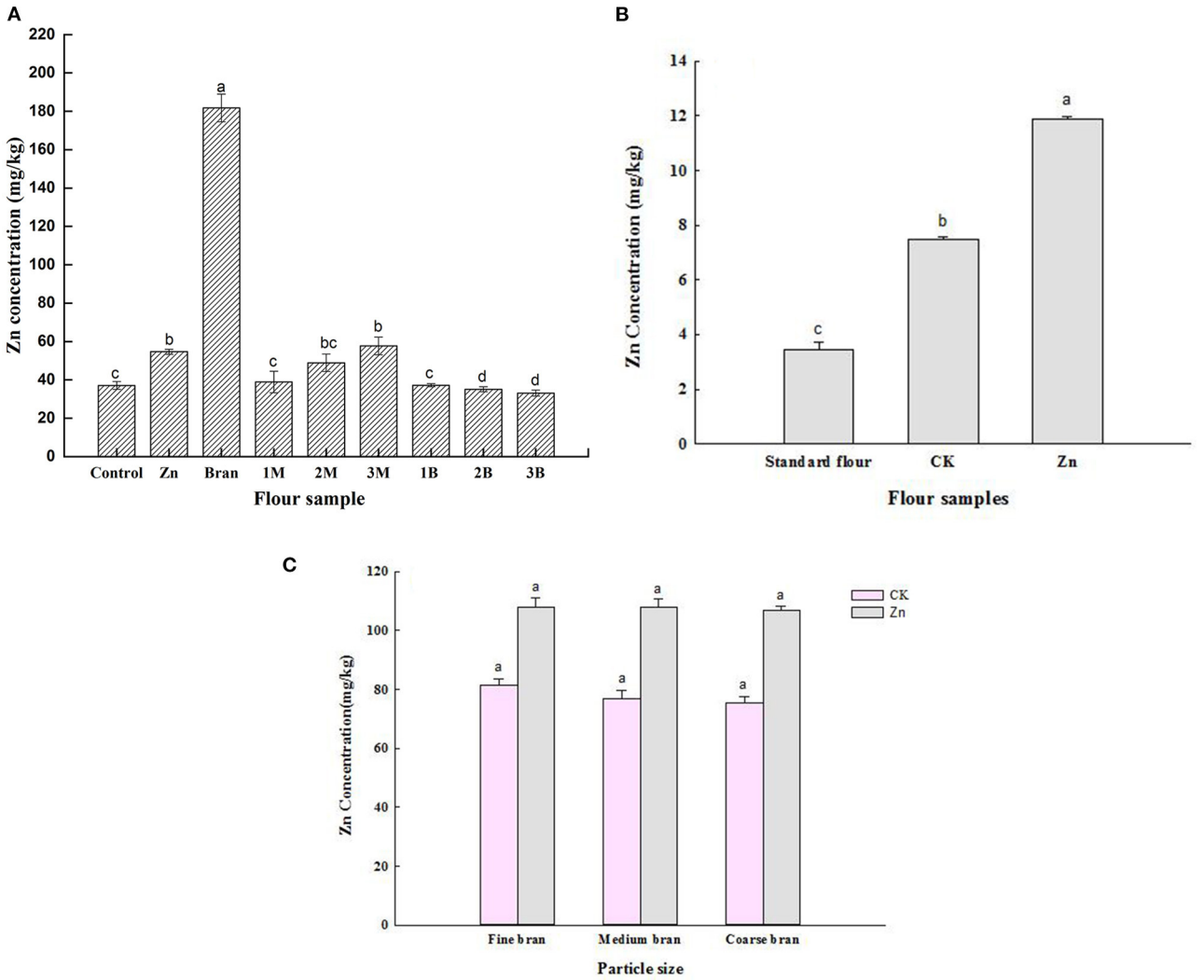

FIGURE 1 | (A) Zn content of whole grain and different grain components. 1M: Core powder 1, 2M: Core powder 2, 3M: Core powder 3, 1B: Hide powder 1, 2B: Hide powder 2, 3B: Hide powder 3. Means with different letters (a–c) for each column showed significant difference ($P < 0.05$). **(B)** Zn content of different flour. Means with different letters (a–d) for each column showed significant difference ($P < 0.05$). **(C)** Zn content of bran with different particles.

sizes would not affect Zn content. These results showed that Zn fertilization effectively increased the Zn concentrations of whole wheat grain relative to the control treatment, and bran was the most Zn-rich part of wheat grains.

Effect of Bran Addition on Flour Quality

Effects of Bran Addition on the Physicochemical Properties of Flour

As can be seen from **Table 1-1**, after the addition of bran, the moisture content of the flour samples in the CK and Zn fertilizer groups gradually decreased with the reduction in bran grain size and significantly decreased with the increase in the addition amount of bran ($p < 0.05$). These results could be attributed to the following: The grinding of small grains required more time and consumed more energy than that of large grains. The heat generated by the processing equipment in this process may be an important reason for water loss. In addition, the whiteness of flour decreased significantly with the increase in bran addition ($p < 0.05$). Whiteness is the major sensory indicator, which is actively correlated with consumers' acceptance. Bran was brownish yellow, and the flour was milky white as usual. The color of the blends gradually deepened and darkened as the amount of bran added to the flour was increased. As can be seen from **Table 1-2**, with the increase in the addition level of the three kinds of bran, the a* and b* values increased and the L* value decreased obviously. Dose-dependent lower L* value indicated bran incorporation darkened the appearance of flour (21). Under the same additive amount, L* decreased with the reduction in bran particle size in the control and Zn fertilizer blends because the even mixing of the small bran particles with the flour reduced the amount of light reflected by the flour surface and decreased brightness.

TABLE 1-1 | The change of physicochemical index of flour after adding different bran.

Bran granularity	Bran addition (%)	Moisture content (%)		Whiteness	
		CK	Zn	CK	Zn
Coarse bran	0	13.94 ± 0.04a	13.87 ± 0.05a	73.85 ± 0.21a	73.40a
	5	13.87 ± 0.04ab	13.81 ± 0.01e	68.00b	68.9 ± 0.42b
	10	13.0.84 ± 0.06b	13.78 ± 0.05d	63.7 ± 0.14c	65.55 ± 0.35c
	15	13.82 ± 0.1bc	13.74 ± 0.06c	61.35 ± 0.35d	62.9 ± 0.42d
	20	13.75 ± 0.02c	13.71 ± 0.07b	58.65 ± 0.21e	60.95 ± 0.07e
Medium bran	0	13.94 ± 0.04a	13.87 ± 0.05a	73.85 ± 0.21a	73.40a
	5	13.64 ± 0.01e	13.87 ± 0.06d	66.80b	68.6 ± 0.14b
	10	13.47 ± 0.01d	13.56 ± 0.04cd	63.65 ± 0.07c	65.85 ± 0.07c
	15	13.19 ± 0.06c	13.11 ± 0.04b	60.90d	64.05 ± 0.07d
	20	13.08 ± 0.01b	12.49 ± 0.01c	58.2 ± 0.14e	62.80e
Fine bran	0	13.94 ± 0.04a	13.87 ± 0.05b	73.85 ± 0.21a	73.40a
	5	13.31 ± 0.06d	13.33 ± 0.48a	68.55 ± 0.21b	69.00b
	10	12.96 ± 0.14c	12.58 ± 0.02a	65.35 ± 0.21c	65.75 ± 0.07c
	15	12.73 ± 0.09b	12.59 ± 0.51a	63.35 ± 0.07d	63.60 ± 0.07d
	20	12.66 ± 0.01a	12.12 ± 0.04a	61.15 ± 0.21e	62.10e

The same alphabets in right side of the same list show no significance (P > 0.05), on the contrary, having significance (P < 0.05).

TABLE 1-2 | The color of the bran flour.

Bran granularity	Bran addition (%)	L*		a*		b*	
		CK	Zn	CK	Zn	CK	Zn
Coarse bran	0	90.53a	90.64a	−0.04a	0.09a	9.35a	9.26a
	5	88.56b	89.08b	0.65b	0.59b	10.49b	9.87b
	10	87.30c	87.92c	0.91c	0.91c	11.23c	10.52c
	15	86.23d	87.15d	1.32d	1.09d	11.64d	11.11d
	20	85.83e	86.46e	1.45e	1.28e	11.91e	11.32e
Medium bran	0	90.53a	90.53a	−0.04a	−0.04a	9.35a	9.35a
	5	88.47b	89.01b	0.66b	0.59b	10.02b	9.56b
	10	86.82c	87.92c	1.26c	0.91c	10.33c	10.03c
	15	85.48d	86.91d	1.59d	1.14d	11.2d	10.51d
	20	84.25e	86.05e	1.91e	1.28e	11.55e	10.96e
Fine bran	0	90.53a	90.64a	−0.04a	0.09a	9.35a	9.26a
	5	88.83b	88.86b	0.44b	0.54b	9.62b	9.31b
	10	86.79c	87.08c	1.06c	1.12c	10.08c	9.62c
	15	84.82d	85.31d	1.37d	1.63d	10.91d	10.43d
	20	83.99e	84.66e	2.02e	1.83e	11.37e	10.05e

The same alphabets in right side of the same list show no significance (P > 0.05), on the contrary, having significance (P < 0.05).

The protein content of the samples is shown in **Figure 2**. With the addition of bran, the protein content of the CK and Zn fertilizer groups increased significantly ($p < 0.05$) and was positively correlated with bran addition level. Generally, wheat bran contains more than 15% high-quality proteins (22). It has been reported that there is a significant positive correlation between grain protein and zinc or iron concentrations (23, 24). In addition, the bran with large particle size retains more aleurone layers, while the aleurone layer contains high protein content. Therefore, the larger the grain size of the bran, the higher the protein content of the flour under the same amount of addition. Moreover, given that the high-quality protein content of bran exceeded 15% (22), the crude protein content of the flour increased after bran addition. Under the same addition level, the protein content of the mixed flour after the addition of coarse bran, medium bran, and fine bran reached 16.1, 16.3, and 17.1%, respectively.

Effects of Bran Addition on the Wet Gluten Content and Gluten Index of Flour

Gluten is not only a nutritional quality character but also a processing quality character. The quality of wheat depends on the

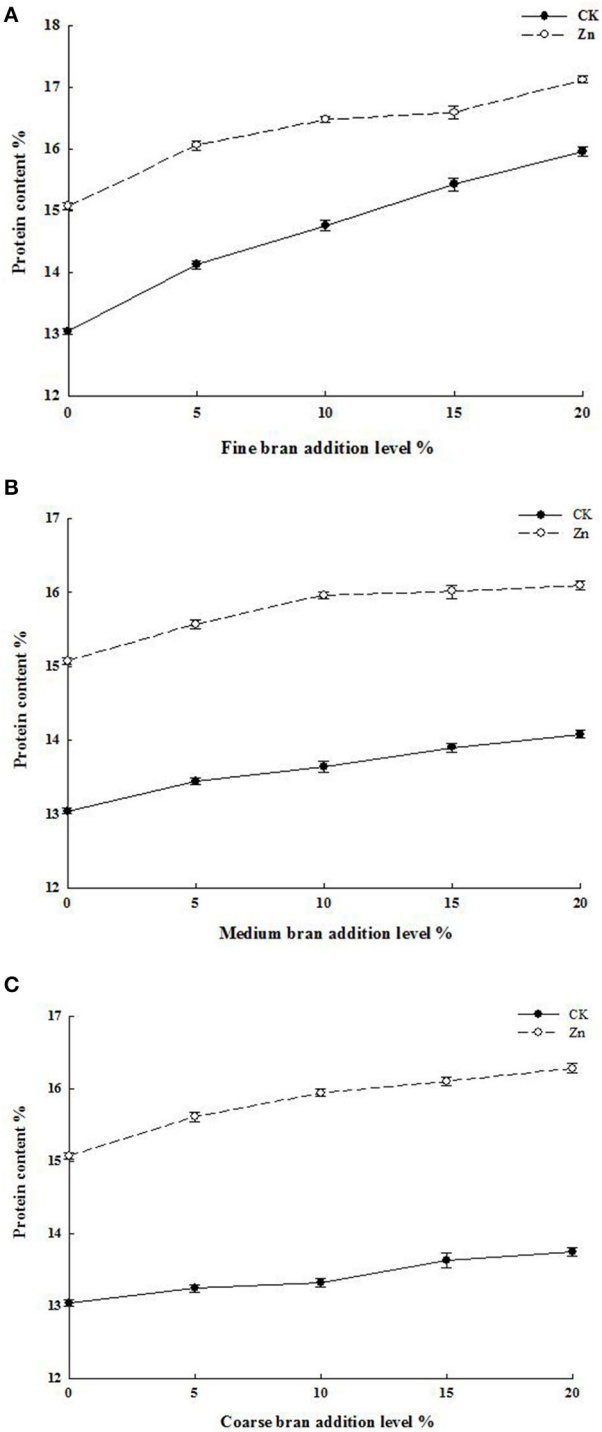

FIGURE 2 | Protein content of flour containing different addition levels and particle sizes of wheat bran. **(A)** Fine bran; **(B)** Medium bran; **(C)** Fine bran.

quality and quantity of gluten. Therefore, wet gluten content and gluten index are important for evaluating the processing quality of wheat. Jian Zhang (25) showed that the wet gluten content and total protein content of flour are significantly and positively correlated. As can be seen from **Table 2-1, 2-2**, with the increase in the addition levels of coarse bran, medium bran, and fine bran, the content of wet gluten first increased and then decreased. The maximum wet gluten content of 38.57% was obtained when medium bran was added at the 5% level into Zn fertilizer flour. At the same particle size, the gluten index decreased significantly with the increase in the added amount of wheat bran ($p < 0.05$), indicating that the addition of bran could affect the formation of gluten in the dough. The possible reasons are as follows: on the one hand, although the protein content increased due to the presence of more bran, the bran protein was mainly dominated by globulin and albumin, and the gluten quality was poorer than that of endosperm protein; on the other hand, the presence of bran had an adverse effect on the gluten network, making it difficult for the gluten to form a strong network structure (26). The highest gluten index was obtained when the bran addition level was 5%, representing the best gluten quality. Moreover, the wet gluten content and gluten index of the flour in the Zn fertilizer group flour were higher than those of the flour in the control group. These results indicated that the application of Zn improved the gluten content and quality of flour.

Effects of Bran Addition on the Sedimentation Value of Flour

Sedimentation value is also an important index for evaluating flour quality. This index reflects the quantity and quality of gluten protein. A high sedimentation volume indicates strong gluten and vice versa. The sedimentation value is significantly related to the cooking quality of flour and depends on the hydration rate and hydration capacity of gluten protein. Upon mixing with water, the hydrophobic bonds, such as hydrogen bonds, of the gluten protein are broken, and the gluten molecule's hydration capability is enhanced such that the swollen flour particles form flocculent precipitates. As can be seen from **Table 3** and consistent with the protein content of the bran flour in the two groups, the sedimentation value of the Zn fertilizer group was higher than that of the control. However, with the increase in the added amount of bran, the sedimentation values of the control and Zn groups decreased significantly ($p < 0.05$) likely because the addition of bran destroyed the network structure formed by gluten and reduced the quality of the dough. This result was consistent with the changes of gluten content and gluten index. The adverse effect of bran addition on gluten network formation could be explained by its role as a filler suspended in the dough (27).

Effects of Bran Addition on the Pasting Properties of Flour

RVA starch pasting properties are closely related to the wheat flour processing performance, food texture, and storage aging performance. It affects the quality of steamed bread, noodles, and bread and is an important indicator of starch quality. The effects of bran addition on the pasting properties of flour are shown in **Tables 4-1**, **4–2**. At a constant bran size and with the increase in the addition level of bran, the peak viscosity, trough viscosity, final viscosity, and setback value decreased significantly ($p < 0.05$). Bran could act as a filler in the flour, wherein it reduced

TABLE 2-1 | The sedimentation value of the CK bran flour.

Flour	Bran granularity	Bran addition (%)				
		0	5	10	15	20
CK	coarse	27.50 ± 0.71a	23.00b	13.00c	9.50 ± 0.71b	9.37 ± 0.71d
	medium	27.50 ± 0.71a	18.00b	16.50 ± 0.71b	14.50 ± 0.71b	12.10 ± 0.71c
	fine	27.50 ± 0.71a	17.50 ± 0.71b	14.50 ± 2.12b	15.50 ± 0.71b	14.00 ± 1.41b

Those with the same letters in the same row indicated that the difference in the same period did not reach the significant level ($P > 0.05$), while those with different letters indicated that the difference reached the significant level.

TABLE 2-2 | The sedimentation value of the Zn bran flour.

Flour	Bran granularity	Bran addition (%)				
		0	5	10	15	20
Zn	coarse	29.00a	24.5 ± 0.71b	19.00c	15.00d	10.50 ± 0.71e
	medium	29.00a	19.5 ± 0.71b	12.00 ± 1.4c	16.00 ± 1.41d	12.00 ± 1.41d
	fine	29.00a	18.00b	11.00c	15.50 ± 0.71c	14.00 ± 1.41d

Those with the same letters in the same row indicated that the difference in the same period did not reach the significant level ($P > 0.05$), while those with different letters indicated that the difference reached the significant level.

TABLE 3 | The gluten content in different bran flour.

Bran granularity	Bran addition (%)	Wet gluten content (%)		Gluten index	
		CK	Zn	CK	Zn
Coarse	0	35.64 ± 0.57b	37.65 ± 0.56b	72.85 ± 0.21a	73.40a
	5	37.64 ± 0.41ab	37.74 ± 0.64ab	68.65 ± 0.07b	68.70b
	10	38.31 ± 022a	38.45 ± 0.24a	63.70 ± 0.14c	65.55 ± 0.35c
	15	34.48 ± 0.26cd	34.3 ± 0.27c	61.35 ± 0.35d	62.91 ± 0.42d
	20	30.62 ± 0.58d	31.02 ± 0.53d	58.65 ± 0.21e	60.95 ± 0.07e
Medium	0	35.64 ± 0.57bc	37.65 ± 0.56ab	73.85 ± 0.21a	73.40a
	5	37.98 ± 1.12bc	38.57 ± 0.54a	66.80b	68.6 ± 0.14b
	10	38.35 ± 1.34a	38.53 ± 0.09ab	63.65 ± 0.07c	65.85 ± 0.07c
	15	38.21 ± 1.09ab	37.42 ± 0.14b	60.90d	64.05 ± 0.07d
	20	33.46 ± 2.70c	36.07 ± 0.39c	58.22 ± 0.14e	62.80e
Fine	0	35.64 ± 0.57b	37.65 ± 0.56b	73.85 ± 0.21a	73.40a
	5	37.62 ± 0.55a	38.02 ± 0.51a	68.55 ± 0.21b	69.00b
	10	34.48 ± 0.26c	34.30 ± 0.57c	65.35 ± 0.21c	65.75 ± 0.07c
	15	32.66 ± 0.42d	32.45 ± 0.52d	63.35 ± 0.07d	63.60 ± 0.07d
	20	31.8 ± 0.61e	31.74 ± 0.47e	61.15 ± 0.21e	62.10e

Those with the same letters in the same row indicated that the difference in the same period did not reach the significant level ($P > 0.05$), while those with different letters indicated that the difference reached the significant level.

the proportion of starch and competed with starch granules for moisture, thus reducing the minimum viscosity values of the bran-containing pastes (28). When the bran concentration was increased, the relative concentration of starch decreased. This effect resulted in a low proportion of expanded starch granules and thus led to a reduction in viscosity. Compared with the control group, the pasting temperature of pastes containing bran were higher. This could be due to the bran absorbed free water, so more energy was needed to destroy the crystal structure of starch granules to make them swell, resulting in an increase in the pasting temperature value (29). As the grain size of the bran increased, the peak viscosity of the flour decreased. The breakdown value of the coarse bran flour was significantly lower than that of the fine and medium bran flours ($p < 0.05$). The size of the bran had no noticeable effect on the minimum and final viscosities of the flour. The setback value is related to the tendency for paste retrogradation. Starch retrogradation occurs in the cooling stage, wherein the amorphous structure of amylose and amylopectin begins to recrystallize through hydrophobic interactions and hydrogen bonds. The competition of the bran

TABLE 4-1 | The pasting properties t in CK bran flours.

Bran granularity	Bran addition (%)	Peak viscosity (RVU)	Trough viscosity (RVU)	Breakdown (RVU)	Final viscosity (RVU)	Setback (RVU)	Peak time (min)	Pasting temperature (°C)
	0	137.21 ± 1.43a	114.67 ± 1.41a	42.5 ± 1.18a	207.92 ± 2.24b	93.25 ± 0.82bc	6.3 ± 0.05a	67.79 ± 0.58c
	5	119.79 ± 0.41c	75.92 ± 1.06d	43.88 ± 0.65a	178.79 ± 2.65d	102.88 ± 1.59b	6.05 ± 0.35a	70.45 ± 0.07b
Fine	10	121.42 ± 3.65a	95.5 ± 3.18bc	41.92 ± 0.47a	230.83 ± 3.54a	135.33 ± 0.35a	6.11 ± 0.12a	75.5 ± 2.12a
	15	120.96 ± 3.59b	85.71 ± 10.31cd	40.25 ± 6.83a	171.58 ± 5.07d	90.88 ± 8.31c	6.08 ± 0.12a	76.3 ± 2.83a
	20	122.08 ± 1.89b	101.54 ± 0.77ab	40.54 ± 2.65a	194.29 ± 0.41c	92.75 ± 1.18bc	6.08 ± 0.26a	78.8 ± 0.42a
	0	137.21 ± 1.43c	114.67 ± 2.03a	42.5 ± 1.18a	207.92 ± 1.58c	93.25 ± 1.52bc	6.3 ± 0.05a	67.79 ± 0.58b
	5	161.00 ± 1.21c	112.5 ± 1.09a	48.50 ± 0.65a	212.92 ± 3.11b	100.42 ± 0.79b	6.27 ± 0.35a	67.45 ± 0.07b
Medium	10	159.83 ± 0.62b	116.5 ± 0.41a	43.50 ± 0.47a	235.83 ± 1.54a	119.5 ± 0.2.33a	6.13 ± 0.07a	72.5 ± 2.12a
	15	134.83 ± 3.08c	96.83 ± 3.541b	40.25 ± 6.83a	187.08 ± 3.21d	90.25 ± 1.83c	6.20 ± 0.12a	76.3 ± 2.83a
	20	150.92 ± 2.40b	94.42 ± 3.187b	44.08 ± 2.65a	182.33 ± 0.91d	87.92 ± 2.01bc	6.19 ± 0.26a	78.8 ± 0.42a
	0	137.21 ± 1.43d	114.67 ± 1.41d	42.5 ± 1.18a	207.92 ± 2.24d	93.25 ± 0.82bc	6.3 ± 0.05a	67.79 ± 0.58a
	5	200.42 ± 1.21c	158.25 ± 1.09b	42.17 ± 0.65a	246.92 ± 3.11b	88.67 ± 0.79b	6.60 ± 0.35a	65.40 ± 0.07a
Coarse	10	229.92 ± 0.62b	186.67 ± 0.41a	43.25 ± 0.47a	306.67 ± 1.54a	120 ± 0.2.33a	6.65 ± 0.07a	64.45 ± 2.12b
	15	192 ± 3.08c	147.17 ± 3.541c	44.83 ± 6.83a	241.17 ± 3.21d	94 ± 1.83c	6.70 ± 0.12a	63.55 ± 2.83b
	20	191.75 ± 2.40b	143.58 ± 3.18c	48.17 ± 2.65a	238.5 ± 0.91c	94.72 ± 2.01bc	6.80 ± 0.26a	61.05 ± 0.42c

At the same granularity, the same alphabets in right side of the same lift of the item of one stage show no significance (P > 0.05), on the contrary, having significance in same column mean significant among treatments at 5% level.

TABLE 4-2 | The pasting properties t in Zn bran flours.

Bran granularity	Bran addition (%)	Peak viscosity (RVU)	Trough viscosity (RVU)	Breakdown (RVU)	Final viscosity (RVU)	Setback (RVU)	Peak time (min)	Pasting temperature (°C)
	0	140.96 ± 2.3a	108.46 ± 9.84a	39.67 ± 5.77a	191.96 ± 4.89a	103.50 ± 8.37a	6.30 ± 0.14a	70.83 ± 0.95a
	5	137.96 ± 10.9b	101.29 ± 3.48b	37.5 ± 1.06b	181.5 ± 3.65b	80.21 ± 6.19c	6.47 ± 0.28a	66.98 ± 0.60b
Fine	10	137.08 ± 3.65b	99.50 ± 0.94b	36.58 ± 4.60bc	184.63 ± 5.01b	94.13 ± 5.95b	6.20 ± 0.19a	62.78 ± 0.67c
	15	129.69 ± 6.05c	73.13 ± 1.47d	35.58 ± 1.06c	175.42 ± 0.47c	96.27 ± 1.03b	6.18 ± 0.07a	70.75 ± 0.78a
	20	108.71 ± 2.53d	89.17 ± 6.36c	33.5 ± 0.35d	170.58 ± 5.66c	101.42 ± 0.71a	6.20 ± 0.02a	69.07 ± 0.94a
	0	140.96 ± 2.3b	101.29 ± 3.48b	39.67 ± 5.77a	191.96 ± 4.89a	90.67 ± 8.37c	6.30 ± 0.14a	70.83 ± 0.95a
	5	123.08 ± 10.9c	88.25 ± 9.84a	38.83 ± 1.06b	171.25 ± 5.66b	80.42 ± 6.19d	6.27 ± 0.28a	67.18 ± 0.60b
Medium	10	151.75 ± 3.65a	111.75 ± 0.94b	34 ± 4.60c	166.33 ± 5.01c	114.58 ± 5.95a	6.20 ± 0.19a	61.75 ± 0.67c
	15	119.71 ± 2.53d	80.83 ± 1.47d	38.17 ± 1.06ab	163.42 ± 0.47d	82.58 ± 1.03c	6.07 ± 0.07a	71.05 ± 0.78a
	20	126.67 ± 6.05bc	85.33 ± 6.36c	34.33 ± 0.35c	168.27 ± 3.65c	85.92 ± 0.71bc	6.13 ± 0.02a	69.07 ± 0.94a
	0	140.96 ± 2.3d	101.29 ± 3.48b	39.67 ± 5.77c	191.96 ± 4.89c	90.67 ± 8.37b	6.30 ± 0.14a	70.83 ± 0.95a
	5	192.42 ± 10.9b	135.08 ± 9.84a	40.75 ± 4.60c	247.83 ± 3.65b	112.75 ± 6.19a	6.27 ± 0.28a	65.70 ± 0.60b
Coarse	10	212.67 ± 3.65a	171.92 ± 0.94b	44.42 ± 1.06b	278.92 ± 5.01a	107.00 ± 5.95b	6.80 ± 0.19a	64.45 ± 0.67c
	15	169.00 ± 2.53c	124.58 ± 1.47d	44.83 ± 0.35b	213.58 ± 0.47bc	89.88 ± 1.03d	6.47 ± 0.07a	64.50 ± 0.78c
	20	171.17 ± 6.05bc	126.33 ± 6.36c	57.33 ± 1.06a	215.00 ± 5.66bc	88.67 ± 0.71d	6.47 ± 0.02a	61.05 ± 0.94d

At the same granularity, the same alphabets in right side of the same lift of the item of one stage show no significance (p > 0.05), on the contrary, having significance in same column mean significant among treatments at 5% level.

for water leads to the redistribution of water in the paste system, resulting in a decrease in starch retrogradation (30). Given that the water retention capacity of fine bran was lower than that of coarse bran, the effect of starch retrogradation inhibition was poor and resulted in a high setback value.

Effects of Bran Addition on the Zn Content of Flour

The Zn content of flour with different addition levels and particle sizes of bran are summarized in **Table 5**. After bran addition, the Zn content of flour increased significantly. The Zn content of bran flour increased significantly ($p < 0.05$) with the increment in the addition level of coarse, medium, and fine bran. Compared with that of the flour without bran, the Zn concentrations of the flour in the Zn fertilizer groups and control groups had enhanced by 5.6–21.7% and 4.35–33.35%, respectively. Obviously, the addition of bran effectively increased the Zn content of flour, and the Zn content of Zn fertilizer flour was significantly higher than that of CK flour ($p < 0.05$). In addition, the different grain sizes of bran had no significant effect on the Zn content of flour.

TABLE 5 | The zinc content of the bran flour.

Bran granularity	Bran addition (%)	Zinc content (mg/kg)	
		CK	Zn
Fine	0	7.50 ± 0.57d	11.85 ± 0.07d
	5	15.05 ± 0.64c	24.45 ± 2.9c
	10	17.00 ± 1.13c	27.95 ± 0.92c
	15	21.85 ± 1.06b	33.65 ± 1.48b
	20	29.05 ± 0.92a	40.85 ± 0.78a
Medium	0	7.50 ± 0.57d	11.85 ± 0.07e
	5	13.10 ± 0.14c	24.20 ± 0.14d
	10	16.10 ± 0.42bc	26.75 ± 0.21c
	15	19.65 ± 0.78b	32.65 ± 1.48b
	20	29.01 ± 2.26a	39.30 ± 0.28a
Coarse	0	7.50 ± 0.57e	11.85 ± 0.07e
	5	13.70 ± 0.71d	21.90 ± 0.42d
	10	16.35 ± 0.07c	26.00 ± 0.42c
	15	29.20 ± 0.42b	32.25 ± 0.21b
	20	28.75 ± 0.07a	37.65 ± 1.06a

At the same granularity, the same alphabets in right side of the same lift of the item of one stage show no significance (P > 0.05), on the contrary, having significance in same column mean significant among treatments at 5% level.

TABLE 6 | The zinc content of the bran steamed bread.

Bran granularity	Bran addition (%)	Zinc content (mg/kg)	
		CK	Zn
Fine	0	16.05 ± 0.78e	25.75 ± 4.59c
	5	20.20 ± 0.14d	40.04 ± 0.42b
	10	27.45 ± 0.21c	47.19 ± 0.7ab
	15	34.00 ± 1.13b	50.35 ± 0.21a
	20	37.91 ± 0.71a	53.90 ± 0a
Medium	0	16.05 ± 0.78e	25.75 ± 4.6c
	5	19.90 ± 0.28d	40.15 ± 1.41b
	10	26.71 ± 1.84c	46.25 ± 3.18ab
	15	31.50 ± 0.28b	49.9 ± 1.27a
	20	36.00 ± 0.71a	53.05 ± 0.78a
Coarse	0	16.05 ± 0.78d	25.75 ± 4.6c
	5	21.75 ± 0.25c	39.25 ± 0.35b
	10	26.47 ± 0.32bc	46.72 ± 0.64ab
	15	32.20 ± 2.83b	49.2 ± 0.14ab
	20	37.25 ± 1.21a	52.75 ± 4.59a

At the same granularity, the same alphabets in right side of the same lift of the item of one stage show no significance (P > 0.05), on the contrary, having significance in same column mean significant among treatments at 5% level.

Effect of Bran Addition on Steamed Bread Quality

Effects of Bran Addition on the Zn Content of Steamed Bread

The effects of bran addition on the Zn content of steamed bread are shown in **Table 6**. The trend of Zn content in steamed bread was consistent with that of flour after bran addition. Specifically, both improved significantly with the increase in the addition level of bran ($p < 0.05$). When the amount of bran exceeded 10%, the change in the Zn content of steamed bread in the Zn fertilizer group was no longer obvious. The Zn content of the steamed bread without bran increased by 73% relative to that of the control group. At the 5% bran addition level, the Zn content of the steamed bread in the Zn fertilizer group increased by 55% and that of the control group increased by 29% on average. At the 20% bran addition level, the average Zn content of steamed bread had improved by almost 106% and that of the CK group increased by 131% on average. Therefore, bran addition had an excellent effect on the Zn content of steamed bread. As the bran retains most of the minerals in grains, it seems to favor the use of integral flour for the manufacture of bread and pasta products.

Effects of Bran Addition on the Specific Volume of Steamed Bread

As can be seen from **Figure 3**, the specific volume of the steamed bread in the control group (**Figure 3A**) and the Zn fertilizer group (**Figure 3B**) decreased with the increase in bran addition. Meanwhile, with the reduction of bran particle size, the specific volume also decreased. Similar result was reported that steamed breads containing smaller size bran had lower specific volume (31). Small bran particles could inhibit the formation of gluten network structure and reduce the gas fixed in the air chamber, and affect the height and volume of the steamed bread (27). The filling of the three-dimensional space structure of the starch–protein matrix increased density. This effect resulted in a reduction in the volume and specific volume of the steamed bread. This trend confirmed the finding that higher bran addition (>7%) led to decreased expansion of dough during kneading (32). Therefore, the optimal bran addition level was 5%.

Effects of Bran Addition on the Texture of Steamed Bread

The textural parameters of steamed bread with different bran additions as obtained through TPA are shown in **Table 7-1, 7-2**. Compared with those of steamed bread without bran, the hardness, gumminess, and chewiness of steamed bread with bran increased with the increase in bran addition, whereas springiness and cohesiveness declined likely because the steric hindrance of bran caused gluten protein dilution (4). Moreover, brain contained rigid dietary fibers and would thus compete with flour in water absorption. The water absorption of bran fiber and the gelatinization of starch during the steaming process increase the viscosity, which may be related to the gumminess and chewiness. In addition, with the decrement in the particle size of bran, the hardness, gumminess, and chewiness of steamed bread increased significantly, whereas springiness and chewiness decreased significantly ($p < 0.05$). Hardness is usually closely related to product acceptability (33). For steamed buns, the soft texture is an ideal quality characteristic. There was a study found that smaller bran particle size resulted in significantly lower hardness in flat bread (34). On the contrary, Li et al. (31) indicated that bread made by mixing hard white flour with fine

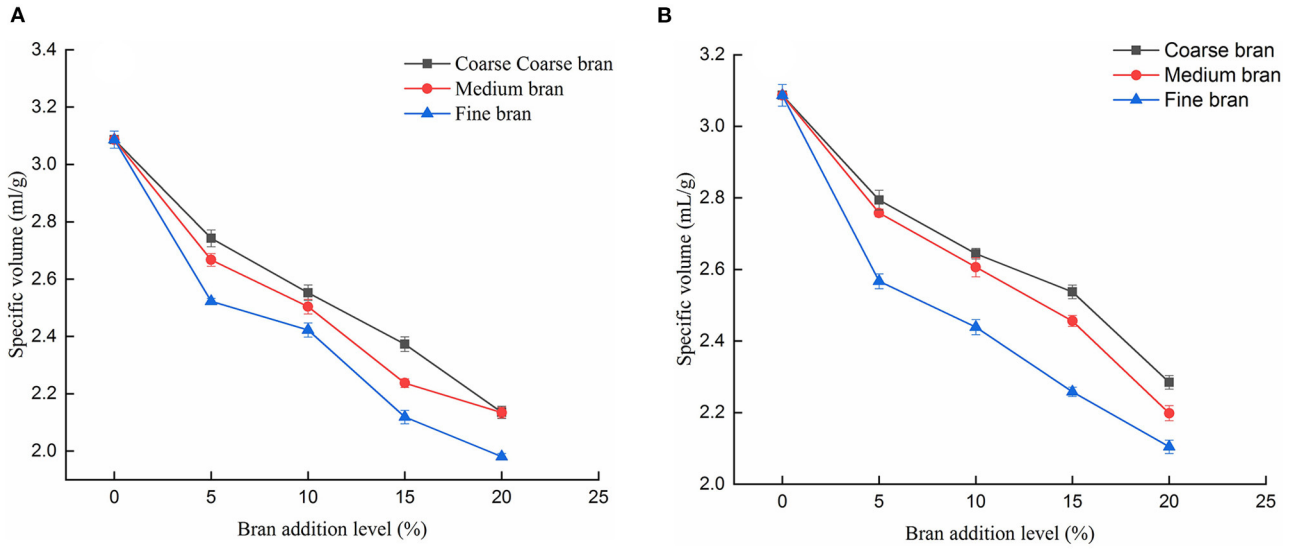

FIGURE 3 | Effect of bran addition on the specific volume of steamed bread. **(A)** control group; **(B)** Zn fertilizer group.

TABLE 7-1 | Texture analysis of CK bran steamed bread.

Granularity	Bran addition/%	Hardness/g	Springiness/%	Cohesiveness	Gumminess	Chewiness
	0	2903.01 ± 57.28e	0.98a	0.85a	2519.32 ± 110.46e	2298.91 ± 120.09e
	5	3641.23 ± 213.01d	0.97b	0.85a	2835.29 ± 61.11d	2667.12 ± 149.28d
Coarse	10	5219.12 ± 282.84c	0.96c	0.84ab	4215.29 ± 205.03c	3871.06 ± 6.98c
	15	6463.96 ± 70.71b	0.94d	0.83ab	5181.51 ± 513.02b	5075.59 ± 180.52b
	20	7410 ± 217.54a	0.93e	0.81b	6228.03 ± 342.17a	5749.17 ± 107.89a
	0	2903.01 ± 57.28e	0.98a	0.85a	2519.32 ± 110.46e	2298.91 ± 120.09e
	5	4432.88 ± 114.02b	0.96ab	0.84b	3598.16 ± 358.75c	3452.9 ± 310.71c
Medium	10	5149.14 ± 104.89c	0.94bc	0.83c	4176.20 ± 174.17c	4039.01 ± 316.75c
	15	7222.15 ± 24.77d	0.94c	0.81d	5568.32 ± 296.74b	5286.76 ± 158.45b
	20	8821.58 ± 25.69e	0.92c	0.8e	6793.77 ± 291.42a	6366.42 ± 327.36a
	0	2903.01 ± 57.28e	0.98a	0.85a	2519.32 ± 110.46e	2298.91 ± 120.09e
	5	4649.69 ± 7.4d	0.95b	0.83b	3836.78 ± 21.3d	3650.63 ± 31.07d
Fine	10	6146.43 ± 169.51c	0.93bc	0.80c	4911.46 ± 131.11c	4492.99 ± 112.14c
	15	8245.61 ± 137.45b	0.92c	0.77d	6179.10 ± 123.33b	6650.93 ± 114.65b
	20	9602.97 ± 315.87a	0.89d	0.75e	7105.42 ± 149.32a	7053.01 ± 175.52a

At the same granularity, the same alphabets in right side of the same lift of the item of one stage show no significance ($P > 0.05$), on the contrary, having significance in same column mean significant among treatments at 5% level.

bran has higher hardness than bread prepared with coarse and medium bran, which was similar to the results of our experiment. This probably because of steamed bread with lower specific volume had denser structure and more compact gas cells and thus increased the steamed bun hardness. The best texture of steamed bread was obtained at the bran addition level of 5%. By contrast, when the amount of bran exceeded 10%, the textural parameters showed significant reductions, and the internal structure was destroyed. In general, the steamed wheat bread added with 5% medium bran was selected as the best product. The results of this study showed that the control group and the foliar Zn group had the same trends.

Effects of Bran Addition on the Sensory Evaluation of Steamed Bread

The sensory scores of the steamed breads indicated that specific volume, surface color, appearance shape, internal structure, spring, tenacity, and odor were affected by the different addition levels and particle sizes of bran The physicochemical properties of wheat bran are quite different from those of refined flour and lead to inferior product quality (with regard to appearance, flavor, and sensory acceptance) of bran dough-based products (35). The sensory scores of the steamed breads with different bran additions are shown in **Table 8-1,8-2**. The addition of bran could affect the fermentation and air-holding capacity of

TABLE 7-2 | Texture analysis of Zn bran steamed bread.

Granularity	Bran addition/%	Hardness/g	Springiness/%	Cohesiveness	Gumminess	Chewiness
	0	2674.66 ± 56.74e	0.97a	0.85a	2512.56 ± 30.25e	2257.04 ± 60.88e
	5	3355.33 ± 5.94d	0.96a	0.84ab	3036.01 ± 11.68d	2871.42 ± 20.34d
Coarse	10	4811.09 ± 23.21c	0.95ab	0.83b	4424.42 ± 57.78c	3972.28 ± 6.36c
	15	6420.49 ± 132.83b	0.93bc	0.81c	5390.94 ± 14.75b	4760.12 ± 65.63b
	20	7710.97 ± 251.89a	0.91c	0.77d	5706.35 ± 78.72a	5323.7 ± 38.82a
	0	2674.66 ± 56.74e	0.97a	0.85a	2512.56 ± 30.25e	2257.04 ± 60.88e
	5	4008.29 ± 140.86d	0.96b	0.85ab	3324.81 ± 11.73c	3144.03 ± 58.25d
Medium	10	5260.99 ± 61.20c	0.94c	0.83b	4159.03 ± 49.90b	4346.87 ± 105.41c
	15	7722.87 ± 141.25b	0.93d	0.81c	5909.49 ± 64.42a	5329.59 ± 82.28b
	20	8205.33 ± 91.96a	0.92e	0.80d	6240.47 ± 36.54a	5846.52 ± 128.10a
	0	2674.66 ± 56.74e	0.97a	0.85a	2512.56 ± 30.25e	2257.04 ± 60.88e
	5	4762.42 ± 7.40d	0.95a	0.81b	3798.44 ± 51.20d	3562.53 ± 49.28d
Fine	10	6346.43 ± 169.51c	0.93b	0.79c	5010.65 ± 122.11c	4502.99 ± 107.14c
	15	8310.21 ± 47.32b	0.91c	0.77d	6157.32 ± 89.35b	6579.42 ± 111.75b
	20	9588.75 ± 125.24a	0.88d	0.76e	7028.33 ± 152.04a	6971.21 ± 169.20a

At the same granularity, the same alphabets in right side of the same lift of the item of one stage show no significance ($P > 0.05$), on the contrary, having significance in same column mean significant among treatments at 5% level.

TABLE 8-1 | The sensory scores of CK bran steamed bread.

Sample	Specific volume (20)	Surface color (10)	Surface structure (10)	Appearance shape (10)	Internal structure (15)	Spring (10)	Tenacity (10)	Viscosity (10)	Odor (10)	Total score
CK	20	9.2	9.0	9.0	13.5	8.5	8.5	8.5	4.7	90.9
CK-C-5	17	8.5	8.0	8.3	10.4	8.0	7.5	8.1	4.8	80.6
CK-C-10	16	7.4	6.5	7.2	9.0	7.5	8.0	7.2	4.5	73.3
CK-C-15	15.5	6.8	7.0	6.0	9.2	7.2	7.0	6.0	4.5	69.2
CK-C-20	14.3	6.0	6.0	5.0	8.7	6.6	6.0	5.8	4.3	62.7
CK-M-5	17	8.5	9.0	8.2	10.6	8.0	8.0	8.5	4.8	82.6
CK-M-10	16	7.5	8.0	8.0	9.9	7.2	8.0	7.2	4.7	76.5
CK-M-15	15.7	6.2	7.3	7.2	8.5	7.0	6.5	6.3	4.6	69.3
CK-M-20	13.2	5.2	7.0	6.5	7.8	6.2	5.0	5.5	4.5	60.9
CK-F-5	16.7	9.0	8.0	8.8	11.7	7.6	6.0	7.5	4.3	79.6
CK-F-10	15	7.7	8.0	8.1	11.0	7.4	5.7	7.4	3.2	73.5
CK-F-15	13.5	6.3	7.0	8.0	7.2	6.2	5.0	6.2	2.7	62.1
CK-F-20	13	5.6	6.0	4.0	6.3	5.0	4.0	4.3	2.0	50.2

CK-C-5, CK flour with 5% coarse bran addition level; CK-M-5, CK flour with 5% medium bran addition level; CK-F-5, CK flour with 5% fine bran addition level and so on.

the dough. Thus, the volume and specific volume of steamed bread changed with bran addition. With the addition of fine bran, the taste of steamed bread worsened, and the smell of steamed bread became unpleasant. Moreover, considering the close fusion of the small-grained bran with the flour, the inner structure of the dough became dense and the unfolding of the gluten network structure was hindered. These effects resulted in the formation of excessively small pores or even prevented the formation of pores. With the addition of coarse bran, the surface of the steamed breads became obviously granular and thus caused distinct discomfort during chewing and swallowing. When the added amount of coarse bran exceeded 5%, the steamed bread exhibited a rough texture and loose internal structure. The total scores of the samples indicated that the steamed bread containing medium-sized bran at the 5% addition level had the highest sensory score and resulted in comparable flavor, and texture relative to control. Numerous negative effects of bran addition on dough and product properties have been reported such as: darker color, dough stickiness increase, specific volume reduction, coarser texture and so on (36). The main problem is the consumer's acceptability of Zn-enriched bran steamed bread. On the basis of the sensory scores, flour physicochemical properties, Zn content, and acceptability of the steamed bread samples, the steamed bread with 5% medium bran was identified

TABLE 8-2 | The sensory scores of Zn bran steamed bread.

Sample	Specific volume (20)	Surface color (10)	Surface structure (10)	Appearance shape (10)	Internal structure (15)	Spring (10)	Tenacity (10)	Viscosity (10)	Odor (10)	Total score
Zn	20	9.1	10.0	9.1	13.5	8.8	8.5	8.5	4.5	92
Zn-C-5	18	8.7	8.0	8.3	10.5	8.5	7.5	8.0	4.8	82.3
Zn-C-10	16.2	8.5	6.5	7.4	10.5	7.6	8.1	7.0	4.6	74.4
Zn-C-15	15.5	7.4	7.0	6.2	10.3	7.2	7.0	6.2	4.2	71
Zn-C-20	14.3	6.3	6.0	5.1	9.4	8.7	6.5	6.0	4.0	66.3
Zn-M-5	17.8	8.8	9.0	8.8	11.0	8.2	8.0	8.0	4.8	84.4
Zn-M-10	16	7.8	8.0	8.5	10.4	7.0	8.2	7.0	4.8	77.7
Zn-M-15	15.8	6.4	7.5	7.2	9.8	7.2	6.5	6.3	4.6	71.3
Zn-M-20	14.7	6.0	7.0	7.0	9.0	6.2	5.0	5.0	4.5	64.4
Zn-F-5	16.4	9.0	8.0	8.8	11.8	8.8	6.0	7.5	4.2	80.5
Zn-F-10	15.5	7.7	8.0	8.0	10.4	7.5	5.7	7.2	3.5	73.5
Zn-F-15	14.2	5.6	7.0	7.8	7.5	6.0	5.0	6.4	3.0	62.5
Zn-F-20	13	5.0	6.0	4.5	6.0	5.5	4.5	4.0	2.0	50.5

Zn-C-5, Zn flour with 5% coarse bran addition level; Zn-M-5, Zn flour with 5% medium bran addition level, Zn-F-5, Zn flour with 5% fine bran addition level and so on.

as the best option under the conditions of this experiment. This result provides scientific knowledge for guiding the production of steamed bread with bran fortified through Zn fertilization.

CONCLUSION

As a result of the foliar application of ZnSO4, the Zn content of wheat grains and flour increased by 47.4 and 58.7%, respectively, which met the target levels for Zn biofortification. The addition level and particle size of wheat bran affected the mixing characteristics and pasting properties of flour and thus weakened mixing tolerance. The addition of wheat bran significantly decreased peak viscosity, trough viscosity, final viscosity, and setback value ($p < 0.05$). However, particle size had no significant effect on pasting properties. The whiteness and L* of the mixed flour gradually decreased with the increment in the particle size and addition amount of bran. The hardness, gumminess, and chewiness of steamed bread showed an upward trend with the increase in bran addition level, whereas springiness and cohesiveness declined. The sensory total scores of steamed bread in the control and Zn fertilizer groups were optimal at the 5% bran addition level. By adding 5% medium bran to wheat flour, the Zn content of the steamed bread in the Zn fertilizer group reached 40.2 mg/kg, whereas that of the steamed bread in the control group was only 25.8 mg/kg. The Zn content of the steamed bran bread was 55.8% higher than that of the control group. This increment indicated that the Zn content of this staple food was enhanced. In conclusion, the results of this study could be useful in the application of wheat bran as an ingredient for enhancing the content Zn of steamed bread. On one hand, we offer a sustainable and low-cost way to provide essential micronutrients (Zn) to people in both developing and developed countries. On the other hand, wheat bran as the main by-product of wheat milling usually has low value but in this way it can be a good source of Zn. The influence of bran on steamed bread structure, nutritional ingredients, and qualities need to be further researched. Meanwhile, further research is needed to minimize the detrimental influence of bran on the quality and sensory acceptance of bran addition products, such as applying physical mode (extrusion, autoclaving and autoclaving) to modify the functional properties of bran and enhance the consumption of bran dough-based products.

DATA AVAILABILITY STATEMENT

The original contributions presented in the study are included in the article/**Supplementary Material**, further inquiries can be directed to the corresponding author/s.

AUTHOR CONTRIBUTIONS

HW and XZ contributed to the design, implementation, and data analysis of the study. HW conducted the experiments, analyzed the data, and wrote the first draft of the manuscript. XZ supervised the findings of this work, verified data analysis, and contributed to the interpretation of results and discussion. All authors contributed to the final manuscript and approved the final version.

FUNDING

This work was supported by Agricultural Variety Improvement Project of Shandong Province (2019LZGC001).

SUPPLEMENTARY MATERIAL

The Supplementary Material for this article can be found online at: https://www.frontiersin.org/articles/10.3389/fnut.2021.761708/full#supplementary-material

REFERENCES

1. Kopittke PM, Lombi E, Wang P, Schjoerring JK, Husted S. Nanomaterials as fertilizers for improving plant mineral nutrition and environmental outcomes. *Environ Sci Nano.* (2019) 6:3513–24. doi: 10.1039/C9EN00971J
2. Phattarakul N, Rerkasem B, Li LJ, Wu LH, Zou CQ, Ram H. Biofortification of rice grain with zinc through zinc fertilization in different countries. *Plant Soil.* (2012) 361:131–41. doi: 10.1007/s11104-012-1211-x
3. Prentice AM, Gershwin ME, Schaible UE, Keusch GT, Victora CG, Gordon JI. New challenges in studying nutrition-disease interactions in the developing world. *J Clin Invest.* (2008) 118:1322–9. doi: 10.1172/JCI34034
4. Zhang Y, Shi R, Rezaul KM, Zhang F, Zou C. Iron and zinc concentrations in grain and flour of winter wheat as affected by foliar application. *J Agric Food Chem.* (2010) 58:12268–74. doi: 10.1021/jf103039k
5. Cakmak I. Enrichment of cereal grains with zinc: agronomic or genetic biofortification? *Plant Soil.* (2007) 302:1–17. doi: 10.1007/s11104-007-9466-3
6. Velu G, Ortiz-Monasterio I, Cakmak I, Hao Y, Singh RP. Biofortification strategies to increase grain zinc and iron concentrations in wheat. *J Cereal Sci.* (2014) 59:365–72. doi: 10.1016/j.jcs.2013.09.001
7. Ozturk L, Yazici MA, Yucel C, Torun A, Cekic C, Bagci A. Concentration and localization of zinc during seed development and germination in wheat. *Physiol Plant.* (2006) 128:144–52. doi: 10.1111/j.1399-3054.2006.00737.x
8. Cakmak I, Kalayci M, Kaya Y, Torun AA, Aydin N, Wang Y. Biofortification and localization of zinc in wheat grain. *J Agric Food Chem.* (2010) 58:9092–102. doi: 10.1021/jf101197h
9. Kim BK, Cho AR, Chun YG, Park DJ. Effect of microparticulated wheat bran on the physical properties of bread. *Int J Food Sci Nutr.* (2013) 64:122–9. doi: 10.3109/09637486.2012.710890
10. Song X, Zhu W, Pei Y, Ai Z, Chen J. Effects of wheat bran with different colors on the qualities of dry noodles. *J Cereal Sci.* (2013) 58:400–7. doi: 10.1016/j.jcs.2013.08.005
11. Zhang J, Li M, Li C, Liu Y. Effect of wheat bran insoluble dietary fiber with different particle size on the texture properties, protein secondary structure, and microstructure of noodles. *Grain Oil Sci Technol.* (2019) 2:97–102. doi: 10.1016/j.gaost.2019.10.001
12. Noort MWJ, van Haaster D, Hemery Y, Schols HA, Hamer RJ. The effect of particle size of wheat bran fractions on bread quality – evidence for fibre–protein interactions. *J Cereal Sci.* (2010) 52:59–64. doi: 10.1016/j.jcs.2010.03.003
13. Pauline M, Roger P, Sophie Natacha Nina NE, Arielle T, Eugene EE, Robert N. Physico-chemical and nutritional characterization of cereals brans enriched breads. *Sci Afr.* (2020) 7:e00251. doi: 10.1016/j.sciaf.2019.e00251
14. Xu X, Xu Y, Wang N, Zhou Y. Effects of superfine grinding of bran on the properties of dough and qualities of steamed bread. *J Cereal Sci.* (2018) 81:76–82. doi: 10.1016/j.jcs.2018.04.002
15. Baumgartner B, Özkaya B, Saka I, Özkaya H. 2018. Functional and physical properties of cookies enriched with dephytinized oat bran. *J Cereal Sci.* (2018) 80:24–30. doi: 10.1016/j.jcs.2018.01.011
16. Sozer N, Cicerelli L, Heiniö R-L, Poutanen K. Effect of wheat bran addition on in vitro starch digestibility, physico-mechanical and sensory properties of biscuits. *J Cereal Sci.* (2014) 60:105–13. doi: 10.1016/j.jcs.2014.01.022
17. Zhu F. Influence of ingredients and chemical components on the quality of Chinese steamed bread. *Food Chem.* (2014) 163:154–62. doi: 10.1016/j.foodchem.2014.04.067
18. Kim Y, Huang W, Zhu H, Rayasduarte P. Spontaneous sourdough processing of Chinese Northern-style steamed breads and their volatile compounds. *Food Chem.* (2009) 114:685–92. doi: 10.1016/j.foodchem.2008.10.008
19. AACC A. *Approved Methods of the American Association of Cereal Chemists*. 10th ed. (2000). Alzuwaid NT, Pleming D, Fellows CM, and Sissons. M. Fortification of durum wheat spaghetti and common wheat bread with wheat bran protein concentrate-impacts on nutrition and technological properties. *Food Chem*. (2021) 334:127497. doi: 10.1016/j.foodchem.2020.127497
20. Kaur N, Kaur H, Mavi GS. Assessment of nutritional and quality traits in biofortified bread wheat genotypes. *Food Chem.* (2020) 302:125342. doi: 10.1016/j.foodchem.2019.125342
21. Hu G, Huang S, Cao S, Ma Z. Effect of enrichment with hemicellulose from rice bran on chemical and functional properties of bread. *Food Chem.* (2009) 115:839–42. doi: 10.1016/j.foodchem.2008.12.092
22. Alzuwaid NT, Pleming D, Fellows CM, Sissons M. Fortification of durum wheat spaghetti and common wheat bread with wheat bran protein concentrate-impacts on nutrition and technological properties. *Food Chem.* (2021) 334:127497. doi: 10.1016/j.foodchem.2020.127497
23. Zhao FJ, Su YH, Dunham SJ, Rakszegi M, Bedo Z, McGrath SP, et al. Variation in mineral micronutrient concentrations in grain of wheat lines of diverse origin. *J Cereal Sci.* (2009) 49:290–5. doi: 10.1016/j.jcs.2008.11.007
24. Velu G, Singh R, Huerta-Espino J, Peña J, Ortiz-Monasterio I. Breeding for enhanced zinc and iron concentration in CIMMYT spring wheat germplasm. *Czech J Genetics Plant Breed.* (2011) 47:S174–7. doi: 10.17221/3275-CJGPB
25. Zhang J , Zhang J , Mengqin L I. The study on the appropriate ranges of important flour traits for making high-quality staple food Man-tou. *J Food Sci*. (2016) 37:30–6.
26. Dong J, Pengchong L, Xiao Y, Ruiling S. Research on the physicochemical properties of whole wheat flour. *Food Industry.* (2018) 39:242–7.
27. Le Bleis F, Chaunier L, Chiron H, Della Valle G, Saulnier L. Rheological properties of wheat flour dough and French bread enriched with wheat bran. *J Cereal Sci.* (2015) 65:167–74. doi: 10.1016/j.jcs.2015.06.014
28. Liu N, Ma S, Li L, Wang X. Study on the effect of wheat bran dietary fiber on the rheological properties of dough. *Grain Oil Sci Technol.* (2019) 2:1–5. doi: 10.1016/j.gaost.2019.04.005
29. Schirmer M, Jekle M, Becker T. Starch gelatinization and its complexity for analysis. *Starch Stärke.* (2015) 67:30–41. doi: 10.1002/star.201400071
30. Ma F, Lee YY, Park E, Luo Y, Delwiche S, Baik B-K. Influences of hydrothermal and pressure treatments of wheat bran on the quality and sensory attributes of whole wheat Chinese steamed bread and pancakes. *J Cereal Sci.* (2021) 102:103356. doi: 10.1016/j.jcs.2021.103356
31. Li Z, Deng C, Li H, Liu C, Bian K. Characteristics of remixed fermentation dough and its influence on the quality of steamed bread. *Food Chem.* (2015) 179:257–62. doi: 10.1016/j.foodchem.2015.02.009
32. Cavella S, Romano A, Giancone T. *The Influence of Dietary Fibres on Bubble Development During Bread Making. Bubbles in Food 2-Novelty, Health and Luxury*. St Paul, MN: Eagan Press (2008). p. 311–22 doi: 10.1016/B978-1-891127-59-5.50035-3
33. Rizzello CG, Cassone A, Coda R, Gobbetti M. Antifungal activity of sourdough fermented wheat germ used as an ingredient for bread making. *Food Chem.* (2011) 127:952–9. doi: 10.1016/j.foodchem.2011.01.063
34. Luc DD, Bo HX, Thomson PC, Binh DV, Leroy P, Farnir F. Reproductive and productive performances of the stress-negative Piétrain pigs in the tropics: the case of Vietnam. *Anim Prod Sci.* (2013) 53:173–9. doi: 10.1071/AN12108
35. Baik BK. Strategies to improve whole wheat bread quality. *Cereal Foods World.* (2019) 64. doi: 10.1094/CFW-64-6-0069
36. Poutanen K, Sozer N , Valle GD. How can technology help to deliver more of grain in cereal foods for a healthy diet? *J Cereal Sci.* (2014) 9:327–36. doi: 10.1016/j.jcs.2014.01.009

Conflict of Interest: The authors declare that the research was conducted in the absence of any commercial or financial relationships that could be construed as a potential conflict of interest.

frontiers in Nutrition

ORIGINAL RESEARCH
published: 13 December 2021
doi: 10.3389/fnut.2021.779595

Application of Zinc and Iron-Based Fertilizers Improves the Growth Attributes, Productivity, and Grain Quality of Two Wheat (*Triticum aestivum*) Cultivars

Muhammad Bilal Hafeez[1], *Yasir Ramzan*[1], *Shahbaz Khan*[2,3]*, *Danish Ibrar*[2], *Saqib Bashir*[4], *Noreen Zahra*[5], *Nabila Rashid*[5], *Majid Nadeem*[1], *Saleem ur Rahman*[1], *Hira Shair*[1], *Javed Ahmad*[1], *Makhdoom Hussain*[1], *Sohail Irshad*[6], *Abdulrahman Al-Hashimi*[7], *Alanoud Alfagham*[7] *and Zeng-Hui Diao*[8]*

[1] *Wheat Research Institute, Ayub Agricultural Research Institute, Faisalabad, Pakistan,* [2] *National Agricultural Research Centre, Islamabad, Pakistan,* [3] *Department of Plant and Soil Sciences, Oklahoma State University, Ardmore, OK, United States,* [4] *Department of Soil and Environmental Science, Ghazi University, Dera Ghazi Khan, Pakistan,* [5] *Department of Botany, University of Agriculture, Faisalabad, Pakistan,* [6] *Department of Agronomy, Muhammad Nawaz Shareef University of Agriculture, Multan, Pakistan,* [7] *Department of Botany and Microbiology, College of Science, King Saud University, Riyadh, Saudi Arabia,* [8] *Guangdong Provincial Engineering and Technology Research Center for Agricultural Land Pollution Prevention and Control, Zhongkai University of Agriculture and Engineering, Guangzhou, China*

Field-based experiments were conducted during wheat cultivation seasons of 2017–2018 and 2018–2019 to minimize the impact of hidden hunger (micronutrient deficiencies) through agronomic biofortification of two wheat cultivars with zinc and iron. Two spring-planted bread wheat cultivars: Zincol-16 (Zn-efficient) and Anaj-17 (Zn-inefficient with high-yield potential) were treated with either zinc (10 kg/ha), iron (12 kg/ha), or their combination to study their effect on some growth attributes (plant height, tillers, and spike length, etc.,), productivity, and quality. No application of zinc and iron or their combinations served as the control. Maximum Zn and Fe contents of grains were improved by sole application of Zn and Fe, respectively. A higher concentration of Ca in grains was observed by the combined application of Zn and Fe. Starch contents were found maximum by sole application of Fe. Sole or combined application of Zn and Fe reduced wet gluten contents. Maximum proteins were recorded in Anaj-17 under control treatments. Zincol-16 produced maximum ionic concentration, starch contents, and wet gluten as compared to Anaj-17. Yield and growth attributes were also significantly ($p < 0.05$) improved by combined application as compared to the sole application of Zn or Fe. The combined application also produced the highest biological and grain yield with a maximum harvest index. Cultivar Anaj-17 was found more responsive regarding growth and yield attributes comparatively. The findings of the present study showed that the combined application of Zn and Fe produced good quality grains (more Zn, Fe, Ca, starch, and less gluten concentrations) with a maximum productivity of bread wheat cultivars.

Keywords: Anaj-17, biofortification, grain quality, micronutrients, wheat growth, Zincol-16

OPEN ACCESS

Edited by:
Velu Govindan, International Maize and Wheat Improvement Center, Mexico

Reviewed by:
Richard Atinpoore Atuna, University for Development Studies, Ghana
Ana Carolina Castro, National University of La Plata, Argentina

***Correspondence:**
Shahbaz Khan
shahbaz2255@gmail.com
Zeng-Hui Diao
zenghuid86@163.com

Specialty section:
This article was submitted to Nutrition and Food Science Technology, a section of the journal Frontiers in Nutrition

Received: *19 September 2021*
Accepted: *10 November 2021*
Published: *13 December 2021*

Citation:
Hafeez MB, Ramzan Y, Khan S, Ibrar D, Bashir S, Zahra N, Rashid N, Nadeem M, Rahman Su, Shair H, Ahmad J, Hussain M, Irshad S, Al-Hashimi A, Alfagham A and Diao Z-H (2021) Application of Zinc and Iron-Based Fertilizers Improves the Growth Attributes, Productivity, and Grain Quality of Two Wheat (Triticum aestivum) Cultivars. Front. Nutr. 8:779595. doi: 10.3389/fnut.2021.779595

INTRODUCTION

Globally, the deficiencies of dietary micronutrients are widespread and pose a major health concern for more than 2 billion people (1–3). After the green revolution, scientist's basic concern is to increase productivity rather than the quality of edible crop parts (4). That is the reason, malnutrition is one of the foremost tasks for agricultural scientists (5). Worldwide, zinc (Zn) and iron (Fe) deficiencies are the most widespread micronutrient disorder. Zn deficiency causes gastrointestinal problems (6), altered reproductive biology, impairments of physical growth (7), DNA damage and cancer development (8), diabetes mellitus, hormone imbalance, respiration issues and high blood pressure, and affects multiple aspects of the immune system. Fe deficiency causes anemia and pregnancy issues (9), tiredness and a poor immunity level, reduced work capacity and intellectual performance, less cognitive development, growth, and reproductive performance (10).

Monotonous and excessive use of wheat-based products has rapidly increased malnutrition. Among cereals, wheat is one of the staple crops, which is being consumed as a staple food for 1.2 billion of the world population (11). Globally, wheat was cultivated in the year 2019 about an area of 214.7 million hectares (M ha) and was the second-highest cereal crop with the production of 749 million tons (MT) after maize (12). In Pakistan (2018), wheat was grown on an area of 8.79 M ha with a production of 25.076 MT that was surplus than country demand (13). People in rural regions fulfilled their 70% daily calories through the wheat, and 60% of the population consumed wheat as a basic dietary food (14). The requirement for wheat to feed the escalating world population is expected to increase up to 40% by 2050 to meet food security (15, 16). According to a survey (17), 25–30% of soil is calcareous and Fe deficient. Around the world, it is estimated that about 50% of soils, under wheat cultivation, are Zn deficient (18). Zn and Fe deficiency is more common in Pakistani soil that has high pH, free $CaCO_3$, and HCO^{3-}, which inhibit the accessibility of Fe and Zn to the plants (16, 19).

Micronutrient-deficient soils are increasing due to the frequent growth of higher-yielding crops and intensive use of fertilizer, i.e., nitrogen, potassium, and phosphorus (20). In plants, Zn is a structural constituent/ activator of many enzymes involved in protein synthesis, regulation of auxin synthesis, carbohydrate metabolism, and membrane integrity (21, 22) and plays an important role in chlorophyll formation, pollen development, and fertilization (23), essential for the regulation of the gene expression needed for the tolerance of abiotic stresses in plants. Under acute zinc deficiency, visible symptoms include chlorosis of leaves, stunted growth, small leaves, and spikelet sterility (24, 25). In plants, Fe plays a vital role in chlorophyll synthesis as it is a component of cytochromes and electron transport (26). Its deficiency decreases the activity of various enzymes such as catalase and peroxidase that contain porphyrin as a prosthetic group (27). Fe chlorosis is also induced by HCO^{-3} that impairs the mechanism of Fe uptake (28). To mitigate the nutrient imbalance, plants use various mechanisms to reduce water loss while maximizing water uptake, including a reduction in the leaf area and osmotic adjustment through the application of liquid seaweed extract, organic compounds, and minerals elements (29–31).

Among various fortification techniques, agronomic biofortification is the most cost-effective, rapid, and sustainable strategy to improve the contents of micronutrients in wheat grains to alleviate the widespread Zn and Fe deficiencies in humans (32). Zinc sulfate ($ZnSO_4$) and iron sulfate ($FeSO_4$) are the most widely applied inorganic fertilizers as sources of Zn and Fe, respectively, due to their high solubility and low cost (33, 34). There is convincing proof about Zn and Fe fertilizer's effectiveness in improving their wheat grain concentrations and economic yield in Zn- and Fe-deficient regions (5, 35). The application of $ZnSO_4$ and $FeSO_4$ is reported as efficient in enhancing the quality of wheat grains (1, 34, 36). Several studies have demonstrated that soil supplementation of micronutrients showed good behavior in increasing their contents in wheat grain (5, 37–39). Exogenous applications of Zn and Fe may be useful to improve the quality of wheat grain with high production. After considering the above notation, a field-based trial was performed to reduce the impact of hidden hunger by assessing the following objective: (i) to compare the yield and physiological response of Zincol-16 (Zn-efficient) and Anaj-17 (Zn inefficient and high yielding) under soil-applied Zn and Fe, (ii) to explore the influence of sole and/or combined application of Zn and Fe on grain quality and yield attributes of wheat cultivars.

MATERIALS AND METHODS

Experimental Field Location and Soil Specification

A 2-year field trial was conducted at Farm Area of Wheat Research Institute (WRI), Faisalabad-Pakistan with longitudes of 73°74 East and latitude of 30°31.5 North with an elevation of 184 m (604 ft.) above the sea level. Faisalabad falls under a semiarid climatic zone due to high evapotranspiration with a mean annual rainfall of about 200 mm. Soil samples from different sites of the study area at 0-cm to 30-cm depth were collected after primary land preparation and prior to conducting the experiment. Estefan et al. (40) protocols were followed for analysis of soil physicochemical properties as presented in **Table 1**. Air-dry soil of 50 g was taken in a 100-ml glass beaker, and 50 ml of deionized water was added and shacked well for mixing. The suspension was allowed to stand for 30 min, and the working sample was prepared. The weather data, including maximum temperature, minimum temperature, average temperature, relative humidity, and rainfall, are presented in **Figure 1**.

Experimental Design and Treatments

Randomized complete block design with factorial (two cultivars and four treatments) arrangement was selected with three replications per treatment. The net plot was 5 × 2.25 m with a row spacing of 22.5 cm. Each experimental unit consists of 10 rows that were 5-m long. Zinc sulfate ($ZnSO_4$) and iron sulfate

TABLE 1 | Physical and chemical analysis of soil of the field trial site.

Characteristics	Units	Value (2017–18)		Value (2018–19)	
Soil depth	**(cm)**	**0–15**	**15–30**	**0–15**	**15–30**
Texture	(Class)	Sandy clay loam	Sandy clay loam	Sandy clay loam	Sandy clay loam
pH		7.5	7.7	7.6	7.5
EC	(dS m^{-1})	2.31	2.36	2.25	2.33
Organic matter	(%)	0.72	0.67	0.73	0.71
Total nitrogen	(%)	0.041	0.038	0.039	0.035
Available P (Olson)	(mg kg^{-1})	4.7	4.4	4.9	5.1
Extractable K (NH_4OAC)	(mg kg^{-1})	300	320	300	330
DTPA Zn	(mg kg^{-1})	0.51	0.47	0.52	0.44
DTPA Fe	(mg kg^{-1})	2.62	2.41	2.75	2.66

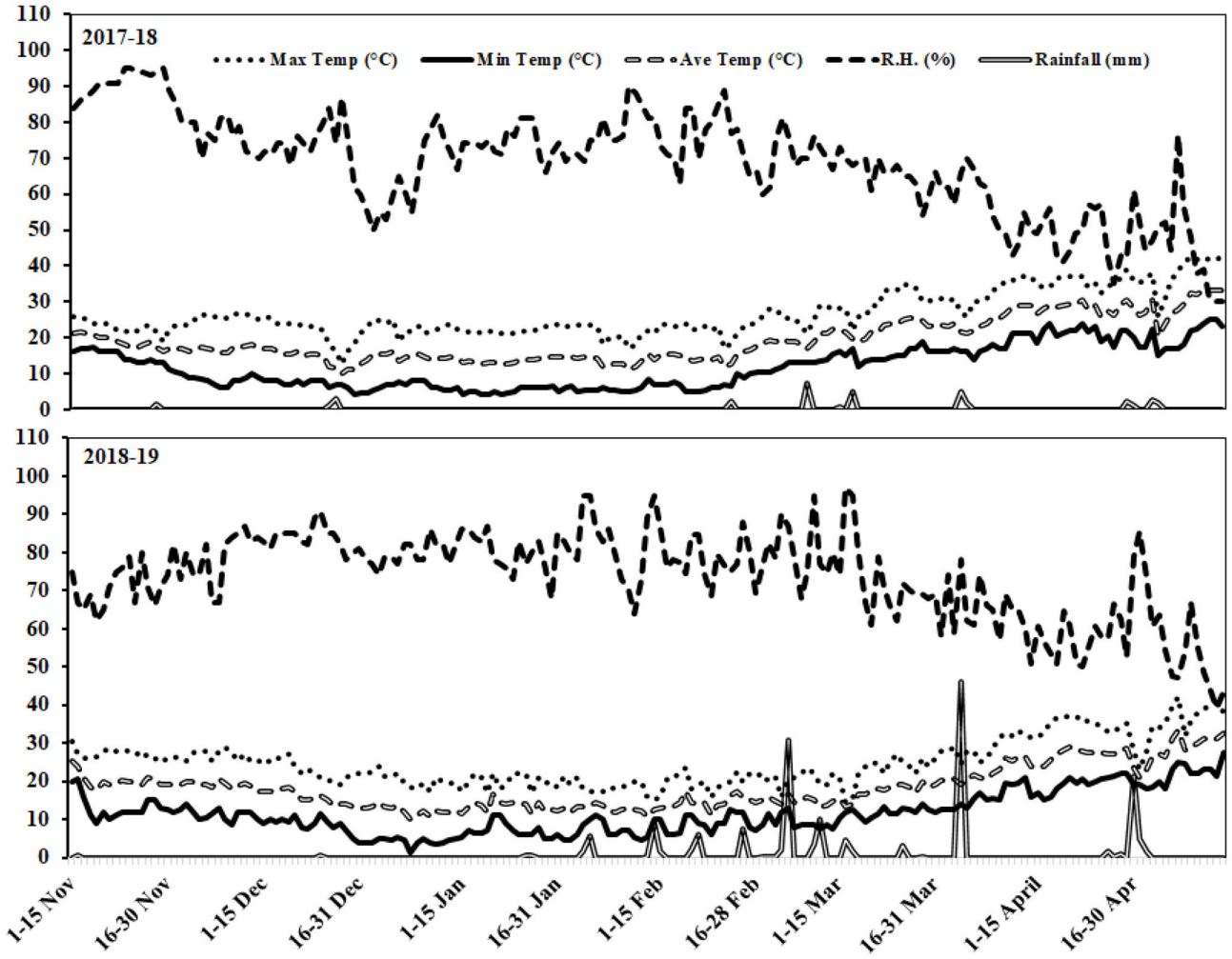

FIGURE 1 | Weather data of the experimental station during 2017–2018 and 2018–2019 growing seasons.

($FeSO_4$) were used as the sources of zinc and iron, respectively. The given below treatment plan was applied to study the above-discussed objectives;

- Control (no soil application of zinc or iron).
- Sole application of zinc at 10 kg ha $^{-1}$.
- Sole application of iron at 12 kg ha $^{-1}$.
- Combined application of zinc and iron at 10 and 12 kg ha^{-1}, respectively.

All the treatments were applied before sowing the crop. Zinc sulfate and iron sulfate were manually spread in the experimental field with recommended fertilizer doses.

Cultivars Used

Two major spring-planted wheat cultivars (Zincol-16 and Anaj-17) were used for the study. Cultivar Zincol-16 is claimed as zinc efficient with low-yield potential, while Anaj-17 is considered zinc inefficient with high-yield potential. Seeds of both cultivars were collected from the gene bank of WRI. The cultivars are being widely grown in wheat-cultivated areas of this region of the world. A recommended seed rate of each cultivar at 100 kg ha^{-1} was used.

Crop Cultivation and Management Practices

After harvesting the previous crop of rice from the field, a deep plow was used to break the hardpan, and stubbles were incorporated into the soil. Before sowing of seeds, seedbed was prepared by using a cultivator two times with the same number of plankings. Seeds of respective cultivars were sown in a well-prepared fine seedbed with the help of a Norwegian planter. Moreover, K, N, and P fertilization were applied at rates of 60 kg ha^{-1}, 114 kg ha^{-1}, and 120 kg ha^{-1}, respectively. Urea (46% N), diammonium phosphate (18% N and 46% P_2O_5), and murate of potash (60% K_2O) fertilizers were used as a source of primary nutrients. At the time of sowing, a complete dose of K and P with 1/3 of N was used as a basal dose. Remaining N was supplied with first and second irrigation with an equal split. Four-time irrigation was applied throughout the season of the wheat crop. Necessary plant protection measures were adopted to keep crops free of pests, weeds, insects, and diseases. All other agronomic practices were kept uniform throughout the course of experimentation. The crop was harvested manually after 160 days of sowing, left in the field for sun drying for a week. After sun-dried, spikes were threshed manually.

Measurement of Quality Parameters

Mineral ions—Zn, Fe, Cu, Mg, and Ca—accumulation was determined in the grains of wheat cultivars (Zincol-16 and Anaj-17) that were collected from each experimental unit during both growing seasons. After threshing the spikes, the grain samples were carefully washed three times with deionized water with each 30 s and were dried at 65°C in an electric oven, typically ranging from ambient to 300°C. Mineral contents, such as Ca, Mg, Cu, Zn, and Fe, in the grains were recorded according to the wet digestion method described by Rashid (41). Atomic absorption spectrum (Skemadzu 7,000) was used to analyze the mineral contents. Starch contents in the wheat grains were determined by following the protocol developed by Edwards (42). Amylose and amylopectin contents were measured through a fraction of 100 mg from each sample. Bradford technique (43) was used to determine the total soluble protein. To extract protein, 0.1 g of grain was grounded using a cooled phosphate buffer (pH 7.8) placed in an ice bath. The homogenate was centrifuged at 15,000 rpm for 5 min at 4°C. The supernatant was used for protein determination.

Measurement of Growth and Yield Parameters

At harvesting, the number of tillers (m^{-2}) was counted. Plant height and spike length were measured accurately with the help of a meter rod. The number of spikelets per spike and the grain number per spike were calculated manually than averaged. At the fully mature stage, an area of 1 m^2 was harvested for the measurement of biological yield. Grain yield was measured by obtaining grains from each experimental unit after threshing. Additionally, 1,000-grain weight was recorded by using weight balance. Harvest index was also calculated with the following formula: grain yield/biological yield × 100.

Statistical Analysis

Recorded data were analyzed and evaluated statistically using a statistical package (Statistix 8.1). Comparison among treatments was made by a two-way ANOVA technique at a CI of 95%. Various letters (a, b, c, etc.) were used to portray the significant difference among treatments *via* LSD as a *post-hoc* test. Microsoft Excel was used for calculation and graphical presentation. Mendeley Desktop (1.19.1) was used for citation and bibliography. Pearson correlation was drawn among different response variables.

RESULTS

Ions Concentrations

There were significant differences ($p \leq 0.05$) in Zn and Fe accumulation in grains of cultivars and soil-applied treatments (**Figure 2**). The interactive effect of fertilizers and cultivars showed no significant difference for the planting season of 2017 and 2018. The sole application of Zn produced maximum Zn contents in the grains while minimum in control for both cultivars (**Figure 2A**). Cultivar Zincol-16 was found more efficient in Zn accumulation as compared to Anaj-17 (**Figure 2**) during both experimental years. Fe accumulation was significantly ($p \leq 0.05$) improved by soil-applied treatments. Maximum improvement was recorded by sole application of Fe, while minimum in control (**Figure 2B**). Zincol-16 accumulated higher content of Fe in grains as compared to Anaj-17 during both experimental years. Based on the findings of the study, significant ($p \leq 0.05$) improvement was recorded regarding the concentrations of Mg, Ca, and Cu in the grains of wheat cultivars by the soil-applied treatments (**Figure 3**). All the treatments enhanced the concentration of Mg in grains as compared to control (**Figure 3A**). Combined application produced the highest concentration of Ca in grains, which were statistically at par with sole Zn application while minimum in control (**Figure 3B**). Zincol-16 accumulated higher concentrations of Mg and Ca in their grains as compared to the Anaj-17 cultivar during the first and second years of experimentation. All the soil-applied treatments significantly ($p \leq 0.05$) increased Cu concentration in the wheat grains as compared to control (**Figure 3C**). Sole application of Zn produced maximum Cu contents in grains, which were statistically at par with a combined application, and sole application of Fe during 2017–2018.

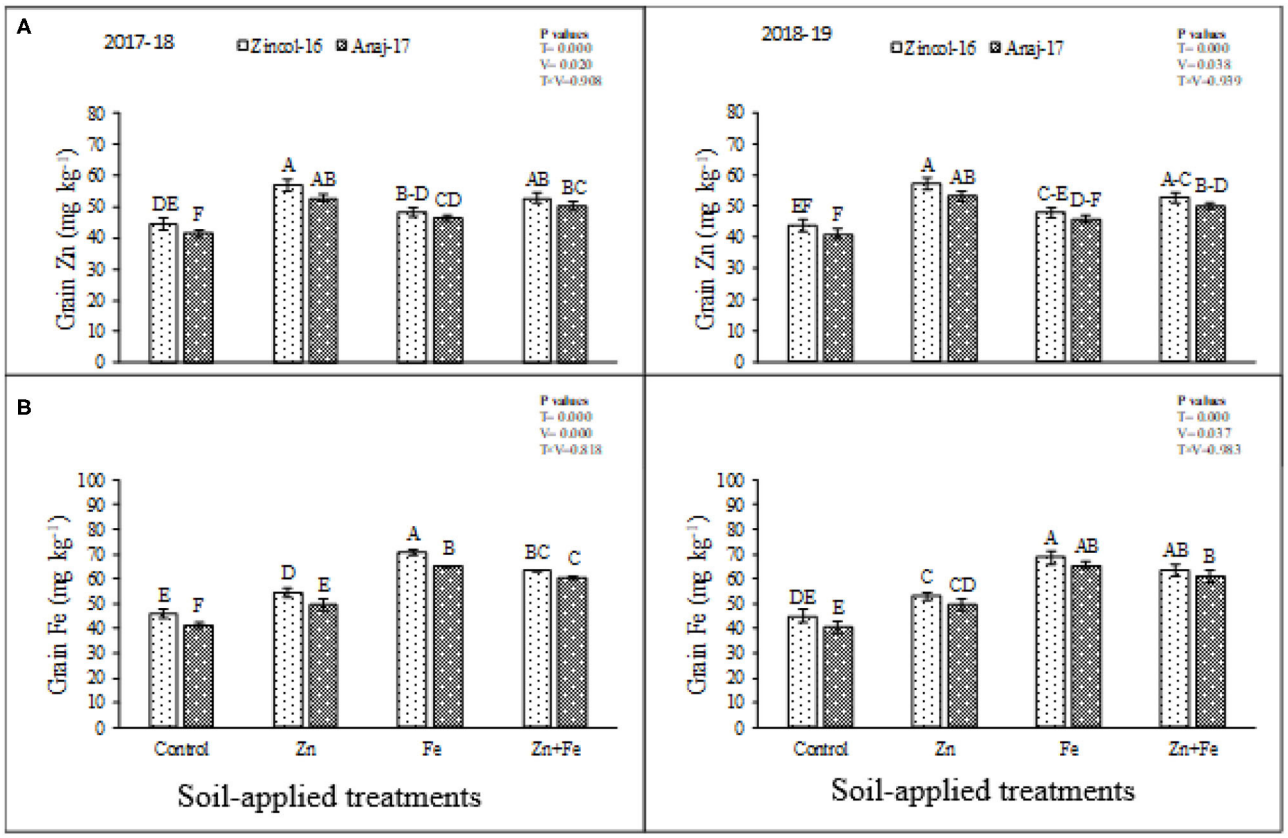

FIGURE 2 | Impact of soil-applied Zn and Fe on Zn **(A)**, and Fe **(B)** contents in grains of wheat cultivars grown during 2017–2018 and 2018–2019 growing seasons. Means sharing the same letter did not differ significantly at $p > 0.05$. Error bars depict the standard error of means.

Starch, Wet Gluten, and Protein Contents

There were significant differences ($p \leq 0.05$) in starch, wet gluten, and proteins concentration among the soil-applied treatments and between the wheat cultivars in the first as well as the second year of experimentation, while their interactive effect was found nonsignificant. Cultivar Anaj-17 synthesized more protein contents under control treatment (**Figure 4A**). Combined application produced the lowest protein contents in the Zincol-16 cultivar. Overall, Anaj-17 performed better regarding protein contents in grains as compared to Zincol-16 in both years of study. Maximum gluten contents were recorded in control, while minimum by combined application of Zn and Fe, which were statistically at par with a sole application of either Zn or Fe (**Figure 4B**). Cultivar Zincol-16 synthesized more gluten contents comparatively than Anaj-16 during 2017 and 2018. Sole application of Fe produced maximum starch concentration in grains while minimum in control. Maximum starch concentration was recorded in Zincol-16, while Anaj-17 accumulated low-starch concentration in their grains. The combined application of Zn and Fe produced more starch contents than the sole application of Zn, while less than the sole application of Fe during both experimental years (**Figure 4C**).

Growth and Yield Parameters

Soil-applied Zn and Fe significantly ($p \leq 0.05$) improved the growth and yield parameters of both wheat cultivars in both seasons of wheat cultivation. The combined application of Zn and Fe at 10 and 12 kg ha^{-1} produced a maximum number of tillers (m^{-2}) (**Table 2**), while the minimum was found in the control treatment. Sole application of Zn and Fe produced 365 and 361 numbers of tillers, respectively, which were statistically at par with each other in the first year of study. Anaj-17 produced a greater number of tillers as compared to Zincol-16 in both years of experimentation. A similar trend was also found in the plant height of both cultivars in response to soil-applied treatments (**Table 2**). Spike length was increased significantly ($p \leq 0.05$) by the soil-applied treatments, and significant variation was also found within the cultivars (**Table 2**). Combined application produced the highest number of spikelets per spike, grains per spike, and 1,000-grain weight (**Table 3**) as compared to sole application of either Zn or Fe, while minimum mean values were found in control throughout the course of the experimentation.

Cultivar Anaj-17 performed better and produced more biological yield, grain yield, and harvest index as compared to Zincol-16, which produced low biological yield, grain yield, and

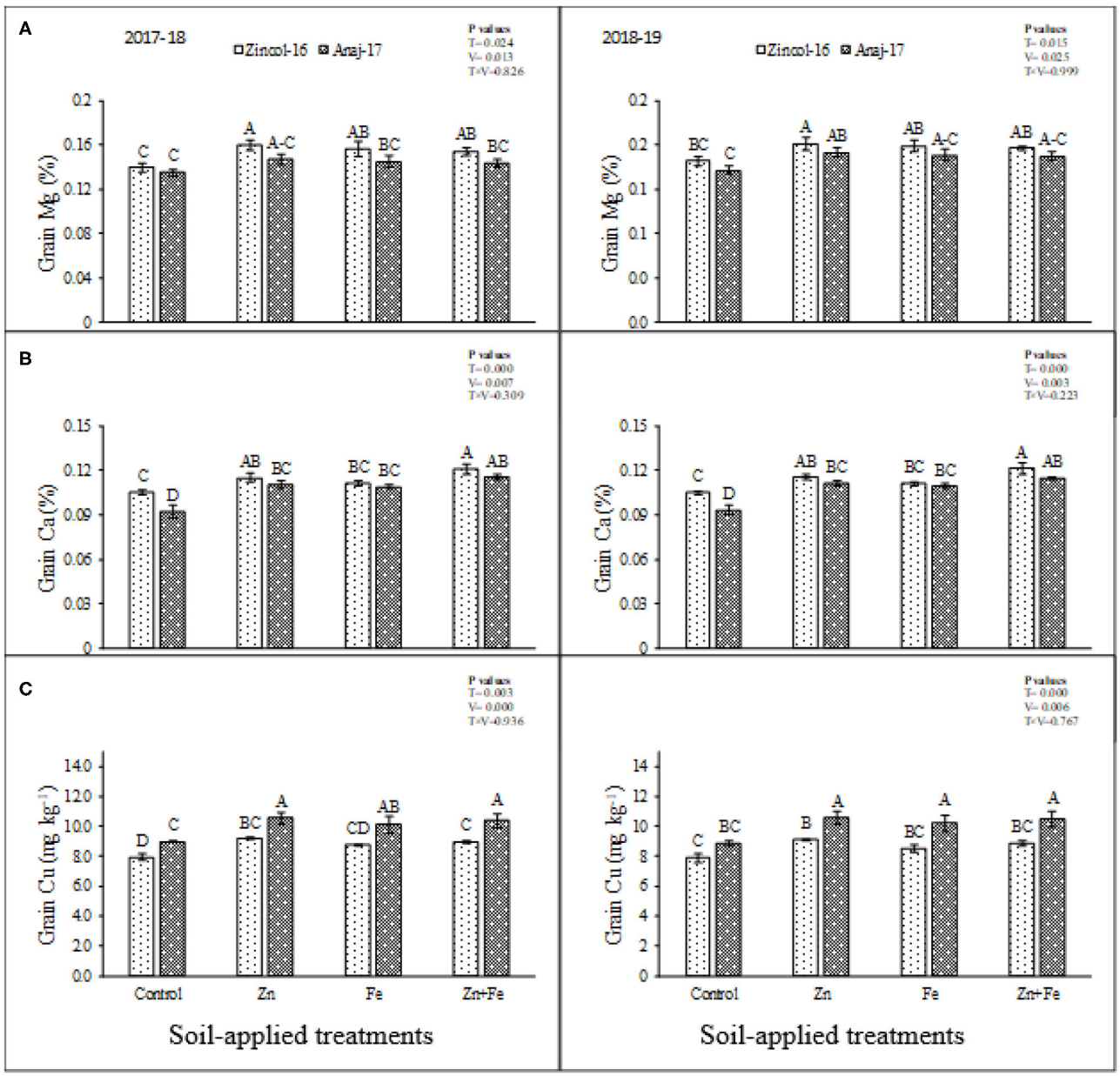

FIGURE 3 | Impact of soil-applied Zn and Fe on Mg **(A)**, Ca **(B)**, and Cu **(C)** contents in grains of wheat cultivars grown during 2017–2018 and 2018–2019 growing seasons. Means sharing the same letter did not differ significantly at $p > 0.05$. Error bars depict the standard error of means.

harvest index (**Table 4**). The combined application of Zn and Fe produced maximum biological yield as compared to other treatments. Sole application of Zn and Fe produced less biomass as compared to combined application, while minimum biomass was produced in control. The highest grain yield was produced by the combined application while the lowest was in control. The sole application of Zn comparatively produced more grain yield than the sole application of Fe. The maximum harvest index was recorded by the combined application while the minimum in control treatment during the first and second years of the experimentation (**Table 4**).

Correlation

Pearson correlation revealed a strong linear relationship among protein and gluten, while the negative correlation with harvest index, grain yield, biological yield, starch, protein, Ca, Mg, Fe, and Zn, while Cu showed a positive correlation with protein and gluten content during the 2017 experimental year. During 2018, biological yield, Cu, grain yield, harvest plus, Fe, Mg, Zn, Ca, and starch showed a linear relationship among them. Similarly, protein and gluten depicted a strong linear relationship among them, while protein and gluten showed a negative correlation with all response variables as shown in **Figure 5**.

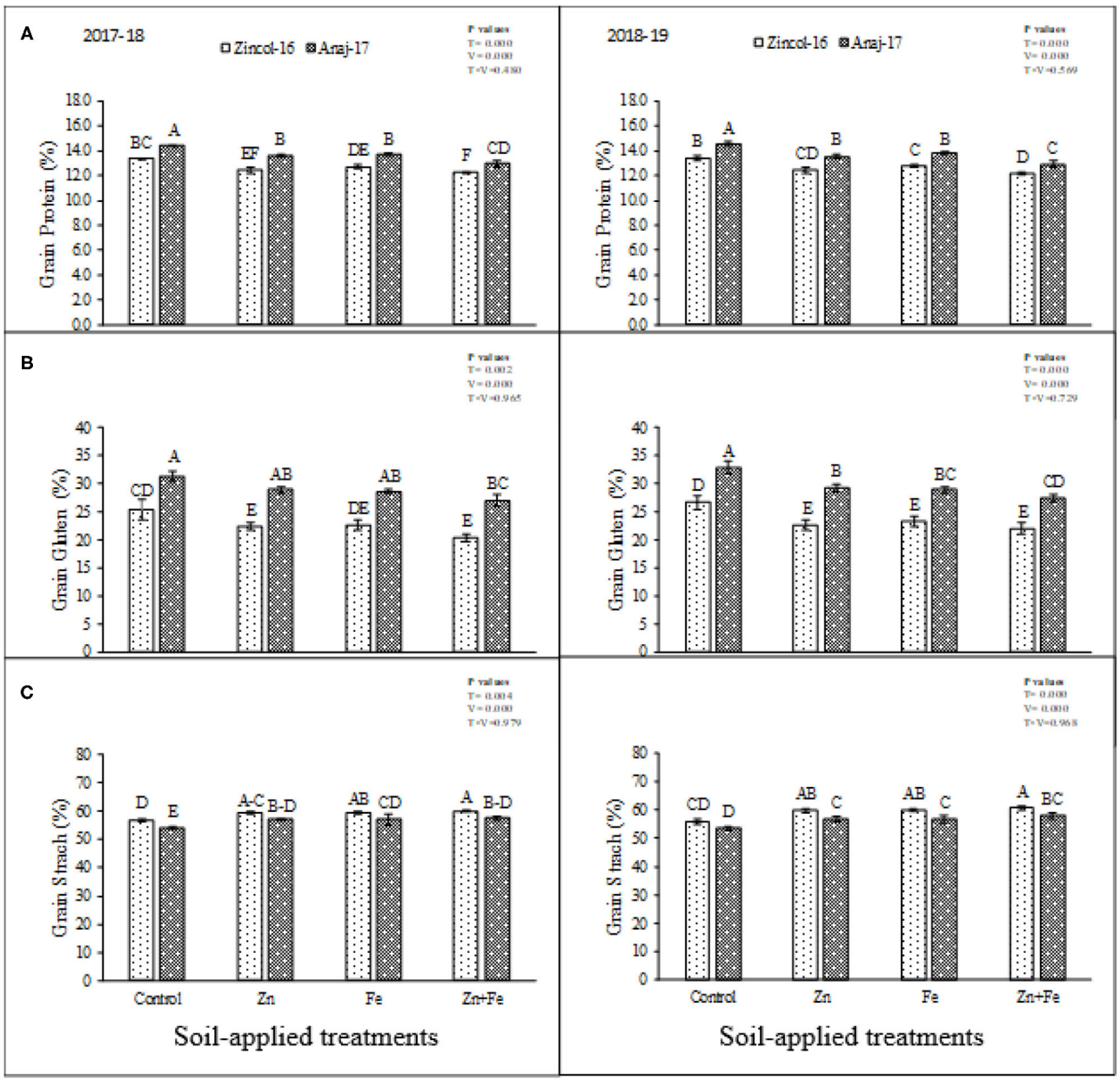

FIGURE 4 | Impact of soil-applied Zn and Fe on grain protein **(A)**, grain gluten **(B)**, and grain starch **(C)** of wheat cultivars grown during 2017-2018 and 2018-2019 growing seasons. Means sharing the same letter did not differ significantly at $p > 0.05$. Error bars depict the standard error of means.

DISCUSSION

This field study explored the effects of soil-applied zinc sulfate and iron sulfate fertilization on crop yield and grain Zn and Fe contents in wheat cultivars, Zincol-16 (Zn enriched) and Anaj-17 (Zn deficient). Micronutrient-deficient soils are increasing due to the frequent growth of exhaustive crops and intensive use of fertilizer, i.e., nitrogen, potassium, and phosphorus (20). The soils having $<0.5\,mg\ kg^{-1}$ DTPA extractable Zn are usually considered as potentially Zn deficient and could be responsive to soil Zn fertilization (44). Rengel (45) stated that calcareous soils are Fe deficient, having high pH. Zn and Fe deficiency is more common in Pakistani soil that has high pH, free $CaCO_3$, and HCO^{-3}, which inhibit the accessibility of Fe and Zn to the plants (16, 19). Based on these criteria, current study soils seemed to be potentially Zn and Fe deficient. Therefore, there was an expectation for enhanced ions contents in grain and yield with soil fertilization of zinc sulfate and iron sulfate.

Mineral accumulation in grains is an imperative indicator for evaluating the capacity of plants to take up the beneficial elements that reveal the biofortification potential of plants. Zn accumulation in grains of cultivars by soil applied treatments

TABLE 2 | Impact of soil-applied zinc ($ZnSO_4$) at 10 kg ha^{-1} and iron ($FeSO_4$) at 12 kg ha^{-1} on a number of tillers, plant height, and spike length of wheat varieties cultivated during 2017-2018 and 2018-2019 growing seasons ($n = 3$).

Treatments	Number of tillers (m^{-2})						Plant height (cm)						Spike length (cm)					
	2017–2018			2018–2019			2017–2018			2018–2019			2017–2018			2018–2019		
	Zincol-16	Anaj-17	Mean (T)	Zincol-16	Anaj-17	Mean (T)	Zincol-16	Anaj-17	Mean (T)	Zincol-16	Anaj-17	Mean (T)	Zincol-16	Anaj-17	Mean (T)	Zincol-16	Anaj-17	Mean (T)
Control	339	350	344C	331	360	345C	101.9	98.8	100.3C	101.6	99	100.3C	9.5	9.7	9.6C	9.6	9.9	9.7C
Sole Zn	358	372	365B	362	379	371B	106	103.3	104.6B	105.7	103.2	104.4B	10.1	10.6	10.3AB	10.1	10.7	10.4AB
Sole Fe	354	368	361B	359	371	365B	104.7	103	103.8B	104.7	102.7	103.7B	9.9	10.3	10.1 B	10	10.4	10.2B
Zn + Fe	367	381	374A	369	387	378A	107.9	105.3	106.6A	107.2	105.1	106.2A	10.4	10.9	10.7 A	10.5	10.8	10.6A
Mean (C)	355 B	368A		355B	374A		105.1A	102.6B		104.8A	102.5B		10.0 B	10.4A		10.0B	10.5A	
LSD	$T = 4.79$; $C = 3.39$; T×C = ns			$T = 5.65$; $C = 4.0$; T×C = ns			$T = 1.80$; $C = 1.27$; T×C = ns			$T = 1.74$; $C = 1.23$; T×C = ns			$T = 0.36$; $C = 0.25$; T×C = ns			$T = 0.27$; $C = 0.19$; T×C = ns		

Different letters within the same column indicate statistically significant differences at $p \leq 0.05$, T, treatment; C, cultivar; T × C, interaction; ns, nonsignificant.

TABLE 3 | Impact of soil-applied zinc ($ZnSO_4$) at 10 kg ha^{-1} and iron ($FeSO_4$) at 12 kg ha^{-1} on number of spikelets per spike, number of grains per spike, and 1,000-grain weight of wheat varieties cultivated during 2017–2018 and 2018–2019 growing seasons ($n = 3$).

Treatments	Number of spikelet's per spike						Number of grains per spike						1,000-grain weight (g)					
	2017–2018			2018–2019			2017–2018			2018–2019			2017–2018			2018–2019		
	Zincol-16	Anaj-17	Mean (T)	Zincol-16	Anaj-17	Mean (T)	Zincol-16	Anaj-17	Mean (T)	Zincol-16	Anaj-17	Mean (T)	Zincol-16	Anaj-17	Mean (T)	Zincol-16	Anaj-17	Mean (T)
Control	16	18	17C	17	18	18C	41	44	43C	42	44	43C	32.4	34.7	33.5D	32.7	34.9	33.8D
Sole Zn	18	19	18B	18	19	19B	47	49	48B	48	49	48AB	36.8	37.8	37.3B	37.1	38.2	37.7B
Sole Fe	18	19	18B	18	19	19B	46	48	47B	47	47	47B	35.5	36.2	35.9C	35.8	36.4	36.1C
Zn + Fe	19	20	20A	19	20	20A	49	51	50A	49	51	50A	38.1	39.2	38.6A	38.4	39.7	39.0A
Mean (C)	18B	19A		18B	19A		46B	48A		46B	48A		35.7B	37.0A		36.0B	37.3A	
LSD	$T = 0.65$; $C = 0.46$; T × C = ns			$T = 0.68$; $C = 0.48$; T × C = ns			$T = 1.27$; $C = 0.89$; T × C = ns			$T = 1.82$; $C = 1.29$; T × C = ns			$T = 1.03$; C = 0.73; T × C = ns			$T = 1.10$; C = 0.78; T × C = ns		

Different letters within the same column indicate statistically significant differences at $p \leq 0.05$, T, treatment; C, cultivar; T × C, interaction; ns, nonsignificant.

TABLE 4 | Impact of soil-applied zinc ($ZnSO_4$) at 10 kg ha^{-1} and iron ($FeSO_4$) at 12 kg ha^{-1} on biological yield, grain yield, and harvest index of wheat varieties cultivated during 2017–2018 and 2018–2019 growing seasons ($n = 3$).

Treatments	Biological yield (t ha^{-1})						Grain yield (t ha^{-1})						Harvest index (%)					
	2017–2018			2018–2019			2017–2018			2018–2019			2017–2018			2018–2019		
	Zincol-16	Anaj-17	Mean (T)	Zincol-16	Anaj-17	Mean (T)	Zincol-16	Anaj-17	Mean (T)	Zincol-16	Anaj-17	Mean (T)	Zincol-16	Anaj-17	Mean (T)	Zincol-16	Anaj-17	Mean (T)
Control	11	11.1	11.1C	11.2	11.5	11.3C	3.2	3.59	3.39D	3.27	3.62	3.45D	28.8	32.7	30.7D	29.4	31.6	30.5C
Sole Zn	11.9	12.1	12.0B	12.2	12.5	12.3AB	3.74	4.12	3.93B	3.8	4.17	3.98B	30.9	34.7	32.8B	31.4	33.4	32.4AB
Sole Fe	11.7	12	11.9B	12	12.4	12.2B	3.61	3.93	3.77C	3.67	4.01	3.84C	30.2	33.5	31.8C	30.7	32.3	31.5BC
Zn + Fe	12.1	12.4	12.3A	12.4	12.7	12.5A	3.98	4.29	4.13A	4.03	4.35	4.19A	32.2	35.4	33.8A	32.6	34.3	33.5A
Mean (C)	11.7B	11.9A		11.9B	12.3A		3.63B	3.98A		3.69B	4.04A		30.5B	34.1A		31.0B	32.9A	
LSD	$T = 0.13$; $C = 0.09$; T×C = ns			$T = 0.13$; $C = 0.09$; T×C = ns			$T = 0.10$; $C = 0.07$; T×C = ns			$T = 0.07$; $C = 0.14$; T×C = ns			$T = 0.78$; $C = 0.55$; T×C = ns			$T = 1.19$; $C = 0.84$; T×C = ns	

Different letters within the same column indicate statistically significant differences at $p \leq 0.05$, T, treatment; C, cultivar; T × C, interaction; ns, nonsignificant.

was significantly improved, and cultivar Zincol-16 was found more efficient in Zn accumulation as compared to Anaj-17 (**Figure 2A**). Iron (Fe) accumulation also was significantly improved by soil-applied treatments. Maximum improvement was recorded by sole application of Fe at 12 kg ha^{-1}. In the case of cultivars, Zincol-16 accumulated higher content of Fe in grains as compared to Anaj-17 (**Figure 2B**). Our results were in line with Zou et al. (39); they stated that soil application of Zn increased Zn contents in wheat grains. The present study also was supported by Zulfiqar et al. (1), who reported Fe soil application increased Fe contents in wheat grains. These results were supported by Ramzan et al. (5), who reported Zn and Fe soil application increased Cu, Mg, and Ca contents in wheat grains. Imtiaz et al. (46) stated that Zn foliage applied had an adverse effect on Cu contents in wheat grains.

Zn and Fe contribute to photosynthesis, chlorophyll formation, metabolism of starch formation, and enzyme carbonic anhydrase, accelerating carbohydrate formation. The maximum concentrations of Zn and Fe are necessary to accumulate suitable carbohydrate contents (47, 48). There were significant differences in starch concentration among the soil-applied treatments and between the wheat cultivars. Our outcomes were supported by Kinaci and Kinaci (49), who reported that Zn soil supplementation significantly increased the starch in barley. Mousavi et al. (50) also reported that Zn soil applied markedly enhanced the starch in the potato. Our outcomes were in contrast with Keram et al. (51), who reported that soil-applied Zn significantly increased wet gluten. Protein contents were also significantly reduced by soil-applied treatments. Ramzan et al. (5) noted that soil-applied Zn and Fe significantly decreased the protein content in spring wheat. Mugenzi et al. (52) reported that Fe and Zn application, either sole or combined, showed a nonsignificant effect on protein content.

The combined application significantly produced maximum growth and yield attributes in wheat cultivars. A number of tillers have key importance in achieving the final yield in a wheat crop. The combined application of Zn and Fe at 10 and 12 kg ha^{-1} produced a maximum number of tillers per unit area. Anajs-17 produced a greater number of tillers as compared to Zincol-16 (**Table 2**). Our findings are also supported by Jalal et al. (53), who stated that the combined application of Zn and Fe significantly enhanced the number of tillers per unit area. They also reported that a number of productive tillers are very important in determining the yield in cereal crops. Outcomes of the present experimentation are also in line with Boorboori et al. (54), who stated that application of Zn and Fe through soil incorporation has a positive influence on tillers, and more tillers were attained by the soil-applied Zn and Fe. Plant height is one of the main parameters that determine the final yield of a crop. Plant height is a function of the combined effect of both genetic and environmental factors. Significant differences were observed in plant height as a result of combined application of Zn and Fe. Combined application produced the highest plant and spike length (**Table 2**) in wheat plants. More height of plants might be due to the involvement of Zn and Fe in cell division, cell expansion, activities of meristematic tissues, and photosynthetic activities.

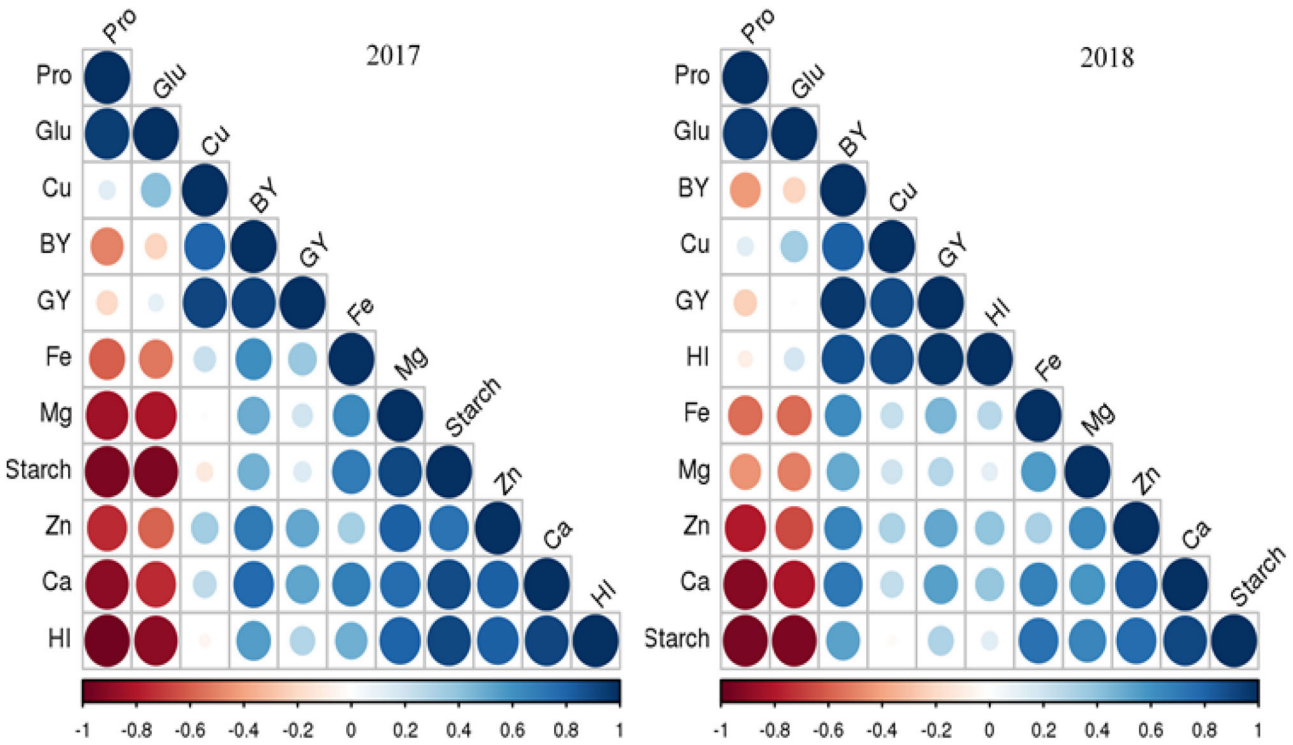

FIGURE 5 | Pearson correlations among different yield attributes and grain quality traits of wheat cultivars grown under soil-applied Zn and Fe.

In the current experimentation, the combined application of Zn and Fe is responsible for a maximum number of grains per spike, 1,000-grain weight, and spikelets per spike (**Table 3**). Zayed et al. (55) reported similar findings that 1,000-kernel weight in rice was significantly enhanced by the mixed application of Zn and Fe as compared to sole application. Bameri et al. (56) concluded from their experimentation that the application of Zn significantly enhanced the grain numbers per spike, productive tillers, 1,000-grain weight, and spike length. Hassan et al. (57) found the positive impact of Zn on the growth parameters of the wheat crop. They stated that the application of Zn improved the Zn dietary standards, more than 1,000-grain weight, the maximum number of grains per spike, as well as spikelets. This, perchance, is because of the fact that Zn is an important element and shows a key role in regulating the auxin concentration throughout the plant body, biosynthesis of indole acetic acid. Zn also controls the physiological and biochemical processes and stimuli for the initiation of primordia regarding reproductive growth. It has a positive influence on the translocation of required metabolites from the source to the sink of plants. In the case of Fe, it is the component of the photosynthetic apparatus as well as its rate and formation of chlorophyll. The application of Fe significantly improved the yield and its contributing factors. It is also reported that enhanced photosynthesis and respiration rates, more crop growth, and improved physiological and biochemical processes were observed by the application of Fe, Zn, and Mn (58). Rehman et al. (31) and Farooq et al. (59) also reported that the application of minerals either alone or in combination with growth promoters improved the growth attributes of crops. Tabaxi et al. (60) stated that the application of various fertilizers or mineral elements improved the agronomic and quality characteristics of crops.

Maximum grain and biological yield, and harvest index were observed by the combined application of Zn and Fe in the current study (**Table 4**). This improvement in the biological and economical yield is due to the fact that zinc has a catalytic and constructive role in the physiological and biochemical activities and in respiration and photosynthesis processes and thus resulting in higher economical yield. Zain et al. (61) concluded that supplementation of nutrients, particularly microelements, is responsible for improved harvest index, biological and grain yields linked with more tillers, number of grains per spike, and 1,000-grain weight. The application of inorganic fertilizers and mineral elements is considered a helpful practice in maintaining crop productivity with improved soil fertility to achieve maximum plant growth and economical yield under stressful conditions (62, 63). The conversion of nitrates to ammonia is also triggered by the Zn that ultimately improves the economical out of a wheat crop. In the present experimentation, the grain yield was also improved by the application of Fe at 10 kg ha^{-1} because Fe is useful for translocation of assimilates and photosynthates from the source toward the sink, particularly grains in the case of wheat. Moreover, Fe is also essential for optimum rates of respiration and photosynthesis that results in maximum accumulation of biomass. Harvest index (HI) is a sign regarding the translocation and partitioning of photosynthates

and dry matter toward reproductive structure like grains in the case of a wheat crop. The findings of the current experimentation are supported by previous studies that the application of various doses of Zn and Fe significantly improved the harvest index of wheat (53) and maize crops (64).

CONCLUSION

Cultivar Zincol-16 produced maximum ions concentration, starch contents, and wet gluten as compared to Anaj-17. Yield and growth attributes, especially the number of tillers, plant height, number of grains, and 1,000-grain weight, were also significantly improved by the combined application of Zn and Fe as compared to the sole application of Zn or Fe. The combined application of Zn and Fe produced the highest biological and grain yield. Cultivar Anaj-17 was found more responsive regarding growth and yield attributes comparatively. Findings of the present experimentation explored that combined application of Zn and Fe at 10 and 12 kg ha^{-1}, respectively, produced good-quality grains with a maximum productivity of bread wheat cultivars grown under calcareous soil.

DATA AVAILABILITY STATEMENT

The original contributions presented in the study are included in the article/supplementary material, further inquiries can be directed to the corresponding author/s.

AUTHOR CONTRIBUTIONS

MBH, YR, and SK proposed the idea and funding was secured by Z-HD, AA-H, and AA. The experiments were conducted by MBH, MN, SR, HS, JA, and MH, as well as data collection. The first draft was prepared by SK, MBH, DI, SB, NZ, NR, and SI. The draft was finalized after careful review by JA, SB, SK, and MH. SK and Z-HD submitted the final draft as corresponding authors. All authors contributed to the article and approved the submitted version.

FUNDING

This work was supported by the Key Realm R&D Program of Guangdong Province (Nos. 2020B1111350002 and 2020B0202080002), the special project in key areas of Guangdong Province Ordinary Universities (No. 2020ZDZX1003), the Guangdong Provincial Special Fund for Modern Agriculture Industry Technology Innovation Teams (No. 2019KJ140), and the National Natural Science Foundation of China (No. 21407155).

ACKNOWLEDGMENTS

The authors acknowledge the Wheat Research Institute, working as a subpart of Ayub Agricultural Research Institute, Faisalabad-Pakistan, for providing the land to conduct the experiment. The authors extend their appreciation to the Researchers Supporting Project number (RSP-2021/219), King Saud University, Riyadh, Saudi Arabia.

REFERENCES

1. Zulfiqar U, Maqsood M, Hussain S, Anwar-ul-Haq M. Iron nutrition improves productivity, profitability, and biofortification of bread wheat under conventional and conservation tillage systems. *J Soil Sci Plant Nutr.* (2020) 13:1–3. doi: 10.1007/s42729-020-00213-1
2. Velu G, Ortiz-Monasterio I, Cakmak I, Hao Y, Singh RP. Biofortification strategies to increase grain zinc and iron concentrations in wheat. *J Cereal Sci.* (2014) 59:365–72. doi: 10.1016/j.jcs.2013.09.001
3. Zhao A, Wang B, Tian X, Yang X. Combined soil and foliar ZnSO4 application improves wheat grain Zn concentration and Zn fractions in a calcareous soil. *Eur J Soil Sci.* (2019) 71:681–94. doi: 10.1111/ejss.12903
4. Cakmak I, Kalayci M, Kaya Y, Torun AA, Aydin N, Wang Y, et al. Biofortification and localization of zinc in wheat grain. *J Agric Food Chem.* (2010) 58:9092–102. doi: 10.1021/jf101197h
5. Ramzan Y, Hafeez MB, Khan S, Nadeem M, Batool S, Ahmad J. Biofortification with Zinc and Iron improves the grain quality and yield of wheat crop. *Int J Plant Prod.* (2020) 14:501–10. doi: 10.1007/s42106-020-00100-w
6. Prasad AS, Bao B, Beck FWJ, Kucuk O, Sarkar FH. Antioxidant effect of zinc in humans. *Free Radic Biol Med.* (2004) 37:1182–90. doi: 10.1016/j.freeradbiomed.2004.07.007
7. Levenson CW, Morris D. Zinc and neurogenesis: making new neurons from development to adulthood. *Adv Nutr.* (2011) 2:96–100. doi: 10.3945/an.110.000174
8. Hotz C, Brown KH. Contents international zinc nutrition consultative group (IZiNCG) technical document. *Food Nutr Bull.* (2004) 25:S94–S200. Available online at: https://archive.unu.edu/unupress/food/fnb25-1s-IZiNCG.pdf
9. Black RE, Allen LH, Bhutta ZA, Caulfield LE, de Onis M, Ezzati M, et al. Maternal and child undernutrition: global and regional exposures and health consequences. *Lancet.* (2008) 371:243–60. doi: 10.1016/S0140-6736(07)61690-0
10. Bouis HE. Plant breeding: a new tool for fighting micronutrient malnutrition. *J Nutr.* (2002) 132:491S−4S. doi: 10.1093/jn/132.3.491S
11. Iqbal MA, Hussain I, Siddiqui MH, Ali E. Ahmad Z. Probing profitability of irrigated and rainfed bread wheat (*Triticum aestivum* L) crops under foliage applied sorghum and moringa extracts in Pakistan. *Custos e Agronegocio.* (2018) 14:2–16. Available online at: https://www.custoseagronegocioonline.com.br/
12. FAO. *Crop Prospects and Food Situation - Quarterly Global Report No. 1, March 2020*. Rome: FAO. (2020). doi: 10.4060/ca8032en
13. GOP Agriculture. Pakistan Economic Survey 2019-20. Islamabad: Government of Pakistan (2019). Available online at: https://www.finance.gov.pk/survey/chapter_20/02_Agriculture.pdf
14. Raza A, Mehmood SS, Shah T, Zou X, Yan L. Applications of molecular markers to develop resistance against abiotic stresses in wheat. In: Hasanuzzaman M, Nahar K, Hossain M, editors. *Wheat Production in Changing Environments*. Singapore: Springer. (2019) p. 393–420. doi: 10.1007/978-981-13-6883-7_15
15. Khaled AAA, Reda OI, Yaser HM, Esmail SM. El Sabagh A. Anatomical, biochemical and physiological changes in some Egyptian wheat cultivars inoculated with Puccinia graminis fSp. *Tritici Fresenius Environ Bull.* (2018) 27:296–305. Available online at: http://www.scopus.com/inward/record.url?eid=2-s2.0-85050878763&partnerID=MN8TOARS
16. Akhtar S, Bangash N, Iqbal MS, Muhammad AA, Habibullah N, Sabir H, et al. Muhammad A. Comparison of foliar and soil applications for correction of iron deficiency in peanut (*Arachis Hypogaea* L). *Pakistan J Bot.* (2019) 51:1121–7. doi: 10.30848/PJB2019-3(13)
17. Vose PB. Iron nutrition in plants: a world overview. *J Plant Nutr.* (1982) 5:233–49. doi: 10.1080/01904168209362954

18. Zhao A. qing, Tian X hong, Cao Y xian, Lu X chun, Liu T. Comparison of soil and foliar zinc application for enhancing grain zinc content of wheat when grown on potentially zinc-deficient calcareous soils. *J Sci Food Agric.* (2014) 94:2016–22. doi: 10.1002/jsfa.6518
19. Imtiaz M, Rashid A, Khan P, Memon MY, Aslam M. The role of micronutrients in crop production and human health. *Pakistan J Bot.* (2010) 42:2565–78. Available online at: http://www.pakbs.org/pjbot/PDFs/42(4)/PJB42(4)2565.pdf
20. Salim N, Raza A. Nutrient use efficiency (NUE) for sustainable wheat production: a review. *J Plant Nutr.* (2020) 43:297–315. doi: 10.1080/01904167.2019.1676907
21. Marschner H. *Mineral Nutrition of Higher Plants*. 2nd ed. San Diego, CA: Academic Press (1995).
22. Rehman A, Farooq M, Ozturk L, Asif M, Siddique KHM. Zinc nutrition in wheat-based cropping systems. *Plant Soil.* (2018) 422:283–315. doi: 10.1007/s11104-017-3507-3
23. Pandey N, Pathak GC, Sharma CP. Zinc is critically required for pollen function and fertilisation in lentil. *J Trace Elem Med Biol.* (2006) 20:89–96. doi: 10.1016/j.jtemb.2005.09.006
24. Cakmak I. Tansley Review No. 111. *New Phytol.* (2000) 146:185–205. doi: 10.1046/j.1469-8137.2000.00630.x
25. Graham RD. Effects of nutrient stress on susceptibility of plants to disease with particular reference to the trace elements. *Adv Bot Res.* (1983) 10:221–76. doi: 10.1016/S0065-2296(08)60261-X
26. Soetan KO, Olaiya CO, Oyewole OE. The importance of mineral elements for humans, domestic animals and plants: a review. *African J Food Sci.* (2010) 4:200–222. Available online at: https://academicjournals.org/article/article1380713863_Soetan%20et%20al.pdf
27. Hsu WP, Miller GW. Iron in relation to aconitate hydratase activity in Glycine max. *Merr BBA Enzymol.* (1968) 151:711–3. doi: 10.1016/0005-2744(68)90027-2
28. Coulombe BA, Chaney RL, Wiebold WJ. Bicarbonate directly induces iron chlorosis in susceptible soybean cultivars. *Soil Sci Soc Am J.* (1984) 48:1297–301. doi: 10.2136/sssaj1984.03615995004800060019x
29. Makawita GIPS, Wickramasinghe I, Wijesekara I. Using brown seaweed as a biofertilizer in the crop management industry and assessing the nutrient upliftment of crops. *Asian J Agric Biol.* (2021) 29:1–10. doi: 10.35495/ajab.2020.04.257
30. Hussain MU, Saleem MF, Hafeez MB, Khan S, Hussain S, Ahmad N, Ramzan Y, Nadeem M. Impact of soil applied humic acid, zinc and boron supplementation on the growth, yield and zinc translocation in winter wheat. *Asian J Agric Biol.* (2021) 30:202102080. doi: 10.35495/ajab.2021.02.080
31. Rehman A, Hassan F, Qamar R. Rehman AU. Application of plant growth promoters on sugarcane (*Saccharum officinarum* L) budchip under subtropical conditions. *Asian J Agric Biol.* (2021) 2:202003202. doi: 10.35495/ajab.2020.03.202
32. Cakmak I. Enrichment of cereal grains with zinc : agronomic or genetic biofortification? *Plant Soil.* (2008) 302:1–17. doi: 10.1007/s11104-007-9466-3
33. Aciksoz SB, Yazici A, Ozturk L, Cakmak I. Biofortification of wheat with iron through soil and foliar application of nitrogen and iron fertilizers. *Plant Soil.* (2011) 349:215–25. doi: 10.1007/s11104-011-0863-2
34. Wang J, Mao H, Zhao H, Huang D, Wang Z. Different increases in maize and wheat grain zinc concentrations caused by soil and foliar applications of zinc in loess plateau, China. *F Crop Res.* (2012) 135:89–96. doi: 10.1016/j.fcr.2012.07.010
35. Yilmaz A, Ekiz H, Torun B, Gültekin I, Karanlik S, Bagci SA, et al. Effect of different zinc application methods on grain yield and zinc concentration in wheat cultivars grown on zinc-deficient calcareous soils. *J Plant Nutr.* (1997) 20:461–71. doi: 10.1080/01904169709365267
36. Rengel Z, Batten GD, Crowley DE. Agronomic approaches for improving the micronutrient density in edible portions of field crops. *F Crop Res.* (1999) 60:27–40. doi: 10.1016/S0378-4290(98)00131-2
37. Chattha MU, Hassan MU, Khan I, Chattha MB, Mahmood A, Nawaz M, et al. Biofortification of wheat cultivars to combat zinc deficiency. *Front Plant Sci.* (2017) 8:1–8. doi: 10.3389/fpls.2017.00281
38. Pahlavan RP-R, Pessarakli M. Response of Wheat plants to zinc, iron, and manganese applications and uptake and concentration of zinc, iron, and manganese in wheat grains. *Commun Soil Sci Plant Anal.* (2009) 40:1322–32. doi: 10.1080/00103620902761262
39. Zou CQ, Zhang YQ, Rashid A, Ram H, Savasli E, Arisoy RZ, et al. Biofortification of wheat with zinc through zinc fertilization in seven countries. *Plant Soil.* (2012) 361:119–30. doi: 10.1007/s11104-012-1369-2
40. Estefan G, Sommer R, Ryan J. *Methods of Soil, Plant, and Water Analysis : A manual for the West Asia and North Africa Region*. 3rd ed. Beirut, Lebanon: International Center for Agricultural Research in the Dry Areas (ICARDA) (2013). p. 65–108. Available online at: https://repo.mel.cgiar.org/handle/20.500.11766/7512
41. Rashid A. *Mapping Zinc Fertility of Soils Using Indicator Plants and Soil Analyses* (1986).
42. Edwards MA, Osborne BG, Henry RJ. Effect of endosperm starch granule size distribution on milling yield in hard wheat. *J Cereal Sci.* (2008) 48:180–92. doi: 10.1016/j.jcs.2007.09.001
43. Bradford MM. A rapid and sensitive method for quantitation or microgram quantities of protein nitiling the principle protein dychinding. *Anal Biochem.* (1976) 72:248–54. doi: 10.1016/0003-2697(76)90527-3
44. Rashid A, Ram H, Zou CQ, Rerkasem B, Duarte AP, Simunji S, et al. Effect of zinc-biofortified seeds on grain yield of wheat, rice, and common bean grown in six countries. *J Plant Nutr Soil Sci.* (2019) 182:791–804. doi: 10.1002/jpln.201800577
45. Rengel Z. Availability of Mn, Zn and Fe in the rhizosphere. *J Soil Sci Plant Nutr.* (2015) 15:397–409. doi: 10.4067/S0718-95162015005000036
46. Imtiaz M, Alloway BJ, Shah KH, Siddiqui SH, Memon MY, Aslam M, et al. Zinc nutrition of wheat: II: interaction of zinc with other trace elements. *Asian J Plant Sci.* (2003) 2:156–60. doi: 10.3923/ajps.2003.156.160
47. Marschner P. *Marschner's Mineral Nutrition of Higher Plants*. 3rd ed. Elsevier Inc (2011).
48. Sturikova H, Krystofova O, Huska D, Adam V. Zinc, zinc nanoparticles and plants. *J Hazard Mater.* (2018) 349:101–10. doi: 10.1016/j.jhazmat.2018.01.040
49. Kinaci G. Kinaci E. Effect of zinc application on quality traits of barley in semi arid zones of Turkey. *Plant Soil Environ.* (2005) 51:328–34. doi: 10.17221/3594-PSE
50. Mousavi SR, Galavi M, Ahmadvand G. Effect of zinc and manganese foliar apllication on yioueld, quality and enrichment on potato (*Solanum Tuberosom L.*). *Asian J. Plant Sci.* (2007)1256–1260. doi: 10.3923/ajps.2007.1256.1260
51. Keram KS, Sharma BL, Sawarkar SD. Impact of Zn application on yield, quality, nutrients uptake and soil fertility in a medium deep black soil (vertisol). *Int J Sci, Environ Technol.* (2012) 1:563–71. Available online at: https://www.ijset.net/journal/69.pdf
52. Mugenzi I, Yongli D, Ngnadong WA, Dan H, Niyigaba E, Twizerimana A, et al. Effect of combined zinc and iron application rates on summer maize yield, photosynthetic capacity and grain quality. *Int J Agron Agric Res.* (2018) 12:36–46. Available online at: https://www.researchgate.net/profile/Niyigaba-Etienne/publication/328281327_Effect_of_combined_zinc_and_iron_application_rates_on_summer_maize_yield_photosynthetic_capacity_and_grain_quality/links/5bc42aab299bf1004c5f477a/Effect-of-combined-zinc-and-iron-application-rates-on-summer-maize-yield-photosynthetic-capacity-and-grain-quality.pdf
53. Jalal A, Shah S, Teixeira Filho MCM, Khan A, Shah T, Hussain Z, et al. Yield and phenological indices of wheat as affected by exogenous fertilization of Zinc and Iron. *Rev Bras Ciências Agrárias Brazilian J Agric Sci.* (2020) 15:1–8. doi: 10.5039/agraria.v15i1a7730
54. Boorboori MR, Eradatmand Asli D. Tehrani MM. Effect of micronutrient application by different methods on yield, morphological traits and grain protein percentage of barley (*Hordeum Vulgare L*) in greenhouse conditions. *Rev Cient UDO Agric.* (2012) 12:128–35. Available online at: http://www.bioline.org.br/pdf?cg12015
55. Zayed BA, Salem AKM. El-Sharkawy HM. Effect of different micronutrient treatments on rice (*Oriza sativa* L) growth and yield under saline soil conditions. *World J Agri Sci.* (2011) 7:179–84. Available online at: https://www.idosi.org/wjas/wjas7(2)/12.pdf
56. Bameri M, Abdolshahi R, Mohammadi-Nejad G, Yousefi K, Tabatabaie SM. Effect of different microelement treatment on wheat (*Triticum aestivum*) growth and yield. *Int Res J Applied and Basic Sci.* (2012) 3:219–23. Available online at: https://www.semanticscholar.org/paper/

Effect-of-different-microelement-treatment-on-wheat-Bameri-Abdolshahi/5bf7d30a012312cbf8e674a2dea490230faa0e3c
57. Hassan MU, Chattha MU, Ullah A, Khan I, Qadeer A, Aamer M, et al. Agronomic biofortification to improve productivity and grain zn concentration of bread wheat. *Int J Agri Bio.* (2019) 21:615–20. doi: 10.17957/IJAB/15.0936
58. Zeidan MS, Mohamed MF, Hamouda HA. Effect of Foliar Fertilization of Fe, Mn and Zn on Wheat Yield and Quality in Low Sandy Soils Fertility. *World J Agri Sci.* (2010) 6:696–9. Available online at: https://citeseerx.ist.psu.edu/viewdoc/download?doi=10.1.1.415.3543&rep=rep1&type=pdf
59. Farooq O, Ali M, Sarwar N, Rehman A, Iqbal MM, Naz T, et al. Foliar applied brassica water extract improves the seedling development of wheat and chickpea. *Asian J Agric Biol.* (2021) 6:696–9. doi: 10.35495/ajab.2020.04.219
60. Tabaxi I, Zisi C, Karydogianni S, Folina AE, Kakabouki I, Kalivas A, Bilalis D. Effect of organic fertilization on quality and yield of oriental tobacco (*Nicotiana tabacum* L.) under mediterranean conditions. *Asian J Agric Biol.* (2021) 60:1–7. doi: 10.35495/ajab.2020.05.274
61. Zain M, Khan I, Qadri RWA, Ashraf U, Hussain S, Minhas S, et al. Foliar application of micronutrients enhances wheat growth, yield and related attributes. *Amer J Plant Sci.* (2015) 6:864–9. doi: 10.4236/ajps.2015.67094
62. Zahid N, Ahmed MJ, Tahir MM, Maqbool M, Shah SZA, Hussain SJ, Khaliq A, Rehmani MIA. Integrated effect of urea and poultry manure on growth, yield and postharvest quality of cucumber (*Cucumis sativus* L.). *Asian J Agric Biol.* (2021) 62:1–9. doi: 10.35495/ajab.2020.07.381
63. Safdar ME, Aslam A, Qamar R, Ali A, Javaid MM, Hayyat MS, Raza A. Allelopathic effect of prickly chaff flower (*Achyranthes aspera* L.) used as a tool for managing noxious weeds. *Asian J Agric Biol.* (2021) 3. doi: 10.35495/ajab.2020.06.370
64. Anwar Z, Basharat Z, Hafeez MB, Khan S, Zahra N, Rafique Z, Maqsood M. Biofortification of maize with zinc and iron not only enhances crop growth but also improves grain quality. *Asian J Agric Biol.* (2021) 64:202102079. doi: 10.35495/ajab.2021.02.079

Conflict of Interest: The authors declare that the research was conducted in the absence of any commercial or financial relationships that could be construed as a potential conflict of interest.

Publisher's Note: All claims expressed in this article are solely those of the authors and do not necessarily represent those of their affiliated organizations, or those of the publisher, the editors and the reviewers. Any product that may be evaluated in this article, or claim that may be made by its manufacturer, is not guaranteed or endorsed by the publisher.

frontiers in Nutrition

ORIGINAL RESEARCH
published: 18 January 2022
doi: 10.3389/fnut.2021.809783

Biofortified Wheat Increases Dietary Zinc Intake: A Randomised Controlled Efficacy Study of Zincol-2016 in Rural Pakistan

Nicola M. Lowe[1], Mukhtiar Zaman[2], Muhammad Jaffar Khan[3†], Anna K. M. Brazier[1], Babar Shahzad[3], Ubaid Ullah[3], Gul Khobana[4], Heather Ohly[1], Martin R. Broadley[5], Munir H. Zia[6], Harry J. McArdle[7], Edward J. M. Joy[8], Elizabeth H. Bailey[5], Scott D. Young[5], Jung Suh[9], Janet C. King[9], Jonathan Sinclair[1] and Svetlana Tishkovskaya[10]*

[1] Centre for Global Development, University of Central Lancashire, Preston, United Kingdom, [2] Department of Pulmonology, Rehman Medical Institute, Peshawar, Pakistan, [3] Institute of Basic Medical Sciences, Khyber Medical University, Peshawar, Pakistan, [4] Abaseen Foundation, Peshawar, Pakistan, [5] School of Biosciences, University of Nottingham, Loughborough, United Kingdom, [6] Research and Development Department, Fauji Fertilizer Company Ltd., Rawalpindi, Pakistan, [7] Department of Nutritional Sciences, University of Nottingham, Loughborough, United Kingdom, [8] Faculty of Epidemiology and Population Health, London School of Hygiene and Tropical Medicine, London, United Kingdom, [9] Children's Hospital Oakland Research Institute, Oakland, CA, United States, [10] Lancashire Clinical Trials Unit, University of Central Lancashire, Preston, United Kingdom

OPEN ACCESS

Edited by:
Velu Govindan, International Maize and Wheat Improvement Center, Mexico

Reviewed by:
Elad Tako, Cornell University, United States
Shahid Hussain, Bahauddin Zakariya University, Pakistan

***Correspondence:**
Nicola M. Lowe
nmlowe@uclan.ac.uk

†*Deceased*

Specialty section:
This article was submitted to Nutrition and Food Science Technology, a section of the journal Frontiers in Nutrition

Received: *05 November 2021*
Accepted: *13 December 2021*
Published: *18 January 2022*

Citation:
Lowe NM, Zaman M, Khan MJ, Brazier AKM, Shahzad B, Ullah U, Khobana G, Ohly H, Broadley MR, Zia MH, McArdle HJ, Joy EJM, Bailey EH, Young SD, Suh J, King JC, Sinclair J and Tishkovskaya S (2022) Biofortified Wheat Increases Dietary Zinc Intake: A Randomised Controlled Efficacy Study of Zincol-2016 in Rural Pakistan. Front. Nutr. 8:809783. doi: 10.3389/fnut.2021.809783

A new variety of zinc biofortified wheat (Zincol-2016) was released in Pakistan in 2016. The primary aim of this study was to examine the effects of consuming Zincol-2016 wheat flour on biochemical and functional markers of zinc status in a population with widespread zinc deficiency. An individually-randomised, double-blind, placebo-controlled cross over design was used. Fifty households were recruited to participate in the study, with each household included at least one woman of reproductive age (16–49 years) who was neither pregnant nor breast feeding or currently taking nutritional supplements. All households were provided with control flour for an initial 2-week baseline period, followed by the intervention period where households were randomly allocated in a 1:1 ratio to receive biofortified flour (group A; $n = 25$) and control flour (group B; $n = 25$) for 8-weeks, then switched to the alternate flour for 8-weeks. The trial has been registered with the ISRCTN (https://www.isrctn.com), ID ISRCTN83678069. The primary outcome measure was plasma zinc concentration, and the secondary outcome measures were plasma selenium and copper concentrations, plasma copper:zinc ratio and fatty acid desaturase and elongase activity indices. Nutrient intake was assessed using 24-h dietary recall interviews. Mineral concentrations in plasma were measured using inductively coupled plasma mass spectrometry and free fatty acids and sphingolipids by mass spectrometry. Linear Mixed Model regression and General Linear Model with repeated measures were used to analyse the outcomes. Based on an average flour consumption of 224 g/day, Zincol-2016 flour provided an additional daily zinc intake of between 3.0 and 6.0 mg for white and whole grain flour, respectively. No serious adverse events were reported. This resulted in significant, increase in plasma zinc concentration after 4 weeks [mean difference 41.5 μg/L, 95% CI (6.9–76.1), $p = 0.02$]. This was not present after 8 weeks ($p = 0.6$). There were no consistent significant effects of the intervention on fatty

acid desaturase and elongase activity indices. Regular consumption of Zincol-2016 flour increased the daily zinc intake of women of reproductive age by 30–60%, however this was not associated with a sustained improvement in indices of zinc status.

Keywords: zinc, biofortified wheat, rural Pakistan, zinc status, micronutrient intake, fatty acid, wheat flour

INTRODUCTION

The Pakistan National Diet and Nutrition surveys have reported widespread micronutrient deficiencies amongst women and children for decades, with those living in rural regions most at risk (1). Although the most recent survey, undertaken in 2018, reported an improvement in zinc status among women of reproductive age (WRA), zinc deficiency still affects 22.1% of WRA, along with vitamin A deficiency (27.3%), iodine deficiency (17.5%) and iron deficiency (18.2%) (2). Current strategies to improve micronutrient status in Pakistan include the National Food Fortification Programme that was launched in 2016, which aims to fortify wheat flour with iron, folic acid, zinc, and vitamin B12, and edible oil/ghee with vitamins A and D. However, the mid-term evaluation of the programme highlighted several challenges to the potential success of the fortification strategy, particularly with respect to the fortification of wheat flour. Key issues include the lack of capacity for effective monitoring and quality control of the fortification process, lack of mandatory legislation for flour fortification and weak consumer demand. In addition, around 20–30% of households (HHs) were found to consume flour milled at the large roller mills which were eligible to participate in the fortification programme, with the majority of HHs consuming flour milled at small local mills, known as "*Chakki*," which fall outside of the current fortification programme and would be impossible to monitor due to the large number, many situated in hard-to-reach rural locations. Conversely, the oil and ghee vitamin fortification programme has a greater potential for success and is supported by government legislation and effective enforcement by the Punjab Food Authority in Punjab Province where much of the national oil and ghee is produced (3).

Biofortification of staple crops with key micronutrients is an alternative strategy for reaching some of the more remote areas of the country, where food fortification coverage is not practical (4, 5). This involves the enhancement of the nutrient content of the crop through traditional selective breeding techniques, genetic modification and/or agronomic techniques including the application of micronutrient fertilisers (4, 6). Globally, several biofortified crop varieties have been released, including iron-rich pearl millet in India (7), zinc-rich rice in Bangladesh (8), zinc-rich wheat in India and Pakistan (9), and vitamin A-rich sweet potato and maize in Africa (10).

To evaluate the success of an intervention, it is necessary to have a reliable and specific biomarker or health outcome measure for the target micronutrient(s). For zinc, this is particularly challenging at the individual level due to the lack of sensitivity and specificity of the indices currently used (11, 12). Plasma zinc concentration (PZC) is frequently used to assess zinc status in populations, however its concentration is under tight homeostatic control and at an individual level, the response to small changes in dietary zinc intake, such as those expected from the consumption of biofortified staples, are subtle, particularly when the additional zinc is consumed with food rather than taken as a supplement (13, 14). In addition, interpretation of PZC is complicated by the presence of concurrent infection, fasted or non-fasted state, and time of day (13, 15). Novel biomarkers have been explored, including enzymes involved in essential fatty acid (EFA) metabolism. Zinc acts as a cofactor in fatty acid desaturase and elongase enzymes, and recent studies have suggested that linoleic acid desaturation and elongation pathways may be sensitive to small changes in zinc intake (16–18). However, more studies are needed to explore this as a robust and sensitive functional indicator for zinc status, particularly from studies conducted in free-living, community settings where confounding co-morbidities may be present.

In Pakistan, a new variety of zinc biofortified wheat (Zincol-2016) was released by HarvestPlus in 2016. The BiZiFED programme was launched in 2017, with the overarching aim of exploring the potential for Zincol-2016 to improve dietary zinc intake with scale-up on a national level (19). The foundation phase of this programme included a double-blind, randomised controlled trial (RCT) with cross-over design. The primary aim of this RCT was to measure outcomes of consuming flour made from a zinc biofortified wheat grain variety, Zincol-2016, on dietary zinc intake and biomarkers of zinc status in a low-resource rural community setting in Pakistan. The secondary aim is to evaluate the potential usefulness of proposed novel biomarkers of zinc nutriture (20). In this paper we present the outcome of consuming Zincol-2016 on dietary zinc intake and plasma zinc and mineral concentrations in the study cohort. We also report the effect of the intervention on proposed novel functional zinc indicators, FADS1, FADS2, and ELOVL5, to explore their potential for the evaluation of the future, larger scale biofortification effectiveness trials.

MATERIALS AND METHODS

A double-blind, individually-randomised, placebo-controlled study with cross-over design was undertaken in a rural community in Pakistan between October 2017 and February 2018. The trial was registered with the ISRCTN registry, study ID ISRCTN83678069 and the study protocol has been published (20). Ethical approval was granted by the lead University (reference no. STEMH 697 FR) and the collaborating institution in Pakistan, Khyber Medical University. The study is reported according to CONSORT statement extension to randomised crossover trials (21).

The recruitment and consent process has been described previously (20). In brief, the target community was comprised of ∼5,000 HHs, served by a Health Centre located near to the brick kilns close to Peshawar in Khyber Pakhtunkhwa (KP) province. The catchment area for this study was comprised of 10 villages, 5 of which were randomly selected for participation in the study. Ten HHs from each village were randomly selected and visited by the study manager to assess their eligibility and willingness to participate in the trial. The inclusion criteria were that the HH included a woman aged 16–49 years who was neither pregnant nor breastfeeding and not currently consuming nutritional supplements. There were no additional inclusion or exclusion criteria. If the head of the HH declined, another house from the same village was randomly selected and the invitation process repeated until 5 HHs had agreed to participate in each village. The primary outcome measure was PZC, and the target was to recruit 50 HHs, based on 5% significance level (two-sided) and 90% power, to detect an increase of plasma zinc concentration of 3.1 μg/dL with standard deviation (SD) 5.9 μg/dL taken from Hambidge et al. (22), with an attrition rate of 20%.

At the start of the 18-week protocol, HHs were randomised by a team member (MJK) to the intervention or control arm of the study using a block design whereby villages were blocks. One member of the team (MZam) who oversaw the logistics of the flour distribution but was not involved in the data collection or analysis, performed the allocation to the study arms. Flour distribution was undertaken by the store manager and community liaison officer, who also had knowledge of the allocation. The remaining team members and all participants were blinded to the allocation until data collection and preliminary statistical analyses were complete. The study comprised a 2-week baseline period, where all fifty HHs were provided with sufficient flour, milled from a standard wheat grain variety (Galaxy- 2013) to meet the HH needs. This was followed by two 8-week intervention periods, where HHs in the intervention arm (group A) received biofortified flour, milled from a zinc-rich variety of wheat (Zincol-2016) and those in the control arm (group B) continued to receive the standard wheat flour (Period 1). After 8 weeks the two groups crossed over with group A receiving the standard flour, and group B receiving the biofortified flour. A washout period between the two intervention periods was not required because part of the experimental design was to examine the shorter-term biomarker response to changes in dietary zinc intakes and zinc homeostatic mechanisms are known to respond rapidly to changes in dietary intake, so a "carry-over" effect was not expected. The participants were visited by the field team for data and sample collection at five timepoints (TP) during the study; during the baseline period (T1); the mid and endpoint of period 1 (T2 and T3, respectively); the mid and endpoint of period 2 (T4 and T5, respectively).

During the study, HHs were asked not to consume any other flour except that which was provided by the study team. Freshly milled flour was delivered to the HHs every 2 weeks, with sufficient quantity for all HH members based on self-reported HH consumption. Compliance was monitored by a member of the study field who visited each HH every 2 weeks to confirm the quantity of flour remaining. In addition, at the end of each timepoint, participants were asked for the number of occasions (meals) when she did not use the flour provided.

Grain Production and Analysis

The grain used to produce both the standard (control) and biofortified flours (intervention) were grown under carefully controlled conditions at a farm in Punjab province. Two genotypes of grain, a standard variety (Galaxy-2013) and a biofortified variety (Zincol-2016) were sown in November 2016 and harvested in May 2017 by our project partner, Fauji Fertilizer Company Ltd. Zincol-2016 had been selectively bred by HarvestPlus for its zinc accumulation properties as well as its resilience to common pests and pathogens, mainly fungal diseases. To increase the potential for zinc uptake into the grain, which is dependent on soil zinc availability (9), zinc fertiliser (Zn 13% as EDTA Zn) was applied to the soil (1.25 kg/ha) before sowing the crop; and foliage ($ZnSO_4 \cdot H_2O$ 33% Zn, applied at 1 kg/ha of product dissolved in 250 L of water) four times during the booting and heading stage. The Galaxy-2013 wheat was grown under standard conditions without additional zinc. Both varieties of grain were manually harvested, threshed mechanically on site and the grain collected into pre-labelled sacks which were transported by road to the study field site in KP. Each sack of grain was manually cleaned to remove any straw and grit before being sent for milling at a local commercial flour mill. A sample of grain (10 g) from the bottom, middle and top of each sack was collected for analysis of the mineral content. An aliquot of each sample was transported to the UK for mineral analysis at the University of Nottingham (UoN) using methods previously described (9, 23). In brief, whole grain was pre-soaked overnight at room temperature in 70% Trace Analysis Grade (TAG) HNO_3 and 2 mL H_2O_2. Samples were then microwave digested (Multiwave 3000 microwave system, Anton Paar Gmbh, Graz, Austria) and the whole-grain zinc and other mineral concentrations determined by inductively coupled plasma-mass spectrometry (ICP-MS; Thermo Fisher Scientific iCAPQ, Thermo Fisher Scientific, Bremen, Germany).

Participant Characteristics and Haematology

The characteristics of the participants, including indicators of socioeconomic status, HH demographics and anthropometric measures of the participating WRA were collected at baseline. These have been reported previously along with dietary diversity data (24). In addition, blood samples were collected at each T to monitor health status throughout the study. Whole blood (non-fasting) was drawn from the antecubital vein through a butterfly needle into plastic vacutainers (BD Diagnostics, Switzerland). Blood (2 mL) was collected into a tube containing Ethylenediaminetetraacetic acid (EDTA) anticoagulant for red blood cell count (RBC), haematocrit, haemoglobin (Hb), mean corpuscular volume (MCV) and mean corpuscular haemoglobin concentration (MCHC). These were measured on whole blood using an automated haematology analyzer (Sysmex XP-100, 19 Jalan Tukang, Singapore).

Dietary Analysis

Diet was assessed using five 24-h recalls collected during the 18-week protocol, at all five timepoints. A minimum of two 24-h recalls are required to estimate nutrient intakes (25). The intention was to establish the usual nutrient intakes in the community, not to examine the effect of the intervention on diet, thus the mean of the five timepoints were used to evaluate intakes in comparison with the dietary guidelines for Pakistan and also to identify any statistically significant differences in nutrient intakes between the two groups that may be confounding factors in the interpretation of the outcome measures. The dietary recalls were conducted by the study nutritionist (GK) using the multiple pass method and portion sizes were estimated using HH measures. In addition, detailed recipes for composite meals were collected to enable accurate entry of ingredients into the nutrient database (Windiets 2017). The Windiet database was augmented using food composition data from Bangladesh (26), and Pakistan (27) to improve the accuracy of the nutrient composition data for foods grown in the region. In addition, white beans, kidney beans and lentils, which are commonly consumed zinc containing foods in the study location, were purchased from the local market and the zinc content measured by ICP-MS at UoN. These values were added to the Windiet database and used in the dietary analysis. Values for the phytate content of individual food items were input manually from the Indian food composition database (28).

Plasma Mineral and Essential Fatty Acid Analyses

For plasma trace mineral analysis, non-fasting whole blood (5 mL) was collected at all five timepoints into trace-element-free tubes containing EDTA anticoagulant. Blood plasma was separated by centrifugation within 40 min of sample collection and stored at −80°C at Khyber Medical University prior to shipping on dry ice to UoN and Children's Hospital Oakland Research Institute (CHORI). Elemental concentrations of zinc in plasma samples were determined at UoN using inductively coupled plasma–mass spectrometry (ICP-MS; Thermo Fisher Scientific iCAPQ, Thermo Fisher Scientific, Bremen, Germany). Full details of the instrument conditions and quality control have been published previously (24). Essential fatty acid (EFA) concentrations in the plasma were measured at CHORI. An Infinity Quaternary liquid chromatography system in tandem with a 6490 Triple Quadrupole mass spectrometer (Agilent Technologies) was used to simultaneously quantify total plasma 18:2n−6 linoleic acid (LA), 18:3n−6 γ -linolenic acid (GLA), 20:3n−6 dihomo-γ -linolenic acid (DGLA), and 20:4n−6 arachidonic acid (ARA) as previously described (14). The proxy indices of the activity of enzymes involved in EFA metabolismwere determined from the ARA:DGLA (FADS1), GLA:LA (FADS2) and DGLA:LA (ELOVL5) ratios, respectively.

Statistical Analysis

The analyses were done on intention to treat basis, as a complete case analysis. Data were analysed using IBM SPSS Statistics Version 28 (Armonk, NY: IBM Corp). The statisticians were blinded to the intervention assignment until the analysis of the primary outcome was complete.

Primary Outcome Analysis

To test for an intervention effect, unadjusted analysis was performed with a paired samples *t*-test based on within participant differences for a PZC in two study periods. The normality assumption was checked and according to Kolmogorov-Smirnov and Shapiro-Wilk tests PZC data were normally distributed.

To explore the effect of the intervention on the primary outcome adjusted for baseline and over all timepoints, Linear Mixed Model (LMM) regression was used which provides a general and flexible approach to accommodate both fixed and random effects. The models included the treatment group (Intervention vs. Control), time and the treatment period (sequence) as fixed effects and the participant as a random effect. PZC at baseline was included as a continuous covariate. The model was chosen on the basis of Bayesian information criteria. To undertake the preliminary tests for carryover effect and period effect, required in cross-over trials (29, 30), a sequence parameter and period parameter were added into the model. Analysis for treatment effect at end points, T3 and T5, was complemented with comparisons of within-subject differences at interim collection points, T2 and T4, and across all four timepoints (T2–T5). An interaction term between study period and intervention effect was considered for inclusion in the model but was not found to be statistically significant so was therefore removed from the final model.

Secondary Outcome Analyses

The intervention effect for the secondary outcomes (plasma mineral concentrations of selenium, copper and copper:zinc ratio) was tested using a LMM with the same fixed and random effects as for the primary outcome, adjusted for baseline. General Linear Model (GLM) analyses with repeated measures were used to explore the within participant effects of time on consuming biofortified flour. According to the most recent dietary recommendations for zinc which were published by the European Food Safety Authority (EFSA) (31), based on a diet of >1,200 mg phytate per day, the Reference Nutrient Intakes (RNI) for WRA is 12.7 mg zinc per day. The Pakistan Dietary Guideline for Better Nutrition (32) set the recommended daily allowances for WRA at 20 mg zinc per day. Therefore, one-sample *t*-tests were utilised to compare the participants' dietary intake of zinc against the reference standards for both the EFSA and Pakistan Dietary Guideline for Better Nutrition. Overall mean nutrient intake between the two study groups were compared using an independent sample *t*-test.

Finally, to explore the linear association between PZC and FADS1 at T3 and T5, Pearson's product moment correlation analyses were adopted.

RESULTS

One hundred and fifty households were assessed for eligibility. Fifty households were recruited to participate in the study which began in October 2017 and ended in February 2018. Baseline participant characteristics have been reported elsewhere (24). Five participants withdrew from the study. The reasons for

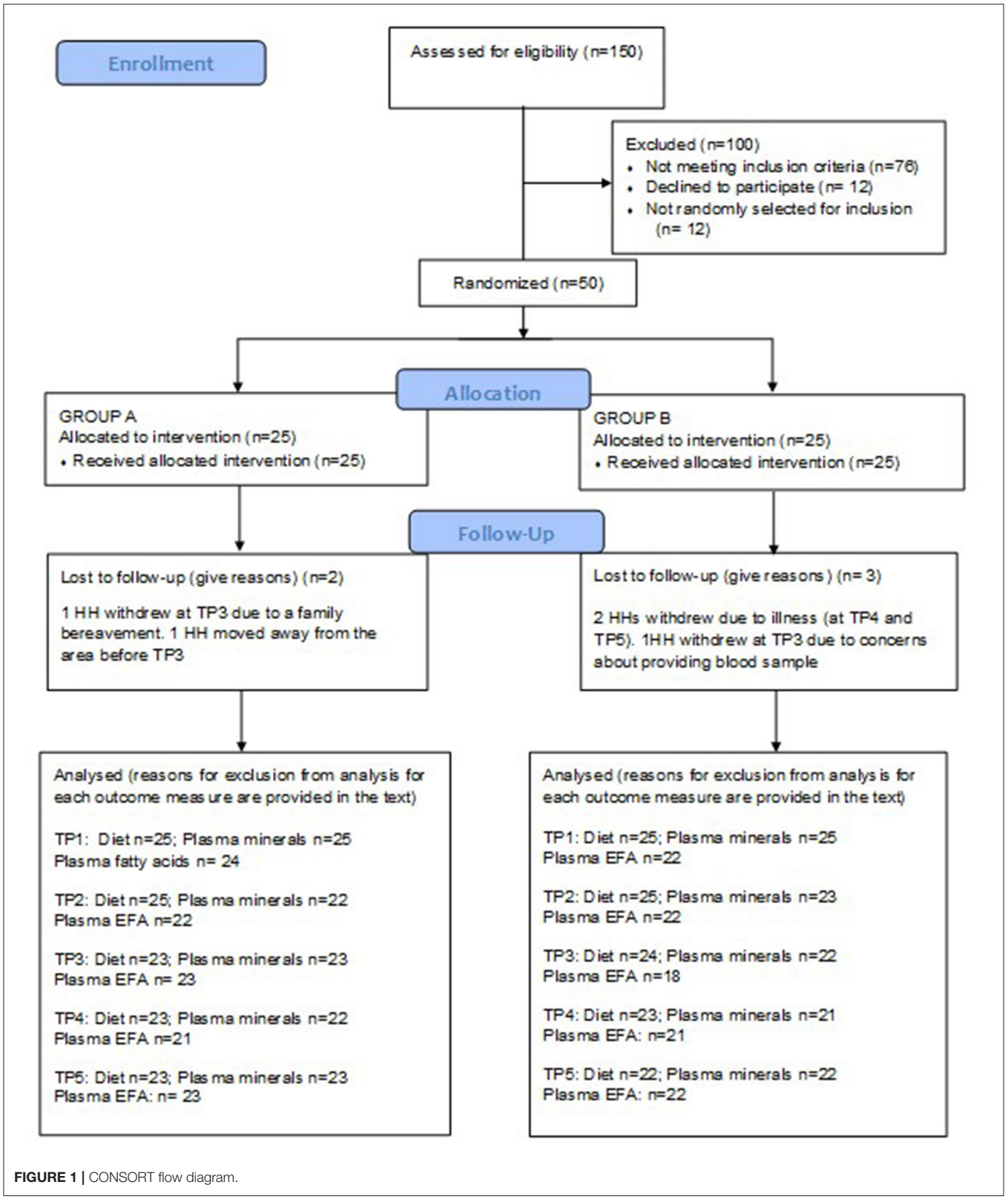

FIGURE 1 | CONSORT flow diagram.

TABLE 1 | Daily dietary nutrient and phytate intake during the randomised controlled trial.

	Timepoint 1[¶]		Timepoint 2[¶]		Timepoint 3[¶]		Timepoint 4[¶]		Timepoint 5[¶]		All timepoints, 1–5	
	Mean	SD	Mean	SD	Mean	SD	Mean	SD	Mean	SD	Mean	SD
Intervention group A[§]	(*N* = 25)		(*N* = 25)		(*N* = 23)		(*N* = 23)		(*N* = 23)			
Energy (kcal/d)	2,002	721	2,071	484	2,076	721	2,081	568	2,079	510	2,048	424
Fat (g/d)	73.7	35.6	69.6	17.7	74.9	37.6	74.8	34.7	74.5	25.3	73.4	17.5
Protein (g/d)	60.3	30.2	60.3	27.6	60.5	32.5	61.1	29.6	64.1	35	61.1	19.3
Carbohydrate (g/d)	266.1	103.7	293	78	281.2	104.9	282.7	82.4	279.9	90.9	277.6	65.2
Iron (mg/d)	17.3	9.2	18.2	7.2	18.7	8.2	18.7	8.2	19.2	9.1	18	5.7
Zinc (mg/d)	9.6	5.5	9.8	4.2	9.8	4.9	9.7	4.6	10.4	5.1	9.7	3.3
Phytate (mg/d)	1,455	804	1,711	779	1,489	833	1,530	786	1,335	694	1,482	562
Phytate/Zn (molar ratio)	15.3	3.4	17.2	3.9	15.2	5	15.7	3.3	12.9	3	15.3	1.9
Intervention group B[§]	(*N* = 25)		(*N* = 25)		(*N* = 24)		(*N* = 23)		(*N* = 22)			
Energy (kcal/d)	2,077	821	2,130	520	2,087	714	2,169	603	2,106	671	2,101	459
Fat (g/d)	83.3	41.6	65.7	28.7	71.5	25.7	68.9	22	77.9	33.2	73.2	15.8
Protein (g/d)	64.8	37.9	69.6	23.9	66.1	40.2	70.8	30.2	59.5	25.6	65.4	17.7
Carbohydrate (g/d)	259.9	118	307.4	67.1	286.9	127.9	308.1	101.9	284	100.1	287.4	68.3
Iron (mg/d)	19.3	12.3	20.3	7.7	19.3	10.8	21.6	8.7	17	6.2	19.4	5.2
Zinc (mg/d)	10.4	5.7	11.2	4.3	10.4	6.1	11.1	4.3	9.1	3.6	10.4	2.6
Phytate (mg/d)	1,295	664	1,741	642	1,562	1,065	1,471	564	1,311	550	1,469	411
Phytate/Zn (molar ratio)	13.2	4.2	16	4.6	14.4	5	13.6	3.9	14.5	3.2	14.5	2.1

[§]*Intervention group A received biofortified flour in period 1 and control flour in period 2 of the study. Intervention group B received control flour in period 1 and biofortified flour in period 2 of the study.*

[¶]*Timepoint 1 = baseline; Timepoint 2 = week 4 of period 1; Timepoint 3 = week 8 of period 1; Timepoint 4 = week 4 of period 2; Timepoint 5 = week 8 of period 2.*

attrition were: unwillingness to provide a blood sample (n = 2), migration out of the area (n = 1), and severe illness (n = 2). The CONSORT flow diagram is provided in **Figure 1**. Some blood samples were lost to individual outcome measure analyses due to non-viability of the sample for various reasons including haemolysis or low sample volume. The number of samples analysed for each outcome are provided in **Figure 1**. The HH adherence to the protocol was good overall. There were no occasions reported during T1 or T3 where study flour was not used for every meal. At T2, one HH reported use of non-study flour for three meals and one HH for 2 meals. At T4, HHs reported using non-study flour for two (1 HH) or three meals (3 HHs), and at T5, there were reports of the use of non-study flour for two (2 HHs) or three (1 HH) meals. In this timepoint, one HH reported not using the study flour for 30 meals (10 days). Incidences of non-compliance were distributed between both study groups, with one from each group at T2, two from each group at T4 and three from group A and two from group B at T5. The HH with the long period of non-compliance was in the control period when this occurred. The HHs reporting non-compliance were different at each of the timepoints.

Diet Analysis

The average macronutrient and zinc intakes for Groups A and B are presented in **Table 1**. The zinc intakes are based on the database analyses, which do not take into consideration the additional zinc intake from the biofortified flour. There were no significant differences in the overall mean (T1–T5) nutrient intakes between the two groups. No participants reported supplement use during the RCT.

TABLE 2 | Nutrient intakes for all participants compared with daily dietary recommendations.

	Nutrient intake		% Energy		
All timepoints	**Mean**	**SD**	**Mean**	**SD**	**PK guidelines**
Energy (kcal/d)	2,074.3	438.3			2,160 kcal/d
Fat (g/d)	73.3	16.5	28.7	4.3	
Protein (g/d)	63.2	18.4	12.1	2.9	0.52/kg = 34.4 g*
Carbohydrate (g/d)	282.5	66.3	54.3	4.0	
Iron (mg/d)	18.7	5.4			30 mg/d
Zinc (mg/d)	10.1	3.0			20 mg/d
Phytate (g/d)	1,475.5	487.3			
Phytate/Zn (molar ratio)	14.9	2.0			

**Mean weight at baseline = 66.3 kg.*

Average nutrient intakes for all participants (Groups A and B combined) were compared with dietary recommendations (**Table 2**). The mean ± SD daily energy intake was 2,074 ± 483 kcal which is commensurate with recommended intakes women with low to moderate activity levels of 1,816–2,234 kcal according to the Pakistan dietary guidelines (32).

The overall mean ± SD dietary intake of zinc was 10.1 ± 3.0 mg per day, and phytate intake averaged 1,476 ± 487 mg per day, giving a mean phytate to zinc molar ratio of 14.9. One sample t-tests showed that dietary zinc intake was significantly

lower than the EFSA recommendations of 12.7 mg/d ($p < 0.001$) and Pakistan Dietary Guideline for Better Nutrition value of 20 mg/d ($p < 0.001$). Based on the mean values for all timepoints completed, only 18% of the participants (9 of the 50) met the ESFA recommended intake, and none met the Pakistan guidelines for either zinc (or iron). For participants in this study, bread contributed almost 40% to the daily energy intake.

Grain Analysis

A total of 203 samples of Galaxy and 172 samples of Zincol-2016 grain were analysed for zinc content. Exploratory statistical analysis of the data revealed that for each wheat variety, a number of outliers were identified which we suspect were due to mislabeling of some of the sample bags during the aliquoting stage for transport to the UoN (UK). Outliers were therefore removed from the analysis if the zinc content was $>1.5 \times$ the interquartile range for the group. Based on this, 32 samples of Galaxy and 33 samples of Zincol-2016 were removed from the final data analysis, reported in **Table 3**.

Estimation of the Daily Zinc Intake From Whole Wheat Flour

The average bread consumption of the women participating in this trial was 324 g per day, taken from the 24-h recalls. Using a local recipe, naan bread contains 69 g of dry wheat flour per 100 g fresh-weight bread, giving an estimated average wheat flour consumption per day of 224 g. Thus, if whole grain Zincol-2016 is consumed, then the daily intake of zinc from flour is $224 \times 0.0493 = 11.0$ mg. If whole grain Galaxy is consumed, then the daily intake of zinc from flour is $224 \times 0.0222 = 5.0$ mg (rounded to 1 decimal place). On the basis of consuming whole grain flour, the additional dietary zinc provided by Zincol-2016 is 6.0 mg per day (rounded to 1 decimal place).

The zinc content of the flour used for baking depends on the amount of bran retained in the flour during the milling process, and the treatment of the flour at the HH level. For this study, the flour was provided "whole" without the bran removed. However, at the HH level, it is common practise for the women to sieve the flour to remove some, or all, of the bran depending on the coarseness of the sieve used and the desired outcome. For example, a fine sieve may be used to produce the whitest flour when baking Paratha, but a coarse sieve used for flour used in the baking of naan or roti. Since the zinc concentration of the bran is typically 3 times greater than that of the white flour (23) and the bran constitutes approximately 25% of the grain weight, removing the bran will reduce the overall zinc content of the flour by ∼50%. Therefore, with all the bran removed, the contribution to daily zinc intake from white flour is estimated to be 5.5 mg for Zincol-2016 and 2.5 mg for Galaxy, a difference of 3.0 mg per day. The increase in daily zinc intake from consuming 224 g biofortified flour per day is estimated to be within the range 3.0 to 6.0 mg per day depending on the bran content of the flour.

TABLE 3 | Zinc content of control (Galaxy) and biofortified (Zincol-2016) wheat grain.

Wheat variety	*N*	Mean (Zinc) mg/kg	SD	Min	Median	Max	95% CI
Zincol-2016	139	49.3	5.6	27.3	49.7	61.3	48.3–50.2
Galaxy	171	22.2	2.9	14.3	22.2	30.9	21.7–22.6

Plasma Mineral Analysis

Mean plasma zinc, copper, and selenium concentrations measured at each of the 5 timepoints are presented in **Table 4**.

Primary Outcome Measure PZC

Testing differences within participants at T3 and T5 for treatment effect with a paired t-test revealed that there was no evidence for a treatment effect [$t = 0.77$ (42 df) and $p = 0.45$]. When the analysis at mid points of period 1 and period 2 (T2 and T4) were performed, evidence of a treatment effect with statistically significant within-subject differences in PZC were demonstrated

TABLE 4 | Plasma Zinc, selenium, and copper concentrations (μg/L) and copper:zinc ratio for groups A and B at each timepoint.

¶T	Flour		Zinc (μg/L)		Selenium (μg/L)		Copper (μg/L)		Copper:Zinc
		N	Mean	SD	Mean	SD	Mean	SD	ratio
Group A									
T1	Control	25	690.8	118.2	95.8	13.7	1,084.7	207.2	1.61
T2	Zn Biofortified	22	664.0	100.8	90.1	13.6	988.5	231.8	1.50
T3	Zn Biofortified	23	670.7	114.0	94.6	15.4	1,035.6	252.2	1.56
T4	Control	22	634.2	93.7	88.7	11.6	902.2	168.6	1.44
T5	Control	23	572.2	89.4	84.2	12.9	904.5	219.4	1.61
Group B									
T1	Control	25	702.3	119.7	97.1	19.6	1,066.0	226.4	1.57
T2	Control	23	621.2	103.7	95.1	16.4	1,027.8	357.2	1.68
T3	Control	22	685.0	107.1	106.4	14.5	1,016.3	209.7	1.52
T4	Zn Biofortified	21	685.9	131.1	98.2	13.4	1,010.4	259.7	1.49
T5	Zn Biofortified	22	601.5	73.4	88.0	15.2	915.2	212.0	1.54

¶*T = Timepoint, where Timepoint 1 = baseline; Timepoint 2 = week 4 of period 1; Timepoint 3 = week 8 of period 1; Timepoint 4 = week 4 of period 2; Timepoint 5 = week 8 of period 2.*

[$t = 2.42$ (40 df), $p = 0.02$]. The mean difference between the intervention and control at mid points T2 and T4 was 41.5 μg/L (SD = 109.7) and mean differences between T2 and T4 in Group A and B were 15.5 μg/L (SD = 118.1) and −66.2 μg/L (SD = 97.4), respectively (**Figure 2**).

From the LMM adjusted for PZC at baseline, the paired differences between the cross over intervention and control groups for the primary end points T3 and T5 are presented in **Table 5**.

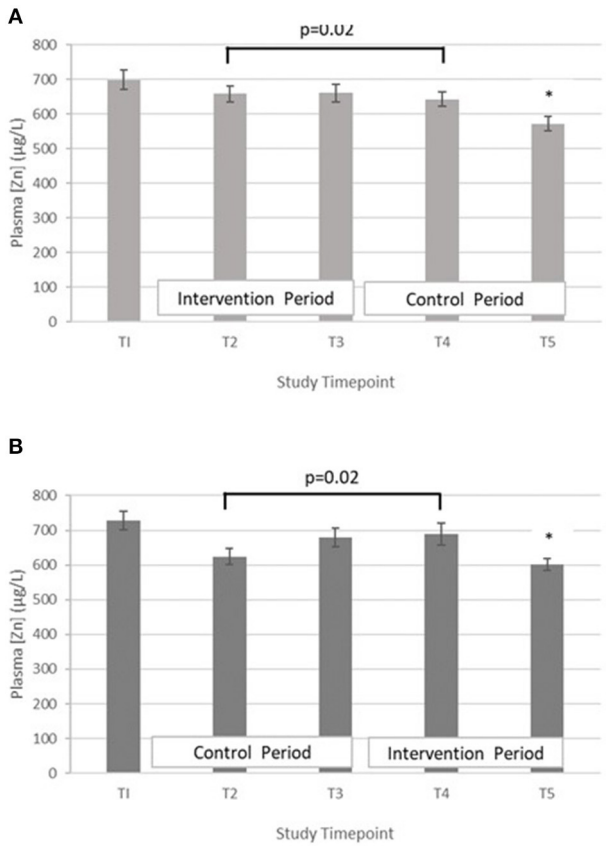

FIGURE 2 | (A) Plasma zinc concentration measured in Group A at baseline (T1), week 4 of period 1 (T2), week 8 of period 1 (T3), week 4 of period 2 (T4) and week 8 of period 2 (T5). Bars indicate estimated marginal means with standard error. *Estimated marginal mean is significantly lower than at all other timepoints, $p < 0.01$. **(B)** Plasma zinc concentration measured in Group B at baseline (T1), week 4 of period 1 (T2), week 8 of period 1 (T3), week 4 of period 2 (T4) and week 8 of period 2 (T5). Bars indicate estimated marginal means with standard error. *Estimated marginal mean is significantly lower than at all other timepoints, $p < 0.01$.

The observed p-value at the sequence parameter in the LMM ($p = 0.46$) indicates that the carry-over treatment effect is statistically insignificant, in agreement with the study assumption that the washout period is not required between the two periods.

To explore the trend of PZC over all four timepoints (T2–T5) (period effect), time was included in the LMM. There was a statistically significant difference in PZC between the four timepoints. Compared to T5, the PZC was greater at T2, T3, and T4, with mean increases of 53.8 μg/L (95% CI 17.6, 90.1 μg/L, $p = 0.004$), 88.2 μg/L (95% CI 52.0,124.5 μg/L, $p < 0.001$) and 73.6 μg/L (95% CI 37.0, 110.1 μg/L, $p < 0.001$), respectively.

Secondary Outcome Measures

The results of the LMM for plasma mineral outcomes are presented in **Table 5**.

Selenium – The treatment effect was not statistically significant. GLM with repeated measures indicated that in group A the plasma selenium concentration was significantly lower at T5 compared with T3 ($p < 0.01$). There were no differences between T2 and T4. A similar pattern was seen within group B, with Se at T5 being significantly lower than T3 ($p < 0.01$), but no significant differences between T2 and T4 (**Figure 3**).

Copper – The treatment effect was not statistically significant. GLM with repeated measures indicated that in group A plasma copper concentration was significantly higher at T3 vs. T5. Within group B, plasma copper concentration was significantly greater in T3 vs. T5 and T4 vs. T2 (**Figure 4**).

Copper:zinc ratio – The treatment effect was not statistically significant. GLM with Repeated measures indicated that there were no significant differences between timepoints in either group A or B (**Figure 5**).

Essential Fatty Acid Analysis

Mean plasma GLA, LA, ARA, and DGLA concentrations for groups A and B are presented in **Table 6**. FADS1 and FADS2 activity indices were determined from the ARA:DGLA and GLA:LA ratios, respectively, and ELOVL5 activity index from the DGLA:LA ratio as previously described (14).

FADS1: GLM with Repeated measures indicated that in group A there were no significant differences between timepoints T3 and T5, or T2 and T4. In Group B there was an increase in FADS1 activity index during the intervention period (between T 3 and 5) that came close to significance, $p = 0.059$, however this followed a marked dip in FADS1 activity at T3 (**Figure 6**). There were no

TABLE 5 | Primary end point (T3 and T5) analysis of differences between intervention and control groups.

Plasma mineral	Intervention, mean (SD), $n = 45$	Control, mean (SD), $n = 45$	Paired differences^, mean with 95% CI	p-value
Zinc (μg/L)	636.8 (101.5)	627.3 (113.8)	10.6 (−32.6, 53.8)	0.62
Selenium (μg/L)	91.4 (15.5)	95.0 (17.6)	−3.6 (−9.4, 2.2)	0.22
Copper (μg/L)	976.7 (238.7)	959.2 (219.7)	11.0 (−64.9, 86.9)	0.77
Copper:zinc ratio	1.6 (0.4)	1.6 (0.4)	−0.03 (−0.2, 0.09)	0.63

^*Intervention minus control. P-values are obtained using Linear Mixed Model adjusted for baseline.*

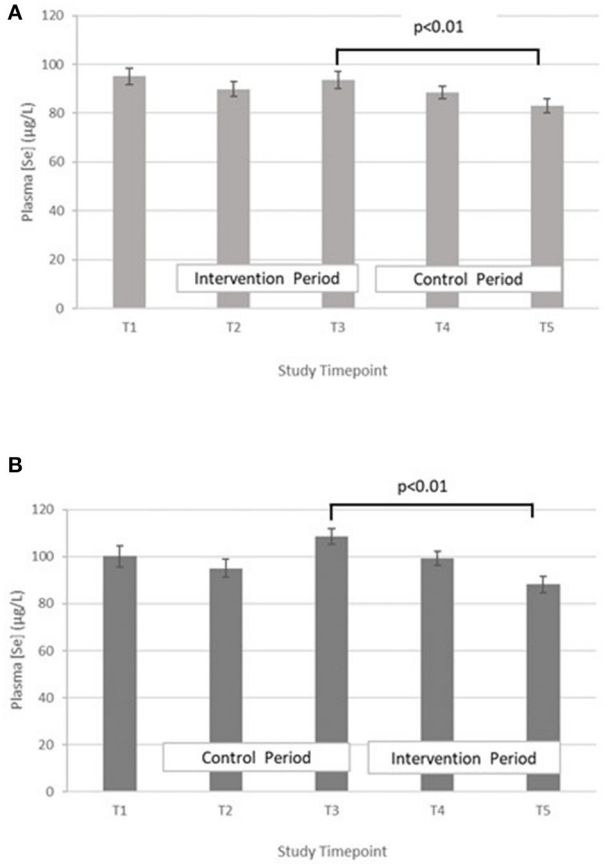

FIGURE 3 | (A) Plasma selenium concentration measured in Group A at baseline (T1), week 4 of period 1 (T2), week 8 of period 1 (T3), week 4 of period 2 (T4) and week 8 of period 2 (T5). Bars indicate estimated marginal means with standard error. **(B)** Plasma selenium concentration measured in Group B at baseline (T1), week 4 of period 1 (T2), week 8 of period 1 (T3), week 4 of period 2 (T4) and week 8 of period 2 (T5). Bars indicate estimated marginal means with standard error.

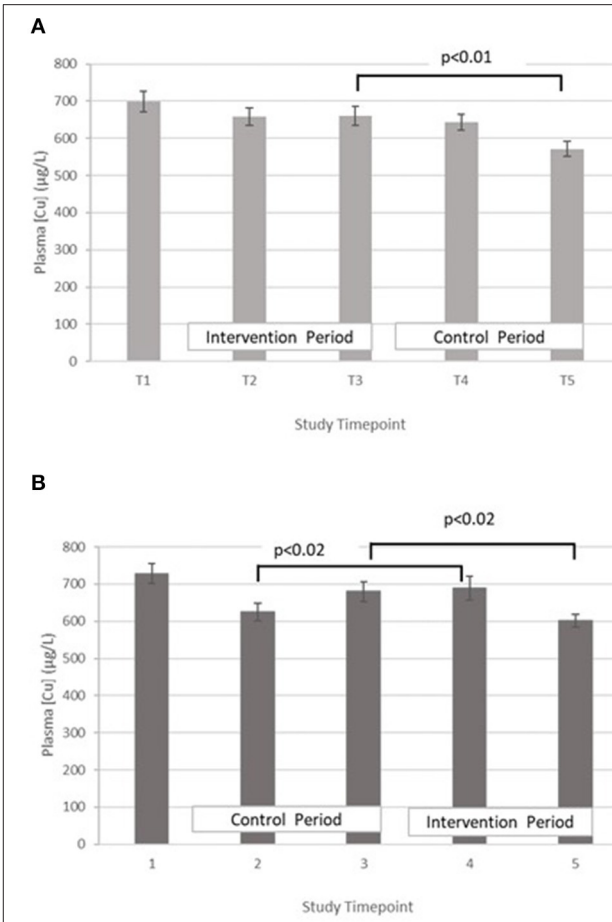

FIGURE 4 | (A) Plasma copper concentration measured in Group A at baseline (T1), week 4 of period 1 (T2), week 8 of period 1 (T3), week 4 of period 2 (T4) and week 8 of period 2 (T5). Bars indicate estimated marginal means with standard error. **(B)** Plasma copper concentration measured in Group B at baseline (T1), week 4 of period 1 (T2), week 8 of period 1 (T3), week 4 of period 2 (T4) and week 8 of period 2 (T5). Bars indicate estimated marginal means with standard error.

significant differences in group B between T2 and T4. Pearson's correlation analyses showed that there were no significant linear associations between PZC and FADS1 at T3 ($r = 0.04$, $p = 0.82$) and T5 ($r = 0.02$, $p = 0.91$).

FADS2, GLA:LA ratio: GLM with Repeated measures indicated that there were no significant differences between timepoints in group A. In group B, FADS2 activity was significantly lower at T5 compared with T3 ($p < 0.001$) (**Figure 7**).

ELOVL5, DGLA:LA ratio. GLM with repeated measures indicated no between timepoints in group A. In group B, ELOVL5 activity was significantly lower at T5 compared with T3 ($p < 0.002$) and higher in T4 compared with T2 ($p = 0.012$) (**Figure 8**).

Routine Haematology and Adverse Effects

No adverse physical adverse effects attributable to the consumption of either the control or intervention flours were reported during the study. Routine haematological indices are summarised in the **Supplementary Table 1** and fell within normal ranges at all timepoints. Following the observation that plasma zinc, selenium and copper concentrations all fell significantly at T5, further investigations into the haematological measures were made, specifically between T4 and T5. GLM repeated measures revealed a significant fall in Hc from T4 to T5 in both groups (group A, $p = 0.048$; group B, $p = 0.003$). This was accompanied by a fall in Hb, but only statistically significant in group B (group A, $p = 0.085$; group B, $p = 0.027$). There were no significant changes in MCV, or MCHC. There was a significant fall in RBC in both groups from T4 to T3 (group A, $p = 0.042$; group B, $p = 0.03$).

DISCUSSION

Biofortification of a staple food is potentially a low-cost, sustainable mechanism of increasing the zinc intake of a population, and for Pakistan, wheat has been selected as the target

staple as wheat flour is used for bread that is consumed with every meal. Zincol-2016 wheat was grown specifically for this study under optimal conditions of zinc fertiliser application and was able to achieve a mean zinc concentration of 49.3 mg/kg. The study showed that replacement of non-biofortified flour with flour milled from Zincol-2016 has the potential to increase dietary zinc intake by 6.0 mg per day, based on the quantities of flour typically consumed by the study participants, depending on the proportion of the bran removed prior to consumption. This is a marked increase in daily zinc intake, against a mean daily intake of 10 mg per day in the study participants (**Table 1**). This compares favourably with a study of agronomically biofortified wheat conducted in India, where addition of zinc rich fertiliser to the foliage resulted in a grain zinc concentration of 30 mg/kg, which translated into an increase of 3 mg per day in the diet of WRA (33). The authors stated that grains should contain between 40 and 60 mg Zn/kg in order to meet the RNI of 15 mg/d. The Zincol-2016 grain zinc content produced in the present study fell within this range, although there was some variability with zinc content ranging from 27.3 to 61.3 mg/kg. It is common practise with HHs in this community to sieve flour prior to use, depending on the type of bread that it is being used for. For Paratha, an oily bread eaten for breakfast, white flour is preferred, whereas for Naan and Roti, a mixed flour is often used. The fractional zinc absorption (FZA) from food depends on the bioavailability which is largely determined by the phytate content of the diet (34). The phytate content of the Zincol-2016 flour is comparable to that of standard varieties (MR Broadley, unpublished data) thus the total amount absorbed from Zincol-2016 is likely to be greater than that of standard varieties due to the higher total zinc content. Further studies on zinc bioavailability from foods made from Zincol-2016 flour are needed to confirm this. In terms of generalizability, the increase in dietary zinc intake calculated from the grain zinc content is presented as a range, depending on the bran content of the flour consumed. Flour consumption for the WRA was estimated from local bread recipes and the amount of bread consumed per day recorded in the 24-h dietary recalls. The mean grain consumption arrived at from this method, 224 g/d, is lower than the estimated national per capita mean grain consumption of 124 kg per year

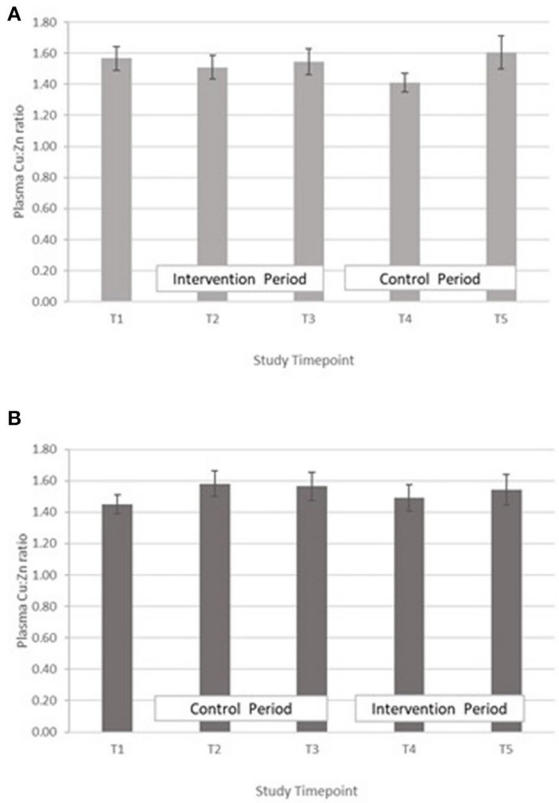

FIGURE 5 | (A) Plasma copper:zinc ratio measured in Group A at baseline (T1), week 4 of period 1 (T2), week 8 of period 1 (T3), week 4 of period 2 (T4) and week 8 of period 2 (T5). Bars indicate estimated marginal means with standard error. **(B)** Plasma copper:zinc ratio measured in Group B at baseline (T1), week 4 of period 1 (T2), week 8 of period 1 (T3), week 4 of period 2 (T4) and week 8 of period 2 (T5). Bars indicate estimated marginal means with standard error.

TABLE 6 | Plasma essential fatty acid concentrations at all timepoints[¶].

	Timepoint 1		Timepoint 2		Timepoint 3		Timepoint 4		Timepoint 5	
	Mean	SD	Mean	SD	Mean	SD	Mean	SD	Mean	SD
Intervention group A	(*N* = 24)		(*N* = 22)		(*N* = 23)		(*N* = 21)		(*N* = 23)	
GLA, mM	0.024	0.011	0.035	0.016	0.032	0.016	0.026	0.011	0.023	0.010
LA, mM	1.421	0.216	1.287	0.197	1.141	0.131	0.957	0.103	0.885	0.086
ARA, mM	0.676	0.195	0.705	0.203	0.679	0.120	0.529	0.100	0.485	0.107
DGLA, mM	0.164	0.056	0.166	0.055	0.167	0.050	0.134	0.041	0.119	0.030
Intervention group B	(*N* = 22)		(*N* = 22)		(*N* = 18)		(*N* = 21)		(*N* = 22)	
GLA, mM	0.026	0.009	0.028	0.009	0.041	0.019	0.027	0.012	0.022	0.009
LA, mM	1.457	0.283	1.301	0.196	1.119	0.170	0.978	0.219	0.858	0.112
ARA, mM	0.696	0.193	0.706	0.186	0.682	0.130	0.573	0.160	0.469	0.084
DGLA, mM	0.169	0.040	0.157	0.033	0.196	0.070	0.148	0.050	0.118	0.038

Linoleic acid (LA); 18:3n−6 γ -linolenic acid (GLA); 20:3n−6 dihomo-γ -linolenic acid (DGLA); 20:4n−6 arachidonic acid (ARA).

[¶]*Timepoint 1 = baseline; Timepoint 2 = week 4 of period 1; Timepoint 3 = week 8 of period 1; Timepoint 4 = week 4 of period 2; Timepoint 5 = week 8 of period 2.*

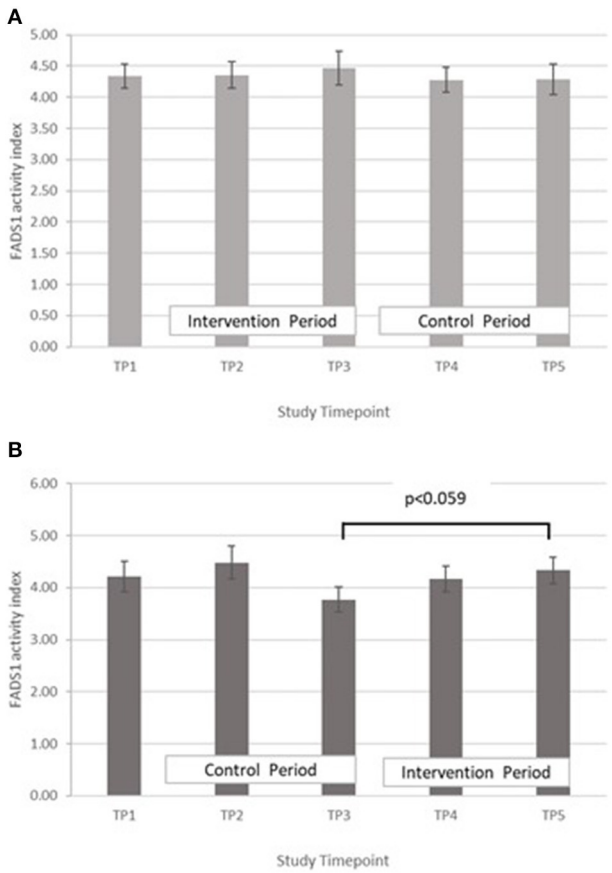

FIGURE 6 | (A) Fatty acid desaturase 1 activity measured in Group A at baseline (T1), week 4 of period 1 (T2), week 8 of period 1 (T3), week 4 of period 2 (T4) and week 8 of period 2 (T5). Bars indicate estimated marginal means with standard error. **(B)** Fatty acid desaturase 1 activity measured in Group B at baseline (T1), week 4 of period 1 (T2), week 8 of period 1 (T3), week 4 of period 2 (T4) and week 8 of period 2 (T5). Bars indicate estimated marginal means with standard error.

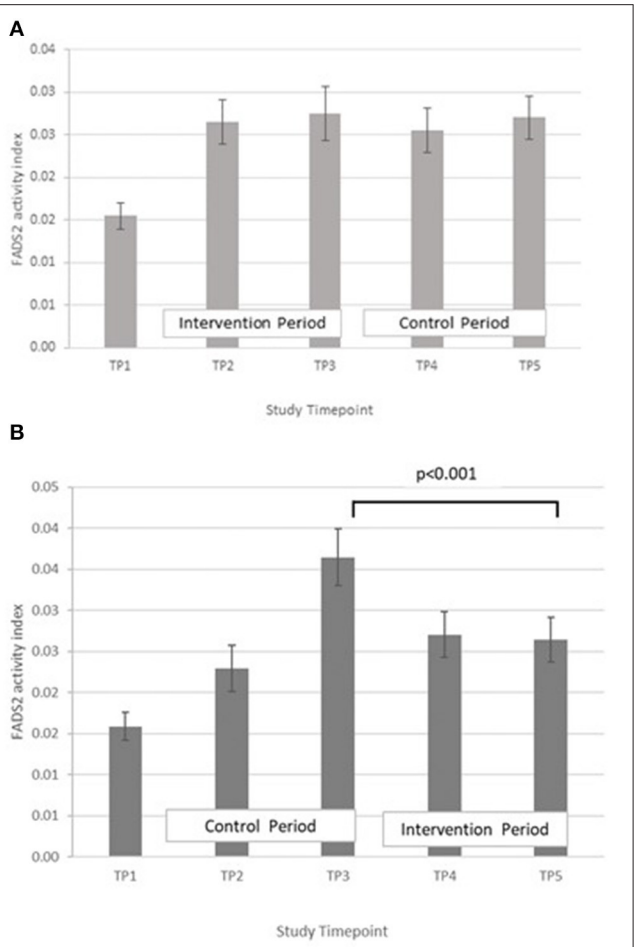

FIGURE 7 | (A) Fatty acid desaturase 2 activity measured in Group A at baseline (T1), week 4 of period 1 (T2), week 8 of period 1 (T3), week 4 of period 2 (T4) and week 8 of period 2 (T5). Bars indicate estimated marginal means with standard error. **(B)** Fatty acid desaturase 2 and elongase-5 activity measured in Group B at baseline (T1), week 4 of period 1 (T2), week 8 of period 1 (T3), week 4 of period 2 (T4) and week 8 of period 2 (T5). Bars indicate estimated marginal means with standard error.

(340 g/d), thus the potential contribution of zinc biofortified grain to the daily zinc intake of the general population of Pakistan could be higher than our estimates for WRA.

To inform the scale of the release of biofortified varieties on a national level, it is important to be able to demonstrate the effect on key indicators of nutritional status and health outcomes. To that end, we examined outcomes arising from consuming biofortified flour for 8 weeks compared with a standard variety in a double-blind cross over RCT. Within group comparisons revealed that there was a significant increase in PZC at the midpoint of the intervention period (4 week) compared with the midpoint of the control (**Figure 2**). However, the difference was not present at the end of the intervention period. A similar finding was reported by Aaron et al. who conducted a study to investigate the impact of consuming of fortified wheat bread on PZC in healthy Senegalese men (35). The RCT had 4 treatment arms: a moderate and a high zinc fortification arms, in which participants were provided with fortified bread containing 7.5 mg zinc or 15 mg zinc, respectively, for 4 weeks which were compared with a control arm (bread without added zinc) and a liquid zinc supplement (15 mg zinc). Fasting blood samples taken at the mid and endpoint of the intervention, and the authors reported that across all timepoints the zinc supplemented group was the only group where PZC increased from baseline. In addition, a RCT of zinc biofortified wheat in India where WRA consumed zinc biofortified flour 6 months also failed to demonstrate an increase in PZC compared to the control, despite a significant improvement in self-reported morbidity (33). Zinc present in blood plasma exchanges rapidly with the liver and other tissues where zinc is required for various functions including metabolism, immune response and protein synthesis (36). In chronic zinc deficiency, it is plausible that following a modest increase in dietary zinc, the additional absorbed zinc is rapidly distributed to restore metabolic functions while PZC

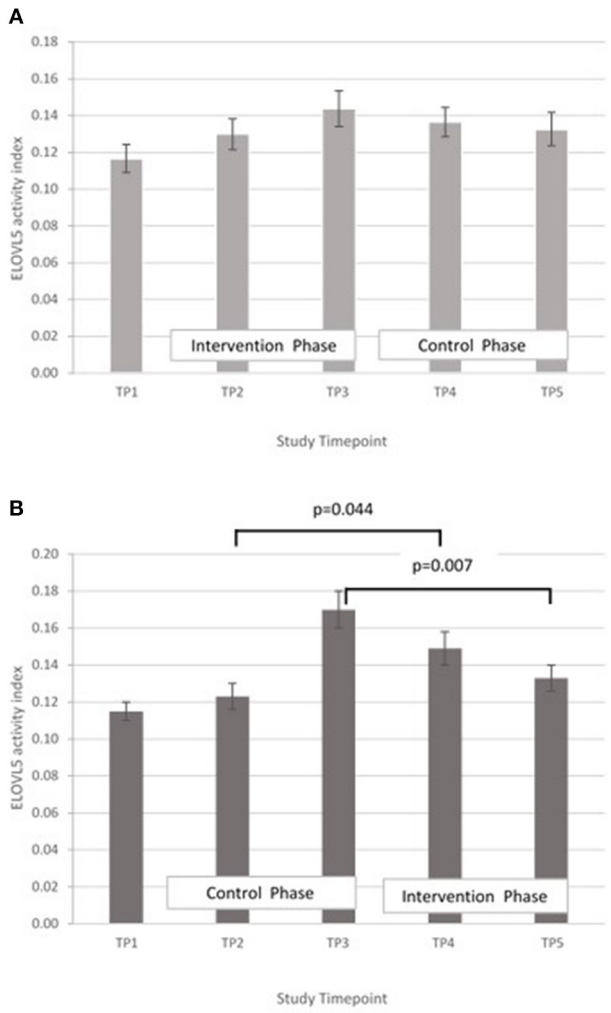

FIGURE 8 | (A) Elongase-5 activity measured in Group A at baseline (T1), week 4 of period 1 (T2), week 8 of period 1 (T3), week 4 of period 2 (T4) and week 8 of period 2 (T5). Bars indicate estimated marginal means with standard error. **(B)** Elongase-5 activity measured in Group B at baseline (T1), week 4 of period 1 (T2), week 8 of period 1 (T3), week 4 of period 2 (T4) and week 8 of period 2 (T5). Bars indicate estimated marginal means with standard error.

remains low, at least until deficiency is more fully resolved. Pinna et al. explored the response of PZC and the exchangeable zinc pool (EZP) of which plasma zinc is a component, to dietary zinc depletion and repletion (37). Participants were provided with a diet containing 13.7 mg zinc per day during the 5-week baseline and repletion phases. Following the baseline period, a moderately deficient diet containing 4.6 mg per day was provided for a 10-week depletion period. The findings indicated that neither PZC nor the size of the EZP responded to this modest (9.1 mg/d) reduction or increase in dietary zinc intake over this time period. Further studies of the longer-term effect of modest increases in dietary zinc intake on PZC following chronic deficiency are needed to explore the homeostatic response and changes in the size of the EZP.

In both groups, a significant decrease in PZC was observed in both groups at T5 (**Figure 2**). This decrease was also observed in the other minerals measured (**Table 4**; **Figures 3–5**), suggesting either a haemodilution effect or a systematic analytical error. Sample batches were randomised for timepoint, therefore a systematic analytical error at T5 is unlikely. In addition, the EFA concentrations also follow a similar trend (**Table 5**), with the lowest values at T5 in both groups. For EFA analysis, sample batches were also randomised for timepoint, and samples were analysed in duplicate and the duplicates were randomised. Further investigation of haematological indices haematocrit (Hc) and haemoglobin concentration, indices of hydration status, also revealed a significant fall in Hc, Hb concentration and RBC between T4 and T5, all of which are consistent with haemodilution. The study took place from October to February 2019 with January and February being the coolest month of the year in Northern Pakistan. Data for T4 and T5 were collected in mid-January and mid-February, respectively, meaning that an impact of a difference in ambient temperature between these 2 timepoints on hydration status is unlikely. There is no evidence from the 24 h recalls for an increase in fluid intake across the 5 Ts. The reason for this fall in blood parameters at T5 therefore remains unclear. Plasma Cu:Zn ratios have also been suggested as an indicator of zinc status (38, 39), with an optimal Cu:Zn ratio of 0.7–1.00 and ratios above 1.5 reflecting an inflammatory response or a decreased Zn status (40). The mean Cu:Zn ratios for the study participants were above or close to 1.5 at all Ts in both groups, and commensurate decreased zinc status as suggested by the low dietary zinc intakes, and low plasma zinc concentrations.

The proxy indices for FADS1, FADS2, and ELOVL5 activities were estimated from the ratio of product to precursor in the pathway involving desaturation and elongation of linoleic acid (18:2 n-6) to form arachidonic acid (20:4 n-6) (14). Massih et al. examined the effect of zinc supplementation (25 mg per day for 13 days) with and without food on FADS1, FADS2, and ELOVL5 activity indices in adult men (14). After adjusting for baseline, they reported a significantly higher FADS1 activity index in participants consuming zinc with a meal, than in those consuming zinc without food. They did not report any significant difference in FADS2 activity index between the two groups and suggested that FADS2 may be less sensitive to changes in zinc nutriture than FADS1. The ELOVL5 activity index tended to increase when zinc was consumed without a meal, but did not reach significance. Data from the present study suggest a rise in FADS1 activity with increased zinc intake, however it failed to reach statistical significance (**Figure 6**). Some significant changes in FADS2 and ELOVL5 activity were observed in group B only but were inconsistent across the study periods (**Figures 7**, **8**) In a study of healthy human volunteers, the LA:DGLA ratio was reported to be significantly higher in participants with relative low dietary intakes when compared with those with higher dietary zinc intakes (41). Similarly, an *in vivo* study using a chicken model (Gallus Gallus) reported that the LA:DGLA ratio measured in erythrocytes was higher in chickens fed a low zinc diet, compared to those consuming a zinc biofortified diet (42). This suggests a decrease in the activity of

either FADS2 or ELOVL5 or both enzymes when dietary zinc is low. This would be consistent with an increase in FADS2 and/or EVOL5 when zinc biofortified flour was consumed in the present study, which was seen in group B at the mid-point of the biofortified flour period (T4) compared with the midpoint of the control flour period (T2), however the reverse was seen at the end of the biofortified period (T5), compared with the end of the control flour period (T3). The blood samples taken for all biochemical analyses were non-fasting, in contrast to previous studies that have reported a relationship between fatty acid metabolism and zinc nutriture from samples taken during the fasted state (14, 17). Perturbations in lipid profiles in response to a recent meal may be masking any subtle changes in EFA ratios due to FADS or ELOVL5 activity in the present study.

A strength of the study is that, to our knowledge, this is the first study that explores the efficacy of a zinc biofortified strain of wheat, Zincol-2016, to improve zinc intake and status in Pakistan. It also provides valuable data on the proposed novel indicators of zinc status, FADS1, FADS2, and ELOVL5, following modest increases in dietary zinc intake in a low resource community setting. The study was double-blind and the cross over design enabled repeated measures analysis under both the intervention and control arms of the study in all participants which enhanced the statistical power in comparison to a two-arm study without cross over as each subject acted as her own control. This provided mitigation to some extent of the limitation of a small sample size, as demonstrated by the power calculation. Another limitation was the relatively short duration of the intervention (8 weeks). In addition, we had intended to measure inflammatory markers of zinc status (CRP and AGP) so that PZC adjustments for the presence of infection could be undertaken, however this was not possible for technical reasons. Ideally, blood samples should be collected in the fasted state to improve consistency and reproducibility of blood biochemical parameters. This was not possible in the present study for logistical and cultural reasons. The study was not powered a priori to detect changes in FADS or ELOVL5 activities, therefore results should be interpreted within this exploratory context. Finally, the high-zinc variety of wheat evaluated in this study, Zincol-2016, was grown under optimal conditions of fertiliser application on a single farm in Punjab province. An effectiveness trial is currently underway to assess the potential of Zincol-2016 to increase dietary zinc intake when grown by farmers living in the vicinity of the study population in KP Province, with some technical support for zinc fertiliser application. Further work is underway to examine Zincol-2016 grain zinc content when grown in different soil conditions, with and without the use of zinc fertiliser.

In summary, the results of this study demonstrate that consuming zinc biofortified flour can have a marked impact on total dietary zinc intake in rural, communities, where diet diversity is low, and there is a reliance on a limited number of plant-based foods and staples to meet energy needs. An increase in the daily zinc intake of between 3.0 and 6.0 mg, did not lead to a sustained, measurable increase in PZC. Some interesting trends towards an increase in FADS activity with increased zinc intake were observed but these did not achieve statistical significance. ELOVL5 activity changed significantly, but inconsistently across the study timepoints. Further studies with a larger sample size and intervention duration are needed to further investigate whether FADS1 and FADS2 activities, estimated from plasma fatty acid ratios, respond sensitively and reliably to modest changes in daily zinc intake.

DATA AVAILABILITY STATEMENT

The raw data supporting the conclusions of this article will be made available by the authors, without undue reservation.

ETHICS STATEMENT

The studies involving human participants were reviewed and approved by STEMH Ethics Committee, University of Central Lancashire, and Khyber Medical University Ethics Committee. The patients/participants provided their written informed consent to participate in this study.

AUTHOR CONTRIBUTIONS

NL, MK, and MZ initiated and conceptualised this RCT within the parent BiZiFED program. MB, HM, EJ, and MHZ were involved in the overall program design including agronomic management of biofortified and reference wheat crop management. JSi and ST performed data analysis. GK collected the dietary data. AB performed the dietary analysis. BS and UU managed the handling of the blood samples and field data collection. HO managed the database and provided support and liaison with the field management team. EB and SY performed the mineral and grain analyses. JK and JSu performed the EFA analyses and were involved in the data interpretation. NL drafted the manuscript. All authors were involved in the revision of the manuscript.

FUNDING

This BiZiFED project was funded by Biotechnology and Biological Sciences Research Council (BBSRC) Global Challenges Research Fund, Foundation Awards for Global Agriculture and Food Systems Research, Grant Number BB/P02338X/1. The Zincol-2016 seed was supplied by HarvestPlus and grown by Fauji Fertilizer Company. The Abaseen Foundation Pakistan facilitated the use of the health centre and access to the community. Funding for the fatty acid analyses was provided by HarvestPlus. The funders were not involved in the design, conduct, or analysis of the trial.

ACKNOWLEDGMENTS

The authors would like to thank the women who participated in this study. Rashid Medhi is gratefully

acknowledged for his oversight of the flour distribution, and community liaison. We thank Lolita Wilson for grain mineral analyses at UoN and Mollie Payne (Lancashire CTU, UCLan) for assistance with the descriptive statistics.

SUPPLEMENTARY MATERIAL

The Supplementary Material for this article can be found online at: https://www.frontiersin.org/articles/10.3389/fnut.2021.809783/full#supplementary-material

REFERENCES

1. Agha Khan University, Pakistan Medical Research Council, Government of Pakistan. *National Nutrition Survey Pakistan.* (2011). Available online at: http://pakresponse.info/LinkClick.aspx?fileticket=BY8AFPcHZQo%3D&tabid (accessed June 01, 2021).
2. UNICEF. *National Nutrition Survey 2018. Key Findings Report*. Ministry of Health Services, Nutrition Wing, Regulation and Coordination, Government of Pakistan, Pakistan (2019). Available online at: https://www.unicef.org/pakistan/media/1951/file/Final%20Key%20Findings%20Report%202019.pdf (accessed June 01, 2021).
3. e.-Pact Consortium. *Evaluation of the Supporting Nutrition in Pakistan Food Fortification Programme. Midterm Evaluation Report.* (2019). Available online at: https://www.opml.co.uk/files/2021-07/mid-term-evaluation-report-food-fortification-programme.pdf?noredirect=1 (accessed June 01, 2021)
4. Gupta S, Brazier AKM, Lowe NM. Zinc deficiency in low- and middle-income countries: prevalence and approaches for mitigation. *J Hum Nutr Diet.* (2020) 33:624–43. doi: 10.1111/jhn.12791
5. Lowe NM, The global challenge of hidden hunger: perspectives from the field. *Proc Nutr Soc.* (2021) 80:283–9. doi: 10.1017/S0029665121000902
6. Joy EJ, Ahmad W, Zia MH, Kumssa DB, Young SD, Ander EL, et al. Valuing increased zinc (Zn) fertiliser-use in Pakistan. *Plant and Soil.* (2016) 411:139–50. doi: 10.1007/s11104-016-2961-7
7. Scott SP, Murray-Kolb LE, Wenger MJ, Udipi SA, Ghugre PS, Boy E, et al. Cognitive performance in Indian school-going adolescents is positively affected by consumption of iron-biofortified pearl millet: a 6-month randomized controlled efficacy trial. *J Nutr.* (2018) 148:1462–71. doi: 10.1093/jn/nxy113
8. Sanjeeva Rao D, Neeraja CN, Madhu Babu P, Nirmala B, Suman K, Rao LVS, et al. Zinc biofortified rice varieties: challenges, possibilities, and progress in India. *Front Nutr.* (2020) 7:26. doi: 10.3389/fnut.2020.00026
9. Zia MH, Ahmed I, Bailey EH, Lark RM, Young SD, Lowe NM, et al. Site-specific factors influence the field performance of a Zn-biofortified wheat variety. *Front Sustain Food Syst.* (2020) 4:135. doi: 10.3389/fsufs.2020.00135
10. Tanumihardjo SA, Ball AM, Kaliwile C, Pixley KV. The research and implementation continuum of biofortified sweet potato and maize in Africa. *Ann N Y Acad Sci.* (2017) 1390:88–103. doi: 10.1111/nyas.13315
11. Lowe NM. Assessing zinc in humans. *Curr Opin Clin Nutr Metab Care.* (2016) 19:321–7. doi: 10.1097/MCO.0000000000000298
12. King JC, Gibson RS, Krebs NF, Lowe NM, Siekmann JH, Raiten DJ. Biomarkers of nutrition for development (BOND)-zinc review. *J Nutr.* (2016) 146:858S−85S. doi: 10.3945/jn.115.220079
13. King JC. Zinc: an essential but elusive nutrient. *Am J Clin Nutr.* (2011) 94:679S−84S. doi: 10.3945/ajcn.110.005744
14. Massih YN, Hall AG, Suh J, King JC. Zinc supplements taken with food increase essential fatty acid desaturation indices in adult men compared with zinc taken in the fasted state. *J Nutr.* (2021) 151:2583–9. doi: 10.1093/jn/nxab149
15. King JC. Yet again, serum zinc concentrations are unrelated to zinc intakes. *J Nutr.* (2018) 148:1399–401. doi: 10.1093/jn/nxy190
16. Knez M, Stangoulis JCR, Glibetic M, Tako E. The linoleic acid: dihomo-gamma-linolenic acid ratio (LA:DGLA)-an emerging biomarker of Zn status. *Nutrients.* (2017) 9:825. doi: 10.3390/nu9080825
17. Chimhashu T, Malan L, Baumgartner J, van Jaarsveld PJ, Galetti V, Moretti D, et al. Sensitivity of fatty acid desaturation and elongation to plasma zinc concentration: a randomised controlled trial in Beninese children. *Br J Nutr.* (2018) 119:610–19. doi: 10.1017/S000711451700366X
18. Hernandez MC, Rojas P, Carrasco F, Basfi-Fer K, Valenzuela R, Codoceo J, et al. Fatty acid desaturation in red blood cell membranes of patients with type 2 diabetes is improved by zinc supplementation. *J Trace Elem Med Biol.* (2020) 62:126571. doi: 10.1016/j.jtemb.2020.126571
19. Ohly H, Broadley MR, Joy EJM, Khan MJ, McArdle H, Zaman M, et al. The BiZiFED project: biofortified zinc flour to eliminate deficiency in Pakistan. *Nutrition Bulletin.* (2019) 44:60–64. doi: 10.1111/nbu.12362
20. Lowe NM, Khan MJ, Broadley MR, Zia MH, McArdle HJ, Joy EJM, et al. Examining the effectiveness of consuming flour made from agronomically biofortified wheat (Zincol-2016/NR-421) for improving Zn status in women in a low-resource setting in Pakistan: study protocol for a randomised, double-blind, controlled cross-over trial (BiZiFED). *BMJ Open.* (2018) 8:e021364. doi: 10.1136/bmjopen-2017-021364
21. Dwan K, Li T, Altman DG, Elbourne D. CONSORT 2010 statement: extension to randomised crossover trials. *BMJ.* (2019) 366:l4378. doi: 10.1136/bmj.l4378
22. Hambidge KM, King JC, Kern DL, English-Westcott JL, Stall C. Pre-breakfast plasma zinc concentrations: the effect of previous meals. *J Trace Elem Electrolytes Health Dis.* (1990) 4:229–31.
23. Khokhar JS, King J, King IP, Young SD, Foulkes MJ, De Silva J, et al. Novel sources of variation in grain Zinc (Zn) concentration in bread wheat germplasm derived from Watkins landraces. *PLoS ONE.* (2020) 15:e0229107. doi: 10.1371/journal.pone.0229107
24. Brazier AKM, Lowe NM, Zaman M, Shahzad B, Ohly H, McArdle HJ, et al. Micronutrient status and dietary diversity of women of reproductive age in rural Pakistan. *Nutrients.* (2020) 12:3407. doi: 10.3390/nu12113407
25. Gibson RS. *An Interactive 24-Hour Recall for Assessing the Adequacy of Iron and Zinc Intakes in Developing Countries HarvestPlus Technical Monograph 8*. Washington, DC and Cali: International Food Policy Research Institute (IFPRI) and International Center for Tropical Agriculture (CIAT) (2008).
26. Shaheen N, Bari L, Mannan MA. *Food composition table for Bangladesh.* Available online at: http://www.fao.org/fileadmin/templates/food_composition/documents/FCT_10_2_14_final_version.pdf, 2013 (accessed November 16, 2018).
27. UNICEF and Ministry of Planning and Development Government of Pakistan. F*ood Composition Table for Pakistan.* (2001). Available online at: https://www.fao.org/fileadmin/templates/food_composition/documents/regional/Book_Food_Composition_Table_for_Pakistan_.pdf (accessed November 16, 2018).
28. Longvah T, Ananthan T, Bhaskarachary K, Venkaiah K. *Indian Food Composition Tables, National Institute of Nutrition (Indian Council of Medical Research).* Hyderabad, India: Department of Health Research, Ministry of Health and Family Welfare, Government of India (2017).
29. Jones B, Kenward MG. *Design and Analysis of Cross-over Trials*. 2nd ed. London: Chapman & Hall/CRC (2003).
30. Senn S. *Crossover-trials in Clinical Research*. 2nd ed. Hoboken, NJ and Oxford, UK: Wiley (2002).
31. EFSA Panel on Dietetic Products. Scientific opinion on dietary reference values for zinc. *EFSA J.* (2014) 12:3844. doi: 10.2903/j.efsa.2014.3844
32. *Pakistan Dietary Guidelines for Better Nutrition*. Rome: Food and Agriculture Organization of the United Nations and Ministry of Planning Development and Reform, Government of Pakistan. (2018).
33. Sazawal S, Dhingra U, Dhingra P, Dutta A, Deb S, Kumar J, et al. Efficacy of high zinc biofortified wheat in improvement of micronutrient status, and prevention of morbidity among preschool children and women - a double masked, randomized, controlled trial. *Nutr J.* (2018) 17:86. doi: 10.1186/s12937-018-0391-5
34. Bel-Serrat S, Stammers AL, Warthon-Medina M, Moran VH, Iglesia-Altaba I, Hermoso M, et al. Factors that affect zinc bioavailability and losses in adult and elderly populations. *Nutr Rev.* (2014) 72:334–52. doi: 10.1111/nure.12105

35. Aaron GJ, Ba Lo N, Hess SY, Guiro AT, Wade S, Brown KH. Plasma zinc concentration increases within 2 weeks in healthy Senegalese men given liquid supplemental zinc, but not zinc-fortified wheat bread. *J Nutr.* (2011) 141:1369–74. doi: 10.3945/jn.110.136952
36. Lowe NM, Green A, Rhodes JM, Lombard M, Jalan R, Jackson MJ. Studies of human zinc kinetics using the stable isotope Zn-70. *Clin Sci.* (1993) 84:113–7. doi: 10.1042/cs0840113
37. Pinna K, Woodhouse LR, Sutherland B, Shames DM, King JC. Exchangeable zinc pool masses and turnover are maintained in healthy men with low zinc intakes. *J Nutr.* (2001) 131:2288–94. doi: 10.1093/jn/131.9.2288
38. Yanagisawa H. Zinc deficiency and clinical practice. *J Jpn Med Assoc.* (2004) 47:359–634. Available online at: https://www.med.or.jp/english/pdf/2004_08/359_364.pdf
39. Malavolta M, Piacenza F, Basso A, Giacconi R, Costarelli L, Mocchegiani E. Serum copper to zinc ratio: relationship with aging and health status. *Mech Ageing Dev.* (2015) 151:93–100. doi: 10.1016/j.mad.2015.01.004
40. Malavolta M, Giacconi R, Piacenza F, Santarelli L, Cipriano C, Costarelli L, et al. Plasma copper/zinc ratio: an inflammatory/nutritional biomarker as predictor of all-cause mortality in elderly population. *Biogerontology.* (2010) 11:309–19. doi: 10.1007/s10522-009-9251-1
41. Knez M, Stangoulis JCR, Zec M, Debeljak-Martacic J, Pavlovic Z, Gurinovic M, et al. An initial evaluation of newly proposed biomarker of zinc status in humans - linoleic acid: dihomo-gamma-linolenic acid (LA:DGLA) ratio. *Clin Nutr ESPEN.* (2016) 15:85–92. doi: 10.1016/j.clnesp.2016.06.013
42. Knez M, Tako E, Glahn RP, Kolba N, de Courcy-Ireland E, Stangoulis JCR. Linoleic acid:dihomo-gamma-linolenic acid ratio predicts the efficacy of Zn-biofortified wheat in chicken (Gallus gallus). *J Agric Food Chem.* (2018) 66:1394–1400. doi: 10.1021/acs.jafc.7b04905

Conflict of Interest: MHZ is employed by Fauji Fertilizer Company.

The remaining authors declare that the research was conducted in the absence of any commercial or financial relationships that could be construed as a potential conflict of interest.

Publisher's Note: All claims expressed in this article are solely those of the authors and do not necessarily represent those of their affiliated organizations, or those of the publisher, the editors and the reviewers. Any product that may be evaluated in this article, or claim that may be made by its manufacturer, is not guaranteed or endorsed by the publisher.

frontiers | Frontiers in Nutrition

REVIEW
published: 12 July 2022
doi: 10.3389/fnut.2022.826131

Wheat Biofortification: Utilizing Natural Genetic Diversity, Genome-Wide Association Mapping, Genomic Selection, and Genome Editing Technologies

Om Prakash Gupta[1†], Amit Kumar Singh[2†], Archana Singh[3], Gyanendra Pratap Singh[1], Kailash C. Bansal[4*] and Swapan K. Datta[5*]*

[1] ICAR-Indian Institute of Wheat and Barley Research, Karnal, India, [2] ICAR-National Bureau of Plant Genetic Resources, New Delhi, India, [3] Department of Botany, Hansraj College, University of Delhi, New Delhi, India, [4] National Academy of Agricultural Sciences, New Delhi, India, [5] Department of Botany, University of Calcutta, Kolkata, India

OPEN ACCESS

Edited by:
Miroslav Nikolic,
University of Belgrade, Serbia

Reviewed by:
Roi Ben-David,
Agricultural Research Organization (ARO), Israel
Xin-Yuan Huang,
Nanjing Agricultural University, China

***Correspondence:**
Gyanendra Pratap Singh
gp.singh@icar.gov.in
Kailash C. Bansal
kcbansal27@gmail.com
Swapan K. Datta
swpndatta@yahoo.com

[†]These authors share first authorship

Specialty section:
This article was submitted to Nutrition and Food Science Technology, a section of the journal Frontiers in Nutrition

Received: 30 November 2021
Accepted: 06 June 2022
Published: 12 July 2022

Citation:
Gupta OP, Singh AK, Singh A, Singh GP, Bansal KC and Datta SK (2022) Wheat Biofortification: Utilizing Natural Genetic Diversity, Genome-Wide Association Mapping, Genomic Selection, and Genome Editing Technologies. Front. Nutr. 9:826131. doi: 10.3389/fnut.2022.826131

Alleviating micronutrients associated problems in children below five years and women of childbearing age, remains a significant challenge, especially in resource-poor nations. One of the most important staple food crops, wheat attracts the highest global research priority for micronutrient (Fe, Zn, Se, and Ca) biofortification. Wild relatives and cultivated species of wheat possess significant natural genetic variability for these micronutrients, which has successfully been utilized for breeding micronutrient dense wheat varieties. This has enabled the release of 40 biofortified wheat cultivars for commercial cultivation in different countries, including India, Bangladesh, Pakistan, Bolivia, Mexico and Nepal. In this review, we have systematically analyzed the current understanding of availability and utilization of natural genetic variations for grain micronutrients among cultivated and wild relatives, QTLs/genes and different genomic regions regulating the accumulation of micronutrients, and the status of micronutrient biofortified wheat varieties released for commercial cultivation across the globe. In addition, we have also discussed the potential implications of emerging technologies such as genome editing to improve the micronutrient content and their bioavailability in wheat.

Keywords: micronutrients, hidden hunger, phytate, QTLs, genome editing

INTRODUCTION

Micronutrient deficiency also known as "hidden hunger," is one of the major global health problems afflicting more than 2 billion people globally (1). Micronutrient deficiency is common among population groups dependent on a single cereal (rice, wheat or maize) diet. These populations lack access to an adequate quantity of fruits, vegetables, dairy products, meats, etc. that are rich in essential minerals and vitamins. Globally, the human populations in Sub-Saharan Africa and South Asia bear the most significant burden of these micronutrient deficiencies (2). Among the micronutrient deficiencies, Iron (Fe), Zinc (Zn), Iodine (I), and Vitamin A deficiencies are the most widespread. Other micronutrient deficiencies include Calcium (Ca) and selenium (Se) that are relatively less widespread but could become more prevalent in the future if not addressed now. The daily intake of these micronutrients recommended dietary allowance (RDA) is vital to sustaining life as they are required for the proper physical and cognitive development, disease prevention, and

overall human well-being. Children less than five years of age, pregnant women, and lactating women are amongst the most vulnerable group to such micronutrient deficiencies.

Fe is required for several processes in the human body, including oxygen transport, electron transport, and DNA synthesis (3). For example, it is a component of oxygen transport proteins, such as hemoglobin and myoglobin. Moreover, Fe is also required for many proteins and enzymes involved in the energy generation, synthesis of neurotransmitters, and proper functioning of the immune system (4). Deficiency of Fe is the leading cause of anemia; nearly 30% of the women of reproductive age (14-59 years of age) and 40% of the children under five years suffer from anemia, globally (5). Similarly, Zn is also a trace element required for proper growth and maintenance of the human body. It acts as an essential cofactor for over 300 enzymes that are involved in vital processes, including cell proliferation, healing of wounds, blood clotting, etc. (6, 7). Zn deficiency has also been associated with increased diarrheal diseases and acute respiratory infections in children under five years of age and is a critical factor contributing to disease burden in developing countries (8). In Africa, 58% of child deaths are estimated to be due to Zn deficiency (9). Se is another important essential trace element needed for a robust immune system, thyroid function and reproduction. It is an essential component of selenoproteins, which act as potent antioxidant protecting cellular components from free radicals (10). Globally, an estimated 1 billion population suffers from Se deficiency, and this number is expected to rise in coming decades, necessitating designing strategies to enhance its dietary intake (11). Ca has also been regarded as one of the essential micronutrients required for the proper growth and development of the human body. It is required for strong bones and teeth and is also involved in many fundamental processes, such as blood coagulation, muscular function, hormonal secretions, nerve impulse transmission, etc. (12). Its deficiency can cause many problems, such as rickets in children, and osteoporosis and osteopenia in adults.

For curbing hidden hunger in the developing world, increasing the content *via* biofortification *vis-à-vis* increasing the bioavailability of both Fe and Zn are the two major approaches. For the first approach i.e., biofortification, significant variation in the level of Fe (up to 88 mg kg^{-1}) and Zn (14 to 190 mg kg^{-1}) has been reported among wild wheat, especially wild emmer wheat (*Triticum turgidum* ssp. *Dicoccoides*) (13), which can be efficiently utilized by wheat breeders to transfer in the background of high yielding and disease resistant hexaploid wheat genotypes. A breeding target of $>$ 59 $\mu g\ g^{-1}$ Fe, and 38 $\mu g\ g^{-1}$ Zn in wheat grains (14) against the baseline level of 30 $\mu g\ g^{-1}$ Fe, and 25 $\mu g\ g^{-1}$ Zn would be sufficient to meet the 30–40% of the average daily requirement of an adult. However, bioavailability of Fe and Zn in wheat is greatly limited due to the presence of phytic acid (PA, 0.4–2.0%), an anti-nutrient (15, 16). [PA]:[Fe and Zn] ratios are very vital in determining the potential bioavailability of the micronutrients and are inversely proportional i.e., higher the molar ratio, lesser the bioavailability and *vice-versa*. For [PA]:[Fe], the ratio should be $<$ 1 (preferably $<$ 0.4) to significantly improve Fe absorption (17), while for [PA]:[Zn] ratios of $<$ 5, 5 to 15, and $>$ 15 have been associated with high (50%), moderate (30%) and low (15%) Zn bioavailability, respectively (18). Therefore, it is desired that wheat genotypes be developed with suitable [PA]:[Fe and Zn] ratios for optimum bioavailability of Fe and Zn to humans and animals.

Generally, three major strategies i.e., dietary diversification, food fortification, and food supplementation were developed to address the problem of micronutrient deficiencies (19). Among these, dietary diversification focuses on modifying food consumption patterns at the individual household level, such as increasing the intake of more nutritious diets like fruits, vegetables, animal foods, etc. However, dietary diversification is not possible in many parts of the world due to poor socio-economic conditions and ethnic dietary choices. Other alternatives like food fortification and micronutrient supplementation for specific life stages and age groups can be considered stopgap measures for tackling micronutrient deficiencies. However, these strategies cannot provide a long-term sustainable solution for nutrient deficiencies in low and middle-income countries. These countries have a large population that lives in extreme poverty and does not have both physical as well as economic access to the adequate quantity of nutritious foods. Further, they cannot afford fortified food products or food supplements (20). Moreover, setting up the infrastructure to develop and distribute fortified foods or even food supplements would require a considerable investment that underdeveloped countries cannot afford. Agro-system diversification can assist local populations to expand their food baskets and solve the problem of micronutrient deficiencies, but it cannot be widely adopted in underdeveloped countries due to small landholdings. Therefore, in the past two decades, a greater emphasis has been laid on biofortification, which refers to increasing the bioavailable nutrient content of food crops either through conventional plant breeding or transgenic approaches. Biofortification is considered the most effective and sustainable approach for addressing the micronutrient deficiencies related problems in humans (21). A recent publication "Wheat and Barley Grain Biofortification" (Elsevier, United Kingdom), would serve as an important ready reckoner for different domains of wheat biofortification (22).

Wheat supplies approximately 20% of the human population's total calories and protein intake worldwide. However, most of the commercial wheat cultivars grown across the world are deficient or have suboptimal levels of micronutrients. It is mainly due to the greater focus of national wheat breeding programs on increasing yield, which has resulted in the erosion of grain minerals and protein contents in improved varieties. For the development of nutrient-dense wheat varieties, the primary prerequisite is to identify donor lines with high concentrations of the targeted micronutrients. Therefore, the need of the hour is to explore natural genetic diversity among the landraces and wild wheat species for grain mineral content and utilize them in the breeding programs for developing biofortified varieties. In 2003, a program in this direction was initiated at CIMMYT, with the support from HarvestPlus. The breeding materials developed under this program have contributed to the development of few

biofortified cultivars with higher grain Zn and Fe concentrations in India, Pakistan, Nepal, Mexico, and Bangladesh (23).

In wheat, conducting molecular studies, especially cloning of genes for any target trait, is considered a very challenging task due to the large and complex genome organization. Therefore, it took many years to clone a grain protein content (GPC) gene (*Gpc-B1*) from an accession of wild emmer wheat (*Triticum turgidum*, *dicoccoides*) (24). Even for the qualitative traits, such as disease resistance, which are generally controlled by a single major gene, cloning the resistance locus has never been easier due to the lack of information on the whole genome-level sequence as well as fully sequenced genes. However, in recent years, the availability of genomic resources such as the gold standard reference sequence of hexaploid wheat (25), reference genome sequences of its progenitor species (26, 27), transcriptome landscape of different tissues of wheat (28–31), single nucleotide polymorphism (SNP) genotyping arrays and genotyping by sequencing (GBS) methods (32) has led to a revolution in the field of wheat genomics. These tools have made it relatively easier to fine map and clone genes of essential traits in cultivated and wild wheat species (33). Further, in recent years, genome-wide association study (GWAS), which uses diverse germplasm lines or multiparent populations, has developed as a powerful tool for high-resolution trait mapping in crops and can be used to map nutritional quality traits using diverse association panels constituted from landraces, synthetics and wild species (34–36). Furthermore, recently, genome editing technologies, including prime editing and base editing have become promising targeted mutagenesis tools for crop improvement (37, 38). The first report of gene editing in wheat was the development of the targeted knockout for the *Mlo* gene that confers resistance against powdery mildew pathogen, *Blumeria graminis f.*sp. *tritici* (39). Since then, there are many reports of gene editing in wheat targeting genes associated with various agronomical and quality traits (40). Recently, nano-technology has also been explored for micronutrient biofortification in wheat. Khan et al. (41) have extensively reviewed the status of nano formulation-based wheat biofortification with a critical analysis of its merits and demerits.

In the present review, we have discussed the current state of knowledge on the existing natural genetic variations for micronutrients content among cultivated and wild wheat germplasm, genes and genomic regions controlling the micronutrient traits, current status of biofortified wheat varieties released for commercial cultivation around the world and potential applications of genome editing tools in the improvement of nutritional quality traits in wheat.

EXPLORING NATURAL GENETIC VARIATION FOR GRAIN MICRONUTRIENTS IN WHEAT AND ITS WILD RELATIVES

Understanding the extent and magnitude of natural genetic variations for various essential nutrients in wheat and its wild species is critical for improving these traits through classical and modern breeding tools. In this context, extensive screening of germplasm collection of wheat and its wild species conserved in genebanks of national and international institutions can facilitate the discovery of novel germplasm donors for various essential nutrients. These donor germplasms can be further exploited in the breeding programs for the development of biofortified wheat varieties. Over the past two decades, several studies have explored cultivated and wild wheat germplasm for variations in grain micronutrient contents. The key findings of some of these studies are briefly presented below.

Iron (Fe), Zinc (Zn), Selenium (Se) and Calcium (Ca) Content

Several studies have reported variation in grain Fe and Zn concentrations of bread wheat cultivars, landraces and wild wheat (42–44). Generally, breeding lines and cultivars have low genetic variation for grain Fe and Zn concentrations compared to landraces, cultivated wheat progenitors and related wild wheat species (unadopted wheat) (45). Several studies show a negative correlation between mineral concentrations and yield, implying that increase in grain yield of wheat varieties was accompanied by a significant decrease in their grain mineral content (45, 46). Evaluation of eighty Iranian wheat cultivars bred over a period of 70 years revealed a significant decrease in grain Fe and Zn concentrations that ranged from 63.56 to 102.19 and 31.65 to 54.06 mg/kg, respectively (46). On the other hand, a wide range of variations for grain Fe and Zn concentrations have been reported in landraces and other unadopted germplasms (43, 44, 47, 48). Qury et al. (43) analyzed a diverse wheat genotype panel comprising of French landraces, elite breeding lines, modern varieties and a set of worldwide germplasm collection which showed variation in grain Zn and Fe concentrations ranging from 15 to 35 mg/kg, and 20 to 60 mg/kg, respectively. However, some unadopted lines of this panel had Fe and Zn concentrations as high as 88 and 43 mg/kg, respectively, which can be exploited to improve the wheat cultivar's mineral concentrations. Another study on fifty landraces and ten varieties revealed higher Fe (24.93 to 66.51 mg/kg) and Zn (18.68 to 38.66 mg/kg) concentrations in landraces as compared to commercial cultivars (48). Recently, novel sources of variation for whole-grain Fe and Zn concentrations were identified in a panel of 245 diverse bread wheat lines derived from crosses between landraces of Watkin collections with a United Kingdom wheat cultivar Paragon (49). Further, the above studies have found that wide variation in grain Fe and Zn concentrations of wheat genotypes across different studies may not be solely due to genotypic differences since environment and soil nutrient status are known to significantly affect these traits, so promising Fe and Zn rich lines identified in these studies must be validated in multilocation trails.

Contrary to widely cultivated wheat, the primary and secondary gene pool of wheat such as *Triticum monococcum*, *Triticum boeoticum*, *T. turgidum dicoccoides*, *Aegilops tauschii, T. spelta* and *Triticum polonicum* are reported to contain wider variation for grain Fe and Zn concentrations (34, 45, 50–52). Among these species, *T. turgidum* ssp. *dicoccoides* is considered the most promising donor for the grain Fe and Zn content.

Cakmak et al. (53) screened a large number of accessions of several wild wheat species and their relatives for grain Fe and Zn concentrations and observed unique variations among the *T. dicoccoides* accessions, which ranged from 14 to 190 mg/kg for Zn and from 15 to 109 mg/kg for Fe. Studies have also identified some accessions with high grain Fe and Zn concentrations in other species as well. Tiwari et al. (52) screened a large number of accessions of *T. boeoticum* and found one accession (pau5088) with higher levels of grain Fe and Zn concentration, 40.1 and 44.6 mg/kg, respectively.

Additionally, some non- progenitor, wild wheat species such as S, U and M genomes have been reported to contain 3-4 times more Fe and Zn than cultivated hexaploid and tetraploid species (51). Velu et al. (54) reported wide genetic variability for Fe and Zn concentration among the introgression lines derived from cultivated species' crosses with wild wheat rich in grain Fe and Zn content. In addition to wild species of wheat, a few non-*Triticum* species such as rye and *Leymus* spp are also rich in mineral nutrient contents. The wheat-alien introgression lines derived from the crosses with *Leymus racemosus*, and also those carrying introgression of 2R, 3R chromosomes of rye contain a high level of Fe and Zn (55).

There are a few reports on the genetic variability of Se concentration in cultivated wheat and its wild relatives as compared to that of Fe and Zn (45, 56, 57). Lyons et al. (56) analyzed the Se concentration of ancestral and wild relatives of wheat, landraces, population, and cultivars grown in Mexico and Australia. The grain Se concentration of this set ranged from 5–720 μg/kg; however, much of this variation was attributed to variation in soil Se content across the locations. Nevertheless, they reported higher variation in diploid species *Ae. tauschi* and rye. Similarly, Zhao et al. (45) also reported limited genetic variability for grain Se concentration in commercial wheat cultivars. Apart from Fe, Zn, and Se, there are very limited genetic variability studies for Ca content in wheat. A study on Indian and Iranian wheat lines showed phenotypic variability for grain Ca content in the range of 104.3 to 663.5 mg/kg (58). Another study that analyzed a diverse panel of 353 wheat varieties, including winter and spring wheat varieties, reported wide variations for grain Ca content ranging from 288.2 to 647.5 mg/kg. Nirvana, a wheat variety from France, had a very high concentration of grain Ca (647.5 mg/kg DW) (59). The wide variability for grain Ca content in the above two studies suggest ample scope for developing biofortified Ca wheat varieties.

Phytate Content

The phytic acid content in wheat grain can significantly affect the bioavailability of minerals such as Fe and Zn during digestion because of their strong ability to bind to metals. Therefore, wheat genotypes with low phytate and high mineral concentration could be immensely useful in breeding programs that aim to develop biofortified verities for essential mineral nutrients. Many studies have analyzed the variability of phytate content among wheat cultivars and germplasm lines (60–62). The analysis of phytic acid content of a set of 65 bread varieties of Pakistan showed variation in the range 0.706–1.113% (60). Another comprehensive study on the collection of global durum cultivars identified a 2-fold variation in phytic acid content ranging between 0.462 to 0.952% (62). Contrary, many other studies have identified higher values for phytic acids (more than 1%) in durum genotypes, which might be attributed to G × E effects (61, 63). The low phytate genotypes identified in various studies may be potentially used as parents for developing wheat varieties with enhanced bioavailable Fe and Zn levels.

GENOMIC REGIONS/GENES CONTROLLING MICRONUTRIENTS IN WHEAT AND ITS WILD RELATIVES

Advancements in genomics, especially the availability of high-throughput genotyping assays such as whole genome re-sequencing, GBS, SNP arrays, etc., have made it easier to perform trait mapping in plant species like wheat with a large and complex genome. Both bi-parental and association mapping approaches have facilitated identifying several QTLs/genomic regions controlling grain minerals content. A brief description of the genomic regions/genes identified in the various studies is presented below.

Genomic Regions/Genes Associated With Grain Fe, Zn, Ca, and Se

In the past two decades, several studies have reported QTLs/candidate genes for grain Fe and Zn concentrations in wheat and its wild species using both QTL and association mapping methods (**Table 1**). Expectedly, most QTLs for Fe and Zn were identified from wild wheat and their relatives because there is a minimal variability for both these minerals in cultivated wheat germplasm. Tiwari et al. (52) were the first to report genetic mapping of grain Fe and Zn using an interspecific mapping population derived from the cross of *T. boeoticum* accession pau5088 (high grain Fe and Zn concentration) with *T. monococcum* accession pau14087. They identified two QTLs for grain Fe and one QTL for Zn. After that, many other studies have employed bi-parental mapping approach and identified QTLs for grain Fe and Zn concentrations on various chromosomes of wheat and its wild relatives (64–69). In the past few years, the association mapping approach has also facilitated identifying genomic regions/QTLs associated with grain Fe and Zn concentrations in diverse association panels constituted using diverse genotypes, including synthetic hexaploid wheat, advanced breeding lines, landraces and cultivars etc. However, most of the reported grain Fe and Zn QTLs have not been found stable across various locations suggesting profound effects of environment and genotype X environment on both these traits. Further, many identified regions have minor effects on grain Fe and Zn concentrations. Therefore, only the significant QTLs for Fe and Zinc identified in various studies should be focused on improving cultivated wheat's mineral contents. Some of the significant QTLs for zinc concentration has been identified on chromosome 1B, 2B, 5A, 1B, 6B (65, 70). Moreover, some studies have identified common genomic

TABLE 1 | Genomic regions/QTLs identified for grain Zn and Fe concentrations in cultivated and wild wheat using biparental and association analysis methods.

Mapping approach	Parentage/association panel	Chromosome	Number of QTLs/genomic regions		Phenotypic variance (%)		References
			Fe	Zn	Fe	Zn	
QTL mapping	*T. boeoticum* (pau5088)x *T. monococcum* (pau14087)	Fe: 2A, 7A (2 QTLs) Zn: 7A (2 QTLs)	3	2	7.0–12.6	9.0–18.0	Tiwari et al. (52)
QTL mapping	Durum wheat (cv. Langdon) X wild emmer (accession G18-16).	Fe: 2A (2 QTLs), 2B, 3A, 3B, 4B 5A, 6A, 6B, 7A, 7B Zn: 2A (2 QTLs), 5A, 6B, 7A, 7B	11	6	2–18	1–23	Peleg et al. (64)
QTL mapping	Xiaoyan 54 and Jing 411	Fe: 2B, 5A, 6A Zn: 5A, 2A, 4B	3	3	3.27–10.78	4.23–9.05	Xu et al. (70)
QTL mapping	PBW343X Kenya Swara	Zn: 1B, 2B, 3A, 4A, 5B	–	5		10.0–15.0	Hao et al. (71)
QTL mapping	Berkut X Krichauff	Fe: 1B Zn:1B,2B	1	2	22.2	23.1–35.90	Tiwari et al. (65)
QTL mapping	Two mapping populations were used: Saricanak98 X MM5/4 Adana99 × 70,711	Fe: 1B, 2A, 2B (2 QTLs), 3A, 6B, 7B Zn: 1B, 1D, 2B, 3A, 3D, 6A, 6B, 7A (2 QTLs), 7B	7	10	9.0–17.	9.00–31.0	Velu et al. (66)
Association mapping	167 *Ae. tauschii*	Fe: 1D, 2D, 3D, 4D, 7D Zn: 2D, 4D, 6D, 7D	5	4	–	–	Arora et al. (114)
QTL mapping	WH542 X a synthetic derivative [*Triticum dicoccon* PI94624/*Aegilops tauschii* (409)//BCN].	Fe: 6D, 7D (2 QTLs) Zn: 1D, 3B, 2D (2 QTLs), 7D (2 QTLs)	3	6	5.61–42.12	5.05–13.07	Krishnappa et al. (69)
Association mapping	369 European elite wheat varieties	Zn: 2A, 3A, 3B, 4A, 4D, 5A, 5B, 5D, 6D, 7A, 7B, 7D	–	40	–	2.5–5.2	Alomari et al. (59)
Association mapping	123 synthetic hexaploid wheat derived from cross *Triticum turgidum* L. × *Aegilops tauschii* Coss.	Fe: 1A (2 QTLs), 3A Zn: 1A, 2A (2 QTLs, 3A (2 QTLs), 3B (3 QTLs), 4A, 4B, 5A (2 QTLs), 6B	3	13	11.2–13.2	1.8–14.1	Bhatta et al. (115)
QTL mapping	Roelfs F2007X Hong Hua Mai/./Blouk #1	Fe: 1A, 2A, 3B, 3D, 4B, 5A, 6B (2 QTLs) Zn: 1B, 2B, 3A, 3B, 3D, 4B, 5A (2 QTLs), 6B, 7A	9	10	2.10–14.56	2.71–14.22	Liu et al. (68)
Association mapping	HarvestPlus Association Mapping panel consisted of 330 wheat lines.	Zn: 1A, 2A (10 QTLs), 2B (11 QTLs), 2D (2 QTLs), 5A (2 QTLs), 6B (2 QTLs), 6D, 7B (7QTLs), 7D	–	39	–	5–10.5	Velu et al. (34)
QTL mapping	WH542 X a synthetic derivative [*Triticum dicoccon* PI94624/*Aegilops tauschii* (409)//BCN].	Fe: 6D, 7D (2 QTLs) Zn: 3B, 1D, 2D (2 QTLs), 7D (2 QTLs)	3	6	5.01–13.07	5.61–42.13	Krishnappa et al. (69)
QTL mapping	Kachu × Zinc-Shakti	Fe: 1B, 1D, 2A, 6A Zn: 1B (2QTLs), 1D, 2A, 2B, 5A, 6B, 7D (2 QTLs)	4	9	3.1–12.3	3.3–10.3	Rathan et al. (116)
Association mapping	205 wheat genotypes comprising cultivars, landraces, and breeding lines	Zn: 2B, 3B, 4B, 7B, 7A Fe: 5A, 6B, 7B, 7D	20	16	8.07–16.23	7.94–12.12	Wang et al. (117)

regions for grain Fe and Zn concentrations, and even some are also associated with other valuable traits such as thousand-grain weight, protein etc. (65, 71). Tiwari et al. (65) had identified two major QTL for grain zinc concentration on 1B and 2B; of these, the QTL on 2B was colocalized with the QTL for grain Fe concentration. Similarly, a significant QTL for grain Zn on 2B co-located with the QTL for grain Fe concentration (66). These studies suggest that simultaneous improvement of both traits is possible using MAS. Compared to Fe and Zn, the QTL mapping studies for grain Se concentration in wheat are rare. A total of five QTLs for Se content were identified on chromosome 3D, 4A, 4D, 5B, and 7D, using two different RIL populations (72). Moreover, in a recent study, Wang et al. (73) identified nine Se concentration QTLs in a mapping population derived from the cross of winter wheat cultivars Tainong18 and Linmai6.

In contrast to grain Fe and Zn content, there is very limited information on genomic regions/QTLs for grain Ca accumulation. A total of 9 QTLs for grain Ca were reported in the RIL mapping population derived from durum and wild emmer wheat (64). In another study, association mapping using a diverse panel of European wheat accessions identified genomic regions for grain Ca accumulation on all the wheat chromosomes except

3D, 4B, and 4D (59). Recently, Alomari et al. (74) identified a major genomic region for grain Ca on the long arm of 5A, which overlapped with gene *TraesCS5A02G542600* that encoded for a transmembrane protein.

INTEGRATION OF GWAS WITH MULTI-OMICS DATA TO ACCELERATE THE DISCOVERY OF CANDIDATE GENES FOR BIOFORTIFICATION TRAITS FROM WHEAT GERMPLASM

Biofortification traits have complex regulations and are governed by many QTLs/genes, which are significantly affected by environment and genotype-environment interactions (75). The expression of some biofortification traits such as grain mineral content involves many processes such as mineral absorption, translocation, redistribution, and re-mobilization to sink, and each of these processes is controlled by many genes. This makes genetic dissection of such traits challenging by utilizing any single genetic or molecular analysis approach (69, 76). The conventional GWAS approach identifies a large number of genomic regions/QTLs that can not be directly utilized in a breeding program (34). Moreover, GWAS does not go beyond simple marker-trait correlation with no proof of causality; therefore, this approach alone may not provide insights on the functional basis of variation in biofortification traits. The above two limitations of GWAS can be overcome by incorporating functionome (multi-omics) data (77). In the past decade, significant technological improvements in the field of "omics" have made it feasible to generate large-scale omics data such as transcriptome, proteome, and metabolome, etc., from a large number of samples at a low cost (78). Integration of GWAS with various multi-omics data would enable a system-level understanding of biofortification traits and has great potential to precisely pinpoint the actual causal variant/candidate gene. There can be two approaches for integrating multi-omics data in GWAS analysis; 1) GWAS is independently performed using biofortification trait profiling data as well as associated omics data i.e., gene expression, proteome and metabolome data of association panel genotypes, and then marker-trait associations results are integrated to interpret pathways and identify causal variant/candidate genes associated with the traits; 2) GWAS is performed only using genome-wide DNA markers and biofortification traits, and then expression, proteome, and metabolite profiling data generated from a few contrasting genotypes of the association panel are mapped to genomic regions associated with the targeted trait to identify the candidate genes (**Figure 1**). The integration of functionome data in GWAS analysis of biofortification traits may not only help identify causal variants responsible for these traits but would also enable their

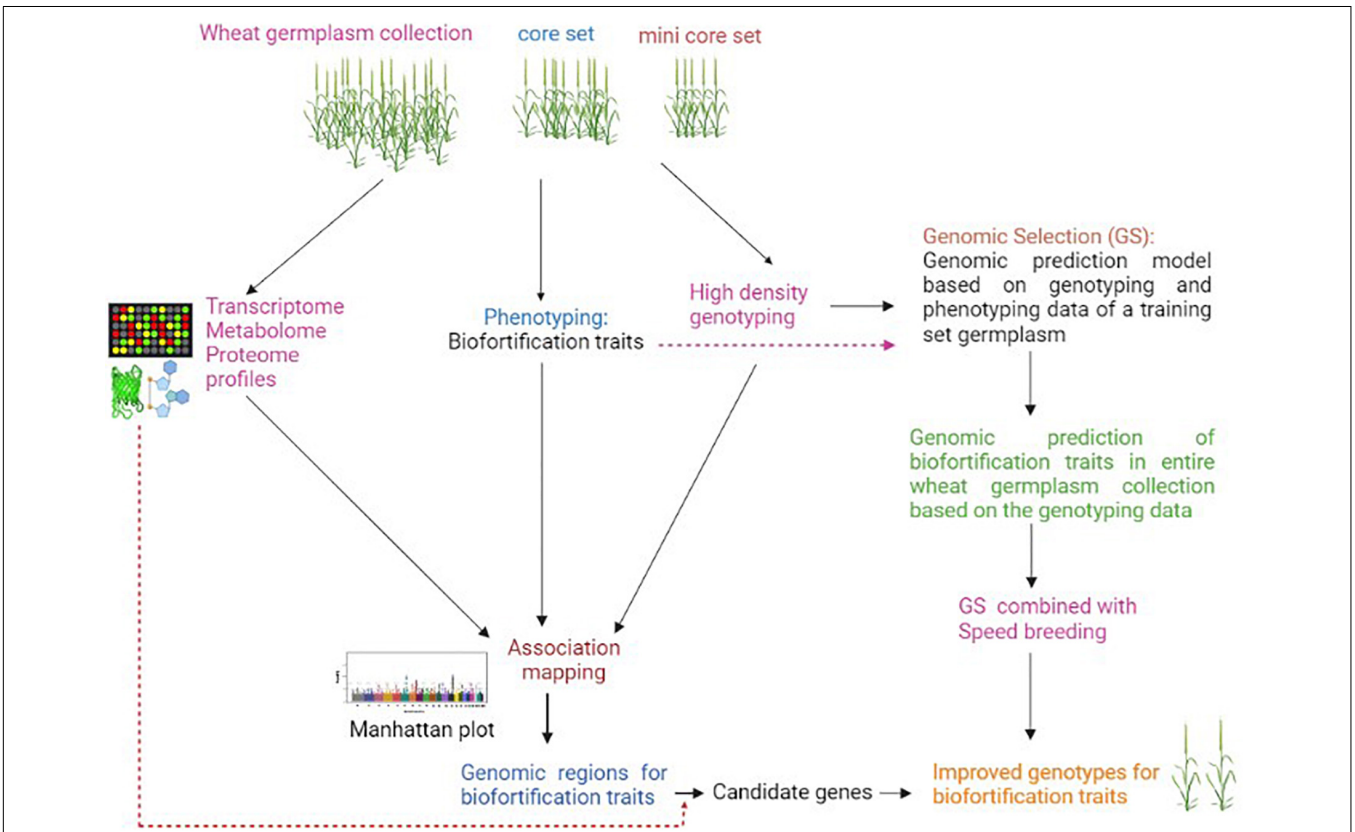

FIGURE 1 | Scheme for integration of omics and genomic selection approaches for accelerating improvement of biofortification traits in wheat.

comprehensive understanding at the cellular, biochemical and molecular levels.

IMPLEMENTATION OF GENOMIC SELECTION AND SPEED BREEDING HAS THE POTENTIAL TO ACCELERATE WHEAT BIOFORTIFICATION

In recent years, with the availability of high throughput and cost-effective genotyping assays, genomic selection (GS) has emerged as a promising genomics-based tool for the improvement of complex traits in crops (79). In GS, the selection of elite genotypes is made using genomic estimated breeding values (GEBVs), which consider all marker effects across the genome. GS enhances breeding efficiency for quantitative traits by reducing breeding cycle duration and selection gain per unit time[1]. This approach has great potential for improving the quality traits with low genetic variance (80). Joukhadar et al. (81) have discussed in detail the potential application of GS in the biofortification of spring wheat. There are already some reports on genomic predictions of micronutrient traits in crops (82–84). Owens et al. (82) were among the first to estimate genomic prediction for a biofortification trait in a crop. They predicted pro-vitamin A content in maize using genome-wide as well as carotenoid pathway-based markers and identified a small number of candidate genes that can be targeted for conversion of elite genotype with low carotenoid content to one that has an orange color grain with higher levels of high pro-vitamin A. In wheat, Velu et al. (83) reported genome-wide predictions for grain Fe and Zn concentrations in a diverse panel of 330 genotypes with prediction accuracies ranging from 0.331 to 0.694 and 0.324 to 0.734, respectively. Another study in wheat also found moderate to high genomic prediction accuracies for various major and minor elements concentration in grains (85). The high genomic prediction accuracies for mineral nutrient traits suggest that GS holds great potential in accelerating breeding for biofortification traits. Further, speed breeding that enables taking up to six generations in one year under glasshouse can be very well combined with GS in different breeding schemes to accelerate genetic gain for biofortification traits (**Figure 1**).

A BRIEF ACCOUNT OF BIOFORTIFIED WHEAT VARIETIES DEVELOPED THROUGH CONVENTIONAL BREEDING

In addition to basic research on micronutrients acquisition, the development of biofortified wheat varieties has recently upscaled with several successful examples. The conventional breeding approach has demonstrated great potential to biofortify hexaploid wheat genotypes by identifying suitable donor genetic resources such as synthetic, wild and primitive wheat genotypes for high Fe and Zn content with enhanced bioavailability. The most promising high Zn and Fe sources are diploid progenitors of hexaploid wheat (*Aegilops tauschii)*, wild emmer (*T. dicoccoides*), einkorn (*Triticum monococcum*), *T. spelta*, *T. polonicum,* and *T. aestivum* landraces. Among wild wheat tested so far, the collections of wild emmer wheat, *Triticum turgidum* ssp. *dicoccoides*, showed a prominent genetic variation of Zn ranging from 14 to 190 mg kg^{-1} and Fe up to 88 mg kg^{-1} (13). Translocation from different *Aegilops spp.* and rye to Pavon 76 background at the International Maize and Wheat Improvement Center (CIMMYT, Mexico) has generated several synthetic hexaploids (SHW), *T. spelta,* and several pre-breeding lines having wider variation in Zn (38 to 72 mg kg^{-1}) and Fe content (32 to 52 mg kg^{-1}) (34).

With these concerted efforts, CIMMYT wheat breeders, in collaboration with other major institutions of India, Pakistan, Bangladesh, Nepal, and Bolivia, have facilitated the development and release of 40 biofortified wheat varieties for commercial cultivation (**Table 2**). Since 2014, A total of 24 biofortified wheat varieties (*T. aestivum*; 16 and *T. durum*; 8) for Fe, Zn and protein have been developed by ICAR-Indian Institute of Wheat and Barley Research, Karnal, Punjab Agricultural University, Ludhiana, ICAR- Indian Agricultural Research Institute, Delhi, Agharkar Research Institute, Pune, University of Agricultural Sciences, Dharwad, Banaras Hindu University, Varanasi and private seed companies and released to Indian farmers for common cultivation at different wheat growing zones of India. Similarly, CIMMYT, in collaboration with important wheat research institutions of Pakistan, Bangladesh, Bolivia, Nepal and Mexico, has developed and released 2, 1, 1, 2, and 1 biofortified wheat varieties, respectively (**Table 2**). Overall, utilization of wild relatives and SHW of wheat in conventional breeding programs have significantly impacted the development of micronutrient biofortified wheat varieties, which is expected to continue with increased bioavailability. Over the next two decades, developing and mainstreaming Zn and Fe in the wheat breeding program at CIMMYT and partner institutions across the globe would undoubtedly enable the release of high-yielding and Fe and Zn biofortified wheat varieties to a more significant percentage of farmers of South Asia to curb hidden hunger of children and pregnant and lactating mothers.

GENETICALLY MODIFIED BIOFORTIFIED WHEAT

While conventional breeding is globally accepted, the absence of desired genetic diversity within the primary, secondary and tertiary gene pools for targeted traits within species (e.g., golden rice) or difficult to breed crops (e.g., banana) can efficiently be managed through genetic engineering technologies as a viable alternative. Also, the development of multi-nutrient cultivars by stacking multiple genes coupled with superior physiological and agronomic traits is often limited with conventional breeding, which can be circumvented by the genetic engineering approach (**Figures 2A,B**). However, wheat being hexaploid is comparatively challenging to transform and therefore needs the development of a robust transformation protocol to harness

[1]https://genomics.cimmyt.org/

TABLE 2 | List of biofortified wheat varieties developed through conventional breeding and released for commercial cultivation around the globe.

Variety	Nutritional quality	Year of release	Developer/sources
India			
DDW 48 (*T. durum*)	Fe: 38.8; Zn: 39.7; Protein: 12.1	2020	ICAR-Indian Institute of Wheat and Barley Research, Karnal, India
DDW 47 (*T. durum*)	Fe: 40.1; Protein: 12.7	2020	
DBW 303	Fe: 35.8; Zn: 36.9; Protein: 12.1	2020	
DBW 187	Fe: 43.1	2018 and 2020	
DBW 173	Fe: 40.7; Protein: 12.5	2018	
WB 02	Zn: 42; Fe: 40	2017	
PBW 771	Zn: 41.4	2020	Punjab Agricultural University (PAU), Ludhiana, India
PBW 752	Fe: 37.1; Zn: 38.7; Protein: 12.4	2018	
PBW 757	Zn: 42.3	2018	
HPBW 01	Zn: 40.6; Fe: 40	2017	
HI 8802 (*T. durum*)	Fe: 39.5; Zn: 35.9; Protein: 13.0	2020	ICAR- Indian Agricultural Research Institute, Regional Station, Indore, India
HI 8805 (*T. durum*)	Fe: 40.4; Protein: 12.8	2020	
HI 1633	Fe: 41.6; Zn: 41.1; Protein: 12.4	2020	
HI 8759 (*T. durum*)	Zn: 42.8; Fe: 42.1; Protein: 12.0	2017	
HI 1605	Zn: 35; Fe: 43; Protein: 13	2017	
HI 8777 (*T. durum*)	Fe: 48.7; Zn: 43.6	2017	
HD 3171	Zn: 47.1	2017	ICAR- Indian Agricultural Research Institute, New Delhi, India
HD 3249	Fe: 42.5	2020	
HD 3298	Fe: 43.1; Protein:12.1	2020	
MACS 4028 (*T. durum*)	Zn: 40.3; Fe: 46.1; Protein: 14.7	2018	Developed by Agharkar Research Institute, Pune, Maharashtra
MACS 4058 (*T. durum*)	Fe: 39.5 Zn: 37.8 Protein: 14.7	2020	
UAS 375	Protein: 13.8	2018	University of Agricultural Sciences, Dharwad, India
BHU-3	High Zn	2014	Banaras Hindu University, Varanasi, India
Abhay	High Zn	2015	Nirmal Seeds, Harvest Plus and Participatory variety selection
Chitra	High Zn	2016	Participatory variety selection
Pakistan			
NR- 421 (Zincol-16)	High Zn (> 6 ppm Zn advantage compared to best local check)	2015	Pakistan Agriculture Research Council/CIMMYT
Akbar-19	High Zn (> 7 ppm Zn advantage compared to best local check)	2019	Faisalabad Agricultural Research Institute/CIMMYT
Bangladesh			
BARI Gom 33	High Zn (7–8 ppm Zn advantage over best check, and also resistance to wheat blast)	2017	CIMMYT, Mexico
Mexico			
Nohely-F2018	High Zn (released in Mexico for the Mexicali valley of northern Sonora region)	2018	CIMMYT, Mexico
Bolivia			
Iniaf-Okinawa	High Zn (> 6 ppm Zn advantage than the local check)	2018	INIAF, Bolivia and CIMMYT, Mexico
Nepal			
Zinc Gahun 1	High Zn (> 6 ppm Zn advantage than the local check)	2020	NARC, Nepal and CIMMYT, Mexico
Zinc Gahun 2			

Grain Fe and Zn conents are expressed in ppm while protein content is expressed in percentage (%).

the full potential of the transgenic approach. As demonstrated in **Figure 2B**, the genetic engineering approach offers limitless cross-kingdom utilization and tacking of desired genes for multi-nutrients target traits improvement, including biotic and abiotic stresses, making it more attractive for farmers to adopt nutritionally improved nutrition wheat varieties. Moreover, it offers simultaneous biofortification of multi nutrients by metabolic engineering (86). However, the three significant bottlenecks of the transgenic approach are the lack of availability of suitable transformation protocol in polyploidy crop such wheat, fear of environmental escape of transgene and global genetically modified organisms (GMO) regulation. Knowledge

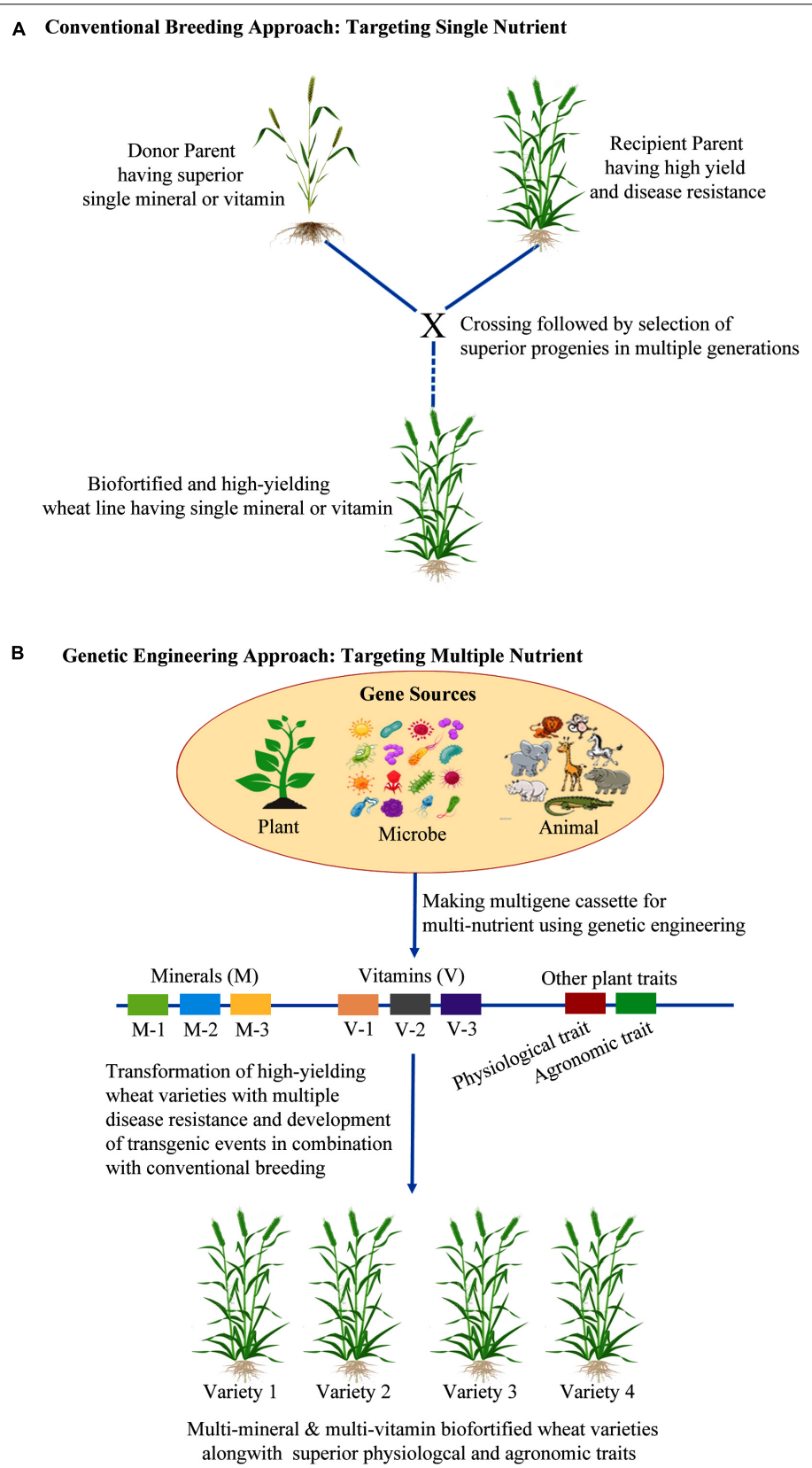

FIGURE 2 | (Continued)

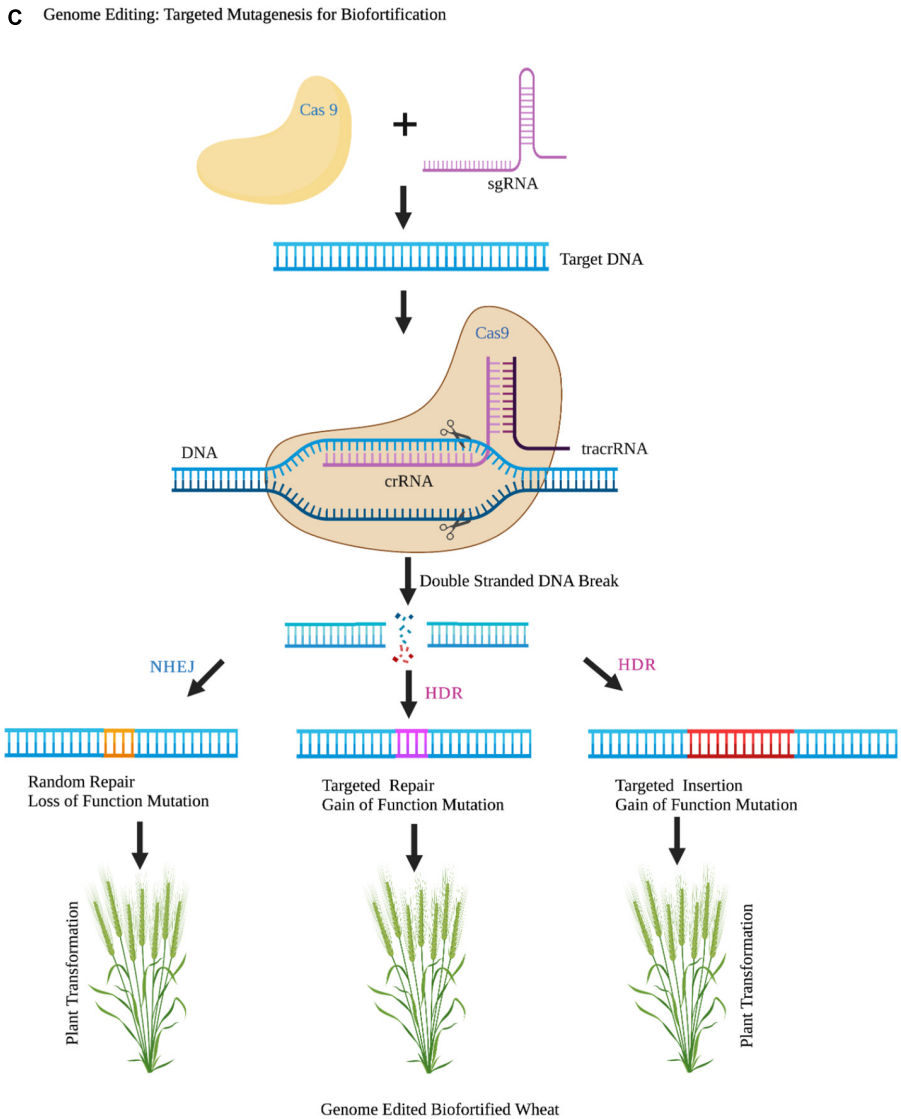

FIGURE 2 | Schematic representation of conventional **(A)** genetic engineering **(B)** and genome editing **(C)** approaches in wheat for targeted biofortifcation of micronutrients. Genetic engineering and genome editing approaches in combination with conventional breeding offers simultaneous incorporation of multi-nutrient (minerals and vitamins) traits along with improved physiological and agronomic features.

gained in identifying and functional characterization of different genes actively associated with uptake and translocation of Fe and Zn can efficiently be used to increase Fe and Zn content in wheat by transgenic approach. Several proofs of concepts using the genetic engineering approaches have been tested with apparently stirring results in wheat for grain Fe and Zn. For example, The *NAM-B1(Gpc-B1)* transcription factor provides an entry point to increase Fe and Zn content. Knowing the critical control points, we can modify expression patterns, downstream targets or binding specificities to augment micronutrient content in grains. Wheat biofortification for Fe and Zn has been achieved using the transcription factor *NAM-B1* (24), which was initially identified for increasing protein content in wild emmer (*Triticum turgidum* ssp *dicoccoides*). In recombinant substitution lines (RSL), the presence of *NAM-B1* allele of *T. dicoccoides* increased Fe and Zn grain concentrations by 18 and 12%, respectively, in addition to 38% higher protein as compared with RSLs carrying the allele from cultivated wheat (*Triticum durum*) (87). Further, the increase in grain Fe and Zn content did not significantly correlate with yield reduction across the five environments (87). This gene is being widely used in breeding programs across several continents (88, 89).

Transgenic approaches involving endosperm-specific expression of wheat ferritin, *TaFer1-A* (90) or soybean ferritin (91) led to 1.5- to 1.9-fold and 1.1- to 1.6-fold increase in grain Fe, respectively alongside increased phytase activity (92). However, the stability of wheat *TaFer1-A* in subsequent generations remains a question. Two independent workers have depicted

that the overexpression of *NICOTIANAMINE SYNTHASE 2* (*OsNAS2*) gene in wheat produced Fe up to 93.1 mg g^{-1} (93) and 80 mg g^{-1} (94) under greenhouse and field conditions, respectively. Connorton et al. (95) demonstrated the doubling of total Fe content in wheat flour by using *VACUOLAR IRON TRANSPORTER 2* (*TaVIT2*) gene, which effectively enhances vacuolar Fe and manganese (Mn) transport in the endosperm. In addition to micronutrients, progress has been made to discourse the challenges of most deficient nutrients like vitamin A and quality proteins in wheat. The provitamin A content of wheat has been enhanced by expressing bacterial *Phytoene synthase (CrtB)* and *Carotene desaturase* gene (*CrtI)* (96, 97). To increase Fe bioavailability, phytase activity was increased by expressing the *Phytochrome* (*phyA)* gene (98), while phytic acid content was decreased by silencing the wheat *ABCC13* transporter gene (99). Protein content, especially essential amino acids lysine, methionine, cysteine, and tyrosine contents in wheat grains, were also attempted to enhance using Amaranthus albumin gene *ama1* (100). Wheat has also been targeted to improve the antioxidant activity by expressing maize regulatory genes *C1*, *B-peru* involved in anthocyanin production (101). The development of biofortified crop varieties either by conventional breeding or transgenic methods is considered a sustainable solution to the problem of micronutrient deficiency. The advantage of this strategy over others like dietary diversification, food fortification, and food supplementation is that once the initial research and development is completed, the benefits of the nutritionally enhanced crops will be sustainable with little further investment. With the advent of powerful reverse genome editing tools such as transcription activator-like effector nucleases (TALENs) and Clustered regularly interspaced short palindromic repeats/CRISPR associated protein 9 (CRISPR/Cas9) coupled with fully sequenced genomes of wheat can be tested as a proof-of-concept for multiple micronutrients biofortification by targeting genes associated with micronutrients uptake and redistribution in different tissues. This will increase the biochemical and physiological pathway's efficiency system biology (pathway reconstruction) and decrease the anti-nutritional factor to increase the bioavailability.

UTILIZING NATURAL GENETIC VARIATION FOR IMPROVING NUTRITIONAL QUALITY THROUGH GENOME EDITING TECHNOLOGIES

Genome editing technologies have emerged as advanced biotechnological, new plant breeding techniques, which offer efficient, target-specific and accurate approaches to engineer genome of a plant. The recent development of CRISPR/Cas9 based genome editing technologies in wheat has shown a ray of hope for improving the nutritional quality of wheat grains (**Figure 2C**). Edited gene constructs generated by these techniques have been delivered to the host genome by PEG-mediated protoplast fusion, particle gun bombardment, or ribonucleoprotein complex. *Since wheat carries a complex hexaploid genome, CRISPR/Cas9—mediated* wheat geminiviral based DNA replicons, delivering RNPs by biolistic method and multiplex editing has proved to be a more appropriate method of genome editing (102, 103). The TALEN and CRISPR/Cas9 systems have already demonstrated their utility for generating abiotic and biotic stress-resistant engineered wheat plants (37). For instance, the mildew resistance locus O (*TaMLO*) gene was edited by CRISPR/Cas9 and TALEN through PEG-mediated protoplast fusion method (39, 104), to achieve resistance to the fungal pathogen. Further, CRISPR/Cas9 genome editing system was applied to engineer dehydration responsive element-binding protein 2 (*TaDREB2*) and wheat ethylene-responsive factor 3 (*TaERF3*) to increase abiotic stress tolerance (105). A more sophisticated technique of multiplexed genome editing with CRISPR/Cas9 has also been demonstrated for wheat using *TaGW, TaLpx* and *TaMLO* genes (103). The gene editing approach has been deployed to improve wheat's grain traits by utilizing the CRISPR/Cas9 RNP delivery of *TaGW2* and *TaGASR7* (negative regulators of grain traits and kernel weight) for increasing kernel weight (102). However, some recent studies have highlighted the use of genome editing for breeding varieties with improved grain quality and increased nutritional value in wheat. CRISPR/Cas9 system was applied to obtain a wheat variety with hypoimmunogenic gluten content by editing α-gliadin genes (40, 106). Similarly, high-amylose modern wheat varieties, needed for better human health, were developed through targeted mutagenesis of the gene *TaSBEIIa* by CRISPR/Cas 9 system (107). Further, the CRISPR/Cas9 editing tool has been demonstrated to be effective in simultaneous editing of multiple genes such as large α- and γ-gliadin gene families in the polyploid bread wheat (106). Other grain quality characteristics such as hardness, starch composition and dough color have been altered in wheat by targeting the *pinb*, *waxy*, *ppo* and *psy* genes (108).

Application of gene-editing techniques is required to be utilized furthermore for biofortification of wheat for enhancing Fe, Zn, Se, Ca and other micronutrient contents. Through QTL mapping and association mapping, information on genomic regions/QTLs responsible for grain Zn and Fe concentrations in different wheat varieties is now available, which can enhance Fe and Zn content in the high yielding varieties. Transgenic technology has been used to generate genetically modified plants with enhanced Fe content as well as better absorption by deploying different genes such as *NAM-B1* transcription factor gene (24), *TaFer1-A* (90, 91), *NAS2* (93, 94), *TaVIT2* (95), and *Phytochrome* (phyA) (98). However, it is recommended that genome editing by CRISPR/Cas9 strategy be applied to provide marker- and foreign DNA- free genetically engineered plants with high Fe content and increased absorption. Attempts are needed to identify and validate genomic regions/QTLs contributing to phytic acid level in wheat grain which can then be engineered to modulate its level by the gene-editing system. For instance, *ABCC13* can be knocked out to reduce the quantity of phytic acid to enhance the concentration of bioavailable minerals. Similarly, future research should focus on enhancing essential amino acid concentration and vitamin levels in wheat. Moreover, *CRISPR/cas9—based genome editing systems can also be utilized to trim the unwanted sequences like*

marker gene, T-DNA region, etc. from the transgenic plants. It is highly recommended that the genome-edited wheat genotypes with improved grain quality characteristics be deployed regularly in wheat breeding programs to enrich the agronomically superior varieties with high nutritional value. It is also envisioned that more recently developed techniques like precise genome editing through base editors, and prime editors are utilized to improve grain quality efficiently and effectively (38, 109).

CONCLUSION AND FUTURE PROSPECTS

Wheat is the most widely cultivated, prominent food crop. There have been several attempts to improve wheat quality and crop yield after the "green revolution". However, the main focus of wheat improvement programs has been on high yield, resulting in high yielding wheat varieties over time but with suboptimal levels of minerals and micronutrients. In order to achieve food and nutritional security, and to provide an adequate supply of calories and nutrients, it is imperative to improve both qualitative and quantitative traits of wheat. Biofortification of wheat can be achieved by exploring natural genetic diversity in wheat and its wild species for higher minerals and phytonutrients through utilizing advanced genomic tools such as QTL mapping and genome-wide association study (GWAS) for mapping nutritional quality traits in wheat, molecular breeding approaches, genomic selection, and genome engineering by transgenic technology and genome editing strategies. Genetic diversity studies have been performed, and few wild relatives of wheat, *T. dicoccoides, Aegilops tauschii, T. dicoccoides*, *T. boeoticun*, *T. spelta*, *T. polonicum,* and *T. aestivum* landraces have been identified that carry relatively higher concentrations of Fe, Zn and Mn. Similarly, QTL mapping and GWAS studies on wheat led to identifying loci responsible for grain Zn and Fe concentrations. Many attempts have been made using transgenic technology to generate wheat with better mineral and micronutrient content and transgenic wheat lines with higher content of Fe, Mn and Vit A have been reported. However, more recently, genome engineering tools like gene editing *via* CRISPR/Cas system, prime editors and base editors have gained much more popularity among scientists over conventional breeding and transgenic technology because of their efficacy, precision, simplicity and robustness.

The significant advantage of genome editing is that it eliminates the foreign DNA/transgene from the final engineered plants. Genome editing by TALEN and CRISPR/Cas 9 system has been employed in wheat to improve stress tolerance and grain yield; however, this system has not been explored as much for biofortification of wheat. Therefore, considering that biofortification of wheat is essential for improving grain quality, genome editing needs to be deployed to improve the content of Fe, Zn, Se, Ca, essential amino acids and decrease the concentration of antinutrients such as phytic acid. Other methods such as multiplex gene editing, transiently expressing CRISPR/Cas9, base editing, prime editing and CRISPR/Cas9 ribonucleoproteins are also promising and should be considered for future research. Exploring natural genetic diversity and broadening the narrow genetic base of hexaploid cultivated wheat varieties is essential and warrants greater attention through whole-genome sequencing of large number of accessions (e.g., the composite core set), and functional genomics for gene discovery associated with agronomic and nutritional traits (110, 111). Such efforts could help generate useful genetic information and genomic resources for accelerating wheat improvement through genome editing (112). Gene editing in germline cells and the CRISPR system carrying RNA interference elements need to be explored in wheat. Similarly, epigenetic genome modifications deserve attention. Also, simulation model-based prediction of superior wheat quality traits under different environmental conditions (113) might accelerate the global wheat nutritional quality program. Hence, utilization of these techniques to improve the nutritional quality of wheat grains and combine them with high yielding traits is emphasized.

AUTHOR CONTRIBUTIONS

OPG, AKS, GPS, KCB, and SKD conceived the idea and designed the outline. OPG, AKS, AS, and KCB drafted the manuscript. OPG, AKS, and AS prepared the illustrations. KCB, GPS, and SKD reviewed and improved the draft. All authors collected, compiled, analyzed, and interpreted the literature and contributed significantly to the article and approved the final version.

FUNDING

OPG and GPS are grateful to the Indian Council of Agricultural Research, Department of Agricultural Research and Education, Government of India for providing financial help under grant no. 1006422, institutional project (CRSCIIWBRSIL 201500900190). AKS, GPS, and OPG acknowledge the financial support received from DBT under the grant BT/Ag/Network/Wheat/2019-20.

ACKNOWLEDGMENTS

We thank the reviewers for critically reviewing the manuscript for its improvement.

REFERENCES

1. Gillespie S, Hodge J, Yosef S, Pandya-Lorch R. *Nourishing Millions: Stories of Change in Nutrition*. Washington, DC: International Food Policy Research Institute (2016).
2. WHO (2017). *Prevalence of Anaemia in Non-Pregnant Women Estimates by WHO Region*. Available online at: https://apps.who.int/gho/data/view.main.ANAEMIAWOMENNPWREG (accessed October 20, 2021).
3. Abbaspour N, Hurrell R, Kelishadi R. Review on iron and its importance for human health. *J Res Med Sci*. (2014) 19:164–74.

4. McDowell LR. *Minerals in Animal and Human Nutrition*. Amsterdam: Elsevier Science BV (2003).
5. World Health Organization [WHO]. *Global Anemia Estimates*. (2021). Available online at: https://www.who.int/data/gho/data/themes/topics/anaemia_in_women_and_children (accessed October 3, 2021).
6. Prasad AS. Zinc: an overview. *Nutrition.* (1995) 1:93–9.
7. Lin PH, Sermersheim M, Li H, Lee P, Steinberg SM, Ma J. Zinc in wound healing modulation. *Nutrients.* (2017) 10:16. doi: 10.3390/nu10010016
8. Bailey RL, West KP Jr, Black RE. The epidemiology of global micronutrient deficiencies. *Ann Nutr Metab.* (2015) 66:22–33. doi: 10.1159/000371618
9. Walker CF, Ezzati M, Black RE. Global and regional child mortality and burden of disease attributable to zinc deficiency. *Eur J Clin Nutr.* (2009) 63:591–7. doi: 10.1038/ejcn.2008.9
10. Mehri A. Trace elements in human nutrition (II)–an update. *Int J Prev Med.* (2020) 11:2. doi: 10.4103/ijpvm.IJPVM_48_19
11. Jones GD, Droz B, Greve P, Gottschalk P, Poffet D, McGrath SP, et al. Selenium deficiency risk predicted to increase under future climate change. *Proc Natl Acad Sci U S A.* (2017) 114:2848–53. doi: 10.1073/pnas.1611576114
12. Pravina P, Sayaji D, Avinash M. Calcium and its role in human body. *Int J Res Pharm Biomed Sci.* (2013) 4:659–68.
13. Cakmak I, Kalayci M, Kaya Y, Torun AA, Aydin N, Wang Y, et al. Biofortification and localization of zinc in wheat grain. *J Agric Food Chem.* (2010) 58:9092–102. doi: 10.1021/jf101197h
14. Ibrahim S, Saleem B, Naeem MK, Arain SM, Khan MR. Next-generation technologies for iron and zinc biofortification and bioavailability in cereal grains. *Crop Pasture Sci.* (2021) 73:77–92.
15. Das, A., Raychaudhuri, U., and Chakraborty, R. (2011). Cereal based functional food of Indian subcontinent: a review. *J. Food Sci. Tech.* 49, 665–672. doi: 10.1007/s13197-011-0474-1
16. Vashishth A, Ram S, Beniwal V. Cereal phytases and their importance in improvement of micronutrients bioavailability. *3 Biotech.* (2017) 7:42. doi: 10.1007/s13205-017-0698-5
17. Hurrell R, Egli I. Iron bioavailability and dietary reference values. *Am J Clin Nutr.* (2010) 91:1461S–7S.
18. Gibson RS. Zinc: the missing link in combating micronutrient malnutrition in developing countries. *Proc Nutr Soc.* (2006) 65:51–60. doi: 10.1079/pns2005474
19. Bhutta ZA, Salam RA, Das JK. Meeting the challenges of micronutrient malnutrition in the developing world. *Br Med Bull.* (2013) 106:7–17. doi: 10.1093/bmb/ldt015
20. Yadava DK, Hossain F, Mohapatra T. Nutritional security through crop biofortification in India: status & future prospects. *Indian J Med Res.* (2018) 148:621–31. doi: 10.4103/ijmr.IJMR_1893_18
21. Welch RM, Graham RD. Breeding for micronutrients in staple food crops from a human nutrition perspective. *J Exp Bot.* (2004) 55:353–64. doi: 10.1093/jxb/erh064
22. Gupta OP, Pandey V, Narwal S, Sharma P, Ram S, Singh GP editors. *Wheat and Barley Grain Biofortification*. 1st ed. Sawston: Woodhead Publishing (2020). p. 364. doi: 10.1016/C2018-0-04173-0
23. Singh R, Velu G. *Zinc-Biofortified Wheat: Harnessing Genetic Diversity for Improved Nutritional Quality*. Bonn: CIMMYT, HarvestPlus, and the Global Crop Diversity Trust (2017).
24. Uauy C, Distelfeld A, Fahima T, Blechl A, Dubcovsky J. A NAC gene regulating senescence improves grain protein, zinc, and iron content in wheat. *Science.* (2006) 314:1298–301. doi: 10.1126/science.1133649
25. International Wheat Genome Sequencing Consortium [IWGSC]. Shifting the limits in wheat research and breeding using a fully annotated reference genome. *Science.* (2018) 361:eaar7191. doi: 10.1126/science.aar7191
26. Avni R, Nave M, Barad O, Baruch K, Twardziok SO, Gundlach H, et al. Wild emmer genome architecture and diversity elucidate wheat evolution and domestication. *Science.* (2017) 357:93–7. doi: 10.1126/science.aan0032
27. Ling H-Q, Ma B, Shi X, Liu H, Dong L, Sun H, et al. Genome sequence of the progenitor of wheat a subgenome *Triticum urartu*. *Nature.* (2018) 557:424–8. doi: 10.1038/s41586-018-0108-0
28. Ramírez-González RH, Borrill P, Lang D, Harrington SA, Brinton J, Venturini L, et al. The transcriptional landscape of polyploid wheat. *Science.* (2018) 361:aar6089. doi: 10.1126/science.aar6089
29. Gupta OP, Pandey V, Saini R, Narwal S, Malik VK, Khandale T, et al. Identifying transcripts associated with efficient transport and accumulation of Fe and Zn in hexaploid wheat (*T. aestivum* L.). *J Biotechnol.* (2020) 316:46–55. doi: 10.1016/j.jbiotec.2020.03.015
30. Gupta OP, Pandey V, Saini R, Narwal S, Malik VK, Khandale T, et al. Transcriptomic dataset reveals the molecular basis of genotypic variation in hexaploid wheat (*T. aestivum* L.) in response to Fe/Zn deficiency. *Data Brief.* (2020) 31:105995. doi: 10.1016/j.dib.2020.105995
31. Gupta OP, Pandey V, Saini R, Khandale T, Singh A, Malik VK, et al. Comparative physiological, biochemical and transcriptomic analysis of hexaploid wheat (*T. aestivum* L.) roots and shoots identifies potential pathways and their molecular regulatory network during Fe and Zn starvation. *Genomics.* (2021) 113:3357–72. doi: 10.1016/j.ygeno.2021.07.029
32. Jia JZ, Zhao G. *Wheat 660 SNP Array Developed by CAAS*. (2016). Available online at: https://wheat.pw.usda.gov/ggpages/topics/Wheat660_SNP_array_developed_by_CAAS.pdf (accessed October 15, 2021).
33. Gadaleta A, Colasuonno P, Giove SL, Blanco A, Giancaspro A. Map-based cloning of *QFhb.mgb-2A* identifies a *WAK2* gene responsible for *Fusarium* head blight resistance in wheat. *Sci Rep.* (2019) 9:6929. doi: 10.1038/s41598-019-43334-z
34. Velu G, Singh RP, Crespo-Herrera L, Juliana P, Dreisigacker S, Valluru R, et al. Genetic dissection of grain zinc concentration in spring wheat for mainstreaming biofortification in CIMMYT wheat breeding. *Sci Rep.* (2018) 8:13526. doi: 10.1038/s41598-018-31951-z
35. Nigro D, Gadaleta A, Mangini G, Colasuonno P, Marcotuli I, Giancaspro A, et al. Candidate genes and genome-wide association study of grain protein content and protein deviation in durum wheat. *Planta.* (2019) 249:1157–75. doi: 10.1007/s00425-018-03075-1
36. Muhu-Din Ahmed HG, Sajjad M, Zeng Y, Iqbal M, Habibullah Khan S, Ullah A, et al. Genome-wide association mapping through 90k SNP array for quality and yield attributes in bread wheat against water-deficit conditions. *Agriculture.* (2020) 10:392. doi:10.3390/agriculture10090392
37. Sharma SK, Gupta OP, Pathaw N, Sharma D, Maibam A, Sharma P, et al. CRISPR-Cas-led revolution in diagnosis and management of emerging plant viruses: new avenues toward food and nutritional security. *Front Nutr.* (2021) 8:751512. doi: 10.3389/fnut.2021.751512
38. Molla KA, Sretenovic S, Bansal KC, Qi Y. Precise plant genome editing using base editors and prime editors. *Nat Plants.* (2021) 7:1166–87. doi: 10.1038/s41477-021-00991-1
39. Wang Y, Cheng X, Shan Q, Zhang Y, Liu J, Gao C, et al. Simultaneous editing of three homoeoalleles in hexaploid bread wheat confers heritable resistance to powdery mildew. *Nat Biotechnol.* (2014) 32:947–51. doi: 10.1038/nbt.2969
40. Sánchez-León S, Gil-Humanes J, Ozuna CV, Giménez MJ, Sousa C, Voytas DF, et al. Low-gluten, non-transgenic wheat engineered with CRISPR/Cas9. *Plant Biotechnol J.* (2018) 16:902–10. doi: 10.1111/pbi.12837
41. Khan MK, Pandey A, Hamurcu M, Gezgin S, Athar T, Rajput VD, et al. Insight into the prospects for nanotechnology in wheat biofortification. *Biology.* (2021) 10:1123. doi: 10.3390/biology10111123
42. Balint AF, Kovacs G, Erdei L, Sutka J. Comparison of the Cu, Zn, Fe, Ca and Mg contents of the grains of wild, ancient and cultivated wheat species. *Cereal Res Commun.* (2001) 29:375–82.
43. Qury FX, Leenhardt F, Remesy C, Chanliaud E, Duperrier B, Balfourier F, et al. Genetic variability and stability of grain magnesium, zinc and iron concentrations in bread wheat. *Eur J Agron.* (2006) 25:177–85.
44. Goel S, Singh B, Grewal S, Jaat RS, Singh NK. Variability in Fe and Zn content among Indian wheat landraces for improved nutritional quality. *Indian J Genet Plant Breed.* (2018) 78:426–32.
45. Zhao FJ, Su YH, Dunham SJ, Rakszegi M, Bedo Z, McGrath SP, et al. Variation in mineral micronutrient concentrations in grain of wheat lines of diverse origin. *J Cereal Sci.* (2009) 49:290–5.
46. Amiri R, Bahraminejad S, Sasani S, Jalali-Honarmand S, Fakhri R. Bread wheat genetic variation for grain's protein, iron and zinc concentrations as uptake by their genetic ability. *Eur J Agron.* (2015) 67:20–6.
47. Guzman C, Peña RJ, Singh R, Autrique E, Dreisigacker S, Crossa J, et al. Wheat quality improvement at CIMMYT and the use of genomic selection on it. *Appl Transl Genomics.* (2016) 11:3–8. doi: 10.1016/j.atg.2016.10.004

48. Heidari P, Etminan A, Azizinezhad R, Khosroshahli M. Genomic variation studies in durum wheat (*Triticum turgidum* ssp. durum) using CBDP, SCoT and ISSR markers. *Indian J Genet.* (2017) 77:379–86.
49. Khokhar JS, King J, King IP, Young SD, Foulkes MJ, De Silva J, et al. Novel sources of variation in grain Zinc (Zn) concentration in bread wheat germplasm derived from Watkins landraces. *PLoS One.* (2020) 15:e0229107. doi: 10.1371/journal.pone.0229107
50. Chhuneja P, Dhaliwal HS, Bains NS, Singh K. *Aegilops kotschyi* and *Aegilops tauschii* as sources for higher levels of grain Iron and Zinc. *Plant Breed.* (2006) 125:529–31.
51. Rawat N, Tiwari VK, Singh N, Randhawa GS, Singh K, Chhuneja P, et al. Evaluation and utilization of *Aegilops* and wild *Triticum* species for enhancing iron and zinc content in wheat. *Genet Resour Crop Evol.* (2008) 56:53–64.
52. Tiwari VK, Rawat N, Chhuneja P, Neelam K, Aggarwal R, Randhawa GS, et al. Mapping of quantitative trait loci for grain iron and zinc concentration in diploid A genome wheat. *J Hered.* (2009) 100:771–6. doi: 10.1093/jhered/esp030
53. Cakmak I, Torun A, Millet E, Feldman M, Fahima T, Korol AB, et al. *Triticum dicoccoides*: an important genetic resource for increasing zinc and iron concentration in modern cultivated wheat. *Soil Sci Plant Nutr.* (2004) 50:1047–54.
54. Velu G, Crespo Herrera L, Guzman C, Huerta J, Payne T, Singh RP. Assessing genetic diversity to breed competitive biofortified wheat with enhanced grain Zn and Fe concentrations. *Front Plant Sci.* (2019) 9:1971. doi: 10.3389/fpls.2018.01971
55. Johansson E, Henriksson T, Prieto-Linde ML, Andersson S, Ashraf R, Rahmatov M. Diverse wheat-alien introgression lines as a basis for durable resistance and quality characteristics in bread wheat. *Front Plant Sci.* (2020) 11:1067. doi: 10.3389/fpls.2020.01067
56. Lyons G, Ortiz-Monasterio I, Stangoulis J, Graham R. Selenium concentration in wheat grain: Is there sufficient genotypic variation to use in breeding? *Plant Soil.* (2005) 269:369–80.
57. Lee S, Woodard HJ, Doolittle JJ. Selenium uptake response among selected wheat (*Triticum aestivum*) varieties and relationship with soil selenium fractions. *Soil Sci Plant Nutr.* (2011) 57:823–32.
58. Pandey A, Khan MK, Hakki EE, Thomas G, Hamurcu M, Gezgin S, et al. Assessment of genetic variability for grain nutrients from diverse regions: potential for wheat improvement. *Springerplus.* (2016) 5:1912. doi: 10.1186/s40064-016-3586-2
59. Alomari DZ, Eggert K, von Wirén N, Pillen K, Röder MS. Genome-wide association study of calcium accumulation in grains of European wheat cultivars. *Front Plant Sci.* (2017) 8:1797. doi: 10.3389/fpls.2017.01797
60. Hussain S, Maqsood M, Miller L. Bioavailable zinc in grains of bread wheat varieties of Pakistan. *Cereal Res Commum.* (2012) 40:62–73.
61. Branković G, Dragičević V, Dodig D, Knežević D, Kandić V, Šurlan-Momirović G, et al. Phytic acid, inorganic phosphorus, antioxidants in bread and durum wheat and their associations with agronomic traits. *Agric Food Sci.* (2015) 24:183–94.
62. Magallanes-López AM, Hernandez-Espinosa N, Velu G, Posadas-Romano G, Ordñez-Villegas V, Crossa J, et al. Variability in iron, zinc and phytic acid content in a worldwide collection of commercial durum wheat cultivars and the effect of reduced irrigation on these traits. *Food Chem.* (2017) 237:499–505. doi: 10.1016/j.foodchem.2017.05.110
63. Tabekha MM, Donnelly BJ. Phytic acid in durum wheat and its milled products. *Cereal Chem.* (1982) 59:105–7.
64. Peleg Z, Cakmak I, Ozturk L, Yazici A, Jun Y, Budak H, et al. Quantitative trait loci conferring grain mineral nutrient concentrations in durum wheat x wild emmer wheat RIL population. *Theor Appl Genet.* (2009) 19:353–69. doi: 10.1007/s00122-009-1044-z
65. Tiwari C, Wallwork H, Arun B, Mishra VK, Velu G, Stangoulis J. Molecular mapping of quantitative trait loci for zinc, iron and protein content in the grains of hexaploid wheat. *Euphytica.* (2016) 207:563–70. doi: 10.1371/journal.pone.0179851
66. Velu G, Tutus Y, Gomez-Becerra HF, Hao Y, Demir L, Kara R, et al. QTL mapping for grain zinc and iron concentrations and zinc efficiency in a tetraploid and hexaploid wheat mapping populations. *Plant Soil.* (2017) 411:81–99. doi: 10.1007/s11104-016-3025-8
67. Krishnappa G, Singh AM, Chaudhary S, Ahlawat AK, Singh SK, Shukla RB, et al. Molecular mapping of the grain iron and zinc concentration, protein content and thousand kernel weight in wheat (*Triticum aestivum* L.). *PLoS one.* (2017) 12:e0174972. doi: 10.1371/journal.pone.0174972
68. Liu J, Wu B, Singh RP, Velu G. QTL mapping for micronutrients concentration and yield component traits in a hexaploid wheat mapping population. *J Cereal Sci.* (2019) 88:57–64. doi: 10.1016/j.jcs.2019.05.008
69. Krishnappa G, Rathan ND, Sehgal D, Ahlawat AK, Singh SK, Singh SK, et al. Identification of novel genomic regions for biofortification traits using an SNP marker-enriched linkage map in wheat (*Triticum aestivum* L.). *Front Nutr.* (2021) 8:669444. doi: 10.3389/fnut.2021.669444
70. Xu Y, An D, Liu D, Zhang A, Xu H, Li B. Molecular mapping of QTLs for grain zinc, iron and protein concentration of wheat across two environments. *Food Crop Res.* (2012) 138:57–62. doi: 10.1016/j.fcr.2012.09.017
71. Hao Y, Velu G, Peña RJ, Singh S, Singh RP. Genetic loci associated with high grain zinc concentration and pleiotropic effect on kernel weight in wheat (*Triticum aestivum* L.). *Mol Breed.* (2014) 34:1893–902. doi: 10.1007/s11032-014-0147-7
72. Pu CX, Han YF, Zhu S, Song FY, Zhao Y, Wang CY, et al. The rice receptor-like kinases DWARF AND RUNTISH SPIKELET1 and 2 repress cell death and affect sugar utilization during reproductive development. *Plant Cell.* (2017) 29:70–89. doi: 10.1105/tpc.16.00218
73. Wang C, Ji J, Zhu F. Characterizing Se transfer in the soil-crop systems under field condition. *Plant Soil.* (2017) 415:535–48. doi: 10.1002/0471142913.faf0102s00
74. Alomari DZ, Alqudah AM, Pillen K, von Wirén N, Röder MS. Toward identification of a putative candidate gene for nutrient mineral accumulation in wheat grains for human nutrition purposes. *J Exp Bot.* (2021) 72:6305–18. doi: 10.1093/jxb/erab297
75. Upadhyaya H, Bajaj D, Das S, Kumar V, Gowda CL, Sharma S, et al. Genetic dissection of seed-iron and zinc concentrations in chickpea. *Sci Rep.* (2016) 6:24050. doi: 10.1038/srep24050
76. Grusak MA, Cakmak I. Methods to improve the crop-delivery of minerals to humans and livestock. In: Broadley MR, White PJ editors. *Plant Nutritional Genomics*. Oxford: Blackwell Publishing Ltd (2005). p. 265–6.
77. Weckwerth W, Ghatak A, Bellaire A, Chaturvedi P, Varshney RK. PANOMICS meets germplasm. *Plant Biotechnol J.* (2020) 7:1507–25. doi: 10.1111/pbi.13372
78. Gupta OP, Deshmukh R, Kumar A, Singh SK, Sharma P, Ram S, et al. From gene to biomolecular networks: a review of evidences for understanding complex biological function in plants. *Curr Opin Biotechnol.* (2022) 74:66–74. doi: 10.1016/j.copbio.2021.10.023
79. Massman JM, Jung HJG, Bernardo R. Genome-wide selection versus marker-assisted recurrent selection to improve gain yield and stover-quality traits for cellulosic ethanol in maize. *Crop Sci.* (2013) 53:58–66. doi: 10.2135/cropsci2012.02.0112
80. Gaikwad KB, Rani S, Kumar M, Gupta V, Babu PH, Bainsla NK, et al. Enhancing the nutritional quality of major food crops through conventional and genomics-assisted breeding. *Front Nutr.* (2020) 7:533453. doi: 10.3389/fnut.2020.533453
81. Joukhadar R, Thistlethwaite R, Trethowan RM, Hayden MJ, Stangoulis J, Cu S, et al. Genomic selection can accelerate the biofortification of spring wheat. *Theor Appl Genet.* (2021) 134:3339–50. doi: 10.1007/s00122-021-03900-4
82. Owens BF, Gore MA, Magallanes-Lundback M, Tiede T, Diepenbrock CH, Kandianis CB, et al. A foundation for provitamin a biofortification of maize: genome-wide association and genomic prediction models of carotenoid levels. *Genetics.* (2014) 198:1699–716. doi: 10.1534/genetics.114.169979
83. Velu G, Crossa J, Singh RP, Hao Y, Dreisigacker S, Perez-Rodriguez P, et al. Genomic prediction for grain zinc and iron concentrations in spring wheat. *Theor Appl Genet.* (2016) 129:1595–605. doi: 10.1007/s00122-016-2726-y
84. Prasanna BM, Palacios-Rojas N, Hossain F, Muthusamy V, Menkir A, Dhliwayo T, et al. Molecular breeding for nutritionally enriched maize: status and prospects. *Front Genet.* (2020) 10:1392. doi: 10.3389/fgene.2019.01392
85. Manickavelu A, Hattori T, Yamaoka S, Yoshimura K, Kondou Y, Onogi A, et al. Genetic nature of elemental contents in wheat grains and its genomic prediction: toward the effective use of wheat landraces from Afghanistan. *PLoS One.* (2017) 12:e0169416. doi: 10.1371/journal.pone.0169416

86. Ludwig Y, Slamet-Loedin IH. Genetic biofortification to enrich rice and wheat grain iron: from genes to product. *Front Plant Sci.* (2019) 10:833. doi: 10.3389/fpls.2019.00833
87. Distelfeld A, Cakmak I, Peleg Z, Ozturk L, Yazici AM, Budak H, et al. Multiple QTL-efects of wheat *Gpc-B1* locus on grain protein and micronutrient concentrations. *Physiol Plant.* (2007) 129:635–43.
88. Randhawa HS, Asif M, Pozniak C, Clarke JM, Graf RJ, Fox SL, et al. Application of molecular markers to wheat breeding in Canada. *Plant Breed.* (2013) 132:458–71.
89. Tabbita F, Lewis S, Vouilloz JP, Ortega MA, Kade M, Abbate PE, et al. Effects of the *Gpc-B1* locus on high grain protein content introgressed into Argentinean wheat germplasm. *Plant Breed.* (2013) 132:48–52.
90. Borg S, Brinch-Pedersen H, Tauris B, Madsen LH, Darbani B, Noeparvar S, et al. Wheat ferritins: improving the iron content of the wheat grain. *J Cereal Sci.* (2012) 56:204–13.
91. Xiaoyan S, Yan Z, Shubin W. Improvement Fe content of wheat (*Triticum aestivum*) grain by soybean ferritin expression cassette without vector backbone sequence. *J Agric Biotechnol.* (2012) 20:766–73.
92. Holm PB, Kristiansen KN, Pedersen HB. Transgenic approaches in commonly consumed cereals to improve iron and zinc content and bioavailability. *J Nutr.* (2002) 132:514S–6S. doi: 10.1093/jn/132.3.514S
93. Singh D, Geat N, Rajawat MVS, Mahajan MM, Prasanna R, Singh S, et al. Deciphering the mechanisms of endophyte-mediated biofortification of Fe and Zn in wheat. *J Plant Growth Regul.* (2017) 37:174–82.
94. Beasley JT, Bonneau JP, Sanchez-Palacios JT, Moreno-Moyano LT, Callahan DL, Tako E, et al. Metabolic engineering of bread wheat improves grain iron concentration and bioavailability. *Plant Biotechnol J.* (2019) 17:1514–26. doi: 10.1111/pbi.13074
95. Connorton JM, Jones ER, Rodríguez-Ramiro I, Fairweather-Tait S, Uauy C, Balk J. Wheat vacuolar iron transporter TaVIT2 transports Fe and Mn and is effective for biofortification. *Plant Physiol.* (2017) 174:2434–44. doi: 10.1104/pp.17.00672
96. Cong L, Wang C, Chen L, Liu H, Yang G, He G. Expression of phytoene synthase1 and carotene desaturase crtI genes result in an increase in the total carotenoids content in transgenic elite wheat (*Triticum aestivum* L.). *J Agric Food Chem.* (2009) 57:8652–60. doi: 10.1021/jf9012218
97. Wang C, Zeng J, Li Y, Hu W, Chen L, Miao Y, et al. Enrichment of provitamin A content in wheat (*Triticum aestivum* L.) by introduction of the bacterial carotenoid biosynthetic genes *CrtB* and *CrtI*. *J Exp Bot.* (2014) 65:2545–56. doi: 10.1093/jxb/eru138
98. Brinch-Pederson H, Olesen A, Rasmussen SK, Holm PB. Generation of transgenic wheat (*Triticum aestivum* L.) for constitutive accumulation of an Aspergillus phytase. *Mol Breed.* (2000) 6:195–206.
99. Bhati KK, Alok A, Kumar A, Kaur J, Tiwari S, Pandey AK. Silencing of ABCC13 transporter in wheat reveals its involvement in grain development, phytic acid accumulation and lateral root formation. *J Exp Bot.* (2016) 67:4379–89. doi: 10.1093/jxb/erw224
100. Tamas C, Kisgyorgy BN, Rakszegi M, Wilkinson MD, Yang MS, Lang L, et al. Transgenic approach to improve wheat (*Triticum aestivum* L.) nutritional quality. *Plant Cell Rep.* (2009) 28:1085–94. doi: 10.1007/s00299-009-0716-0
101. Doshi KM, Eudes F, Laroche A, Gaudet D. Transient embryo specific expression of anthocyanin in wheat. *In Vitro Cell Dev Biol.* (2006) 42:432–8.
102. Zhang Y, Liang Z, Zong Y, Wang Y, Liu J, Chen K, et al. Efficient and transgene-free genome editing in wheat through transient expression of CRISPR/Cas9 DNA or RNA. *Nat Commun.* (2016) 7:12617. doi: 10.1038/ncomms12617
103. Wang W, Pan Q, He F, Akhunova A, Chao S, Trick H, et al. Transgenerational CRISPR-Cas9 activity facilitates multiplex gene editing in allopolyploid wheat. *CRISPR J.* (2018) 1:65–74. doi: 10.1089/crispr.2017.0010
104. Shan Q, Wang Y, Li J, Gao C. Genome editing in rice and wheat using the CRISPR/Cas system. *Nat Protoc.* (2014) 9:2395–410. doi: 10.1038/nprot.2014.157
105. Kim D, Alptekin B, Budak H. CRISPR/Cas9 genome editing in wheat. *Funct Integr Genomics.* (2018) 18:31–41.
106. Jouanin A, Schaart JG, Boyd LA, Cockram J, Leigh FJ, Bates R, et al. Outlook for coeliac disease patients: towards bread wheat with hypoimmunogenic gluten by gene editing of α-and γ-gliadin gene families. *BMC Plant Biol.* (2019) 19:333. doi: 10.1186/s12870-019-1889-5
107. Li J, Jiao G, Sun Y, Chen J, Zhong Y, Yan L, et al. Modification of starch composition, structure and properties through editing of TaSBEIIa in both winter and spring wheat varieties by CRISPR/Cas9. *Plant Biotechnol J.* (2021) 19:937–51. doi: 10.1111/pbi.13519
108. Zhang S, Zhang R, Gao J, Song G, Li J, Li W, et al. CRISPR/Cas9-mediated genome editing for wheat grain quality improvement. *Plant Biotechnol J.* (2021) 19:1684–6. doi: 10.1111/pbi.13647
109. Zong Y, Wang Y, Li C, Zhang R, Chen K, Ran Y, et al. Precise base editing in rice, wheat and maize with a Cas9-cytidine deaminase fusion. *Nat Biotechnol.* (2017) 35:438–40. doi: 10.1038/nbt.3811
110. Dutta M, Phogat BS, Kumar S, Kumar N, Kumari J, Pandey AC, et al. Development of core set of wheat (*Triticum spp.*) germplasm conserved in the National Genebank in India. In: Ogihara Y, Takumi S, Handa H editors. *Advances in Wheat Genetics: From Genome to Field*. Berlin: Springer (2015). p. 33–45. doi: 10.1007/978-4-431-55675-6_4
111. Phogat BS, Kumar S, Kumari J, Kumar N, Pandy AC, Singh TP, et al. Characterization of wheat germplasm conserved in the Indian National Genebank and establishment of a composite core collection. *Crop Sci.* (2020) 61:604–20. doi: 10.1002/csc2.20285
112. Li S, Zhang C, Li J, Yan L, Wang N, Xia L. Present and future prospects for wheat improvement through genome editing and advanced technologies. *Plant Commun.* (2021) 2:100211. doi: 10.1016/j.xplc.2021.100211
113. Mohan D, Sendhil R, Gupta OP, Pandey V, Gopalareddy K, Singh GP. Wheat quality index: new holistic approach to identify quality superior genotypes. *Cereal Res Commun.* (2022). doi: 10.1007/s42976-022-00254-5
114. Arora S, Cheema J, Poland J, Uauy C, Chhuneja P. Genome-wide association mapping of grain micronutrients concentration in *Aegilops tauschii*. *Front Plant Sci.* (2019) 10:54. doi: 10.3389/fpls.2019.00054
115. Bhatta M, Baenziger PS, Waters BM, Poudel R, Belamkar V, Poland J, et al. Genome-wide association study reveals novel genomic regions associated with 10 grain minerals in synthetic hexaploid wheat. *Int J Mol Sci.* (2018) 19:3237. doi: 10.3390/ijms19103237
116. Rathan ND, Sehgal D, Thiyagarajan K, Singh R, Singh A-M, Govindan V. Identification of genetic loci and candidate genes related to grain zinc and iron concentration using a zinc-enriched wheat 'zinc-shakti'. *Front Genet.* (2021) 12:652653. doi: 10.3389/fgene.2021.652653
117. Wang, W., Guo, H., Wu, C., Yu, H., Li, X., Chen, G., et al. (2021). Identification of novel genomic regions associated with nine mineral elements in Chinese winter wheat grain. *BMC Plant Biol.* 21:311. doi: 10.1186/s12870-021-03105-3

Conflict of Interest: The authors declare that the research was conducted in the absence of any commercial or financial relationships that could be construed as a potential conflict of interest.

Publisher's Note: All claims expressed in this article are solely those of the authors and do not necessarily represent those of their affiliated organizations, or those of the publisher, the editors and the reviewers. Any product that may be evaluated in this article, or claim that may be made by its manufacturer, is not guaranteed or endorsed by the publisher.

Advantages of publishing in Frontiers

OPEN ACCESS
Articles are free to read for greatest visibility and readership

FAST PUBLICATION
Around 90 days from submission to decision

HIGH QUALITY PEER-REVIEW
Rigorous, collaborative, and constructive peer-review

TRANSPARENT PEER-REVIEW
Editors and reviewers acknowledged by name on published articles

Frontiers
Avenue du Tribunal-Fédéral 34
1005 Lausanne | Switzerland

Visit us: www.frontiersin.org
Contact us: frontiersin.org/about/contact

REPRODUCIBILITY OF RESEARCH
Support open data and methods to enhance research reproducibility

DIGITAL PUBLISHING
Articles designed for optimal readership across devices

FOLLOW US
@frontiersin

IMPACT METRICS
Advanced article metrics track visibility across digital media

EXTENSIVE PROMOTION
Marketing and promotion of impactful research

LOOP RESEARCH NETWORK
Our network increases your article's readership